# Geochemistry of the Mafic Sequences in the Cloncurry District, Queensland: Implications for crustal accretion and prospectivity.

Thesis submitted in accordance with the requirements of the University of Adelaide for an Honours Degree in Geology/Geophysics

Jack Kameron Maughan

November 2016


THE UNIVERSITY of ADELAIDE

# THE GEOCHEMISTRY OF THE MAFIC SEQUENCES IN THE CLONCURRY DISTRICT, QUEENSLAND: IMPLICATIONS FOR CRUSTAL ACCRETION AND PROSPECTIVITY.

## ABSTRACT

The Cloncurry District, Queensland, is a classic Iron Oxide Copper Gold (IOCG) terrain. However, the geochemical characteristics of the numerous mafic intrusives (dominantly dolerite dykes), which are often spatially and temporally associated with mineralisation, have never been studied in detail. Specifically, the newly described dolerite-associated Great Australia-Taipan-Mongoose-Magpie (GATPMM) deposits are thought to represent a distinct Cu-Co-carbonate-rich, Au-poor style of IOCG mineralisation that has not been documented elsewhere in the district. Trace element geochemistry provides evidence that these dykes formed from lower crust fractionation and magmatic ascent throughout intracontinental extension. There is significant REE links to previously studied granites of the Naraku and Williams Batholith within the district, indicating a similar melt source for both igneous lithologies. Geochronological studies of hydrothermal titanite (1515± Ma) and apatite (1177±37 Ma and 1179±41 Ma) from the Mongoose prospect provide constraints on the age of initial intrusion and alteration and provide evidence for thermal-tectonic activity within the Eastern Succession ca. 1100-1200 Ma, possibly related to the Albany-Fraser and/or Musgravian Orogeny's. Geochemical relationships between mineralised dolerite samples from the CuDECO Rocklands deposit and local barren dolerite samples are also analysed and display geochemical similarity. This is consistent with the interpretation that dolerite geochemistry alone is not an indicator of prospectivity and is not linked to the distribution of mineralisation.

## KEYWORDS

Geochemistry, Cloncurry, Geochronology, Mafic, Dykes, Mineralisation, Melt Source, Rifting.

**TABLE OF CONTENTS**

Title ..... i
Abstract ..... i
Keywords ..... i
List of Figures ..... 3
1 Introduction ..... 5
2 Geological Setting ..... 6
2.1 Regional Geology ..... 6
2.2 Alteration ..... 8
2.3 Cloncurry Dolerites ..... 10
3 Methods ..... 12
3.1 Fieldwork and Sampling ..... 12
3.2 Petrological Analysis ..... 15
3.3 Geochemical Analysis ..... 15
3.4 Geochronology ..... 16
3.5 Data Processing ..... 18
4 Observations and Results ..... 18
4.1 Petrology ..... 18
4.1.1 Grain Size and Textures ..... 19
4.1.2 Mineralogy ..... 19
4.1.3 Alteration ..... 20
4.1.4 CuDECO Petrology ..... 23
4.2 Geochemistry ..... 25
4.2.1 Major Elements ..... 25
4.2.2 Trace & Rare Earth Elements ..... 28
4.2.3 Tectonic Discrimination Plots ..... 34
4.2.4 CuDECO Geochemistry ..... 38
4.3 Geochronology ..... 40
4.3.1 Standards ..... 40
4.3.2 Titanite ..... 41
4.3.3 Apatite ..... 42
5 Discussion ..... 43
5.1 Melt Source ..... 43
5.2 Tectonic Implications ..... 46

5.3 Geochronology ..... 49
5.4 CuDECO Dolerites and Exploration Implications ..... 50
6 Conclusions ..... 51
7 Future Research ..... 52
Acknowledgments ..... 52
References ..... 54
APPENDIX 1: Extended Methods ..... 59
APPENDIX 2: Petrology ..... 82
APPENDIX 3: Geochemistry ..... 114
APPENDIX 4: Geochronology ..... 142

**LIST OF FIGURES**

Figure 1. Cover sequences of the Eastern Succession. ..... 7
Figure 2. A chronostratigraphic history of the Mount Isa Inlier. ..... 9
Figure 3. The GATPMM paragenetic sequence stages based upon Taylor (2013). ..... 10
Figure 4. A sample location map with Mt Isa Inlier inset. ..... 14
Figure 5. The textures and shape of hydrothermal titanite and apatite. ..... 17
Figure 6. Petrography images of the varying grain size within the mafic samples. ..... 21
Figure 7. Petrography images of alteration in field samples ..... 22
Figure 8. Petrogrpahy and SEM images of CuDECO samples. ..... 24
Figure 9. a) AFM diagram and b) TAS diagram. ..... 26
Figure 10. Bi-varite plots of major element oxides. ..... 27
Figure 11. Bi-variate plots of trace elements. ..... 29
Figure 12. Cr-Y plot and Ni-Y plot. ..... 30
Figure 13. Th/Ta vs La/Ta diagram. ..... 31
Figure 14. A MORB normalised spider diagram. ..... 32
Figure 15. Grouped Nb/Yb-Th/Yb diagram. ..... 33

Figure 16. Grouped REE spider diagram. ..... 33

Figure 17. Ti-V diagram. ..... 36

Figure 18. Ti-Zr diagram. ..... 36

Figure 19. Tectonic discrimination diagrams. ..... 37

Figure 20. Grouped Nb/Yb-Th/Yb diagram with CuDECO samples. ..... 39

Figure 21. Grouped REE spider diagram with CuDECO samples. ..... 39

Figure 22. The weighted average mean of titanite and apatite standard ages. ..... 40

Figure 23. Tera-Wasserberg Concordia diagram for D16 titanite with weighted inset. 41

Figure 24. Tera-Wasserberg Concordia diagram for D16 apatite with weighted inset. . 42

Figure 25. Tera-Wasserberg Concordia diagram for D18 apatite with weighted inset .. 43

Figure 26. An incomplete liquid-solid separation scenario. ..... 46

Figure 27. A cartoon summary of proposed tectonic history. ..... 48

# 1 INTRODUCTION

The Proterozoic Eastern Succession of the Mount Isa Inlier, North-West Queensland, consists mainly of ca. 1800–1600 Ma metasedimentary and metavolcanic sequences with a complex and protracted history of regional scale metamorphism and alteration (Foster & Austin, 2008; Mark et al., 2006). These sequences are host to igneous intrusions such as the ca. 1500-1550 Ma felsic Naraku and Williams Batholith (Wyborn, 1998), but are also intruded by mafic dykes and sills of possible dates ranging from ca. 1100 to 1800 Ma (Young & Lane, 2015; Carter et al., 1961). The igneous intrusions located in the Cloncurry District of the Eastern Succession are of particular interest because of their spatial and possible temporal relationship with Cu-Au (Co) mineralisation of the area. The Cloncurry District is a classic Iron Oxide-Copper-Gold (IOCG) terrain and hosts a range of ore deposits including a distinctive vein hosted Cu-Co-carbonate-rich, Au-poor style of IOCG mineralisation (Oliver et al., 2008). These carbonate-rich deposits are often hosted within and associated with mafic intrusives, forming a geographical trend following the southern boundary of the Naraku Batholith. The trend containing these deposits is informally named the Great Australia, Taipan, Mongoose, and Magpie (GATPMM) Trend and is the focus of this study.

To understand the relationship between these intrusions and mineralisation, it is necessary to understand the relationship between the mafic dykes and the tectonic evolution of the Eastern Succession. The dykes are poorly understood in regards to their paleotectonic setting of intrusion, age, paragenetic sequence and their textural, mineralogical and geochemical relationships. Dolerite is the dominant lithology, with some variation of

grain size to include meta-basalt and/or meta-gabbro with a highly variable alteration history.

This project analysed 17 rock chip field samples, 90 reverse circulation (RC) drilling pulps and 6 dolerite drill core samples for whole rock geochemistry, including major element, trace element and REE. This data has been used to; determine the evolution of the melt source from which these intrusives were sourced, attempt to distinguish between different intrusive episodes, generate discrimination diagrams to define geological constraints on the palaeotectonic setting and to geochemically compare mineralised and barren dykes for exploration benefit. Petrographical analysis has been utilised to define textural and mineralogical properties of each of the field and drill core samples, which together with geochemical data, have been used in attempt to discriminate separate intrusive events. Additionally, geochronological U-Pb dating of hydrothermal apatite and titanate has constrained ages of alteration and mafic intrusion within the Eastern Succession and may have implications for mineral exploration.

# 2 GEOLOGICAL SETTING

## 2.1 Regional Geology

The Mt Isa Inlier can be split into 3 major geological zones; The Western Succession, Kalkadoon-Leichardt belt and The Eastern Succession (Blenkinsop et al., 2008). All of these zones contain a variety of lithologies including; deformed basement rocks, sedimentary packages including calc-silicates, turbidites, carbonates, shales, and quartzites, pre- and syn-depositional bi-modal volcanics, I- to A-type granitic intrusions and widespread mafic intrusions (Foster & Austin, 2008; Young & Lane, 2015).

Basement rocks and overlying sedimentary packages have been assigned to one of three unconformity bound cover sequences (Betts et al., 2007) as shown in Figures 1 and Figure 2.

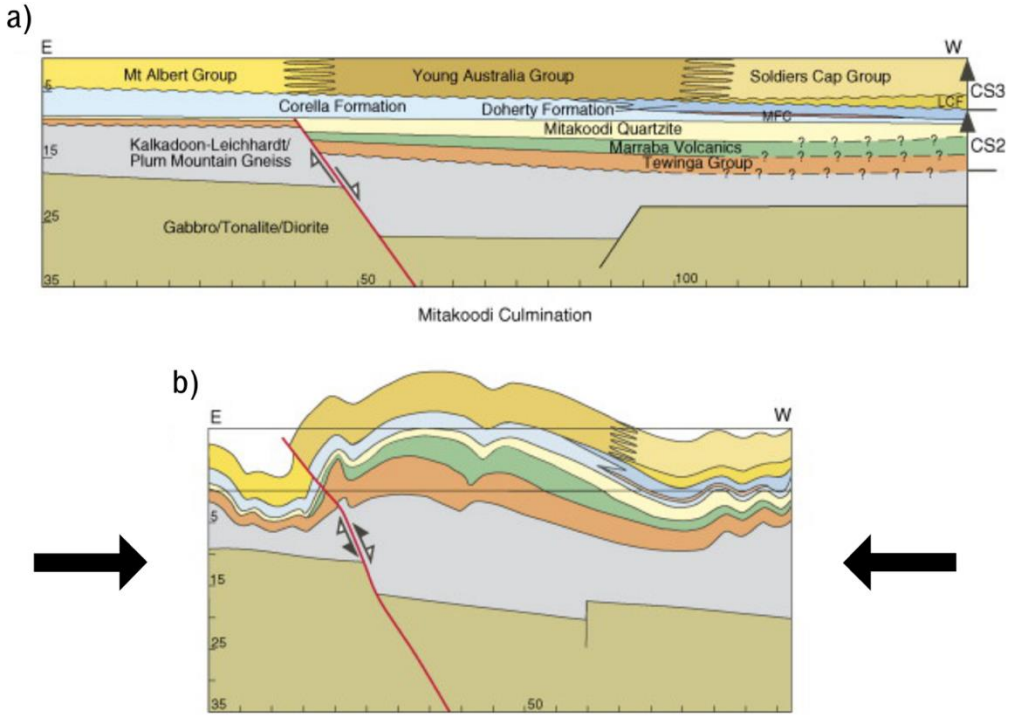


**Figure 1. A cartoon taken from Foster & Austin (2008), and modified by Blenkinsop et al. (2008) showing a) The cover sequences within the Eastern Succession with extensional faults and b) The East-West compressional basin inversion and the reactivation of faults. Mafic dykes cross-cut all of these units.**

Initial deformation of the Mount Isa Inlier, known as the Barramundi Orogeny (1800 Ma), records the final stages of continental growth in the North Australian Craton. This was followed by tectonic extension and the formation of the intraplate Leichardt, Calvert and Isa superbasins (Foster & Austin, 2008; Betts et al., 2007; Abu Sharib & Sanislav, 2013). Over the next ~200 Myr these basins underwent sedimentation, elevated heat flow, magmatism and repeated extension and contraction (Betts et al., 2007).

Basin inversion and associated metamorphism (ca. 1600-1500 Ma) affected the inlier on a crustal scale (Blenkinsop et al., 2008) and caused the cessation of sedimentation. The

period of high temperature (>650°C) metamorphism and crustal accretion has been termed The Isan Orogeny (Foster & Austin, 2008; Betts et al., 2007) and has been confined to two possible events; 1) N-NW shortening due to thin skinned flat slab subduction (1600-1580 Ma) and 2) the thick skinned continent Laurentia colliding with the Australian plate causing basin closure (1550-1500 Ma) (Oliver et al., 2008; Abu Sharib & Sanislav, 2013). Large scale normal faults that formed during extension were reactivated during this contraction, providing potential pathways for magmatic intrusions (Blenkinsop et al., 2008) (Figure 1).

## 2.2 Alteration

The Eastern Succession of the Mount Isa Inlier is a classic example of crustal scale metasomatism (Betts et al., 2007) with many styles of alteration and subsequent mineralisation represented, hosting Cu, Au, Pb, Zn, Co, Mo, Fe, U and REE deposits (Pollard, Mark, & Mitchell, 1998).

Paragenetically early alteration include regional Na(-Ca) events, which took place over several periods, with the earliest dated to 1750-1730 Ma (Betts & Giles, 2006). The second regional Na (-Ca) event is related to the alkaline to subalkaline granitic intrusions of the ca. 1550-1500 Ma Williams-Naraku Batholith (Oliver et al., 1985: Wyborn, 1998: Baker et al., 2010). This event was then oveprinted by local K-Fe enrichment (Wyborn, 1998: Mark et al., 2006). The general element fluxuation of the Eastern Succession includes an increase in K, Rb and Ba with a decrease in Na, Ca, Sr, P and Y (Mark et al., 2006).

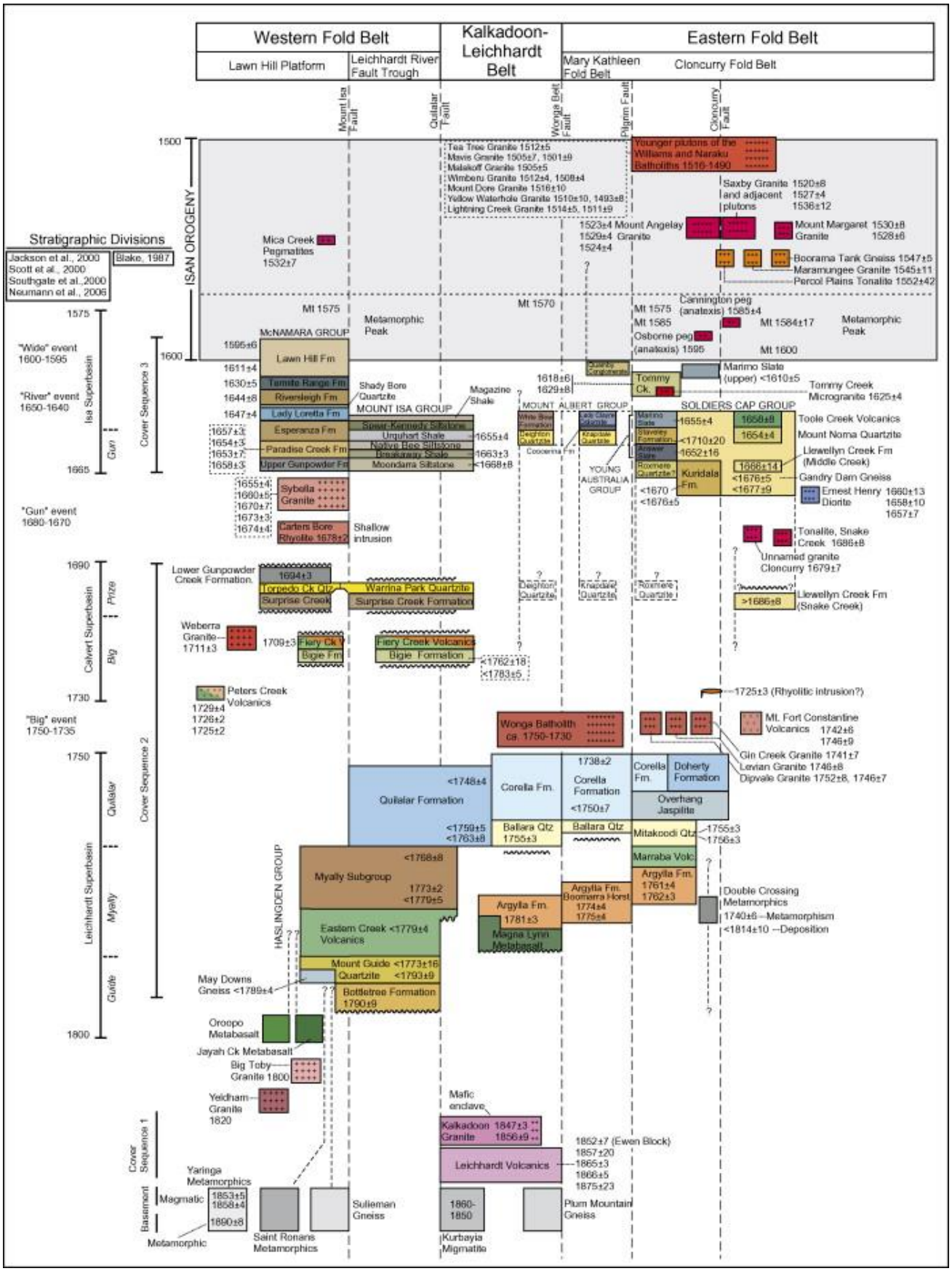


**Figure 2. A chronostratigraphic history of the Mount Isa Inlier (Foster & Austin, 2008). The mafic dykes that are the subject of this thesis are noticeably absent from this diagram and have yet to be ascribed to a cover sequence.**

Previous paragenetic studies of the GATPMM Trend have indicated a complex alteration history (Taylor, 2013). Initially, mafic rocks in the area were proposed to be abundant in plagioclase, ferromagnesian minerals such as pyroxenes and disseminated Fe-Ti-oxide minerals such as titanite-magnetite (Taylor, 2013). Amphibolite facies metamorphism and proceeding alteration in this area altered the plagioclase feldspars to albite, the pyroxenes to amphiboles (actinolite and hornblende) and overprinted these minerals with a range of alteration minerals including (but not limited to); magnetite, scapolite, sericite, biotite, chlorite, quartz, carbonates and epidote (Taylor, 2013). Figure 3 shows the interpereted paragenetic sequence of alteration related minerals within the GATPMM Trend.

| Great Australia Mine (GAM) Alteration Paragenetic Sequence | |
|---|---|
| Alteration Sequence | Characteristics |
| 1. Magnetite (Titanite) | Early Na-Ca related |
| 2. Biotite | K-Fe related |
| 3. Albite-Scapolite | Coarse grained and hydrothermal |
| 4. Amphibole (Carbonate – Quartz) | Hydrothermal origin |
| 5. Pyrite- Chalcopyrite- Carbonate | Cu-Co mineralising Stage |
| 6. Epidote-Chlorite-Apatite | Retrograde stage |

**Figure 3. The paragenetic sequence stages based upon Taylor (2013), with an interpreted general decrease in temperature with time.**

## 2.3 Cloncurry Dolerites

Limited previous research on the mafic intrusives of the Mount Isa Inlier have found that they generally range from amphibolite grade facies to unaltered dolerites (Ellis & Wyborn, 1984: Carter et al., 1961: Blake, 1987). Dolerites have previously been grouped

according to their relative levels of alteration and/or metamorphism, textural and mineralogical characteristics, with Carter et al. (1961) suggesting 8 groups of dolerite-metadolerite and Ellis & Wyborn (1984) proposing 4 groups of dolerite dykes in the Eastern Succession. Mafic intrusions in the Mount Isa Inlier in general are noted to be emplaced within structural traps such as faults and fold crests (Carter et al., 1961), to be tholeiitic in composition with 10-20% $Fe_2O_3$ content (Oliver et al., 2008) and are interpreted to have formed over a <600 Ma period (Blake, 1987).

The youngest intrusive age recorded is 1116±12 Ma, dated from Rb-Sr isotopes (Page, 1983) and the oldest date via field relationships is pre-1880 Ma (Carter et al., 1961). However, some dating methods may be unreliable due to hydrothermal alteration and post-metamorphism thermal spikes. Spikings et al. (2001) recorded four separate rapid cooling events within the Eastern Succession, from 1490-1410 Ma, 1280-1050 Ma, 740-640 Ma and 600-500 Ma based upon $^{40}Ar/^{39}Ar$ data of hornblende, biotite, muscovite and alkali-feldspar. Temperatures of >300ºC were reached in the first two thermal spikes potentially affecting mineral closure temperatures and in turn geochronological studies (Spikings et al., 2001).

The dykes in the area of this study cross cut all existing lithologies, except for the Williams and Naraku Batholith (Foster & Austin, 2008), consistent with the interpretation that they are one of the final lithologies accreted within the Eastern Succession. Mafic dykes can form in a number of tectonic regimes including; extensional, back arc, subduction and post-collisional settings. (Goldberg, 2010; Scarrow et al., 1998; Khan et al., 2007; Williams et al., 2001). However, intraplate rifting and extension is a favoured

environment for the formation of the mafic dykes of the Eastern Succession (Abu Sharib & Sanislav, 2013). A recent seismic line (Korsch et al., 2012) provides evidence for a possible suture zone for a westward subducting slab, which has been proposed previously as the driving factor for the Mount Isa Inlier formation and basin closure (Oliver et al., 2008, Betts et al., 2007, Gibson et al., 2008). The Mount Isa Inlier is proposed to have once been a continental margin, undergoing a complex history of extension, contraction and subduction (Korsch et al., 2012; Korsch & Doublier, 2016; Gibson et al., 2016). The previously studied mafic dykes are believed to be emplaced during pre- (ca. 70 Myr) and syn-contractional tectonism of the Isan Orogeny (Abu Sharib & Sanislav, 2013; Gibson et al., 2008).

# 3 METHODS

## 3.1 Fieldwork and Sampling

17 mafic intrusive rock chips (D01 to D18, with D12 excluded) were collected from the GATPMM trend for analysis (locations displayed in Figure 4). Samples were collected from known ore deposits and Mount Isa Mines Resource Development prospects including Mt Glorious (D01), Eternal (D02), Fifi (D03), D-Ring (D04), Walton (D05, D07, D08), Wilgar (D06) Remedy (D09, D10), Monakoff (D11), Battleaxe (D13, D14) Tapian (D15) and Mongoose (D16, D17, D18) (Figure 4). Samples were collected from mafic outcrops using a sledgehammer or geological pick and placed into marked calico bags. Sample locations were entered into a Garmin GPSMap 62s handheld GPS, with AGD-84 54K UTM zone co-ordinate system. Fresh samples were selected from the outcrops where possible.

Six dolerite drill core samples were also collected from diamond drill hole DODH068 (Las Minerale trend) of CuDECO's Rocklands Operation, where mineralization is closely associated with dolerites. Samples were taken at 52m and 59m (above ore zone), 115m and 121m (within ore zone) and 151m and 173m (below ore zone). Approximately 30cm length of quarter core was placed into calico bags and marked accordingly. For both field and CuDECO samples, a thin section was made by Ingham Petrographics, QLD for petrographical analysis.

A total of 90 reverse circulation (RC) drill samples were also sampled. The drill samples were collected during exploration drilling at Battleaxe, CHUM, Double Oxide, Magpie, Thebe and Turf Club prospects in 2014 and are representative of the mineralised dolerites encountered in the Cloncurry district (Figure 4). The original RC samples were collected from 1m composite RC sample bags, with spear sampling of the bags completed at 2m intervals. The samples were originally assayed by ALS Townsville in 2014 for analysis suite of major and trace elements. The remaining laboratory pulps were resampled for this project. A spoonful of each pulp sample was placed into a zip-lock sample bag, with a duplicate samples and a standard (OREAS45d) inserted every 15 samples.

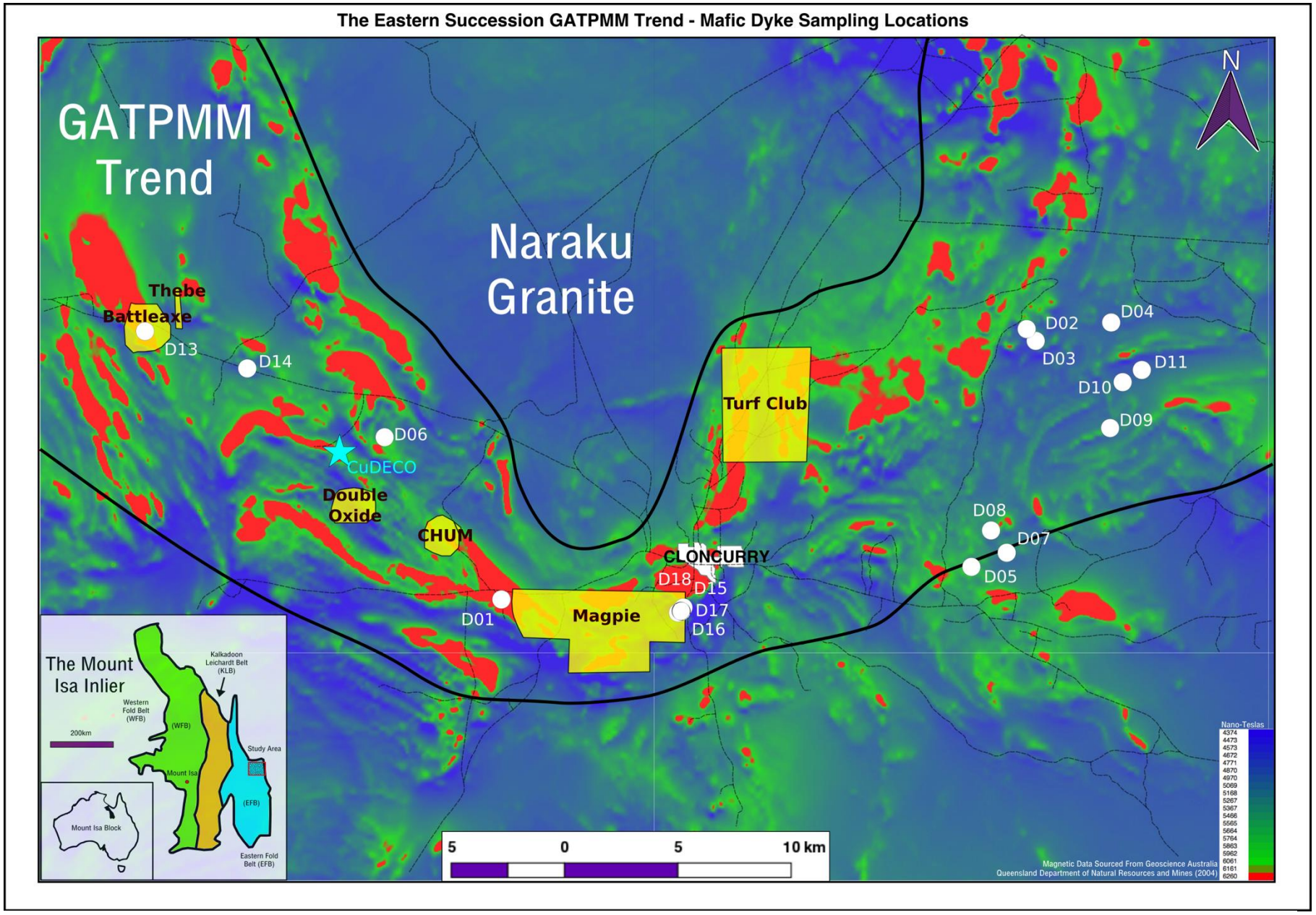


**Figure 4. A magnetics density map with locations of field samples (white circles), CuDECO Rocklands Las Minerale open pit (blue star) and sampled pulp drilling fields (Richardson, 2003). Inset is a simplified cartoon of the 3 geological zones within The Mount Isa Inlier.**

### 3.2 Petrological Analysis

Initial lithological and mineralogical analysis of all samples was completed using a hand lens and a scribe, with field and sample images taken from an 8 megapixel iPhone 6 camera. An Olympus BX-51 Research System Microscope, along with an external Olympus BX-UCB light source was utilized for optical petrography analysis of all thin sections. Transmitted light through both a cross polarizer and a plane polarizer was used to identify the main constituent minerals, while reflected light was used to differentiate sulphides and opaque minerals within the CuDECO thin sections. Petrographical images were taken using the Olympus DP21 camera system.

Four CuDECO thin sections (D20, D21, D22 and D23) were carbon coated and underwent analysis within the FEI Quanta 600 MLA Scanning Electron Microscope (SEM) at Adelaide Microscopy. Spectrum peak analysis was used to determine elemental compositions of specific minerals with back scatter electron (BSE) images of samples also taken.

### 3.3 Geochemical Analysis

All samples, including hand sample, drill core and pulp samples, were sent to Australian Laboratory Services (ASL), Townsville, for geochemical analysis. Analysis included Inductively Coupled Plasma – Mass Spectrometry (ICP-MS) and Inductively Coupled Plasma –Atomic Emission Spectrometry (ICP-AES) on instrumentation ME-MS61 and ME-MS81, with additional with X-ray fluorescence spectrometry (XRF) on instrumentation ME-XRF06 (ALS Minerals, 2006b). Major element oxides of field and CuDECO samples (D01-D24) were analysed by ME-XRF06, after being crushed, ignited,

fused with a lithium borate flux and moulded into a disk. Trace element and rare earth element (REE) compositions of field and CuDECO samples were analysed by a combination of ME-MS61 and ME-MS81. Initially a portion of the sample was fused with a lithium borate flux at 1000$^{o}$C before being dissolved with $HNO_3$ and $HCl_3$ concentrate, the solution was then analysed by ICP-MS. Any remaining concentrate that was not analysed (base metals and sulphides) was diluted again and run through either ICP-MS or ICP-AES (ALS Minerals, 2006a; ALS Minerals, 2009). Unfortunately, due to unsatisfactory portion amounts, samples D10, D14 and D24 could not be analysed for REE. Major element and trace element concentrations for all pulp data was analysed by ME-MS61 after being portioned, dissolved by nitcric, hydrofluoric, hydrochloric and perchloric acids (4-acid digest) and then diluted to create an analysable concentrate. Similarly, to ME-MS81, if base metals and sulphides were not being sufficiently analysed, diluted hydrochloric acid was added and ICP-MS was run again. All samples and concentration data was received in excel spreadsheet format for data processing. A quality assurance and quality control report was completed to determine accuracy of instrumentation (Appendix 2).

### 3.4 Geochronology

Two field samples were chosen for U-Pb dating (D16 and D18 from Mongoose). Samples were selected as having the highest Zr concentration as determined by spot-analysis using the Olympus Delta 50kV Premium on site in Cloncurry. Following Payne et al. (2008), samples were crushed, milled and sieved between 79um – 400um mesh before undergoing panning, heavy liquid separation and Frantz magnetic separation. The remaining ‘heavy’ portion of the sample was viewed under an Olympus SZ61 binocular microscope for grain picking and selected grains were placed upon an teflon mount and

set in epoxy resin. The set blocks were polished, carbon coated and mineralogy was confirmed using the FEI Quanta 600 MLA Scanning Electron Microscope (SEM) at Adelaide Microscopy. The grains were a combination of hydrothermal apatite and titanite that were mapped using BSE images. Both apatite and titanite grains, ranging 50-200 micron (Figure 5) had abundances of $Si^{28}$, $Cl^{35}$, $Ca^{43}$, $Ti^{49}$, $Zr^{91}$, $Hg^{202}$, $Pb^{204}$, $Pb^{206}$, $Pb^{207}$, $Pb^{208}$, $Th^{232}$ and $U^{238}$ analysed by the Agilent 7700S with ASI M-50 laser ablation system (ICP-MS). Standards for both minerals were used to account for common $Pb^{207}$ concentrations, downhole fractionation and instrument drift. Apatite, standards were NIST610 glass, Madagascar Apatite, Mt McClure apatite and Durango apatite. Titanite standards were NIST610 glass, GJ-1 zircon and Khan titanite. Elemental concentrations and ratio data was exported as comma separated value (.csv) files.

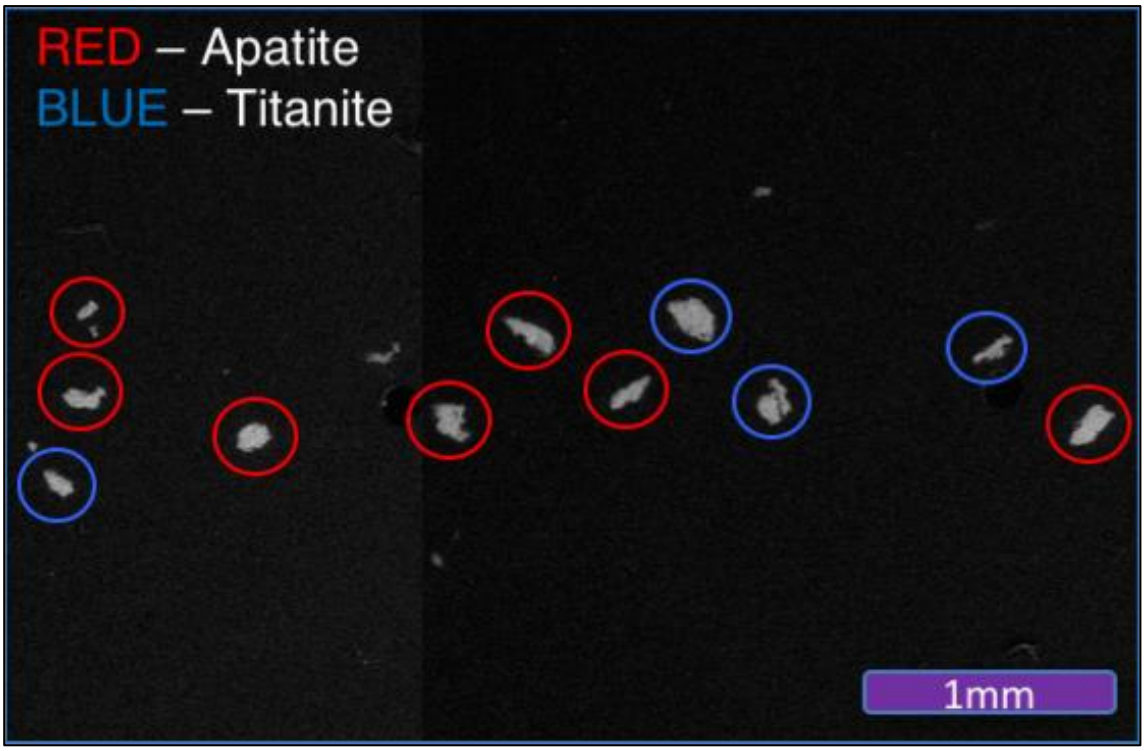


**Figure 5. The textures and form of hydrothermal titanite and apatite within sample D16 from Mongoose. Back scatter electron image taken using the SEM Quanta 600 at Adelaide Microscopy.**

### 3.5 Data Processing

GPS files were opened and mapped in QGIS 2.14, with additional magnetic and infrastructural data sourced from the Queensland Government (Richardson, 2003). Maps were exported and customized in Inkscape-XQuartz 2.7.9.

Geochemical data files were first imported and re-arranged in Microsoft Excel 2016, before being imported into ioGAS 6.1. Negative or zero quantities were given null values, and major element oxides were normalized due to loss on ignition (LOI) percentages to account for loss of water within minerals. Bivariate and spider plots were drafted in excel while discrimination diagrams were plotted in ioGAS using existing diagram templates. All ioGAS plots were customized as scalable vector graphics (SVG) files in Inkscape-XQuartz 2.7.9.

Geochronological data files were imported into Igor-Iolite version 3 to be normalised to Madagascar (apatite) and GJ-1 (titanite) and corrected for common Pb. The U-Pb data reduction scheme VizualAge_UcomPbine was incorporated following Chew et al. (2014). They were then exported as a metadata file, before being manipulated within the excel add-in Isoplot 4.0. All geochronological related diagrams or figures were imported and customized in Inkscape-XQuartz 2.7.9.

## 4 OBSERVATIONS AND RESULTS

### 4.1 Petrology

Samples were collected from isolated, small outcrops that were commonly <5m wide and <20m long, with the result that lithological contacts and relationships were difficult to

establish in the field. However, mafic dykes were observed intruding through multiple units including Mount Norna Quartzite and Toole Creek Volcanics of the Soldiers Cap Group, Calc-Silicates of the Corella Formation, Mitakoodi Quartzite, and various granites. The intrusions are commonly associated with faults or lithological contacts (Foster & Austin, 2008) (Figure 1).

### 4.1.1 GRAIN SIZE AND TEXTURES

Field samples range from basaltic to gabbroic in texture with varying grain sizes recorded from 0.05mm to 6mm (Figure 6). Several samples (D02, D09, D10 and D13) display an apparent orientated foliation. Some samples (D01, D02, D09, D11, D13, D15 and D16) display veining and fracturing with a variety of different mineral infill, while some samples (D06, D07, D15 and D17) have poryphyroblastic textures. Sample D04 is petrographically unique as it is apparently unaltered, displaying plagioclase, orthopyroxene and lamellae textured clinopyroxene (Figure 7I).

### 4.1.2 MINERALOGY

Minerals common within most samples include albitic plagioclase, actinolite, hornblende, magnetite, scapolite, biotite, chlorite, epidote with minor titanite, apatite, pyrite, pyroxenes and quartz. Within the coarse grained samples, albite is generally present as elongated, bladed crystals, surrounded by irregular anhedral hornblende and actinolite grains. The fine grained samples generally have little to no visible albitic plagioclase and contain abundant epidote and hydrous minerals (biotite, chlorite and hornblende). Where present, porphyroblasts are composed of albite, epidote, chlorite and scapolite.

Petrographical analysis indicates that these rocks were originally composed of abundant plagioclase, intergrown with ferromagnesian minerals such as clinopyroxene and Ti-Fe oxide minerals such as titanite or magnetite, before being altered to their current mineralogy. This interpretation is consistent with the previously mentioned paragenetic history of the Cloncurry District (Taylor, 2013).

### 4.1.3 ALTERATION

All field samples show an extensive and complex alteration history, with the exception of sample D04, which has only been affected by weak sericitic alteration (Figure 7I and 7J). Magnetite is a common alteration product in all samples, regularly associated and intergrown with titanite. It is most commonly seen altering along hornblende or pyroxene cleavages as seen in Figure 7B, but is also disseminated within the foliated fabrics of finer-grained samples (Figure 7H). The abundance of biotite alteration varies between samples but is considered to be of retrograde origin in the fine grained samples (Figure 7G), whereas coarse grained samples show biotite altering from amphiboles (Figure 7F). Plagiolcase has been altered to albite, and then continued to be affected by sericitic (white mica) alteration and scapolite alteration. Scapolite alteration occurs along the boundary of albite grains, and within twinning planes and fractures (Figure 7A). Clinopyroxene within coarse grained samples alters to green amphiboles such as hornblende and actinolite, an observation that is consistent with the interpretation that the abundance of hornblende is because of alteration of ferromagnesian pyroxenes. Epidote alteration is the most prominent late-stage alteration in fine grained metamorphosed samples, overprinting retrograde chlorite-biotite-actinolite fabrics and disseminated quartz grains (Figure 7D and 7E). Apatite appears to be coeval with the epidote stage alteration appearing in most samples as euhedral hexagonal grains. Veins and fractures within all

samples are generally carbonate rich with occasional quartz and albite association, except for sample D15, which contains a hornblende-chlorite vein hosting sulphides such as pyrite

The alteration paragenesis for the suite of field samples can be compared to that of Taylor (2013). The relative intensity of each alteration stage varies significantly between all samples, with the albite-scapolite stage being the most intense within the sequence. Not all samples are affected by every alteration stage illustrating that structural localisation of alteration fluid pathways is an important factor, particularly with regard to the sulphide mineralization stage, represented in samples D13 and D15.

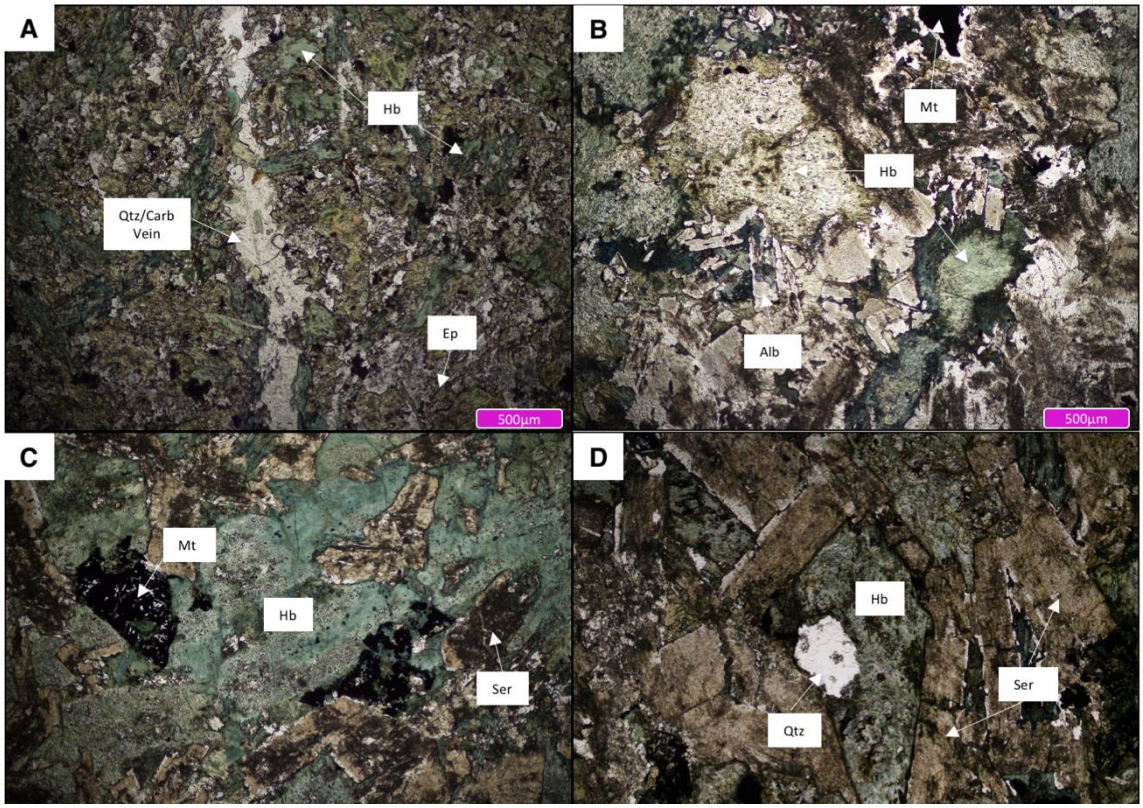


**Figure 6. Representative XPL images of the varying grain size within the mafic samples. Diagram A) shows a finer grained sample (D11), with the higher abundances of epidote and hydrous minerals, B) medium grained dolerite (D18) with a combination of albite and sericite altered albite, C) gabbro (D07) with magnetite and sericite alteration and D) gabbro with the largest grain size within the suite (D13).**

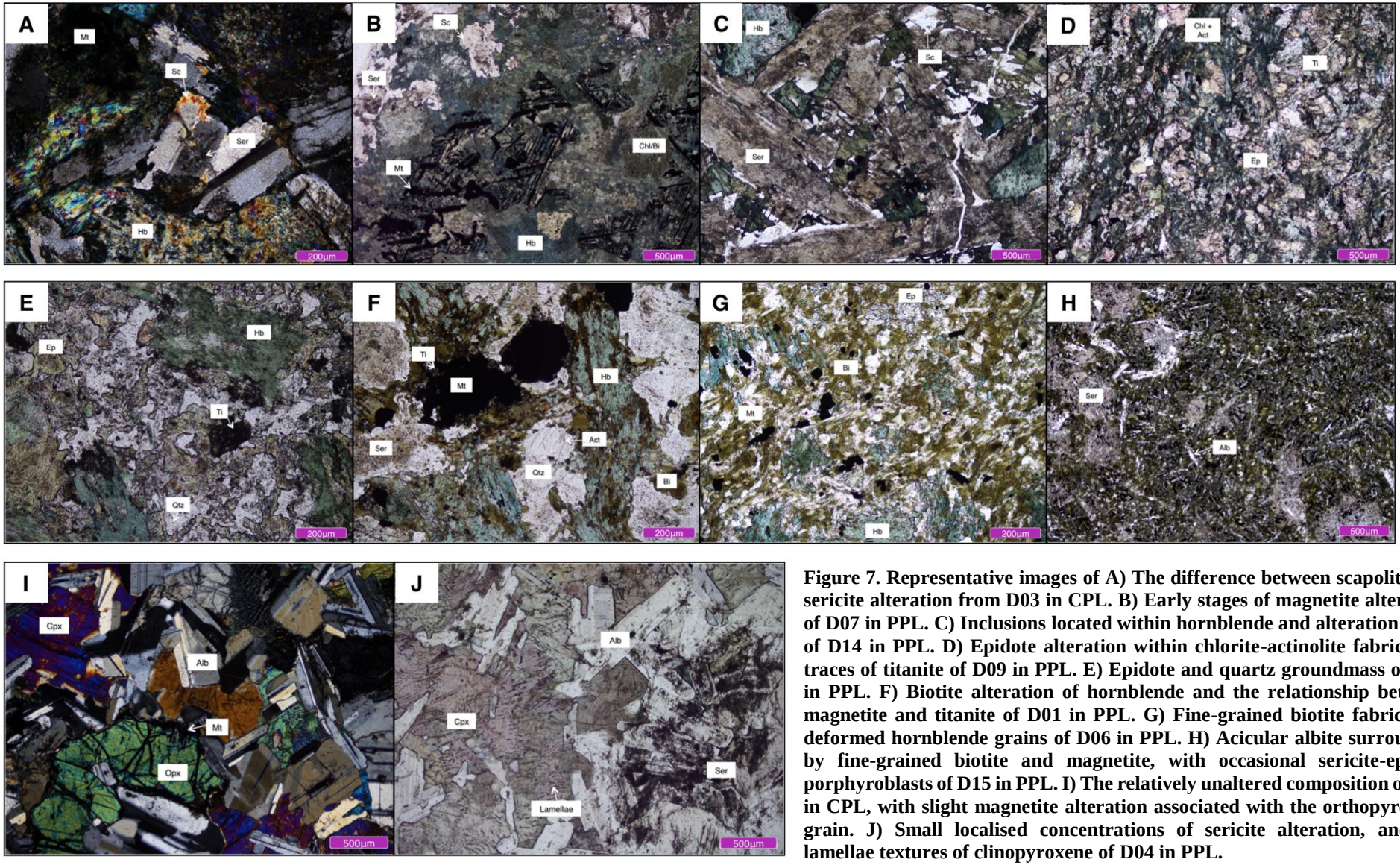


**Figure 7. Representative images of A) The difference between scapolite and sericite alteration from D03 in CPL. B) Early stages of magnetite alteration of D07 in PPL. C) Inclusions located within hornblende and alteration types of D14 in PPL. D) Epidote alteration within chlorite-actinolite fabric with traces of titanite of D09 in PPL. E) Epidote and quartz groundmass of D11 in PPL. F) Biotite alteration of hornblende and the relationship between magnetite and titanite of D01 in PPL. G) Fine-grained biotite fabric with deformed hornblende grains of D06 in PPL. H) Acicular albite surrounded by fine-grained biotite and magnetite, with occasional sericite-epidote porphyroblasts of D15 in PPL. I) The relatively unaltered composition of D04 in CPL, with slight magnetite alteration associated with the orthopyroxene grain. J) Small localised concentrations of sericite alteration, and the lamellae textures of clinopyroxene of D04 in PPL.**

**Key: Mt-Magnetite, Ser-Sericite, Sc-Scapolite, Hb-Hornblende, Bi,-Biotite Chl-Chlorite, Act-Actinolite, Ti-Titanite, Ep-Epidote, Qtz-Quartz, Alb-Albite, Cpx-Clinopyroxene (Augite) and Opx-Orthopyroxene.**

### 4.1.4 CUDECO PETROLOGY

The six dolerite samples from CuDECO Rocklands Las Minerales ore zone host chalcopyrite-carbonate bearing veins and associated disseminated mineralization (Figure 8). The mineralised dolerites are mainly comprised of albitic plagioclase, sericite, hornblende, chlorite, biotite, actinolite, magnetite, pyrite and chalcopyrite with accessory titanite, apatite, calcite and epidote. Average grain size varies from 0.5mm (D20) to 2mm (D22) over a distance of <100m, possibly indicating more than one generation of dolerite is present. Plagioclase is yellow in CPL and ranges from relatively unaltered (D23) to sericitic albite (D24) with biotite inclusions. Hornblende is also observed altering to biotite in most samples. The two samples within the ore body contain no significant hornblende and are dominated by bioitite. Late stage barite-biotite veins were identified through SEM analysis of the samples along with Cu-sulphide hosted quartz-carbonate veins (Figure 8G and H), which is consistent with other district deposits (Williams et al., 2015). Chalcopyrite, hosted within quartz-carbonate veins, is the main economic sulphide mineral, with trace amounts of galena, molybdenum and native Au also present.

The paragenetic sequence of the CuDECO dolerites is similar to that of the field samples and Great Australia deposit (Taylor, 2013). However, epidote-chlorite alteration and late stage biotite-barite veins are not observed at Great Australia.

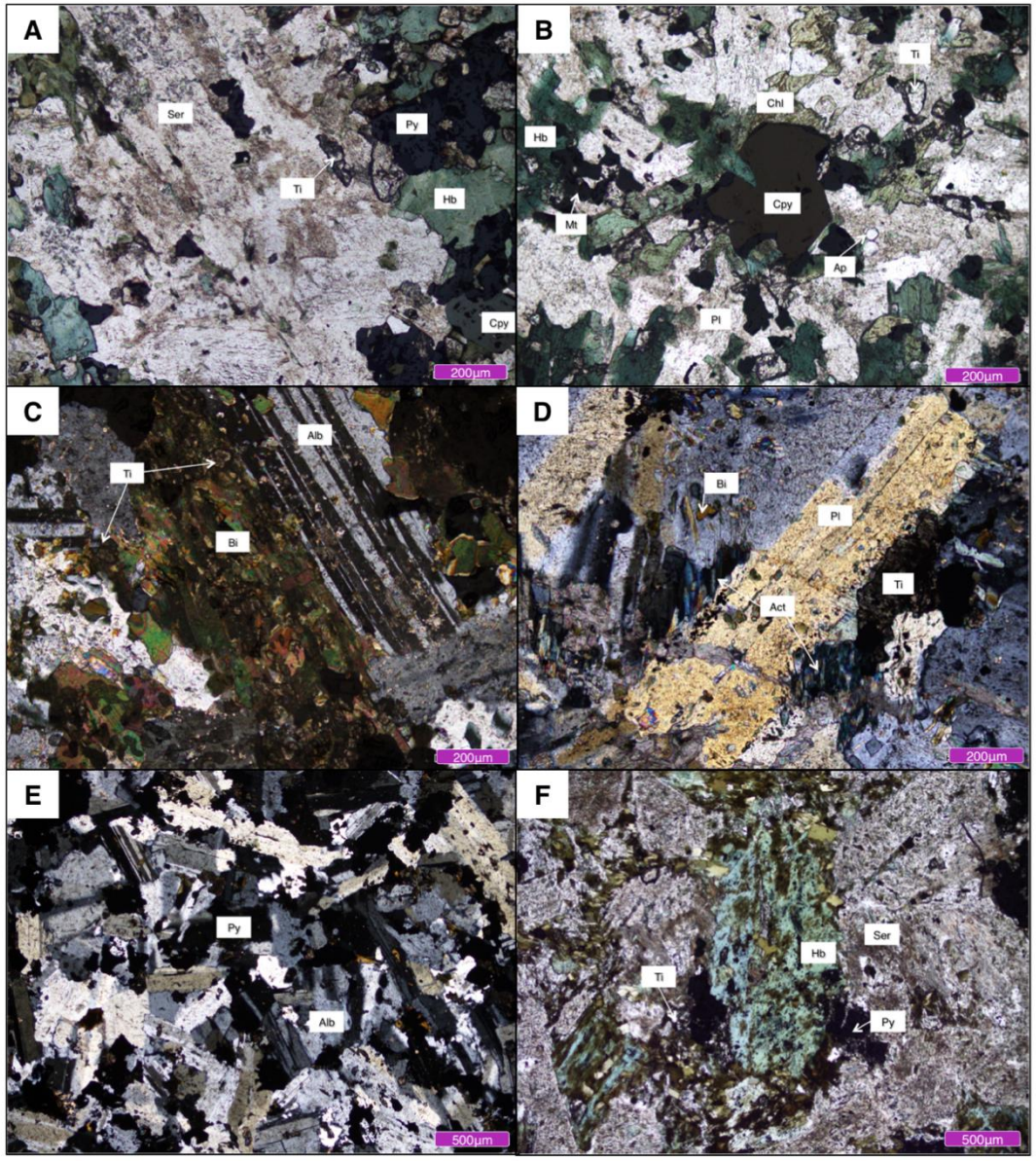


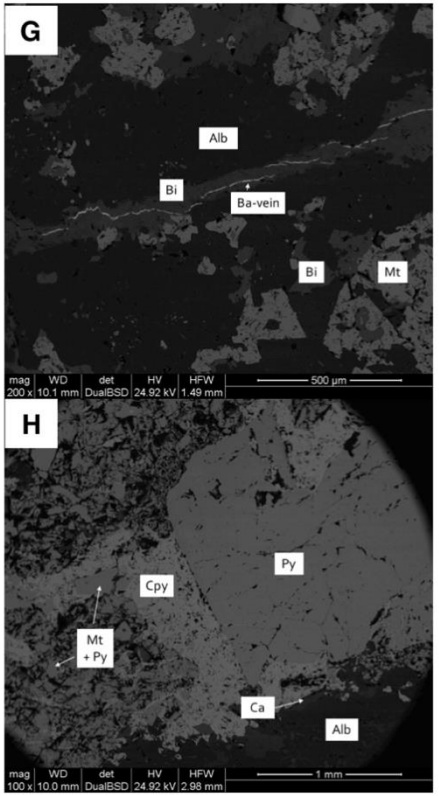


**Figure 8. Representative images of A) Moderate levels of sericite alteration and hornblende dominated D19 in PPL. B) Disseminated chalcopyrite mineralisation associated with titanite and apatite of D20 in PPL. C) Albite and late stage biotite with titanite inclusions of D21 in CPL. D) Yellow-blue coloured plagioclase with inclusions and needle-like actinolite of D22 in CPL. E) The relatively unaltered composition of D23 in CPL and F) The alteration of twinned hornblende to biotite along fractures of D24 in PPL. G) Late stage barite-biotite veining in sample D23. H) Sulphide mineralisation of pyrite and chalcopyrite with magnetite within a carbonate vein.**

**Key: Mt- Magnetite, Ser-Sericite, Sc-Scapolite, Hb-Hornblende, Bi,-Biotite, Act-Actinolite, Ti-Titanite, Ap-Apatite, Ep-Epidote, Qtz-Quartz, Pl-Plagioclase Alb-Albite, Cp-Chalcopyrite and Py- Pyrite.**

## 4.2 Geochemistry

### 4.2.1 MAJOR ELEMENTS

Field samples have a wide range in major oxide compositions, including $Fe_2O_3$ (3.62-22.7 wt%), $TiO_2$ (0.42-3.5 wt%), CaO (2.8-17.9 wt%), $SiO_2$ (41.3-52.9 wt%) and especially alkalies (0.21-8.3 wt%) with lesser variance in oxides such as $Al_2O_3$ (11.9-16.9 wt%) and MgO (1.64-9.3 wt%). The chemical composition of all the samples are considered tholeiitic (Figure 9A) (Irvine & Baragar, 1971; Kuno, 1968) with the majority of field samples plotting as a basalt, and others plotting as either picrobasalt, trachybasalt or basalt-andestite (Figure 9B) (Le Maitre et al., 1989). Sample D08 and D09 are compositionally defined as picrobasalt, with D08 being the most abundant in $Fe_2O_3$ (22.7 wt%) and $TiO_2$ (3.48 wt%), and D09 sharing the same high $Fe_2O_3$ characteristic (18.2 wt%). Sample D15 is classified as a trachybasalt and contains the lowest CaO value (2.8 wt%) and the highest K2O value (5.1 wt%). D10 is classified as the basalt-andesite and retains a low MgO (1.6 wt%) and $Na_2O$ (0.25 wt%) but also has the highest $SiO_2$ (52.9 wt%) concentration. The loss on ignition (LOI) ranges from 0.41 wt% in unaltered sample D04, up to 2.55-3.82 wt% in the fine grained epidote altered samples D09, D10 and D11.

Bi-variate diagrams are used for both major oxides and trace elements to determine any magmatic differentiation trends within the suite of rocks studied. In Figure 10, major oxides of field and RC samples are plotted against MgO with underlying data of mid ocean ridge basalt (MORB), back arc basin (BAB) and the Red Sea Rift for geochemical comparison (Melson et al., 2002; Sarbas, 2008; GEOROC, 2016). The plots show significant scatter in the MgO vs $SiO_2$, CaO and alkalies but a generally linear relationship

on MgO vs $Al_2O_3$, $TiO_2$ and $P_2O_5$ plots, with significant correlation to the values of MORB. Due to the high mobility of these major elements and the alteration affects seen in the petrographical results, these bi-variate plots are not an accurate representation of magmatic differentiation.

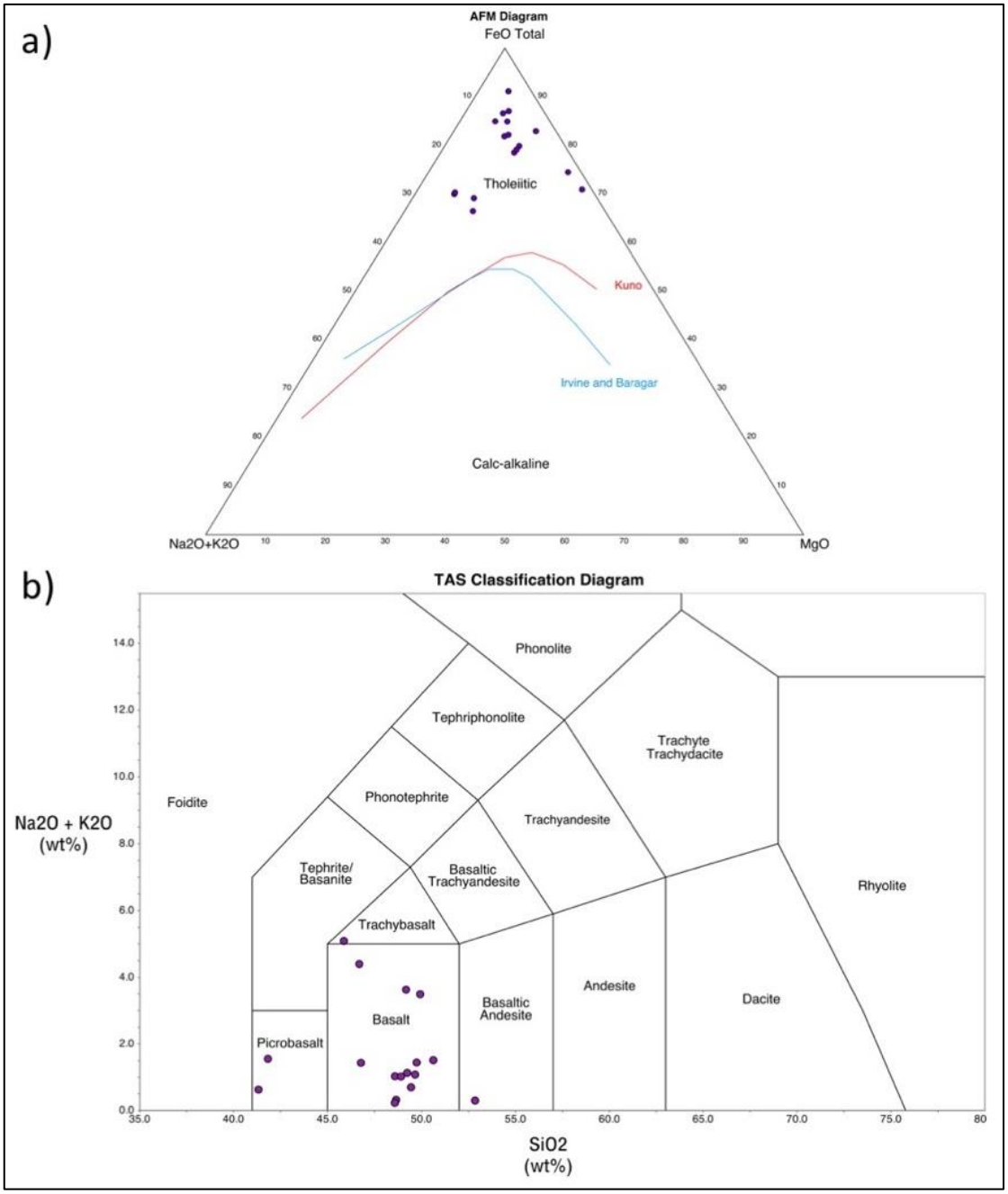


**Figure 9. a) The AFM diagram of Kuno (1968) and Irvine & Baragar (1971), displaying that the field samples (purple circles) are highly tholeiitic and b) the TAS diagram of Le Maitre et al. (1989) indicating samples are generally basaltic in composition.**

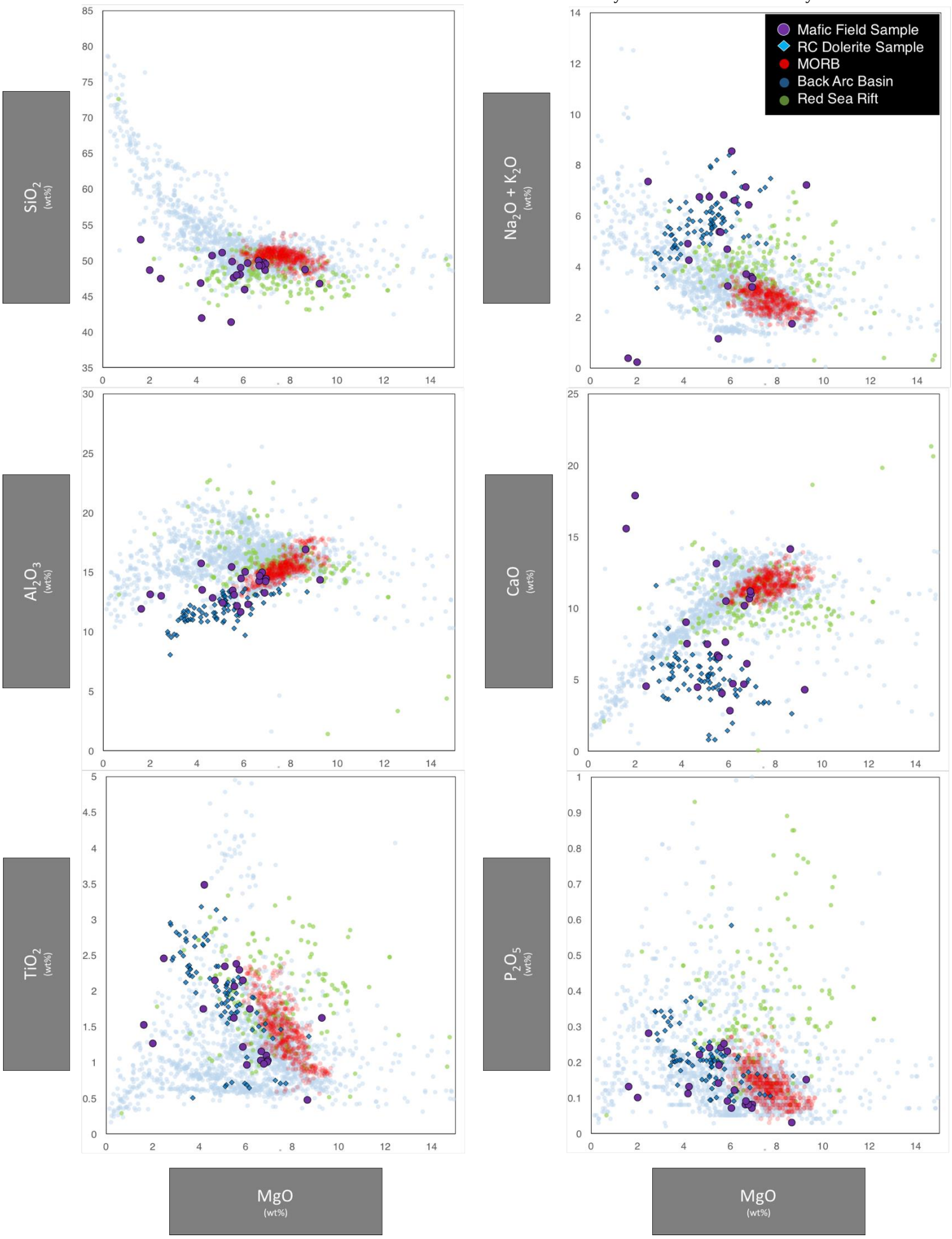


**Figure 10. Bi-varite plots of major element oxides.**

### 4.2.2 TRACE & RARE EARTH ELEMENTS

Trace elements are considered to be the best geochemical proxy for identifying magmatic evolution due to their immobility during post-magmatic events, such as the alteration and metamorphism (Pearce, 2008). Trace elements plotted against immobile element Zr display a large variation in concentration with a positive correlation between most immobile elements (Figure 11) and unaltered sample D04 having the lowest concentrations. Significant scatter is noticeable in Rb vs Zr due to Rb mobility during alteration. All plots show varying comparisons to the underlying fields of MORB, BAB and Red Sea Rift, but generally follow the same trend as MORB. Mobile transition metals Ni and Cr have been plotted against immobile element Y following DeLong & Chatelain, (1989) (Figure 12a and b), with the inclusion of RC pulp samples, displaying a linearly decreasing trend. There is a noticeable exponential curve to the data trend, indicative of a differentiating liquid composition during fractionation (Rollinson, 2003). A Th/Ta vs La/Ta diagram (Figure 13) following Srivasta et al. (2014a) shows the majority of samples plotting with similar values to the lower crust (Rudnick & Gao, 2003). Ba, Rb K, Pr, Sr, and Mo display large variances in concentration because of alteration and have not been plotted on any discriminating diagrams, (Figure 14).

Pearce's (2008) Th/Yb vs Nb/Yb discrimination diagram, which uses Nb anomalies to determine subduction related tectonic regimes, is used to split the samples into two separate groups (Figure 15). From here a different colour scheme will be incorporated to distinguish groups. Samples in Group 1 (THEBE2-4, D01, D02, D03, D13, D15, D16,

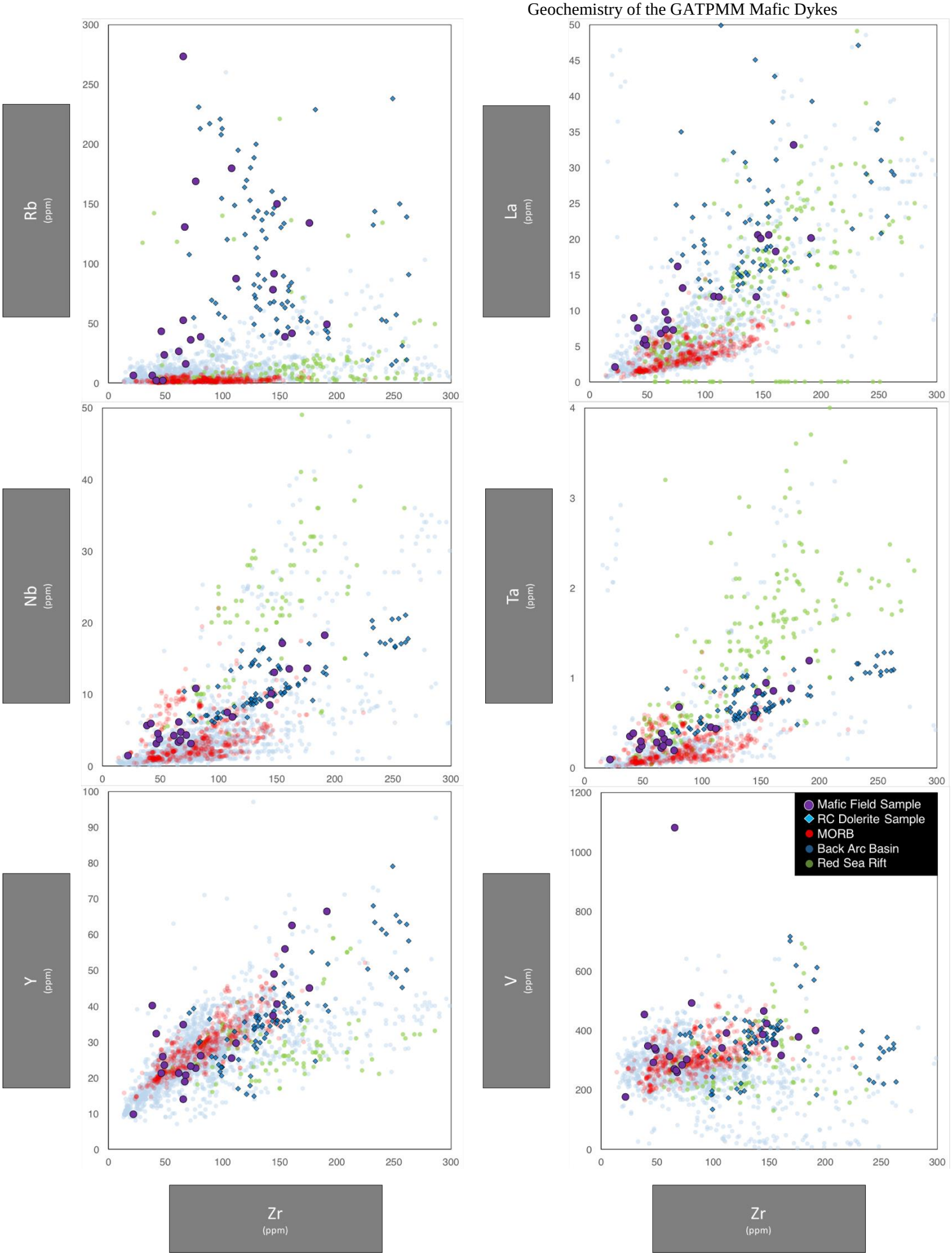


**Figure 11. Bi-variate plots of trace elements.**

D17 and D18) are coloured green and plot within the mixed field of continental arc and oceanic arc, with Group 2 (THEBE5, D04, D05, D07, D08, D09 and D11), coloured pink, plotting with the lowest Th/Yb ratio. Sample D06 and THEBE1 are not assigned to a group due to their outlier characteristics.

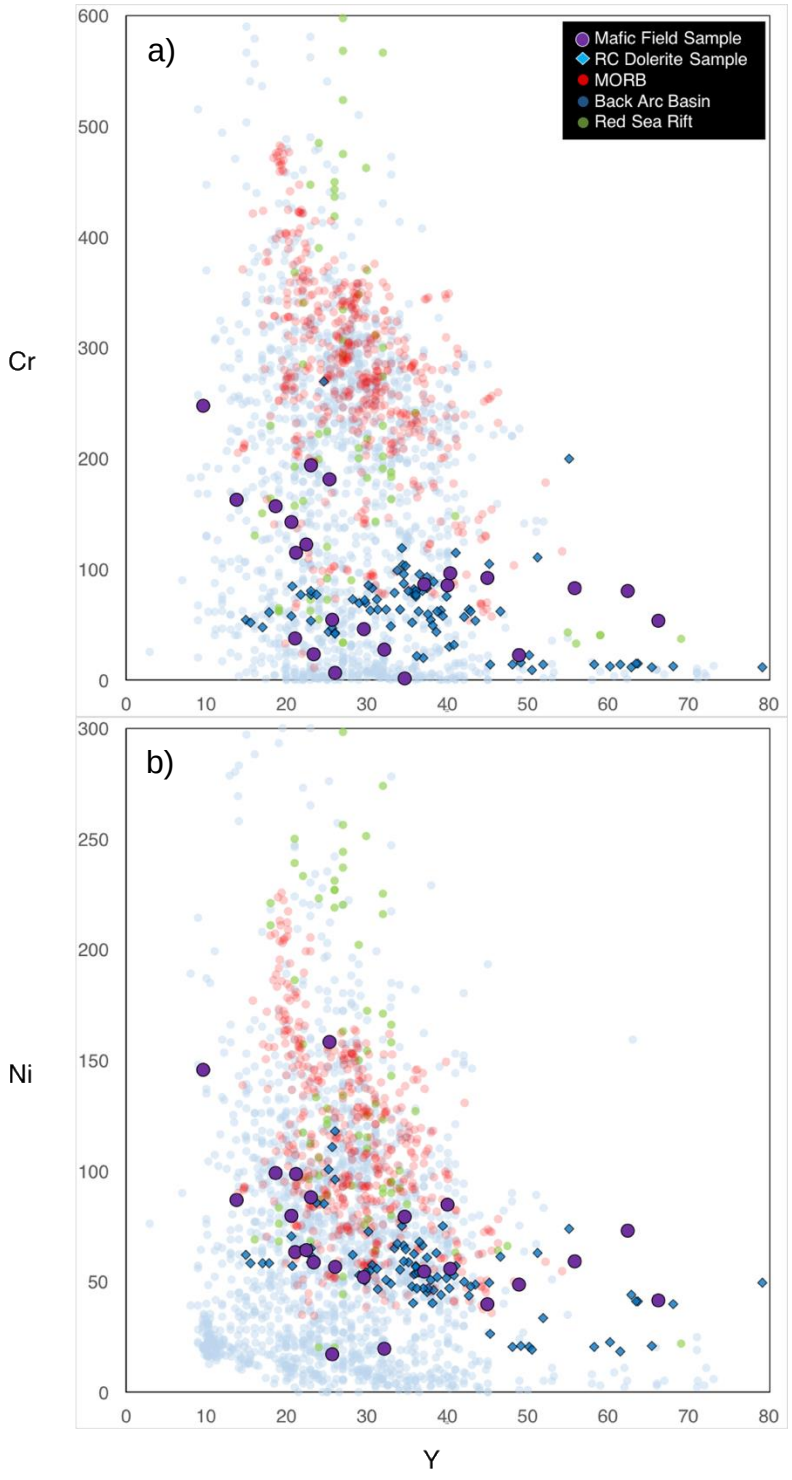


**Figure 12. a) Cr-Y plot and b) Ni-Y plot showing a slightly exponential trend of field and pulp data, indicative of slight liquid differentiation during fractionation.**

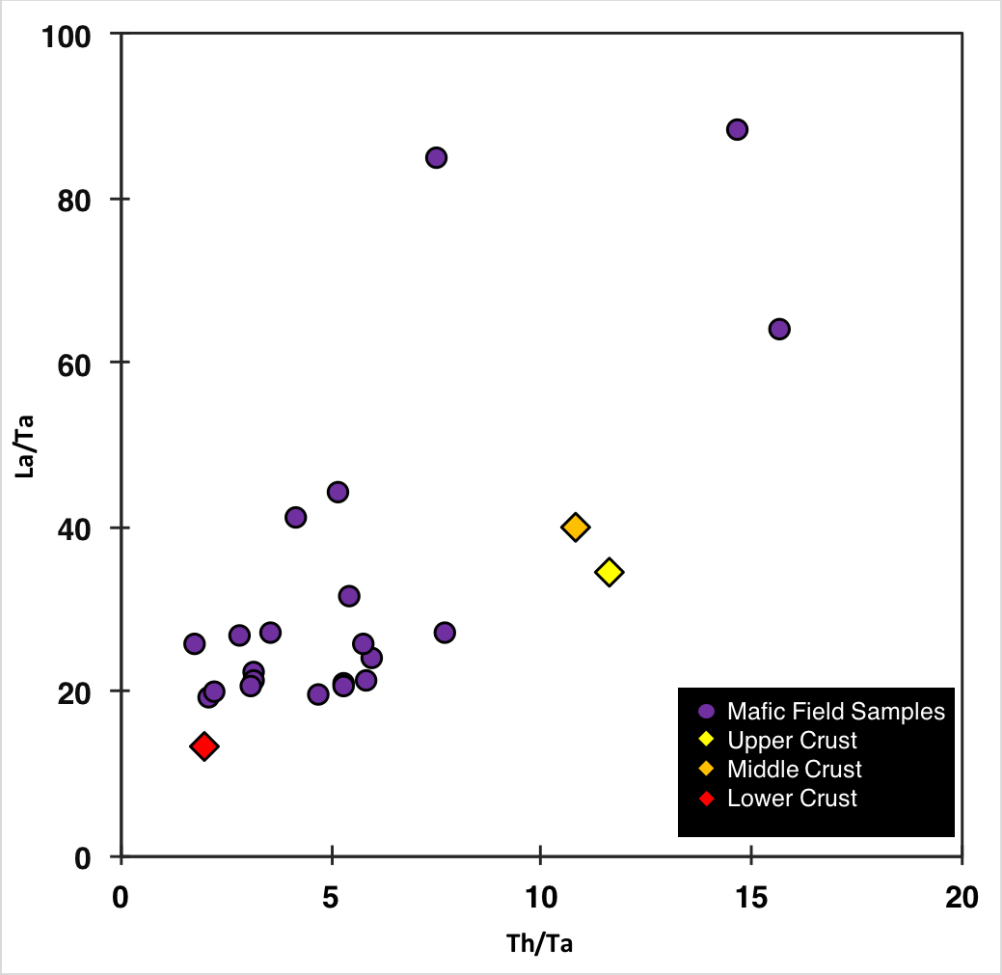


**Figure 13. Th/Ta vs La/Ta diagram following Srivasta et al. (2014a) displaying a similar composition between the field samples and the average lower crust (Rudnick & Gao, 2003).**

The assigned groups present a uniform array of REE concentrations (Figure 16), except for minor Eu anomalies in samples D04, D09 and D15. All samples normalised to MORB (Sun & McDonough, 1989) display negative anomalies in subduction mobile elements Ta and Nb, with Group 1 generally presenting the highest concentration of REE and Group 2 containing the lowest, with sample D04 being the least concentrated in REE.

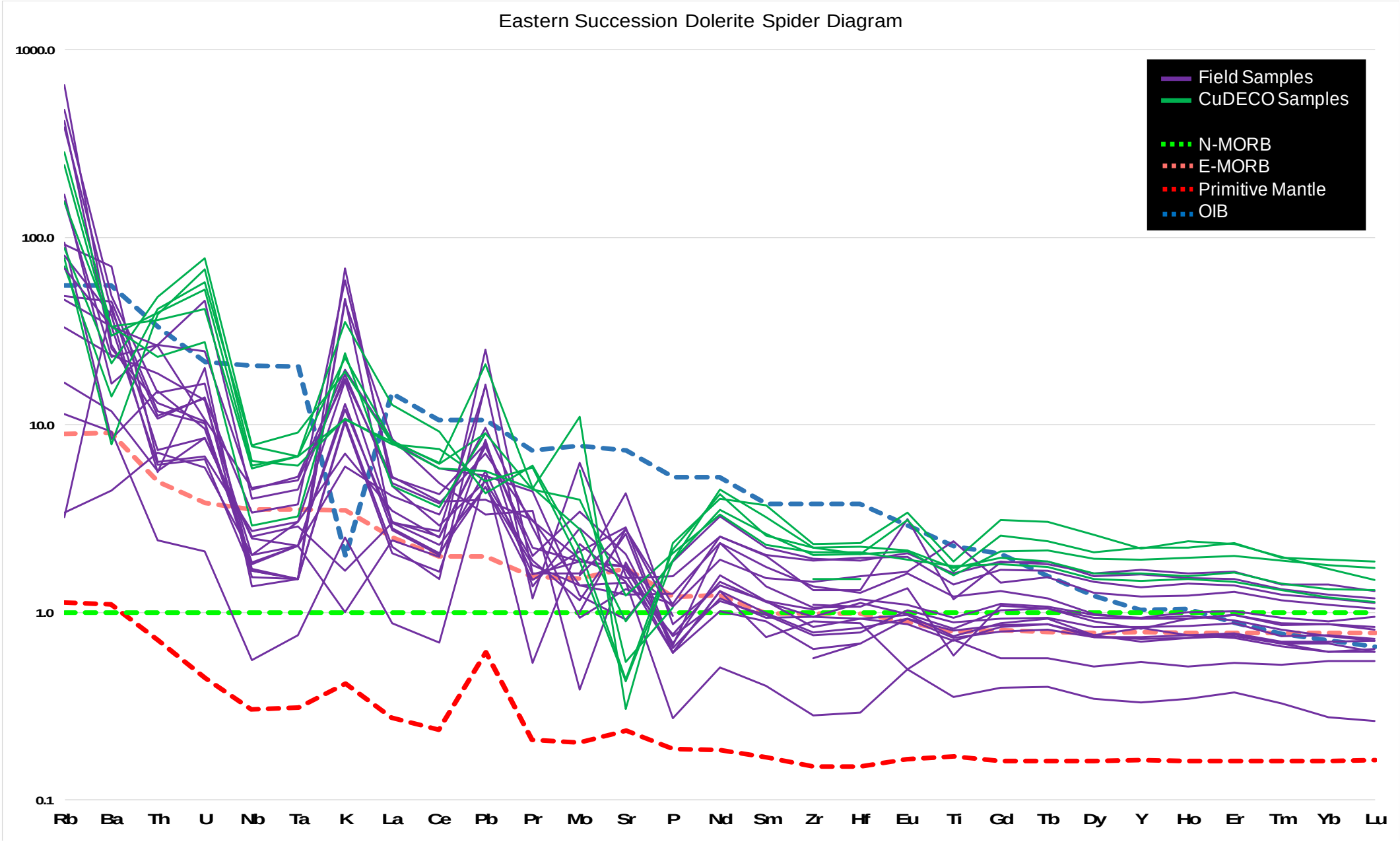


**Figure 14. A MORB normalised spider diagram for various trace elements of both field and CuDECO samples (Sun & McDonough, 1989).**

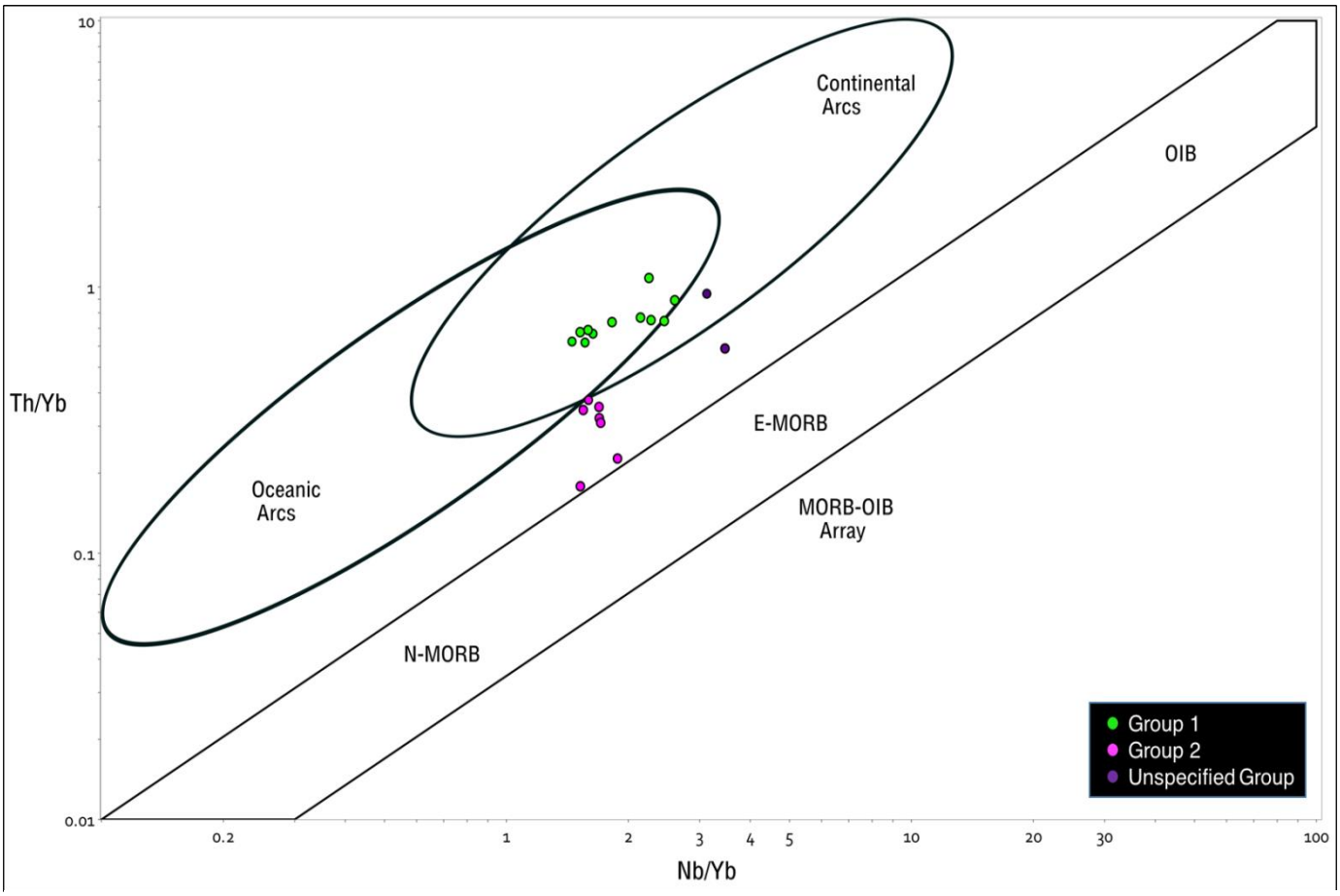


**Figure 15. The Nb/Yb-Th/Yb diagram of Pearce (2008) displaying two separate clusters of data for each Group, potentially displaying separate mafic intrustive events within the Eastern Succession.**

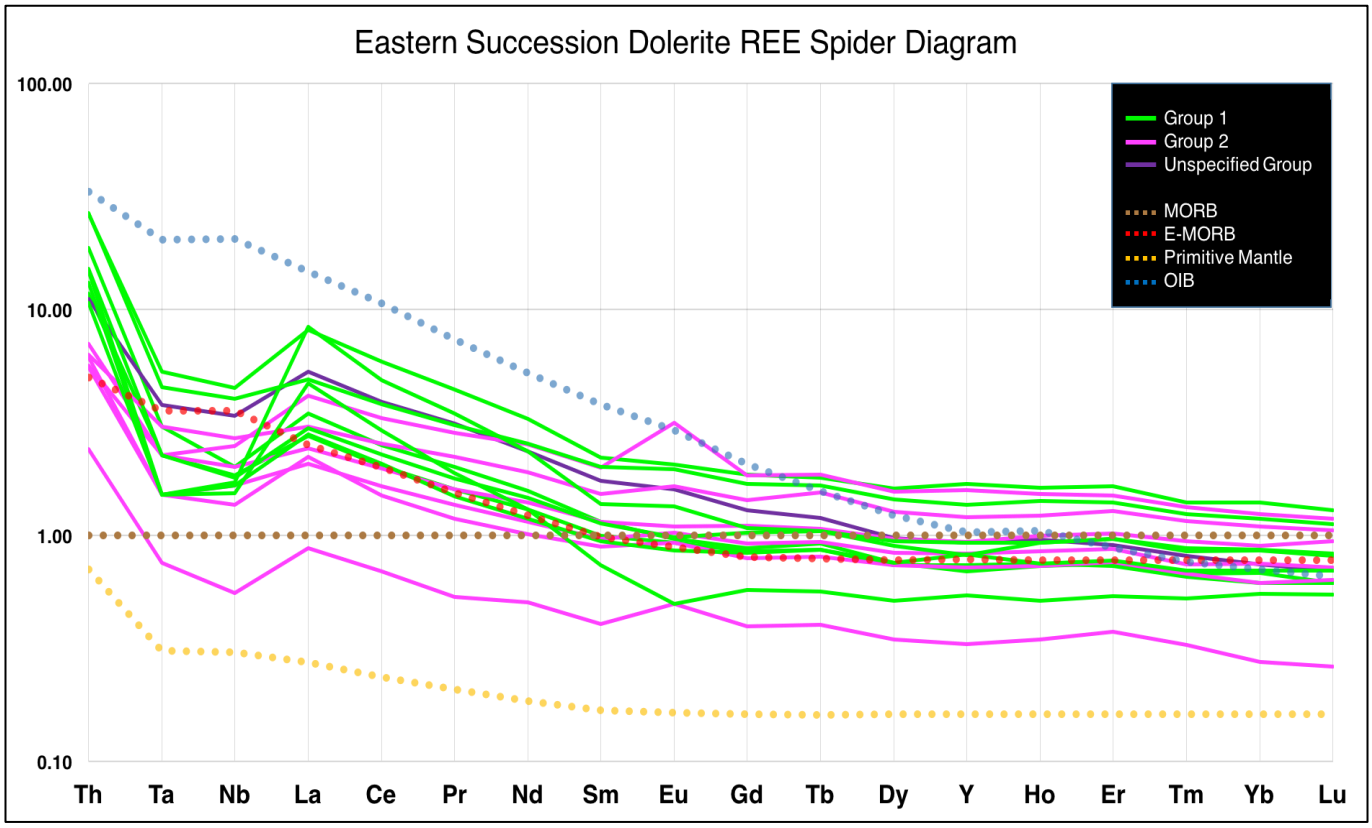


**Figure 16. The grouped REE spider diagram normalised to MORB with values from Sun and McDonough (1989).**

### 4.2.3 TECTONIC DISCRIMINATION PLOTS

Several discrimination plots have been examined to determine the tectonic environment responsible for forming the mafic dykes. Samples have remained grouped to help determine any further geochemical similarities. Data fields have been created from RC pulp data to determine if there is any geochemical signatures between separate intrusive events.

The Ti-V discrimination diagram of Shervais (1982), uses vanadium as a proxy for oxygen fugacity in magma due to is three existing valence states (Rollinson, 1993). The majority of samples (Figure 17) plot within the island arc basalt (IAB) field, with three samples plotting within the mid ocean ridge basalt (MORB) field. There are no significant differences between the two chosen groups and pulp fields. However, no members of Group 2 plot within the MORB field.

The Ti-Zr and Ti-Zr-Y diagrams of Pearce and Cann (1973) are used to discriminate between different types of basalts and the tectonic setting they formed in (Rollinson, 1993). The Ti-Zr diagram (Figure 18) presents a majority of samples plotting within the ‘mix’ field, with samples from Group 1 plotting within and close to the calc-alkaline basalt (CAB) field, with higher Zr/Ti values than Group 2. Similarly, in the Ti-Zr-Y diagram (Figure 19A), the majority of samples plot within a mixed field of MORB, CAB and island arc tholeiites (IAT) with samples from Group 1 plotting with higher Zr values, while Group 2 samples plot near the IAT field with higher Y concentration.

The La-Y-Nb diagram of Cabanis and Lecolle (1989) discriminates between basalts sourced from mid ocean ridges and continental/oceanic arcs. Figure 19B displays Group 1 plotting almost entirely within the back-arc (BA) field, and Group 2 plotting within a combination of fields. Interestingly the RC pulp fields, in addition to the field samples, produce a curved trend from the BA field through to the La apex within the arc calc-alkaline (ACA) field.

The Zr-Th-Nb diagram of Wood (1980) discriminates between MORB and VAB (Figure 19C). Grouped samples are noticeably separate, with Group 1 plotting as a cluster within volcanic arc basin (VAB)-CAB field and showing significant association to pulp fields. Group 2 also has samples plotting within the VAB-CAB field but also within the MORB fields that form a linear trend pointing towards the Th apex.

The Zr-Nb-Y diagram of Meschede (1986) (Figure 19D) is another discrimination between MORB and within-plate basalt (WPB). Both sample Groups 1 and 2 plot within the MORB field, minus a few samples plotting along the field border. There is no significant connection between pulp fields and field samples. Group 2 samples tend to plot closer to the Y apex within the MORB field whereas Group 1 clusters closer to the pulp fields.

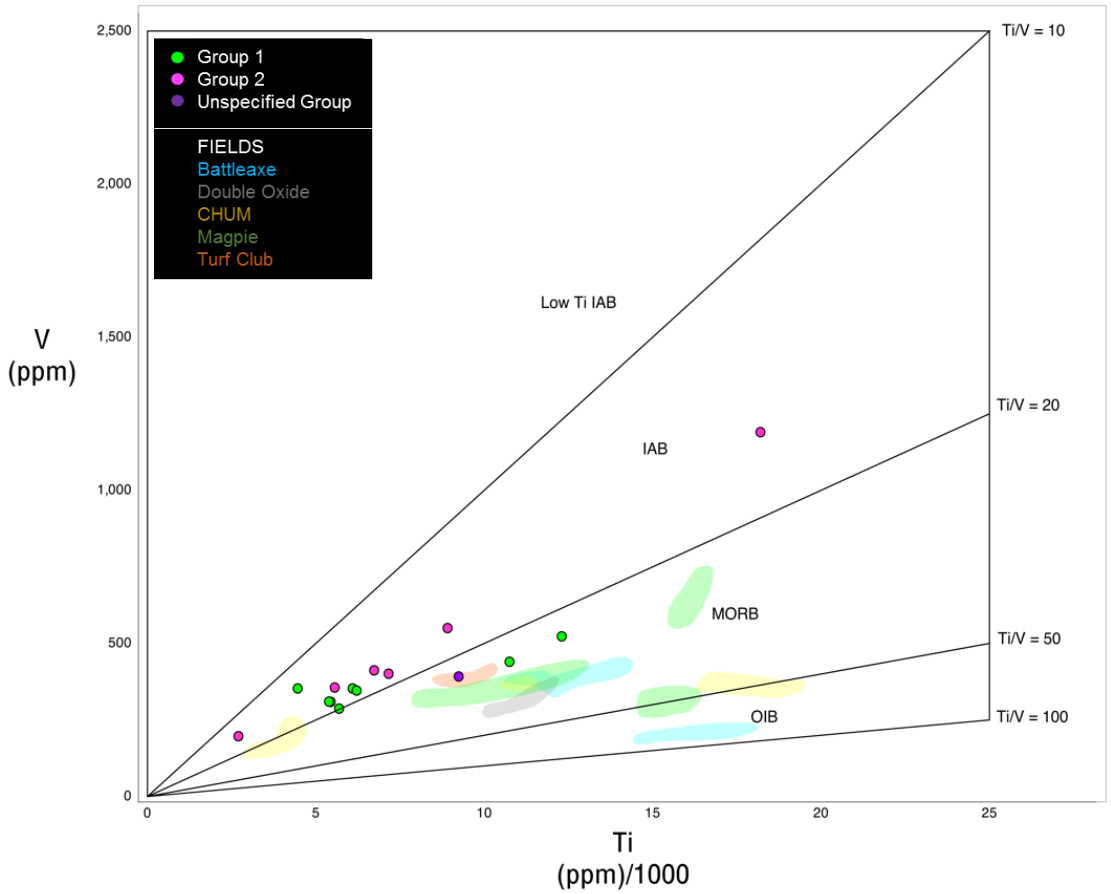


**Figure 18. Ti-V diagram of Shervais (1982), displaying field samples and RC sample fields of various locations plotting predominantly within the Island Arc Basalt and Mid Ocean Ridge Basalt fields.**

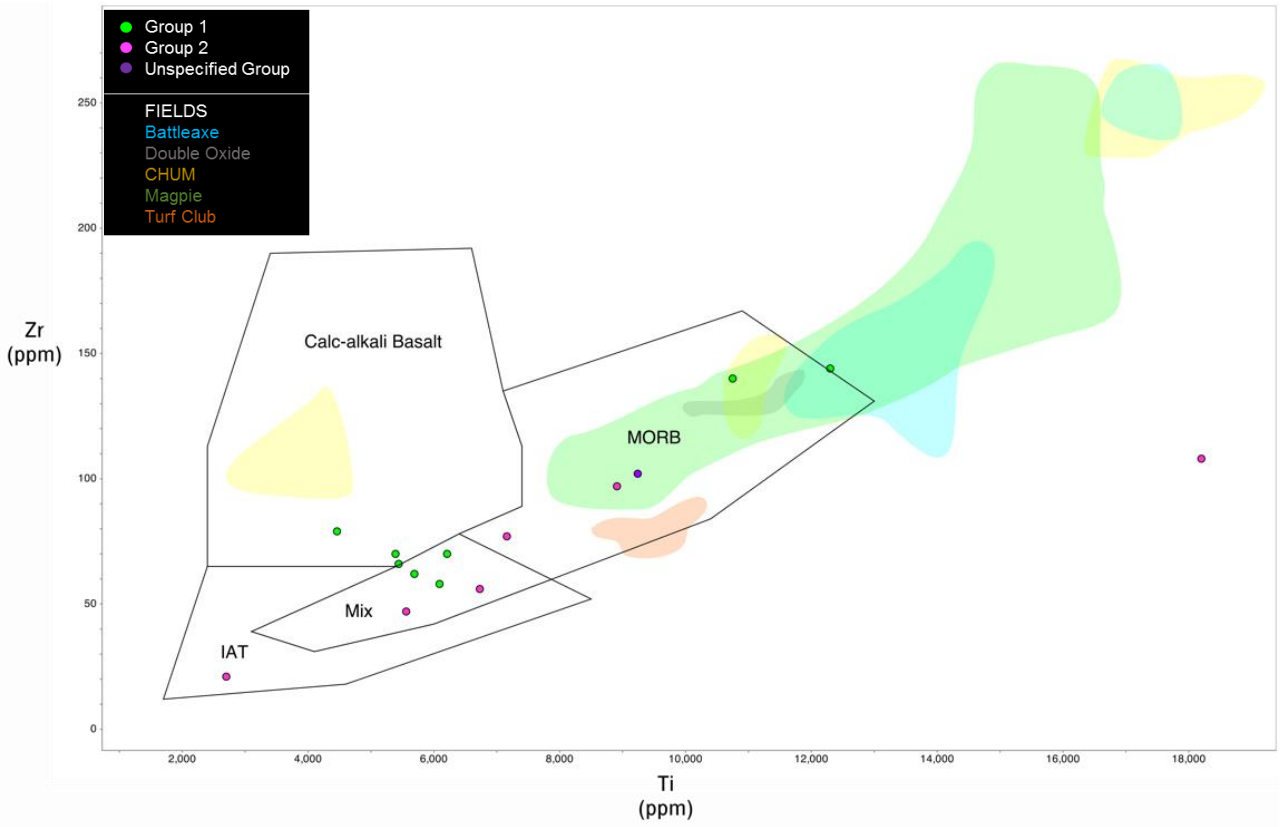


**Figure 17. Ti-Zr diagram of Pearce and Cann (1973), displaying field samples and RC sample fields of various locations plotting predominantly within the Mixed Basalt Field and the Mid Ocean Ridge Basalt field.**

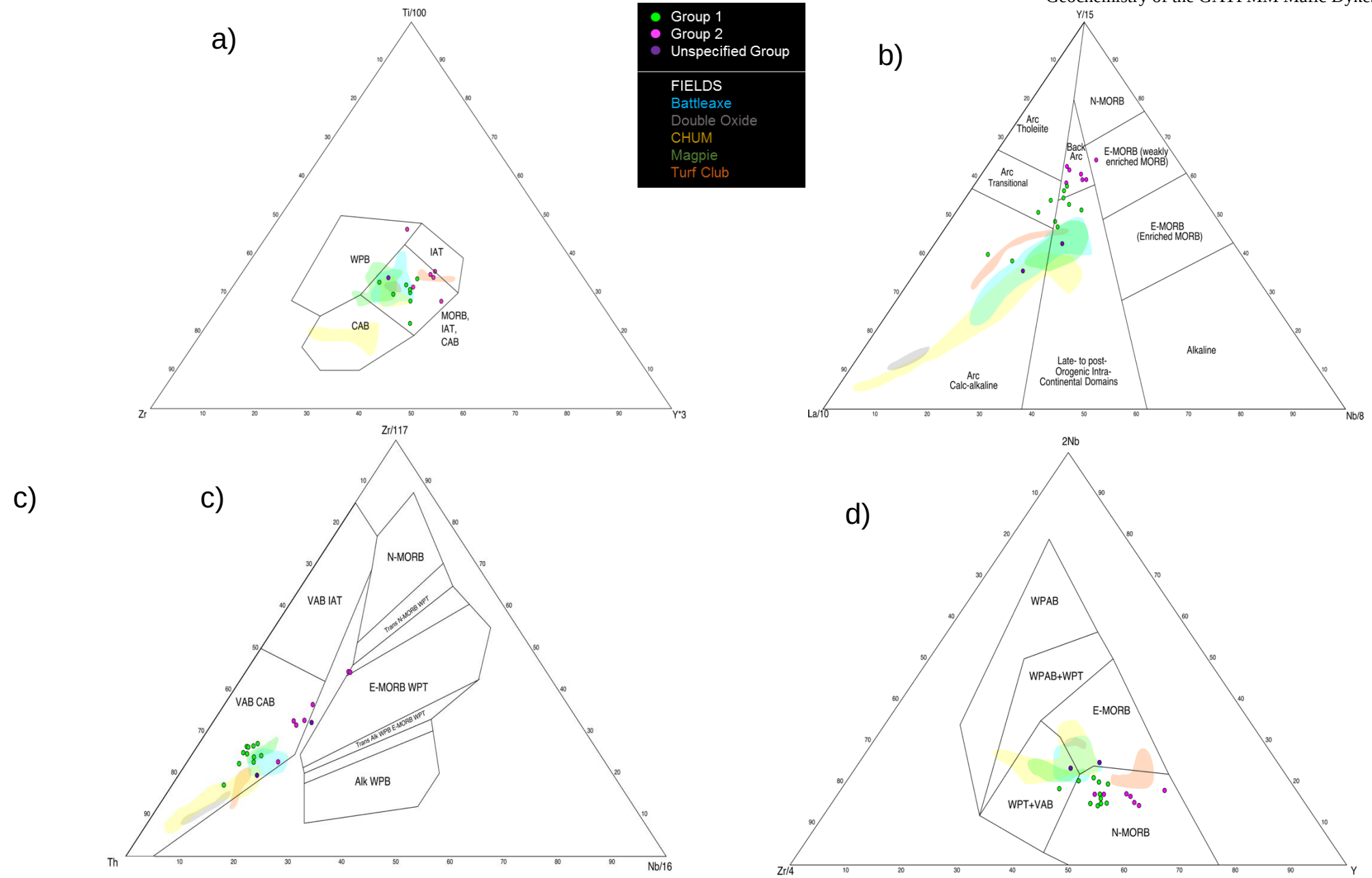


**Figure 19. Geochemical discrimination diagrams used to define tectonic and melt source characteristics. a) Ti-Zr-Y diagram of Pearce and Cann (1973), b) La-Y-Nb diagram of Cabanis and Lecolle (1989), c) Zr-Th-Nb diagram of Wood (1980) and d) Zr-Nb-Y diagram of Meschede (1986).**

### 4.2.4 CUDECO GEOCHEMISTRY

Geochemically, the six CuDECO drill core samples show similar characteristics to the GATPMM field samples, including a wide range of major oxide concentrations and LOI values (0.93-3.94 wt%). There is a significant decrease in Sr values compared the field samples (Figure 14), however, this is likely due to the Cu-carbonate mineralising veins within the samples. Generally, the CuDECO samples possess higher concentrations of most trace elements, and retain a uniform spread with the other samples on REE spider diagrams (Figure 21).

When plotted on Pearce's (2008) Th/Yb vs Nb/Yb discrimination diagram, the CuDECO samples plot within the continental arc field, clustering close to the initially outlying sample THEBE1 (Figure 20), initiating another possible grouping. On all tectonic discrimination diagrams, the CuDECO dolerites plot generally within MORB fields, showing no significant correlation to previously existing groupings or pulp sample fields, and displaying no noticeable differences to field samples.

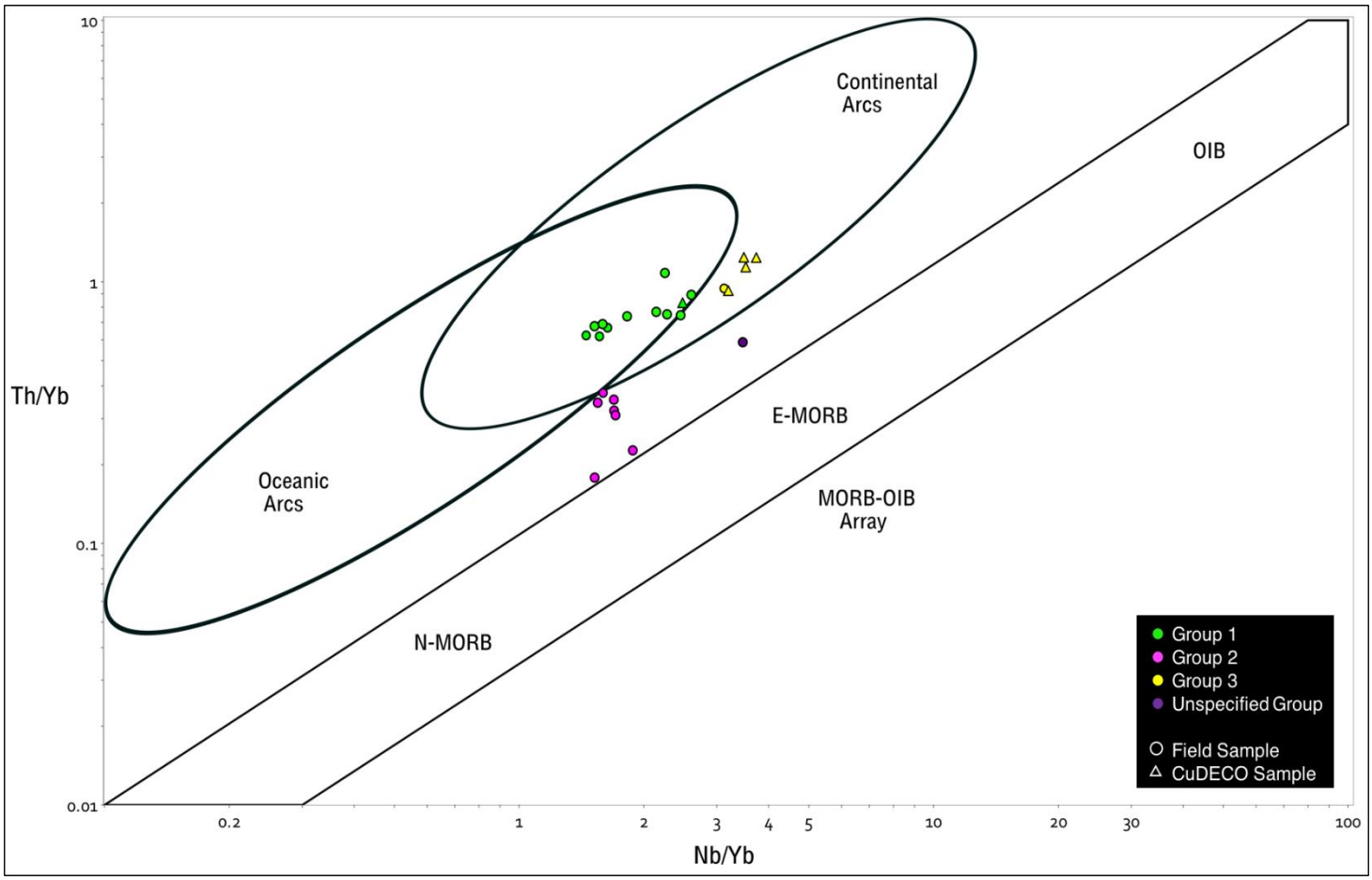


**Figure 20. The Nb/Yb-Th/Yb diagram of Pearce (2008) displaying the two seperate clusters of field samples and the mineralised samples of CuDECO. CuDECO samples plot within a separate cluster, within close proximity to THEBE1 sample, except for sample D22 which plots within the Group 1 field.**

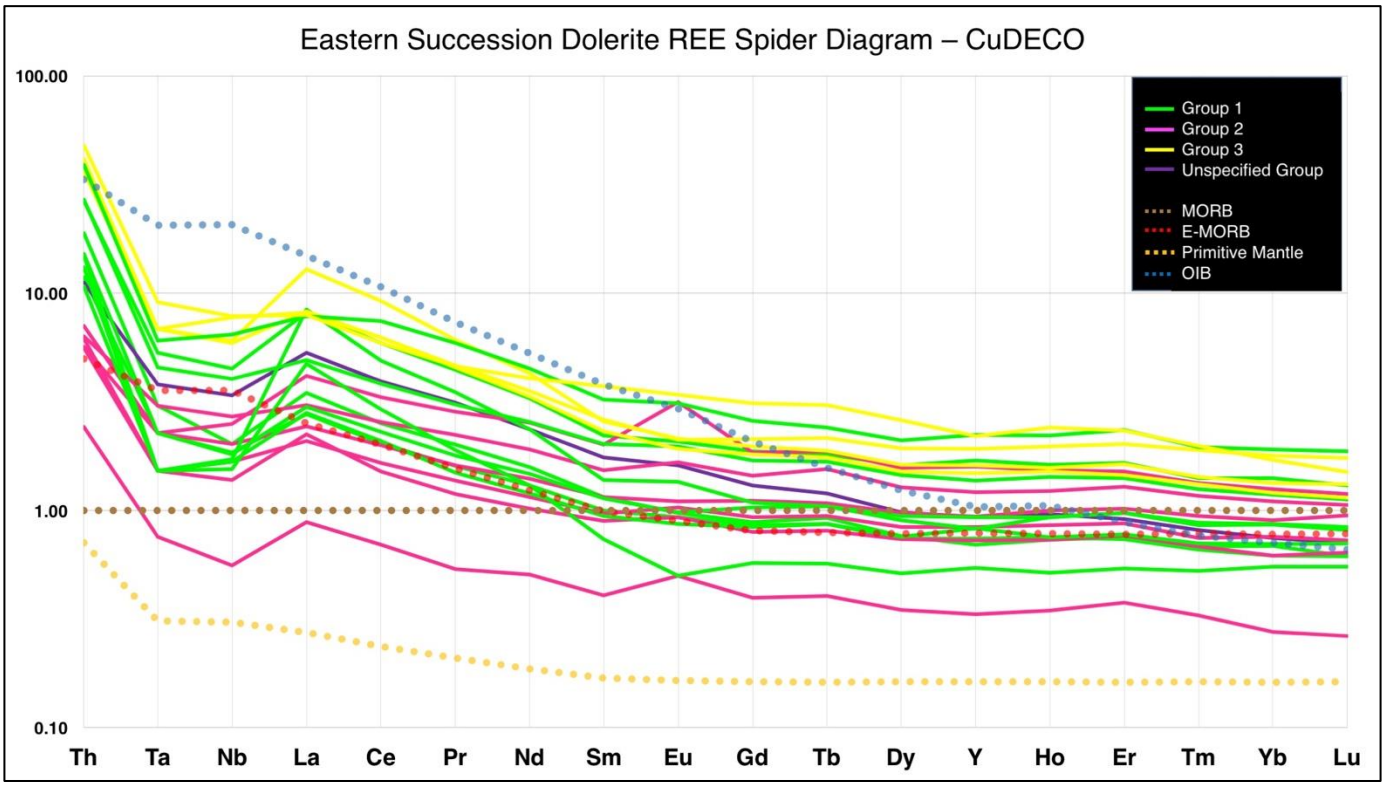


**Figure 21. The grouped REE spider diagram normalised to MORB with values from Sun and McDonough (1989), including the mineralised samples from CuDECO.**

## 4.3 Geochronology

### 4.3.1 STANDARDS

Primary standards, Madagascar apatite and GJ zircon, were used for apatite and titanate dating respectively. The Madagascar apatite was corrected for common Pb following Chew, Petrus, & Kamber (2014), while the GJ zircon standard presumably contains no common Pb. Secondary Apatite standards, Mt McClure and Durango, and a secondary titanate standard, Khan, were used to correct for instrument drift and downhole fractionation (Chew et al., 2011). Known corrected $^{207}$Pb weighted mean ages for Mt McClure apatite, Durango apatite and Khan titanite are 524.6±3.2 Ma, 32.20±0.51 Ma and 520.7±3.8 Ma respectively (Chew et al., 2014). Both known standard ages and calculated standards ages in this study use Madagascar as the primary standard for apatite. However, the known standard age for Khan was measured with OLT1 titanite as the primary standard, instead of GJ zircon as this study has incorporated (Chew et al., 2014). The $^{207}$Pb corrected weighted average of secondary standards for apatite are within error

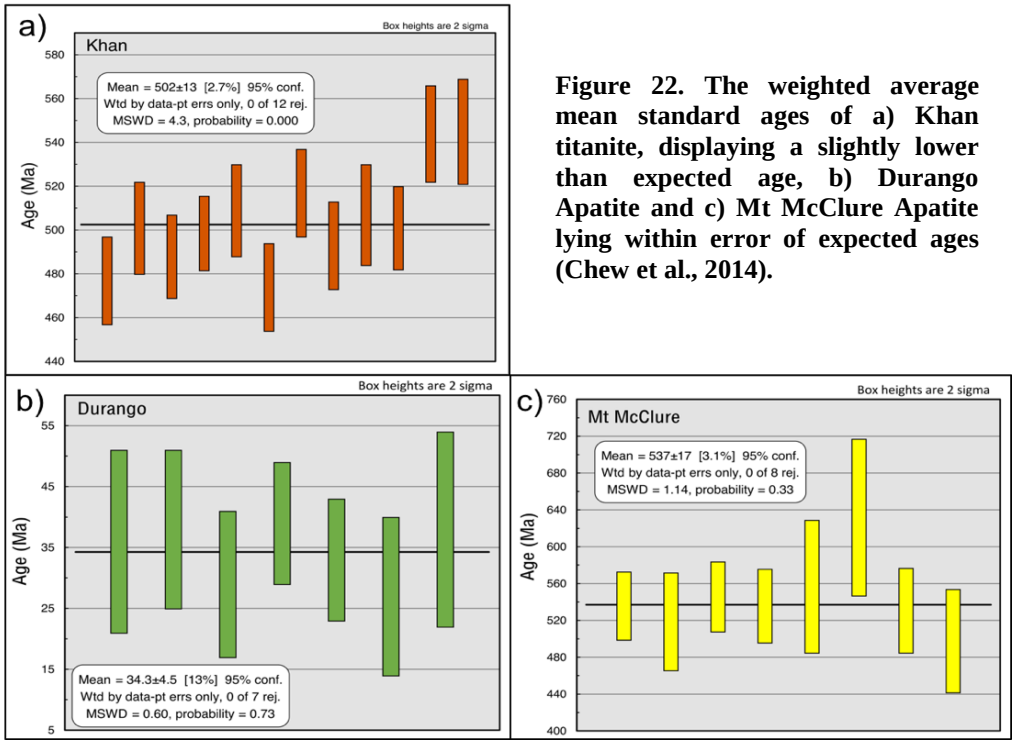


**Figure 22. The weighted average mean standard ages of a) Khan titanite, displaying a slightly lower than expected age, b) Durango Apatite and c) Mt McClure Apatite lying within error of expected ages (Chew et al., 2014).**

of known age, confirming no appreciable presence of error in the data (Figure 22). However, the secondary standard Khan in the titanite study was not within error by 2 Myr, possibly giving the final results a slightly younger age then what is considered to be the true age.

### 4.3.2 TITANITE

U-Pb dating of titanite from sample D16 showed strong discordance due to varying levels of incorporated common Pb. The 16 titanite grains produced a lower intercept of 1570 +71/-120 Ma (MSWD=0.80) on the T-W plot, with an erroneous upper intercept and hence an inaccurate common Pb line, which is also due to tight clustering of samples

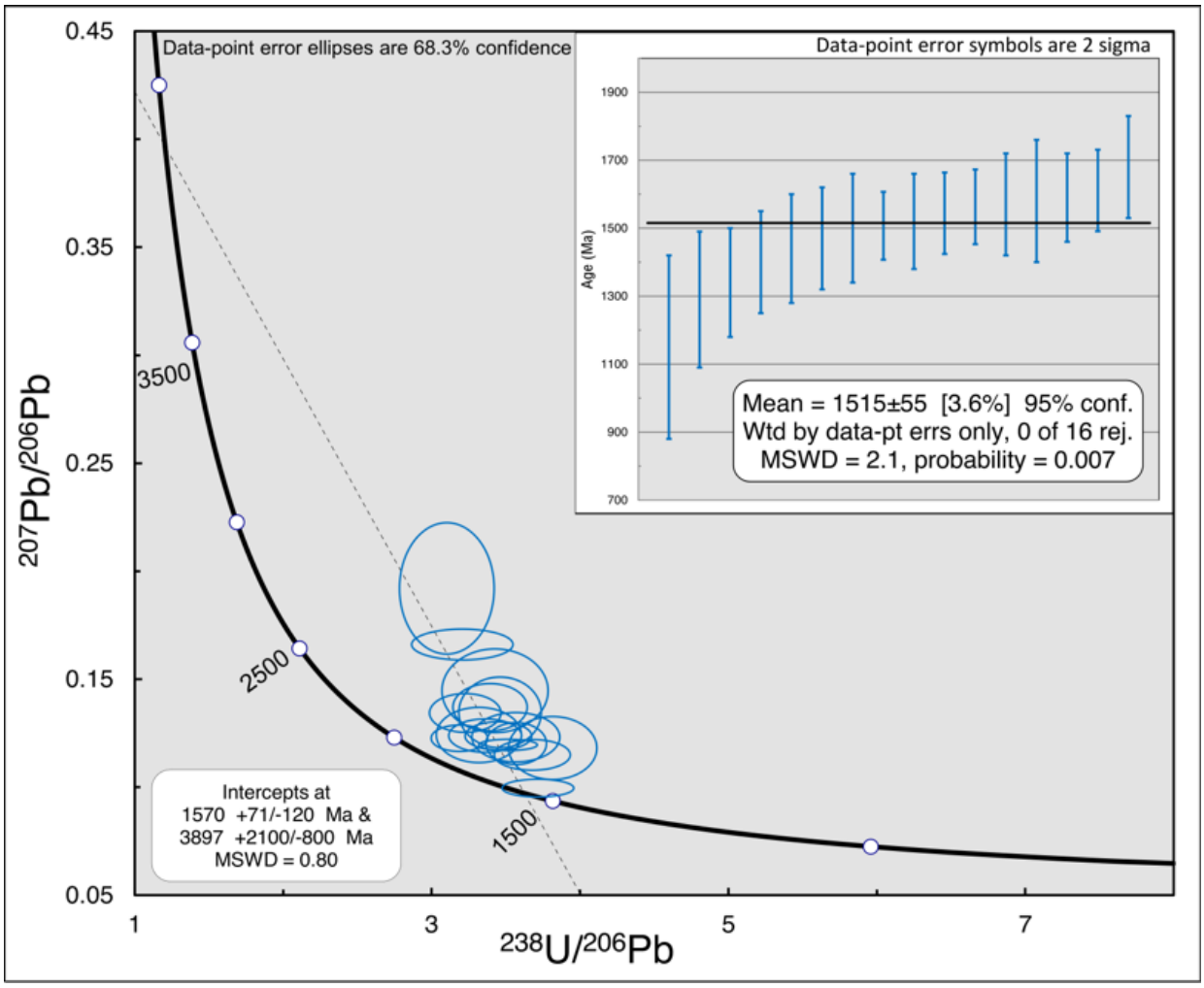


**Figure 23. Tera-Wasserberg Concordia diagram for titanite from dolerite sample D16 from Mongoose with an inset $^{207}$Pb corrected Weighted Average plot presenting a calculated age of 1515±55 Ma. Conf=confidence, wtd=weighted, data-pt=data point, errs=errors and rej=rejected.**

(Figure 23). The weighted average $^{207}$Pb-corrected plot yielded an age of 1515±55 Ma (MSWD=2.1) (Figure 22).

### 4.3.3 APATITE

U-Pb apatite dating from two samples (D16 and D18) show strong discordance due to varying levels of internal common Pb (Gawęda et al., 2014). The 27 apatite grains of D16 and the 14 grains of D18 present Tera-Wasserburg (T-W) lower intercepts of 1148±86 Ma (MSWD=1.03) and 1099 +140/-11000 Ma (MSWD=0.85) respectively (Figure 23 and 24). Due to the tight clustering of samples on the T-W plots, the upper and lower intercept values are erroneous and do not produce an accurate common Pb line. Weighted

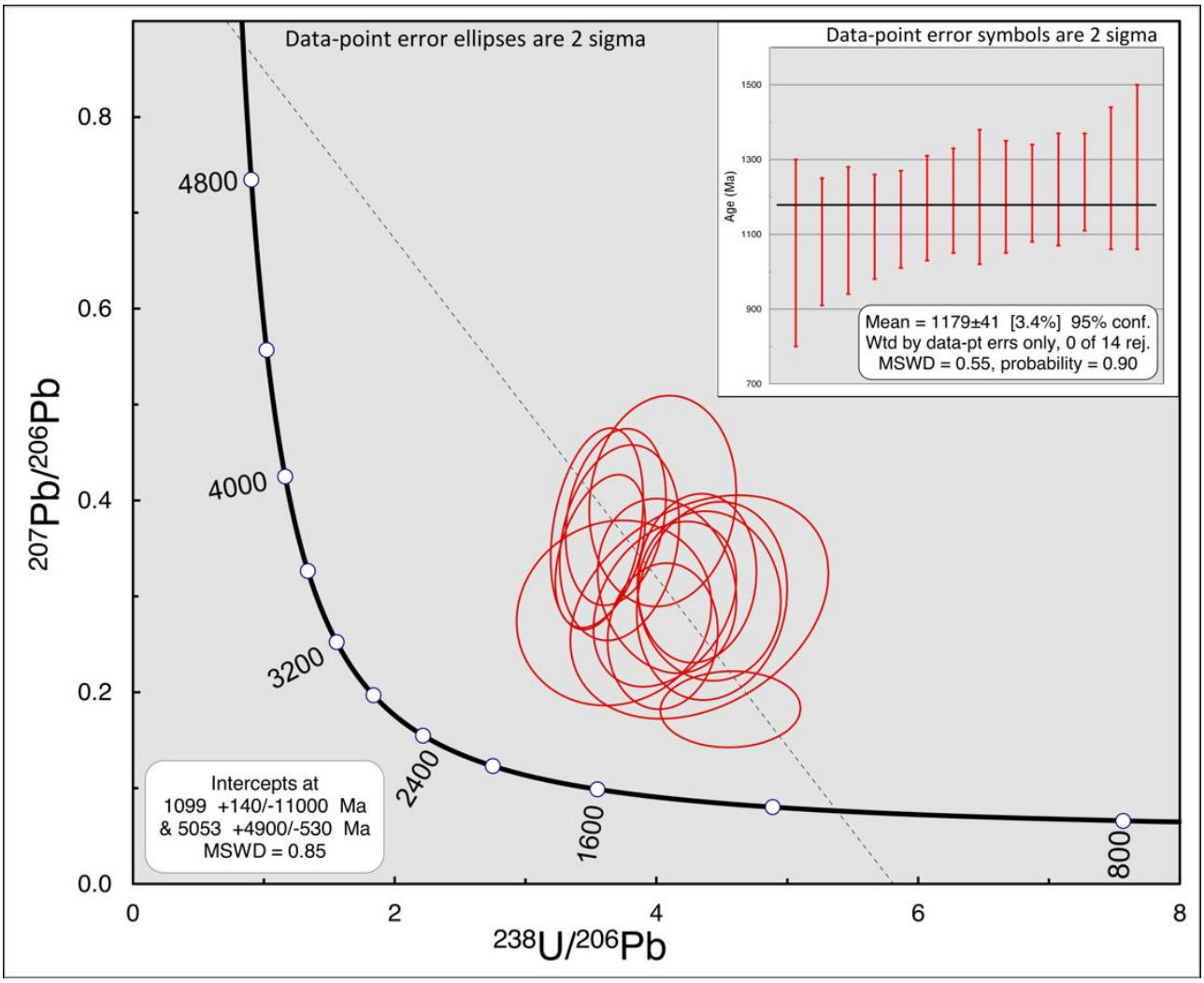


**Figure 24. Tera-Wasserberg Concordia diagram for Apatite from dolerite sample D16 from Mongoose with an inset $^{207}$Pb corrected Weighted Average plot presenting a calculated age of 1179±41 Ma. Conf=confidence, wtd=weighted, data-pt=data point, errs=errors and rej=rejected.**

average $^{207}$Pb-corrected plots with 2-sigma error bars yield an age of 1179±41 Ma (MSWD=0.55) and 1177±37 Ma (*MSWD=1.3) for both D16 and D18 respectively (Figure 24 and 25).

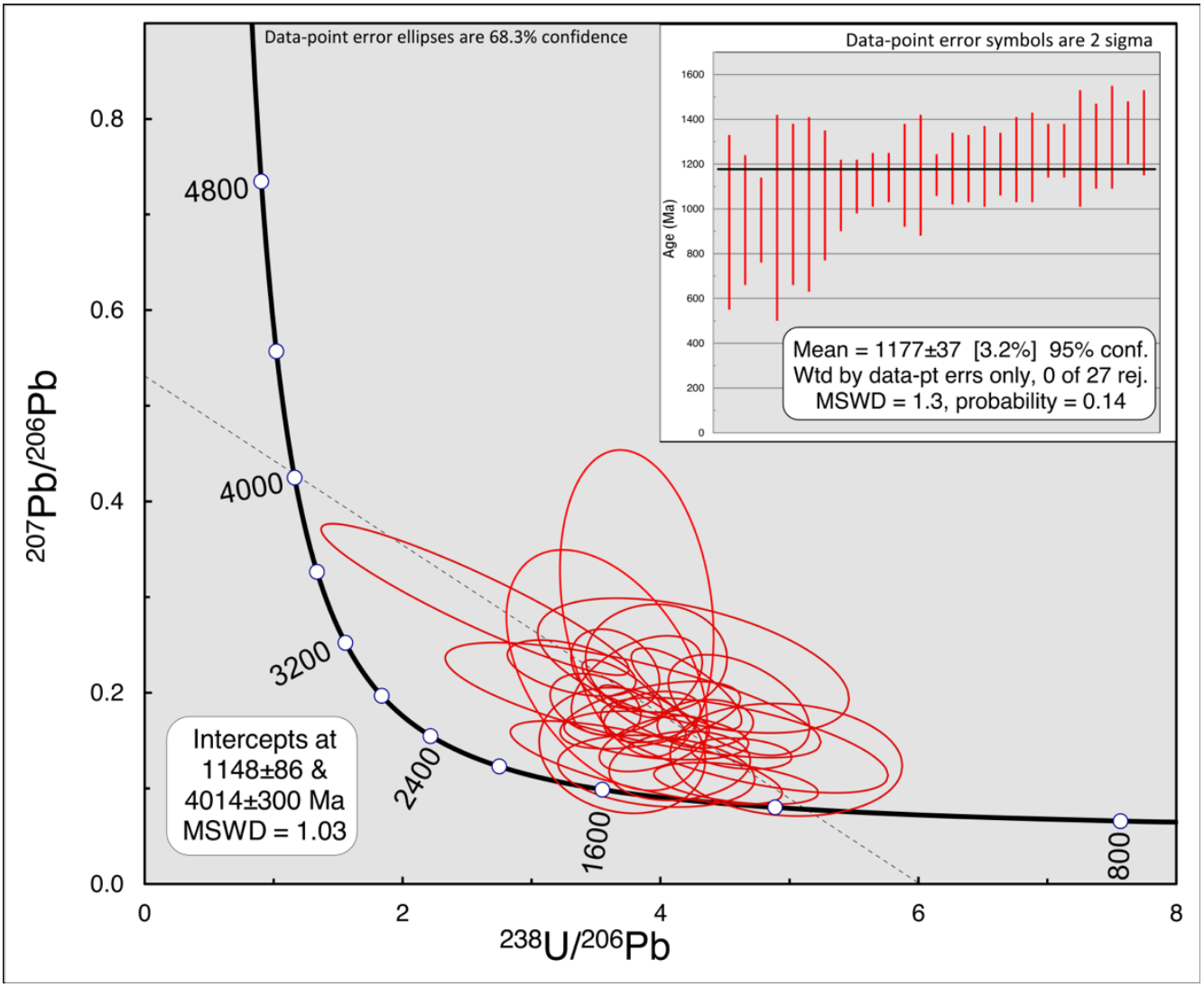


**Figure 25. Tera-Wasserberg Concordia diagram for Apatite from dolerite sample D18 from Mongoose with an inset $^{207}$Pb corrected Weighted Average plot presenting a calculated age of 1177±37 Ma. Conf=confidence, wtd=weighted, data-pt=data point, errs=errors and rej=rejected.**

## 5 DISCUSSION

### 5.1 Melt Source

Despite the variable and significant alteration history of the mafic dyke samples, the linear trend of trace element bi-variate plots and the uniform trend of samples on the REE spider

plot indicates a single source of melt for all samples, (Rollinson, 1993; Cai et al., 2010) consistent with the work of Ellis & Wyborn (1984). Relatively elevated values of MgO, Cr, Ni, low $SiO_2$ values and a similar trend between samples and primitive mantle compositions (Figure 13) indicate that these rocks were derived from a primary mantle source. These characteristics are especially noticeable in the unaltered sample D04 which has MgO, Cr and Ni values of 8.66 wt%, 247 ppm and 145.5 ppm respectively (Mandal et al., 2012; Xiong et al., 2014).

The slight exponential trend in Ni-Cr vs Y diagrams (Figure 12) is likely representative of the transition between olivine and feldspar/pyroxene fractionation, with most samples plotting towards the feldspar/pyroxene end of the fractionation trend. The lack of olivine and the large abundances of plagioclase and relict pyroxene in petrographical analysis are consistent with the interpretation that the primary melt source may have resided and undergone fractionation within the lower crust, consistent with the hypothesis of Rubenach et al. (2008).

Some crustal assimilation of source melt is present, shown by an enrichment of Pb (Figure 14) and a general enrichment of LILE (Cai et al., 2010). However, the lack of noticeable enrichment of crustally rich elements Zr and Hf (Figure 13) (Cai et al., 2010: Srivastava et al., 2014b) and the Th/Ta vs La/Ta plot of Srivasta et al. (2014a) showing samples plotting with similar values to that of the lower crust, it is precluded that there is an absence of significant upper crustal contamination during magma ascent (Rudnick & Gao, 2003).

There is a large range of trace element compositions (eg. Nb 1.4-10.8ppm), indicating that mineral accumulation and pure-fractionation were not the only processes taking place in this system. It is proposed that some incomplete liquid-solid separation may have taken place, with trace and REE being incorporated into residual phases of minerals to create a REE depleted source (Janoušek et al., 2015). This would require an initially REE rich melt source, as seen in the geochemical studies of the I-type Naraku Granite (Wyborn, 1998; Pollard et al., 1998). The local granite lithology is proposed to have originated from an enriched melt of gabbroic composition with a significant phase of plagioclase fractionation (Pollard et al., 1998). This melt is believed to have been emplaced between 1500-2300 Ma, and is the source for all granites within the Eastern Succession, which are believed to have formed in association with extensional events (Wyborn et al., 1988). It is likely that source of melt for both mafic dykes and the Naraku Granite are the same, confirming a relatively REE enriched source and confirming an incomplete liquid-solid separation phase as seen in Figure 26.

The variation of grain sizes within the field samples is evidence of a range of cooling rates indicating different relative timing and depths of intrusions. This is consistent with the interpretation that multiple individual, temporally and spatially related, intrusive events are recorded in the Cloncurry District. The plotted samples on the Th/Yb vs Nb/Yb diagram of Pearce (2008), including CuDECO samples, display promising groupings of geochemically defined episodic intrusions. However, in comparison to all other geochemical data and the RC data fields it is difficult to distinguish defined events, suggesting that mafic intrusions were continuously emplaced within the Eastern Succession. There is no apparent spatial relationship between the geochemical signature

of individual samples and there are no identified preferential orientations of dykes in the field, providing evidence for a dynamic and complex structural setting of emplacement.

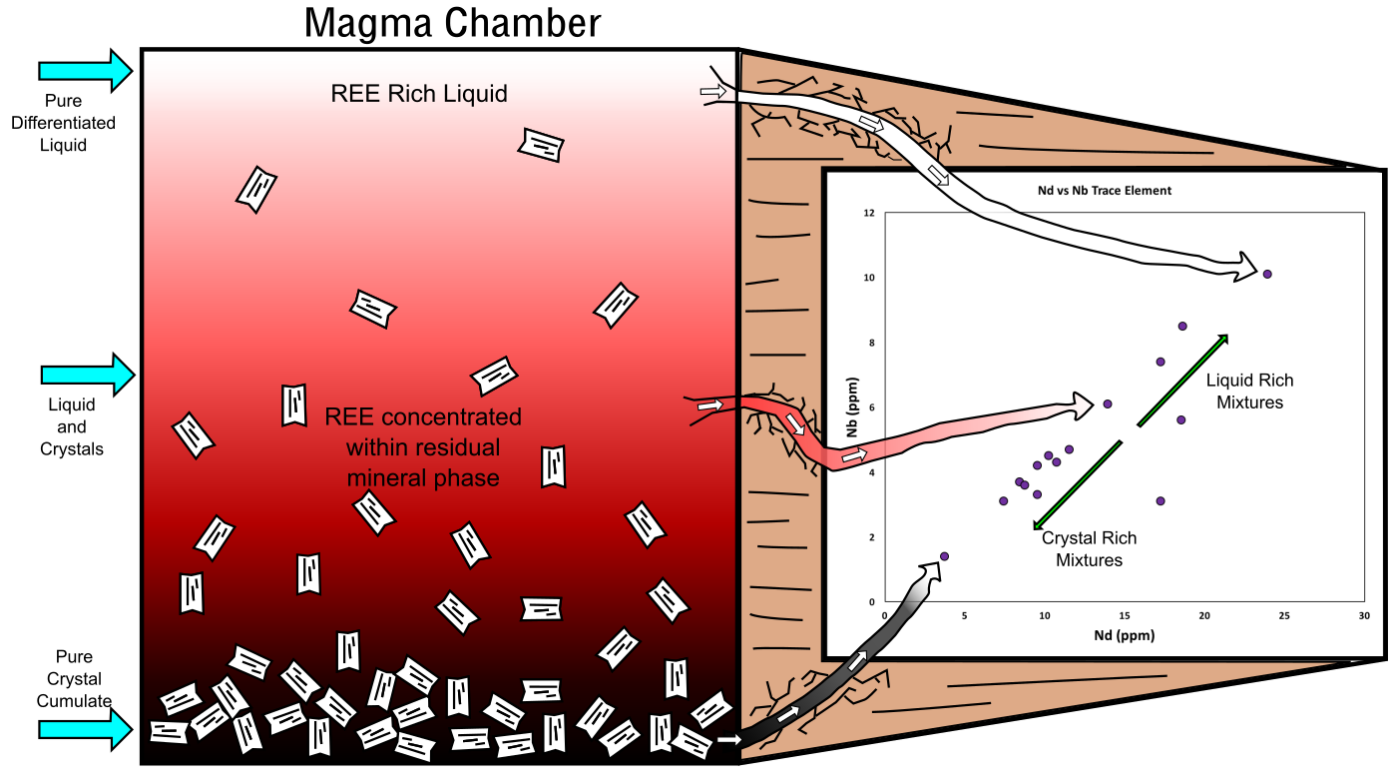


**Figure 26. An incomplete liquid-solid separation scenario following Janoušek et al. (2015) providing a solution to the large range of trace element concentrations within the sample suite.**

## 5.2 Tectonic Implications

Tectonically, the samples display anorogenic MORB like characteristics, showing; similar characteristics on bi-variate plots, similar trends on REE spider plots to N-MORB and E-MORB values of Sun & McDonough (1989), plotting within MORB fields of most tectonic discrimination diagrams and being of tholeiitic composition. There is a significant depletion in Nb and Ta, indicating subduction related processes (Pearce, 2014; Xiong et al., 2014). However, this may be due to some degree of partial melting of the Nb-Ta rich lower crust during fractionation and extension (Kelemen et al., 1993).

The MORB-like compositions and cross cutting relationships of sedimentary packages indicate that the mafic dykes likely formed within the last stages of continental extension,

to the point that a mid-ocean ridge was almost formed, prior to basin inversion and west dipping subduction. A region of high seismic velocity (6.9-7.3 km/s) directly underlying the Cloncurry region at 20km depth, previously defined as a plagioclase abundant magmatic source of igneous rocks (Goncharov et al., 1998; Goncharov & Wyborn, 1997) has recently been recognised as a thickening section of a large half-graben (Gibson et al., 2016), supporting large scale extension. Samples show a low ratio of $TiO_2$/Yb (<0.7), indicative of shallow melting within the mantle (Pearce, 2014). The moho in the area ranges from 40-51km deep with a relatively undefined transitional depth, because of interpreted basaltic rocks at this depth (Gibson et al., 2016).

It is proposed that the shallow melting characteristics and the large variance in moho depths indicates an upwelling magmatic source that fractionated slowly within the crust. During later stages of intracontinental extension, the magma continually migrated to the surface. During basin inversion of the Isan Orogeny, the upwards migrating mafic melt resulted in a widespread raising of the geothermal gradient, aiding the high temperature metamorphism recorded in the Inlier (Rubenach et al., 2008). The mafic dykes were continually emplaced during extension and contraction, cross-cutting existing dykes. The recent discovery of the Gidyea suture zone (Korsch et al., 2012) beneath the Cloncurry Region has provided a tectonic regime that incorporates intracontinental rifting followed by basin inversion due to west-dipping plate subduction. Figure 27 provides a simplified tectonic scenario; however it is unusual for melt to reside within the crust for such a long period, postulating that there may have been reheating of the ca. 1850 Ma mafic dyke sources within the lower crust (Carter et al., 1961).

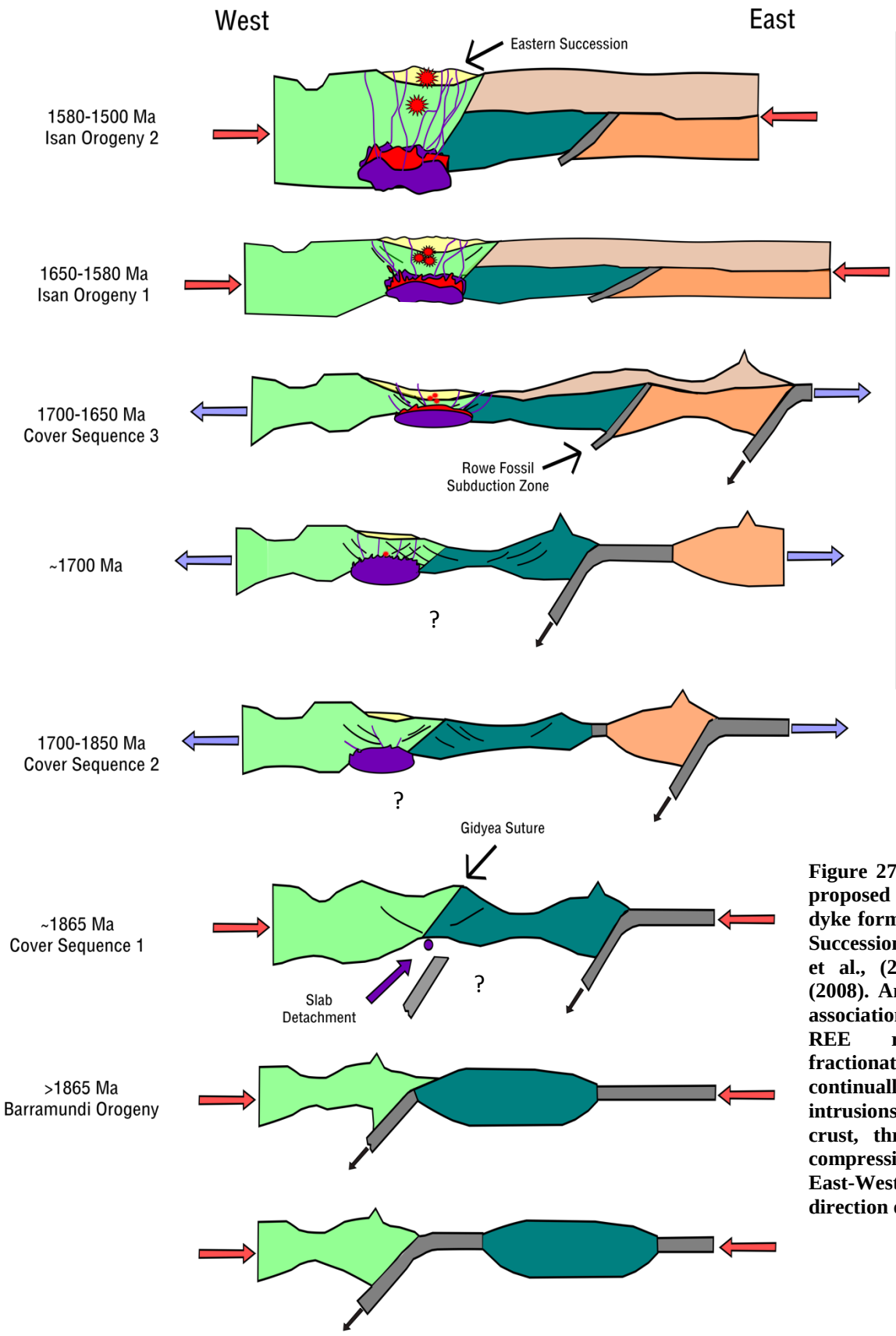


**Figure 27. A cartoon summary of proposed tectonic history of mafic dyke formation within the Eastern Succession, modified from Korsch et al., (2012) and Oliver et al, (2008). An intracontinental rift in association with an upwelling of REE rich mafic source, fractionated within the lower crust, continually emplacing mafic intrusions into the overlying upper crust, throughout extension and compression of the Isan Orogeny. East-West arrows indicate general direction of tectonic stress.**

## 5.3 Geochronology

Based on petrographical studies, the titanite and apatite within sample D16 and D18 from Mongoose have been defined as having a hydrothermal origin. In accordance with the local paragenesis (Taylor, 2013) it is proposed that titanite formation was early, coeval with magnetite, and that apatite was late stage and associated with epidote alteration. Previous ages of unmetamorphosed dolerites have been studied in the Eastern Succession, including the Rb-Sr isotope age of the 1116±12 Ma Lakeview Dolerite (Page, 1983), the K-Ar dating of pyroxenes within 1135±62 Ma and 1179±44 Ma dolerites (Tanaka & Idnurm, 1994) and the Ar-Ar dating of hornblende within the 1457±5 Ma Tommy Creek Block Dolerite (Spikings et al., 2001).

The titanite age of 1515±55 Ma is coeval with the intrusions of the Naraku Granite (Page & Sun, 1998; Foster & Austin, 2008), which is proposed to be one of the driving forces of economic mineralization of the Eastern Succession (Oliver et al., 2008). For example, a mineralization date of ca. 1510 Ma for the Ernest Henry deposit (Mark et al., 2006) corresponds well to the titanite age generated by this study. The relatively large error within the titanite data of this project makes it difficult to constrain temporal events such as the Ernest Henry mineralisation, but it is likely that the hydrothermal titanite age provides an age of initial magnetite alteration within the GATPMM district. As the titanite is hydrothermal, the mafic intrusions within the Mongoose region must have intruded prior to 1515±55 Ma.

The apatite ages of 1177±37 Ma and 1179±41 Ma are very young in comparison to any orogenic related alteration of the Mount Isa Inlier (Foster & Austin, 2008). However, they

are comparable to previously dated dolerites of Page (1983) and Tanaka & Idnurm (1994). Apatite has been petrographically identified as one of the last minerals to form within these samples, their presence indicates that there was reheating thermal event during this time period that caused the growth/resetting of apatite and may have interfered with the dating of some previously documented ages. Spikings et al. (2001) states that there was a thermal peak within the Mount Isa Inlier at ca. 1100 Ma, reaching temperatures of up to 350°C. The temperature for apatite U-Pb reset is ca. 480°C (Chew et al., 2011; Farley, 2002) and pyroxene K-Ar reset is ca. 600°C (Cassata et al., 2011), so based on existing evidence, the proposed thermal spike of 350°C is insufficient in resetting these minerals. However, there is undoubtedly some coincidental activity involved between the previously documented ages of intrusions and the studied apatite ages, this may be related to similarly aged tectonic activity of the ca. 1150-1200 Ma Albany Fraser Orogeny of south Western Australia and the Musgravian Orogeny of central Western Australia (Betts & Giles, 2006; Spikings et al., 2001). Further research is required to confirm these possible links.

### 5.4 CuDECO Dolerites and Exploration Implications

The petrological and geochemical similarity of the Cu-Au mineralised dolerite dykes from CuDECO Rocklands to the field sampled dolerites are consistent with the interpretation that they originate from the same parent melt. The drill core samples have the highest values of REE concentrations indicating they likely formed in the latter stages of liquid fractionation and possibly some of the last mafic dykes to intrude the Eastern Succession postulating that mineralisation in the GATPMM Trend may have been coeval or just prior to the most recent dyke emplacements. However, the reason for some mafic

dykes hosting mineralisation and others being barren cannot be determined solely by geochemical or petrographical means.

## 6.0 CONCLUSIONS

- Alteration has significantly replaced original mineralogy and major oxide concentrations of mafic dykes within the GATPMM Trend.
- The melt source resided within the lower crust and underwent complex fractional crystallisation of REE, dominantly through a plagioclase phase with negligible crustal contamination.
- Separate intrusive events cannot be geochemically grouped, suggesting it is more likely that mafic dykes were continually emplaced throughout the formation of the Eastern Succession.
- The REE enriched source of the mafic dykes is likely to be the same as the I-type Williams-Naraku Granite.
- Intracontinental rifting and lithospheric thinning due to extension caused the upwards migration of mafic melts, which continually migrated throughout the basin inversion of the Mount Isa Inlier.
- The emplacement of mafic dykes and the Naraku-Williams batholith was a driving force of raised temperatures during ca. 1600-1500 metamorphism.
- Hydrothermal titanite ages from Mongoose are likely to represent the influx of Fe-rich fluids associated with early magnetite alteration within the GATPMM Trend.
- Apatite ages are within range of previously documented intrusion ages, but are likely to represent the timing of a thermal event from an external source; most likely related to the Albany-Fraser Orogeny and/or the Musgravian Orogeny.

- The geochemical signature of the mineralised dolerite dykes at CuDECO's Rocklands deposit are consistent with the interpretation that they were sourced during the final stages of melt extraction.
- There are no petrographical or geochemical methods to discriminate Cu-Au mineralised mafic intrusions from their spatially and temporally associated barren counterparts.

## 7.0 FUTURE RESEARCH

Isotopic dating and analysis of mafic rocks within GATPMM Trend is difficult to complete accurately due to the high alteration levels. It is suggested that sample D04 from Walton is analysed isotopically due to its relatively unaltered characteristics to gain a better understanding of the melt source emplacement age. The depletion of Sr within CuDECO samples should be further studied by looking at the Sr compositions of other carbonate vein hosted lithologies within the area and defining if the depletion is a unique geochemical characteristic or due to the similar mobility characteristics of Ca and Sr. U-Pb dating of minerals within CuDECO samples is also suggested to further constrain the mineralising events within the GATPMM Trend.

## ACKNOWLEDGMENTS

I would like to say a massive thank you to my primary supervisor Dr Richard Lilly for continual help and accessibility throughout the year, and managing to keep all the A.W.E.S.O.M.E.S team in line. Thanks to the Mount Isa Resource Development team for financially supporting this project, in particular to Emmanuel Wembenyui for sharing a wealth of knowledge of the Eastern Succession and willingness to help throughout the year. Thanks to Michael Hawtin from CuDECO Rocklands for supplying the option of mineralised dolerite samples, widening the scope of this project. Many thanks need to go to Ben Wade at Adelaide Microscopy and James Hall and Stijn Glorie with the AFT group for continual guidance and use of apatite and titanite standards. John Foden and Martin Hand need to be acknowledged for several conversations regarding geochemistry and geochronology, steering the project in the right direction, and Katie Howard for supplying

necessary training requirements. The honours 2016 cohort must be thanked, in particular ‘yeah the boys’ for making such an enjoyable year, and finally Aunty Vic for her unprecedented care.

## REFERENCES

Abu Sharib, A. S. A. A., & Sanislav, I. V. (2013). Polymetamorphism accompanied switching in horizontal shortening during Isan Orogeny: Example from the Eastern Fold Belt, Mount Isa Inlier, Australia. *Tectonophysics, 587*, 146-167. doi:10.1016/j.tecto.2012.06.051

ALS Minerals, (2006a). Geochemical Procedure - ME- MS61.

ALS Minerals, (2006b). Whole Rock Geochemistry ME-XRF06.

ALS Minerals, (2009). Geochemical Procedure - ME- MS81.

Baker, M. J., Crawford, A. J., & Withnall, I. W. (2010). Geochemical, Sm–Nd isotopic characteristics and petrogenesis of Paleoproterozoic mafic rocks from the Georgetown Inlier, north Queensland: Implications for relationship with the Broken Hill and Mount Isa Eastern Succession. *Precambrian Research, 177*(1-2), 39-54. doi:10.1016/j.precamres.2009.11.003

Betts, P., & Giles, D. (2006). The 1800–1100Ma tectonic evolution of Australia. *Precambrian Research, 144*(1-2), 92-125. doi:10.1016/j.precamres.2005.11.006

Betts, P. G., Giles, D., Schaefer, B. F., & Mark, G. (2007). 1600–1500 Ma hotspot track in eastern Australia: implications for Mesoproterozoic continental reconstructions. *Terra Nova, 19*(6), 496-501. doi:10.1111/j.1365-3121.2007.00778.x

Blake, D. H. (1987). Geology of the Mount Isa Inlier and environs, Queensland and Northern Territory (Vol. 225). Canberra: Australian Government Publishing Services.

Blenkinsop, T., Huddlestoneholmes, C., Foster, D., Edmiston, M., Lepong, P., Mark, G., Austin, J., Murphy, F., Ford, A., & Rubenach, M. (2008). The crustal scale architecture of the Eastern Succession, Mount Isa: The influence of inversion. *Precambrian Research, 163*(1-2), 31-49. doi:10.1016/j.precamres.2007.08.011

Cabanis, B., & Lecolle, M. (1989). The La/10-Y/15-Nb/8 diagram - a tool for discrimination volcanic series and evidencing continental-crust magmatic mixtures and or contamination. *Comptes Rendus De L Academie Des Sciences Serie Ii, 309*(20), 2023-2029.

Cai, K., Sun, M., Yuan, C., Zhao, G., Xiao, W., Long, X., & Wu, F. (2010). Geochronological and geochemical study of mafic dykes from the northwest Chinese Altai: Implications for petrogenesis and tectonic evolution. *18*(4), 638-652.

Carter, E. K., Brooks, J.H & Walker, K.R. (1961). *The Precambrian mineral belt of North-Western Queensland* (Vol. Bulletin 51). Tasmania: Mercury Press.

Cassata, W. S., Renne, P. R., & Shuster, D. L. (2011). Argon diffusion in pyroxenes: Implications for thermochronometry and mantle degassing. *Earth and Planetary Science Letters, 304*(3), 407-416. doi:10.1016/j.epsl.2011.02.019

Chew, D. M., Petrus, J. A., & Kamber, B. S. (2014). U–Pb LA–ICPMS dating using accessory mineral standards with variable common Pb. *Chemical Geology, 363*, 185-199. doi:10.1016/j.chemgeo.2013.11.006

Chew, D. M., Sylvester, P. J., & Tubrett, M. N. (2011). U–Pb and Th–Pb dating of apatite by LA-ICPMS. *Chemical Geology, 280*(1-2), 200-216. doi:10.1016/j.chemgeo.2010.11.010

DeLong, S., & Chatelain, C. (1989). Complementary trace-element fractionation in volcanic and plutonic rocks: imperfect examples from ocean-floor basalts and

gabbros. *Contributions to Mineralogy and Petrology, 102*(2), 154-162. doi:10.1007/BF00375337

Ellis, D. J., & Wyborn, L. A. I. (1984). Petrology and geochemistry of Proterozoic dolerites from the Mount Isa Inlier. *Journal of Australian Geology & Geophysics, 9*, 19-32.

Farley, K. A. (2002). (U-Th)/He Dating: Techniques, Calibrations, and Applications. *Reviews in Mineralogy and Geochemistry, 47*(1), 819-844. doi:10.2138/rmg.2002.47.18

Foster, D., & Austin, J. (2008). The 1800–1610Ma stratigraphic and magmatic history of the Eastern Succession, Mount Isa Inlier, and correlations with adjacent Paleoproterozoic terranes. *Precambrian Research, 163*(1-2), 7-30. doi:10.1016/j.precamres.2007.08.010

Gawęda, A., Szopa, K., & Chew, D. (2014). LA-ICP-MS U-Pb dating and REE patterns of apatite from the Tatra Mountains, Poland as a monitor of the regional tectonomagmatic activity. *Geochronometria, 41*(4). doi:10.2478/s13386-013-0171-0

GEOROC. (2016). Geochemistry of Rocks of the Oceans and Continents.

Gibson, G. M., Meixner, A. J., Withnall, I. W., Korsch, R. J., Hutton, L. J., Jones, L. E. A., Holzschuh, J., Costelloe, R. D., Henson, P. A., & Saygin, E. (2016). Basin architecture and evolution in the Mount Isa mineral province, northern Australia: Constraints from deep seismic reflection profiling and implications for ore genesis. *Ore Geology Reviews, 76*, 414-441. doi:10.1016/j.oregeorev.2015.07.013

Gibson, G. M., Rubenach, M. J., Neumann, N. L., Southgate, P. N., & Hutton, L. J. (2008). Syn- and post-extensional tectonic activity in the Palaeoproterozoic sequences of Broken Hill and Mount Isa and its bearing on reconstructions of Rodinia. *Precambrian Research, 166*(1-4), 350-369. doi:10.1016/j.precamres.2007.05.005

Goldberg, A. S. (2010). Dyke swarms as indicators of major extensional events in the 1.9-1.2Ga Columbia supercontinent. *Journal of Geodynamics, 50*(3 4), 176.

Goncharov, A. G., Lizinsky, M. D., Collins, C. D. N., Kalnin, K. A., Fomin, T. N., Drummond, B. J., & Platonenkova, L. N. (1998). Intra-Crustal “Seismic Isostasy” in the Baltic Shield and Australian Precambrian Cratons from Deep Seismic Profiles and the Kola Superdeep Bore Hole Data *Structure and Evolution of the Australian Continent* (pp. 119-137): American Geophysical Union.

Goncharov, A. G., & Wyborn, L. (1997). Balanced petrology of the crust in the Mount Isa region. *AGSO Research Newsletter, 26*, 13-16.

Irvine, T. N., & Baragar, W. R. A. (1971). A Guide to the Chemical Classification of the Common Volcanic Rocks. *Canadian Journal of Earth Sciences, 8*(5), 523-548. doi:10.1139/e71-055

Janoušek, V., Moyen, J. F., Martin, H., Erban, V., & Farrow, C. (2015). *Geochemical Modelling of Igneous Processes - Principles And Recipes in R Language Bringing the Power of R to a Geochemical Community*. Berlin, Heidelberg: Springer Berlin Heidelberg.

Kelemen, P. B., Shimizu, N., & Dunn, T. (1993). Relative depletion of niobium in some arc magmas and the continental crust: partitioning of K, Nb, La and Ce during

melt/rock reaction in the upper mantle. *Earth and Planetary Science Letters, 120*(3), 111-134. doi:10.1016/0012-821X(93)90234-Z

Khan, T., Murata, M., Karim, T., Zafar, M., Ozawa, H., & Hafeez-Ur-Rehman, H. (2007). A Cretaceous dike swarm provides evidence of a spreading axis in the back-arc basin of the Kohistan paleo-island arc, northwestern Himalaya, Pakistan. *Journal of Asian Earth Sciences, 29*(2), 350-360. doi:10.1016/j.jseaes.2006.04.001

Korsch, R. J., & Doublier, M. P. (2016). Major crustal boundaries of Australia, and their significance in mineral systems targeting. *Ore Geology Reviews, 76*, 211-228. doi:10.1016/j.oregeorev.2015.05.010

Korsch, R. J., Huston, D. L., Henderson, R. A., Blewett, R. S., Withnall, I. W., Fergusson, C. L., Collins, W. J., Saygin, E., Kositcin, N., Meixner, A. J., Chopping, R., Henson, P. A., Champion, D. C., Hutton, L. J., Wormald, R., Holzschuh, J., & Costelloe, R. D. (2012). Crustal architecture and geodynamics of North Queensland, Australia: Insights from deep seismic reflection profiling. *Tectonophysics, 572-573*, 76-99. doi:10.1016/j.tecto.2012.02.022

Kuno, H. (1968). Origin of andesite and its bearing on the Island arc structure. *Bulletin Volcanologique, 32*(1), 141-176. doi:10.1007/BF02596589

Le Maitre, R. W., Streckeisen, A., Zanettin, B., Le Bas, M. J, Bonin, B., Bateman, P., Bellieni, G., Dudek, A., Efremova, S., Keller, J., Lameyre, J., Sabine, P. A., Schmid, R., Sørensen, H., & Woolley, A. R. (1989) International Union of Geological Sciences. Subcommission on the Systematics of Igneous. *A classification of igneous rocks and glossary of terms : recommendations of the International Union of Geological Sciences Subcommission on the Systematics of Igneous Rocks*. Oxford Boston: Blackwell.

Mandal, A., Ray, A., Debnath, M., & Paul, S. (2012). Petrology, geochemistry of hornblende gabbro and associated dolerite dyke of Paharpur, Puruliya, West Bengal: Implication for petrogenetic process and tectonic setting. *Journal of Earth System Science, 121*(3), 793-812. doi:10.1007/s12040-012-0195-5

Mark, G., Oliver, N. H. S., & Williams, P. J. (2006). Mineralogical and chemical evolution of the Ernest Henry Fe oxide–Cu–Au ore system, Cloncurry district, northwest Queensland, Australia. *Mineralium Deposita, 40*(8), 769-801. doi:10.1007/s00126-005-0009-7

Melson, W. G., O' Hearn, T., & Jarosewich, E. (2002). A data brief on the Smithsonian Abyssal Volcanic Glass Data File. Geochemistry, Geophysics, Geosystems, 3(4), 1-11. doi:10.1029/2001GC000249

Meschede, M. (1986). A method of discriminating between different types of mid-ocean ridge basalts and continental tholeiites with the Nb-Zr-Y diagram. *Chemical Geology, 56*(3), 207-218. doi:10.1016/0009-2541(86)90004-5

Oliver, N., Butera, K., Rubenach, M., Marshall, L., Cleverley, J., Mark, G., Tullemans, F., & Esser, D. (2008). The protracted hydrothermal evolution of the Mount Isa Eastern Succession: A review and tectonic implications. *Precambrian Research, 163*(1-2), 108-130. doi:10.1016/j.precamres.2007.08.019

Oliver, N. H. S., Pearson, P. J., & Holcombe, R. J. (1985). Chronology of magmatism, skarn formation, and uranium mineralization, Mary Kathleen, Queensland, Australia

discussion. *Economic Geology, 80*(2), 513-517. doi:10.2113/gsecongeo.80.2.513-A

Page, R. W. (1983). Chronology of magmatism, skarn formation, and uranium mineralization, Mary Kathleen, Queensland, Australia. *Economic Geology, 78*(5), 838-853. doi:10.2113/gsecongeo.78.5.838

Page, R. W., & Sun, S. S. (1998). Aspects of geochronology and crustal evolution in the Eastern Fold Belt, Mt Isa Inlier∗. Australian Journal of Earth Sciences, 45(3), 343-361. doi:10.1080/08120099808728396

Payne, J. L., Hand, M., Barovich, K. M., & Wade, B. P. (2008). Temporal constraints on the timing of high-grade metamorphism in the northern Gawler Craton: implications for assembly of the Australian Proterozoic. *An International Geoscience Journal of the Geological Society of Australia, 55*(5), 623-640. doi:10.1080/08120090801982595

Pearce, J. A. (2008). Geochemical fingerprinting of oceanic basalts with applications to ophiolite classification and the search for Archean oceanic crust. *Lithos, 100*(1-4), 14-48. doi:10.1016/j.lithos.2007.06.016

Pearce, J. A. (2014). Immobile Element Fingerprinting of Ophiolites. *Elements, 10*, 101-108.

Pearce, J. A., & Cann, J. R. (1973). Tectonic setting of basic volcanic rocks determined using trace element analyses. *Earth and Planetary Science Letters, 19*(2), 290-300. doi:10.1016/0012-821X(73)90129-5

Pollard, P. J., Mark, G., & Mitchell, L. C. (1998). Geochemistry of post-1540 Ma granites in the Cloncurry District, Northwest Queensland. *Economic Geology, 93*(8), 1330-1344. doi:10.2113/gsecongeo.93.8.1330

Richardson, L. M. (2003). *Index of Airborne Geophysical Surveys, Seventh Edition.*

Rollinson, H. (1993). *Using Geochemical Data: evaluation, presentation, interpretation*. New York: Pearson Education Limited.

Rubenach, M., Foster, D., Evins, P., Blake, K., & Fanning, C. (2008). Age constraints on the tectonothermal evolution of the Selwyn Zone, Eastern Fold Belt, Mount Isa Inlier. *Precambrian Research, 163*(1-2), 81-107. doi:10.1016/j.precamres.2007.08.014

Rudnick, R. L., & Gao, S. (2003). Composition of the Continental Crust. In R. L. Rudnick (Ed.), *The Crust, Volume 3*: Elsevier.

Sarbas, B. (2008). The GEOROC Database as Part of a Growing Geoinformatics Network. Paper presented at the Geoinformatics 2008–Data to Knowledge, Potsdam.

Scarrow, J. H., Leat, P. T., Wareham, C. D., & Millar, I. L. (1998). Geochemistry of mafic dykes in the Antarctic Peninsula continental-margin batholith: a record of arc evolution. *Contributions to Mineralogy and Petrology, 131*(2 3), 289.

Shervais, J. W. (1982). Ti-V plots and the petrogenesis of modern and ophiolitic lavas. *Earth and Planetary Science Letters, 59*, 101-118.

Spikings, R. A., Foster, D. A., Kohn, B. P., & Lister, G. S. (2001). Post-orogenic (<1500 Ma) thermal history of the Proterozoic Eastern Fold Belt, Mount Isa Inlier, Australia. *Precambrian Research, 109*(1), 103-144. doi:10.1016/S0301-9268(01)00143-7

Srivastava, R. K., Jayananda, M., Gautam, G. C., Gireesh, V., & Samal, A. K. (2014a). Geochemistry of an ENE–WSW to NE–SW trending ~2.37Ga mafic dyke swarm of

the eastern Dharwar craton, India: Does it represent a single magmatic event? *Chemie der Erde - Geochemistry, 74*(2), 251-265. doi:10.1016/j.chemer.2013.07.007

Srivastava, R. K., Kumar, S., Sinha, A. K., & Chalapathi Rao, N. V. (2014b). Petrology and geochemistry of high-titanium and low-titanium mafic dykes from the Damodar valley, Chhotanagpur Gneissic Terrain, eastern India and their relation to Cretaceous mantle plume(s). *Journal of Asian Earth Sciences, 84*, 34-50. doi:10.1016/j.jseaes.2013.07.044

Sun, S. S., & McDonough, W. F. (1989). Chemical and isotopic systematics of oceanic basalts: implications for mantle composition and processes. *Geological Society, London, Special Publications, 42*(1), 313-345. doi:10.1144/GSL.SP.1989.042.01.19

Tanaka, H., & Idnurm, M. (1994). Palaeomagnetism of Proterozoic mafic intrusions and host rocks of the Mount Isa Inlier, Australia: revisited. *Precambrian Research, 69*(1), 241-258. doi:10.1016/0301-9268(94)90089-2

Taylor, R. G. (2013). *Comments Regarding the Taipan prospect, Great Australia mine, Cloncurry. Suggested paragenesis, genetic overview and rock photography*. Retrieved from

Williams, H., Turner, S., Kelley, S., & Harris, N. (2001). Age and composition of dikes in Southern Tibet: New constraints on the timing of east-west extension and its relationship to postcollisional volcanism. *Geology, 29*(4), 339.

Williams, M. R., Holwell, D. A., Lilly, R. M., Case, G. N. D., & McDonald, I. (2015). Mineralogical and fluid characteristics of the fluorite-rich Monakoff and E1 Cu-Au deposits, Cloncurry region, Queensland, Australia: Implications for regional F-Ba-rich IOCG mineralisation. *Ore Geology Reviews, 64*, 103.

Wood, D. A. (1980). The application of a Th Hf Ta diagram to problems of tectonomagmatic classification and to establishing the nature of crustal contamination of basaltic lavas of the British Tertiary Volcanic Province. *Earth and Planetary Science Letters, 50*(1), 11-30. doi:10.1016/0012-821X(80)90116-8

Wyborn, L. (1998). Younger ca 1500 Ma granites of the Williams and Naraku Batholiths, Cloncurry district, eastern Mt Isa Inlier: Geochemistry, origin, metallogenic significance and exploration indicators. *Australian Journal of Earth Sciences, 45*(3), 397-411. doi:10.1080/08120099808728400

Wyborn, L. A. I., Page, R. W., & McCulloch, M. T. (1988). Petrology, geochronology and isotope geochemistry of the post-1820 Ma granites of the Mount Isa Inlier: mechanisms for the generation of Proterozoic anorogenic granites. Precambrian Research, 40, 509-541. doi:10.1016/0301-9268(88)90083-6

Xiong, F., Ma, C., Jiang, H. a., Liu, B., & Huang, J. (2014). Geochronology and geochemistry of Middle Devonian mafic dykes in the East Kunlun orogenic belt, Northern Tibet Plateau: Implications for the transition from Prototethys to Paleotethys orogeny. *Chemie der Erde - Geochemistry, 74*(2), 225-235. doi:10.1016/j.chemer.2013.07.004

Young, L. J. &. Lane, R.P (Cartographer). (2015). Marraba - Sheet 6956.

**APPENDIX 1: EXTENDED METHODS**

# 1. Materials and Methods

A total of 109 dolerite samples were examined for this project. The 109 samples consisted of 18 field samples, 6 drill core samples and 90 pulp samples. Each sample was collected from within the Cloncurry District, including Rocklands, Battleaxe, Mt Glorious, Eternal, Fifi, D-Ring, Walton, Wilgar, Remedy, Monakoff, Taipan, Mongoose, CHUM, Double Oxide, Magpie and Turf Club. Each of the 109 samples were sent to ALS (Australian Laboratory Services) Townsville for whole rock geochemical analysis. 5 samples were also chosen for Zircon and Nd/Sr dating. Each of the field samples and core samples were also sent to (WHERE) to be cut for thin sections for petrographical analysis. QGIS software was used for mapping and ioGAS software was used for geochemical data analysis once a QAQC (Quality Assurance and Quality Control) report was completed.

## *1.1 SAMPLING*

### 1.1.1 Field Sampling

**Materials**

Calico bag
Hammer
Garmin GPSMap 62s (AGD-84 54K UTM zone)
Scribe
Hand lens

**Methods**

Dolerites were found in the field using existing knowledge and magnetic/radiogenic maps of the survey area.
Dolerites were identified using hand lens and scribe, labelled from D01-D18.
Dolerites were smashed into dinner plate sized pieces and placed in calico sampling bags.
GPS point was used to place dolerite data on a map.
Sent away for assay, with 5 large sized samples also collected for dating. Dating ability based on handheld XRF zirconium values.

18 dolerite field samples were taken from the Cloncurry District in March 2016. The sample locations were based on existing knowledge of the area and radiometric maps of the area projected on QGIS. Areas with high uranium (blue) were chosen for sampling due to the association of uranium with mafic rocks. The points of high uranium given on the map were entered into a Garmin GPSMap 62s handheld GPS, with AGD-84 54K UTM zone co-ordinate system. Once at the outcrop, a hand lens and scribe would be used to confirm lithology, and a sledgehammer would be used to collect approximately 5kg of dolerite sample. The sample is then placed into calico bags and marked according to location, date and sample ID. The sample ID varies from D01 to D18 in accordance to sample number. Once the sample is collected, a GPS point is taken for mapping purposes. From each of the samples, a section is sent to Ignham Petrology to be cut for thin section petrography and a hand sample analysis is completed, focusing on mineralogy, grain size and alteration. Of the 18 field samples 5 samples were chosen for dating. These samples were D12, D14, D16, D17 and D18. All 18 samples were sent to ALS Townsville for a whole rock geochemistry report.

## 1.1.2 Core Sampling

### Materials

Diamond Drill Rig
Core Trays

**Methods**
Samples were chosen from CuDeco drill core at 6 random intervals, selections were based on lithology from reports and identification within the core shed. 6 samples were chosen in total, 2 from below the ore zone, 2 from within the ore zone and 2 from above the ore zone. Samples sent away for assay.

6 dolerite samples were taken from CuDeco Rocklands drill core. The core is drilled from a diamond drill rig with ID DODH068 within the Rocklands tenement. Of the 6 samples, 2 are taken from below the rocklands ore body, 2 are taken from within and 2 are taken from above. The sampling is randomly spaced and purely based on the lithology of the core. The sample lithology is dolerite which is decided from previous drill core reports and general identification. From each of the samples, a section is sent to (WHERE) to be cut for thin section petrography and a hand sample analysis is completed, focusing on mineralogy, grain size and alteration. All 6 samples were sent to ALS Townsville for a whole rock geochemistry report.

## 1.1.3 Pulp Sampling

**Materials**
Pulp data sheet analysis
Reverse circulation drill rig
Rock chips

1m RC bags

**Methods**

2014 (BATTLEAXE)
Rock chips collected from drill rig cyclone in 1m RC bags
Spear sampling used at every 2m interval
Speared samples tipped into calico bags, tied and then placed into poly-weave bags
Sent away for assay
2016
Pulp from previous assay withdrawn from pulp shed in accordance with dolerite locations of previous assay.
Sent away for assay

A total of 90 dolerite samples were sampled from pulp, originally in the form of rock chips from a reverse circulation (RC) drill rig cyclone. The drill rigs were located in Battle-axe, CHUM, Double oxide Magpie and Turf Club, and chosen for dolerite sampling due to their large spread around the study area. The rock chips were placed in 1m RC bags, with spear sampling completed at 2m intervals. The speared samples were poured into calico bags, tied and placed into poly-weave bags. They were sent to ALS Townsville in 2014 for whole rock analysis. The pulp remains from the first assay were re-located from the Cloncurry Barracks pulp-shed. The pulps were chosen based on their lithology. A spoonful of each pulp sample was placed into a sample bag. A duplicate sample was taken at every 15 pulp samples, and was followed by a standard sample. The standard sample was OREAS45d which was sourced from Ore Research and Explorations. The samples and standards were sent to ALS Townsville for a whole rock geochemistry report.

## *1.2 ALS WHOLE ROCK GEOCHEMISTRY*

### ME-MS61 ICP-MS and ICP-AES (ALS Resource)

**Materials**

0.25g prepared sample
perchloric acid
nitric acid
hydrofluoric acid
hydrochloric acid
inductively coupled plasma - atomic emission spectrometry
inductively coupled plasma - mass spectrometry

**Methods**

Sample is digested by the 4 acids.
Residue is topped up with dilute hydrochloric acid.
Then analysed by ICP-AES.
Sample is then diluted again if necessary
Analysed by ICP-MS.
Results corrected for spectral interelement interferences
Element data acquired (TRACE AND BASE METALS)

All field, drill and pulp samples were sent away for a whole rock geochemistry assay to ALS (Australian Laboratory Services) in Townsville. Several laboratory techniques were used to determine either major element oxide percentages, major and trace element abundances and/or rare earth element abundances.

ME-MS61 Inductively Coupled Plasma – Mass Spectrometry (ICP-MS) and Inductively Coupled Plasma – Atomic Emission Spectrometry (ICP-AES) were used to determine major and trace elements of all 17 field, 6 drill core and 90 RC pulp samples. Each sample was sectioned into a 0.25g portion, which is then digested by nitcric, hydrofluoric, hydrochloric and perchloric acids. The residue from this digestion is topped up with dilute hydrochloric acid and then analysed by ICP-AES. The remaining sample is diluted again if the concentrations of bismuth, mecury, silver, tungsten and molybdenum are high, and then analysed by ICP-MS. All results are corrected for spectral interelement interferences. It is possible not all elements can be quantatively extracted. ICP-AES and ICP-MS give the near-total concentrations for base metals and trace elements.

### ME-XRF06 (ALS resource)

**Materials**

0.9g Calcined/ignited sample
9.0g of Lithium Borate Flux
Auto-fluxer
X-ray fluorescence spectrometry

**Methods**

Calcined-ignited sample added to lithium borate flux and mixed.

Fused inside autofluxer between 1050-1100 degrees celcious.
A disc is prepared from the resulting melt and analysed by X-ray fluorescence spectrometry.
Element oxide is acquired (MAJOR OXIDES)

17 dolerite field samples and 6 drill core samples were analysed using ME-XRF06 for their concentrations of major element oxides. The samples were sectioned into 0.9g portions, then calcined or ignited before being added to and mixed with 9.0g of lithium borate flux (50 % - 50 % $Li_2 B_4 O_7$ – $LiBO_2$). The sample and flux are then fused inside an autofluxer between 1050-1100 degrees celcius. The resulting melt is then molded into a disk and analysed by X-ray fluorescence spectrometry, which gives major element oxide concentrations as a weight percentage.

## ME-MS81 ICP-MS (ALS resource)

**Materials**

0.2g prepared sample
0.9g lithium metaborate flux
ICP-MS
100ml of 4% HNO3 and 2%HCl3 solution

**Methods**

Add the sample to the lithium metaborate flux
Mix well and add to the furnace at 1000 degrees celcius
Resulting melt is cooled down and diffused in the 100ml solution
The solution is then analysed by ICP-MS
Sample decomposition is Lithium Metaborate Fusion (ULTRA TRACE)

15 out of the 17 field samples and 5 out of 6 drill core samples were analysed by ME-MS81 ICP-MS for their REE concentrations. 3 of the total samples could not be analysed due to their small sample size from previous analysis. The analaysed samples were sectioned into 0.2g portions and added to 0.9g of lithium metaborate flux. The two substances are mixed then fused at 1000 degrees celcius, then cooled and dissolved in 100ml of 4% HNO3 and 2% $HCl_3$ solution. This solution is then analysed by ICP-MS. However, base metal oxides and sulphides may often not be completely dissolved by the lithium borate fusion technique or become volatile, and therefore not quantitative. To analyse base metals and sulphides, 4-acid digestion was undertaken, with the same steps seen in MS61- ICPMS. All REE elements were determined using this method.

## *DATING*

## Samples

**Materials**

Field samples
Olympus Delta 50kV Premium hand-held XRF

### Methods

Samples for dating were chosen as good fresh rocks, good sized samples and were of the higher Zr composition as determined by spot-analysis by the Olympus Delta 50kV Premium.
5 samples were chosen, D12 from Monakoff, D14 from Battleaxe and D16-D18 from Mongoose

4 dolerite samples were chosen, D14 from Battleaxe and D16-D18 from Mongoose for zircon dating. Samples for dating were chosen as fresh rocks, 30cm^2 sized and were of the highest Zr concentration as determined by spot-analysis by the Olympus Delta 50kV Premium. All dating procedures took place within the University of Adelaide and Adelaide Microscopy.

## Jaw Crusher

### Materials

Jaw Crusher
Paper towel
Ethanol
Air Compressor
Safety equipment (glasses, hearing protection and closed in shoes)
Butchers paper

### Methods

Clean and remove any possible sample contamination from machine, chute, using air compressor, paper towel and ethanol.
Close machine and turn on, ensure jaws aren't hitting each other
Place fist sized samples into crusher.
Samples may be removed and ready for use.
Clean and remove any possible sample contamination from machine, chute, using air compressor, paper towel and ethanol.


Prior to use, the jaw crusher was completely blown down and wiped in ethanol to remove any possible contaminations. All interior and exterior parts including chute, crushing pads and landing tray were cleaned. Butchers paper was placed onto the landing tray before crushing commenced to reduce contamination. Following this, each sample was crushed independently and removed from the jaw crusher and placed on a clean bench. After a sample was crushed, a full compressor and ethanol clean was completed to avoid contamination.

## Sieve Shaker

### Materials

Sieve Shaker
Sieves
Paper towel
Ethanol
Air Compressor
Safety equipment (glasses, hearing protection and closed in shoes)

**Methods**

Clean and remove any possible sample contamination from sieve shaker container and machine using air compressor, paper towel and ethanol.
Place 79 micron and 400 micron mesh sheets within the sieve container to separate the ziron particles
Place crushed samples onto the largest mesh
Turn sieve shaker on for as long as required.
Remove container from sieve shaker and place on clean butchers paper to avoid contamination
Remove larger sample pieces and place on clean butchers paper to avoid contamination
Place sample dust between the two mesh sheets into sample bags to be used for zircon/monazite dating.
Clean and remove any possible sample contamination from sieve container and machine, using air compressor, paper towel and ethanol.


## Disk Mill

### Materials

Disk Mill
Paper towel
Ethanol
Air Compressor
Safety equipment (glasses, hearing protection and closed in shoes)

### Methods

Clean and remove any possible sample contamination from machine, disks, using air compressor, paper towel and ethanol.
Close machine and turn on, ensure disks aren't hitting each other
Place gravel sized samples into machine and let grind to dust.
Samples may be removed and ready for use in the sieve shaker, disks can be moved closer together to further grind gravel to finer dust.
Clean and remove any possible sample contamination from machine, disks, using air compressor, paper towel and ethanol.

Prior to use, the disk mill was completely blown down and wiped in ethanol to remove any possible contaminations. All interior and exterior parts including chute, crushing disks and landing tray were cleaned. Following this, each sample was crushed independently and removed from the jaw crusher and placed on a clean bench. After a sample was crushed, a full compressor and ethanol clean was completed to avoid contamination.

## Panning

### Materials

Pans (1 large 1 small)
Water squirt bottle
Paper towel
Funnels
Large beakers
Funnel Stand

Filter paper
Oven

**Methods**
Clean and remove any possible sample contamination from pans, funnels beakers etc.
Tip adequate (100g) amount of sample into large pan and fill with water and empty to remove any suspended particles.
Repeat until relatively dense material remains
Pour sample into the small pan and fill large pan with water
Pan sample into the larger pan until adequate amount of sample remains for zircon portion.
Pour both samples into separate funnels with filter paper inside over a beaker.
Let sample dry, or place in oven.
Clean all equipment with water and paper towel to avoid contamination.

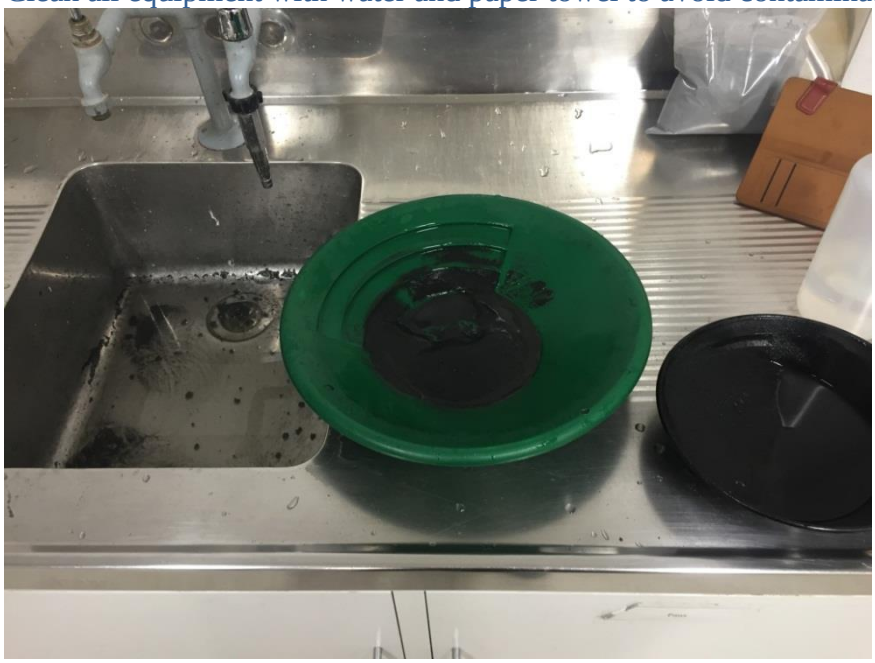

## Hand Magnet Separation

**Materials**
Hand magnet (REE) in plastic sealed bag
Paper
Kim whipes

**Methods**
Lay the sample out on paper
Cover the magnet in kim wipes and scan over the sample to remove any extrememly magnetic minerals
Place the magnectic minerals onto another piece of paper
Keep both samples
In between each sample change the paper and kim wipes to avoid contamination

## Frantz

### Materials

Frantz
Air Compressor
Paper

### Methods

Clean every component of the franz using compressed air.
Follow the instructions for using the frantz (regarding safe power preocedures)
Repeat the Frantz separation at 0.5A, 1.0A and 1.75A to remove the maximum amount of minerals
Clean the Frantz out for each separate sample.

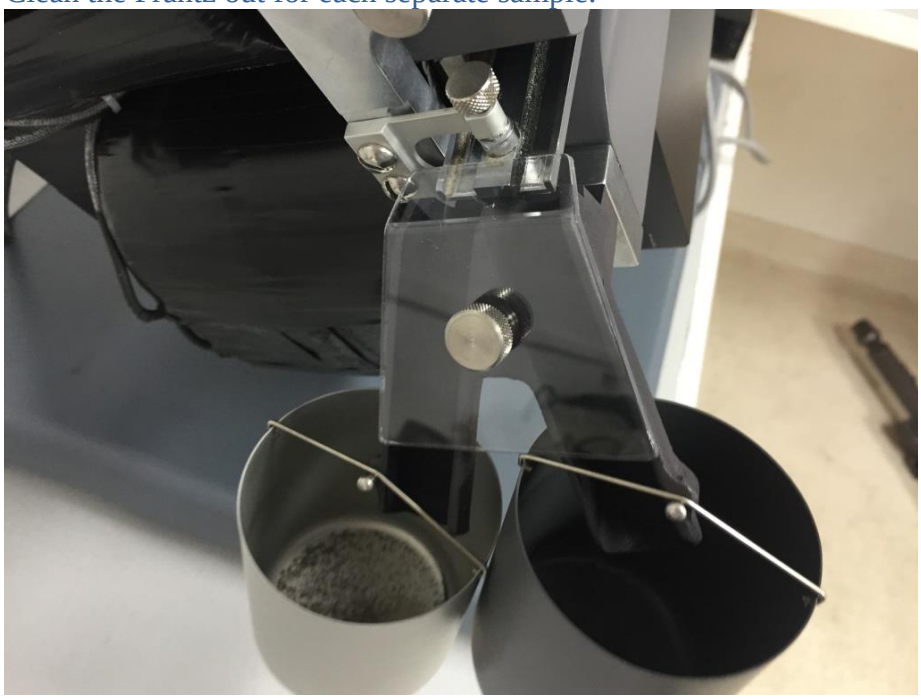

## Heavy Liquid Separation

### Materials

Dry Ice – cryo gloves
Funnels
Beakers
Plastic test tubes
Heavy liquid
deionised water
Filter paper
Hot plate
Small paint brush
Vial

### Methods

Pour approximately 10g of sample into plastic tubes and fill with approximately 8ml of heavy liquid, shaking well with a lid on

Allow samples to stand in heavy liquid until the heavy minerals have sunk and the lighter minerals are floating
Place the bottom of the test tube into the dry ice and allow the bottom half to freeze
Set up beakers underneath funnels and place filter paper inside the funnels
Once the bottom half of test tubes have frozen, pour the top half into the filter paper laced funnel and allow heavy liquid to be caught in the beaker
Leave heavy mineral portion to defrost
Once the heavy mineral portion has defrosted, pour into another funnel over a beaker, and used deionised water to ensure every grain is removed from the test tube
Once the portions have completely dripped through return the heavy liquid to its container to be used again, and return the diluted heavy liquid to its designated container
Use the hot plate to remove any residue liquid, ensuring the sample is completely dry
Using a small paint brush, place the heavy mineral sample in a vial ready for picking.

## Hand Picking

**Materials**

Microscope x2
Light
Glass dish

Pick
Zircon Mount
Double Sided Tape
Ethanol
Paper towel

**Methods**

Ensure the glass dish is clean from any previous grains by wiping with ethanol and paper towel
Remove the cylindrical section of the zircon mount and place double sided sticky tape to the surface of the mount, and place under the first microscope and turn the light on
Pour approximately 5g of zircon sample into the dish.
Place glass dish under the microscope and turn the light on
Adjust the focus and zoom of both microscopes
Identify zircons based on their shape and size, elongated grains with smooth to rounded edges, may be varying in colour but generally clear
Once a zircon has been identified, rub the pick on your skin to collect a small amount of oil for the grain to stick to
Pick up the grain and transfer it to the mount, place on the double sided sticky tape
Line the zircons along the mount
Once an adequate amount of zircons have been picked (50 for dolerite) remove the sample from the dish and clean with ethanol again to avoid contamination
Turn off the microscope lights.

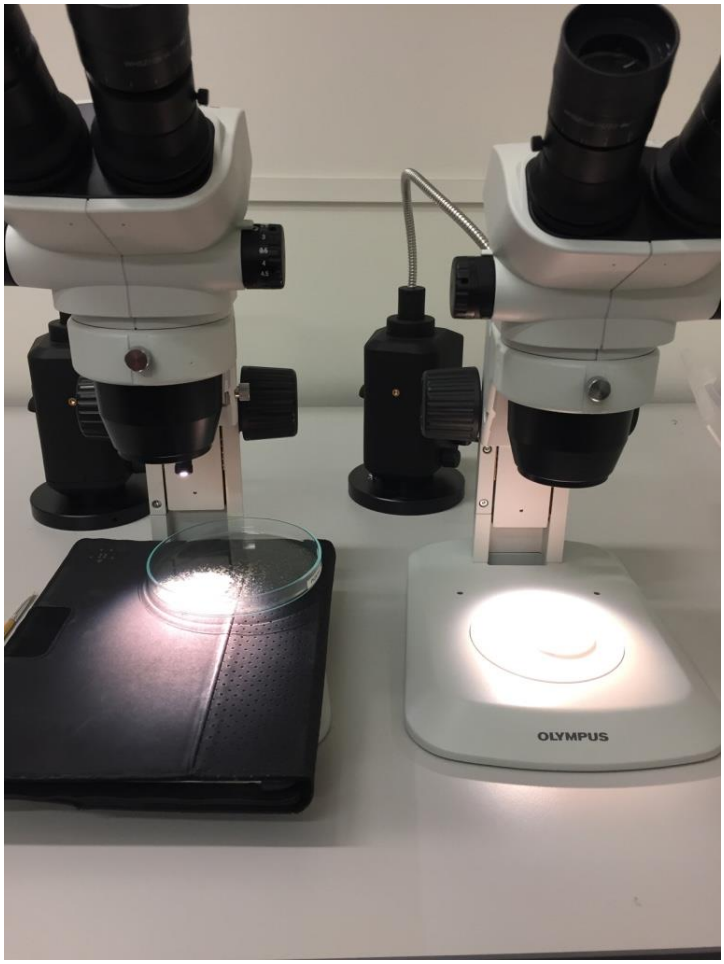


## Epoxy Resin

### Materials

Epoxy
Hardener
Rubber Gloves
Electric Scales
Paper towel
Pop-stick
50ml plastic beakers
zircon mounts
Vasoline
Oven

### Methods

Place paper towel down over work space to avoid epoxy spills
Using rubber gloves, rub vasoline on the inside of the zircon mount to allow an easy release once epoxy has set
Place paper towel and one plastic beaker onto the scales and set to zero
Following the ratios of 5ml Epoxy and 1.15ml Hardner per mount, pour the necessary amount of epoxy into the plastic beaker, immediately cleaning any spills or droplets.

Set the scales to zero again with the epoxy filled beaker, and pour necessary amount of hardener into the beaker.
Immediately clean any spills or droplets with paper towel.
Using the pop-stick, stir the sample until the liquid goes clear
If there is an abundant amount of bubbles, place the beaker in the oven for up to two minutes to allow the bubbles to rise to the top and be scraped away to the side by the pop-stick
Slowly pour the clear epoxy resin into the zircon mount to avoid bubbles, filling to approximately 1cm from the bottom
Allow at least 6 hours to set
Once the resin has set, remove the hardened epoxy disk from the zircon mount.
Sample is ready for polishing

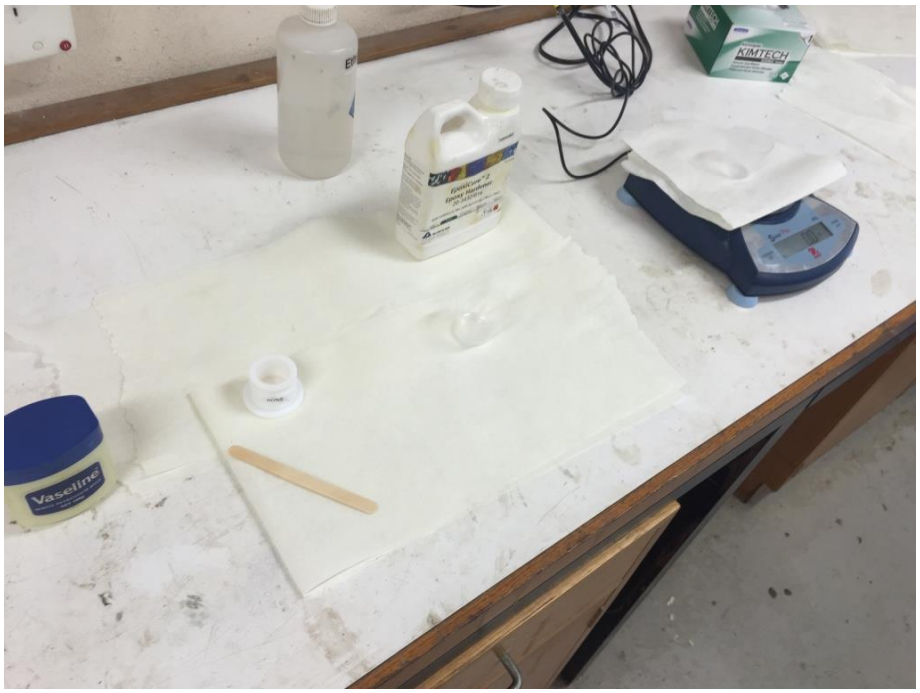


## Polishing

### Materials

Knuth Rotor polishing disk
DP-U4 polishing cloth lap
Soniclean sonic bath
Kim wipes
Microscope
Blue and Green Diamond Paste
Blue and Brown polish cloth

### Methods

Remove epoxy resin from mount
Analyse mount for zircons under microscope
Using water and the Knuth rotor polishing disk, polish epoxy block (figure eight) on zircon surface until a matte coloured finish is shown, must be dry

Contiunally examine sample under microscope to ensure no damage to zircons is done
Apply green diamond paste to surface of zircon and place firmly into the DP-U4 polishing lap, which has the blue polish cloth mounted
Turn on both the DP-U4 main polishing table and the small rotor to ensure continual movement of the epoxy blocks
Keep rotating cloth wet and leave running for ten minutes
After ten minutes, replace the blue cloth with the brown cloth, and apply blue diamond paste to the zircon surface of the mount
Apply the same process for the brown cloth and allow the DP-U4 cloth lap to run for ten minutes
After ten minutes, place epoxy blocks inside a sonic bath and run for 5 minutes to ensure they are completely cleaned and rid of dirt.
Ensure everything is returned and powered off safely, epoxy blocks are ready to be carbon coated for SEM CL imaging


## SEM

### Methods

Place mount with carbon tape into mount stand.

Turn on SEM and allow vacuum seal.
Set SEM visual contrast manually using gold as a standard
Locate apatite and titanate grains and record location via BSE images

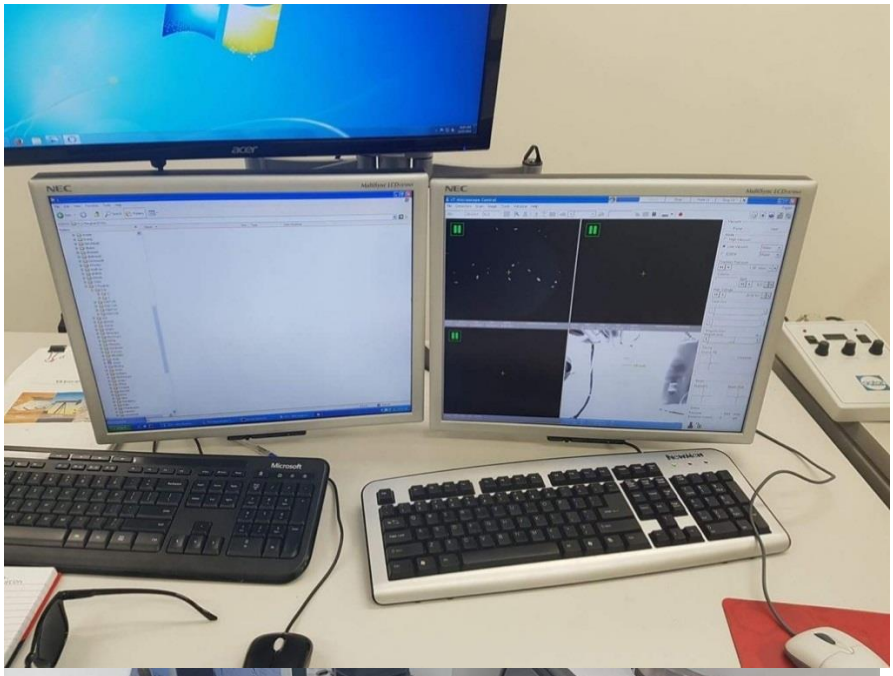

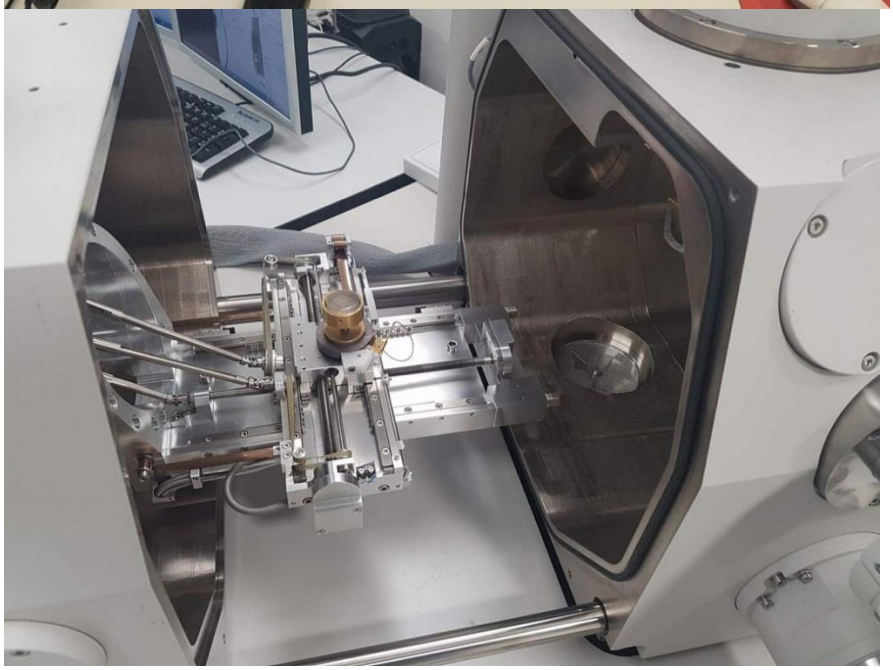

## Resonetics Laser

### Methods

Place standards and sample within laser slot
Take image of mount and locate sample grains
Align laser beam and orientation
Locate all grains to be ablated and tag them

Locate and tag standards to the necessary amount, making sure to adjust laser accuracy on each shot
Set laser to 30 micron diameter and make sure correct elements are selected.
Run laser for designated samples

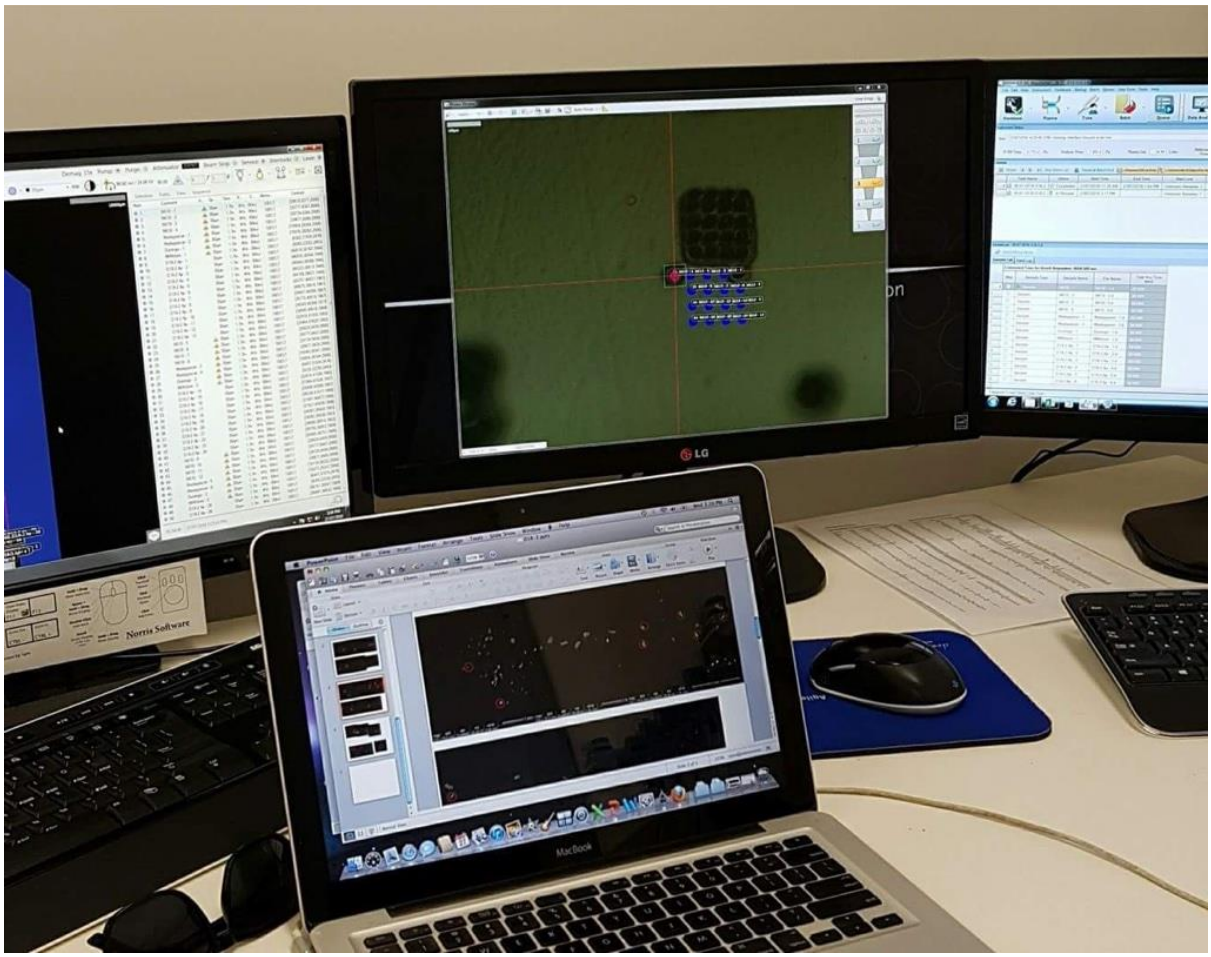


## Iolite 6.37

### Methods

Import all csv. Files from the laser into one iolite file
Set times of interval to get the optimum amount of U-Pb readings of samples and standards and to remove the ‘dead’ time.
Apply info seen in photo before crunching the data.
Remove any botch samples and continue to crunch data until happy.
Export the whole file and save.

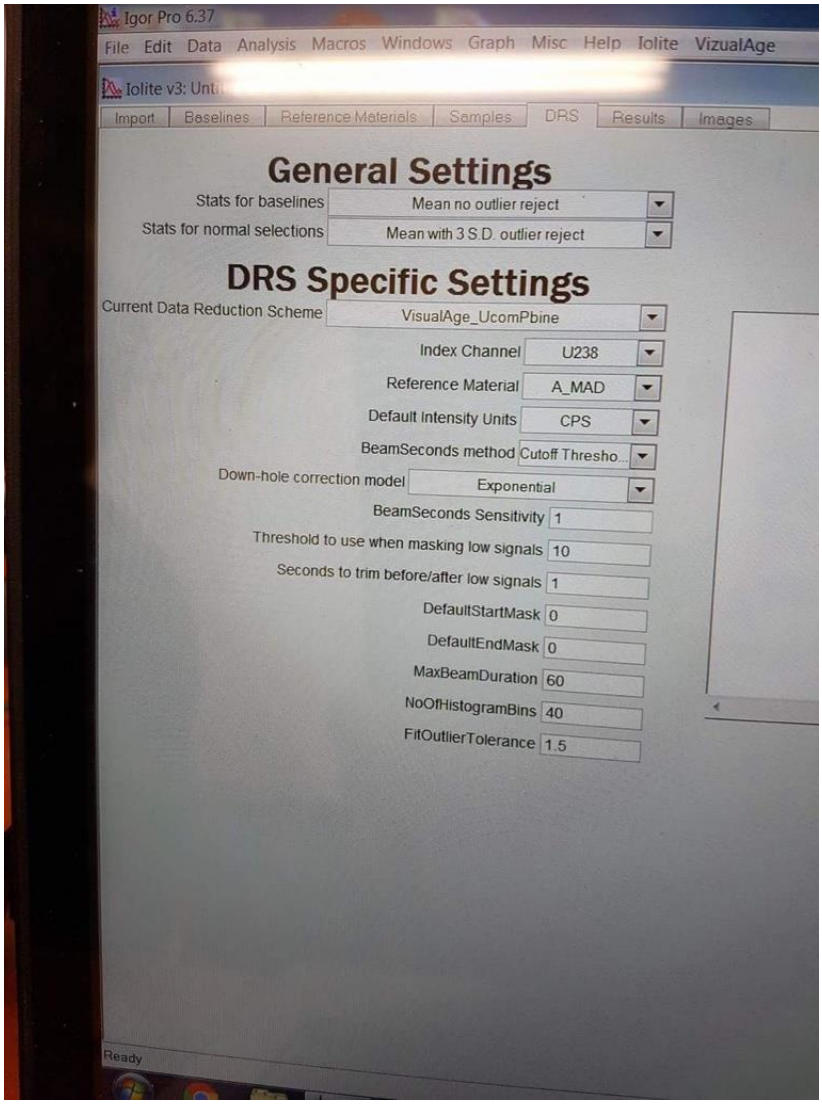


## Isoplot

### Methods

Import saved files from iolite and create terra-wasserburg plots
Remove samples to constrain error if necessary
Use samples to create weighted standard deviation plot of age.
Save save save.

## ***MAPPING***

### Materials

QGIS 2.14
MIM data files, radiometrics, magnetics, gravity
Field GPS points
Geology of Cloncurry field data (http://www.ga.gov.au/metadata-gateway/metadata/record/gcat_a05f7892-b45e-7506-e044-00144fdd4fa6/Geology+of+the+Cloncurry)

Mt Isa inlier geology http://www.ga.gov.au/metadata-gateway/metadata/record/gcat_a05f7892-b5ae-7506-e044-00144fdd4fa6/Mount+Isa+Inlier+1%3A100+000+geology%3A+lithostratigraphy+and+chronostratigraphy

**Methods**
Using downloaded data of the Cloncurry region sourced from MIMRD and online, and gps data points, maps of the study area are created on QGIS to gain understanding of the area geographically and geologically.

# ***GEOCHEMICAL ANALYSIS***

## QAQC

**Materials**
Microsoft Excel 15.21.1

**Methods**
Before analysis can be conducted a Quality Assurance and Quality Control report must be completed. The report involves comparing the OREAS45d standards sent in with the dolerite samples with their certified values and the 95% confidence intervals. If standard data matches the existing data, the assay data is useable. Duplicates were also taken of the data and plotted against each other to determine precision. If the data plots within a line of regression the data is useable. This QAQC report uses the elements Al, Ca, Cu, Co, Mn, Zn, V, La and Ce.

## Petrography

**Materials**
Thin sections
Microscopes (BRAND)

**Methods**
From each of the 18 field samples and 6 core samples collected, a part of each sample was designated for thin section and sent away to (WHERE). The thin sections were looked at and analysed under microscope (BRAND) and be mineralogicaly analysed.

## ioGAS

**Materials**
ioGAS 6.1

**Methods**
ioGAS 6.1 will be used to create classification and discrimination diagrams of the dolerite data. The diagrams that will be created will mostly follow the textbook ‘Using Geochemical Data’ by Hugh Rollinson, which explains how and why each diagram is used, and also diagrams from more recent papers involving basaltic or doleritic lithologies.

References (6)

- B-Axe drill report
- Als Resources
- Mapping resources
- Hugh Rollinson textbook

## SEM

### Materials

Carbon Coated Samples
SEM Qanta 600

### Methods

Load carbon coated samples onto SEM Stage

## APPENDIX 2: PETROLOGY

DO1




| LOCATION | Mt Glorious |
|---|---|
| EASTINGS | 439907 |
| NORTHINGS | 7708475 |
| LITHOLOGY | Dolerite |
| FIELD COMMENTS | Sheared zone of dolerites in-between quartzite |

## Petrography Report

| Sample ID | DO1 Mt Glorious | Doleritic<br>Fractures<br>Slight Green Tinge |
|---|---|---|

| Mineral | Primary/ Second | Size (mm) | Abundance % | Characteristics |
|---|---|---|---|---|
| Albite | S | 1-2 | 30 | Dominant and replacing plagioclase |
| Plag | P-S | 0.5-2 | 20 | Most unaltered plag is along fractures, which is |
| HB | P-S | 0.2-0.8 | 15 | Strong relationship with biotote, could be chlorite |
| Mag | S | 0.2-0.5 | 10 | Very replacive strong cob-web textures amd rimmed with sphene |
| Biotite | P | 0.1-1 | 10 | Borders hornblende but also has strongly formed crystals |
| Sphene | S | 0.5 | 5 | High relief generally localized around magnetite |
| Quartz | S | 0.5-0.8 | 5 | Forms mostly along veins |
| Act | S | 0.1-0.3 | 5 | Mainly in veins or the edges of hornblende |
| | | | | |

**Veins and fractures dominaly plag and quartz, with actinolite and sphene included**

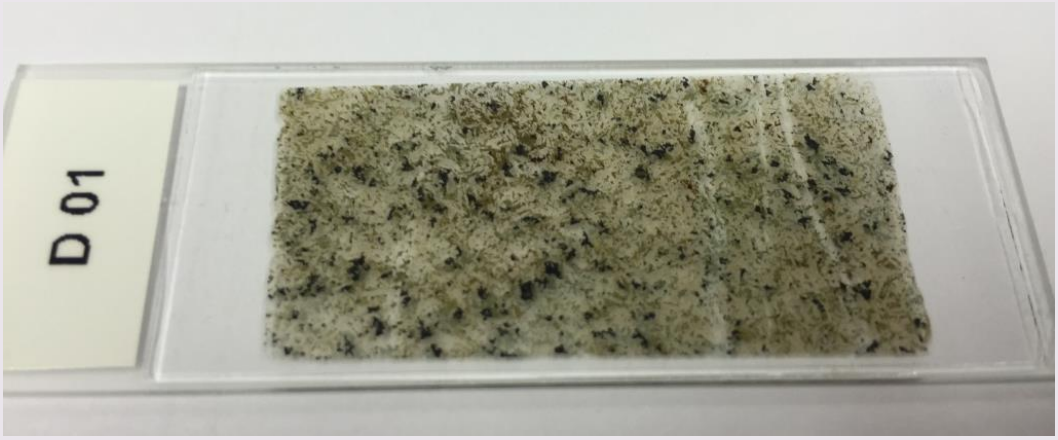

# DO2

| LOCATION | Eternal |
|---|---|
| EASTINGS | 463077 |
| NORTHINGS | 7720393 |
| LITHOLOGY | Dolerite |
| FIELD COMMENTS | Sample taken along the calc-silicate boundary |

## Petrography Report

| Sample ID | DO2 Eternal | Doleritic<br>Very Green<br>Long Parallel Fractures |
|---|---|---|

| Mineral | Primary/ Second | Size (mm) | Abundance % | Characteristics |
|---|---|---|---|---|
| Sericitic albite | P | 1-3 | 40 | Some grains surrounded by orange mineral, scapolite |
| HB | Both | 1-3 | 30 | Strong shapes but can be fractured with chlorite infill |
| Sericite | I | 1-2 | 10 | Replaces Albite |
| Chlorite | I | 1-3 | 10 | Not pleochroic and very pale green |
| Mag | I | 0.5-1 | 7 | Very placive |
| Epidote | I | 0.1-0.2 | 1 | Strong relief and birefringence |
| Titanite | I | 0.2-0.5 | 1 | Small grains inside of HB |
| Scapolite | I | 0.5 | 1 | Mantles around albite veins |
| | | | | |

Some albite are fractured with chlorite veins through them, can also show cross hatch twinning.
Veins are chlorite based but done seem to fracture through any other minerals, could be a slide technicality.

# DO3


| LOCATION | Fifi |
|---|---|
| EASTINGS | 463475 |
| NORTHINGS | 7719872 |
| LITHOLOGY | Dolerite |
| FIELD COMMENTS | Truncating calc-silicates and granite |

## Petrography Report

| Sample ID | DO3 Fifi | Doleritic Slight Green Tinge |
|---|---|---|

| Mineral | Primary/ Second | Size (mm) | Abundance % | Characteristics |
|---|---|---|---|---|
| Albite | P | 0.5-2 | 40 | Lots of small grains mainly fractured |
| HB | P | 1-3 | 30 | Large grains with very high relief |
| Scapolite | S | 1-4 | 10 | Parallel extinction, massive and orange-grey |
| Epidote | S | 0.1-0.5 | 5 | Forming within scapolite mass |
| Mag | S | 0.5-2 | 5 | Mainly alters within HB |
| Sericite | S | 0.5-2 | 5 | Smaller abundances taking over albite |
| Chlorite | S | 1-3 | 5 | Possibly HB |
| | | | | |
| | | | | |

**Scapolite appears with parallel extinction and appears to encompass epidote, small dark unidentifiable mineral also noticed within sample.**

# DO4

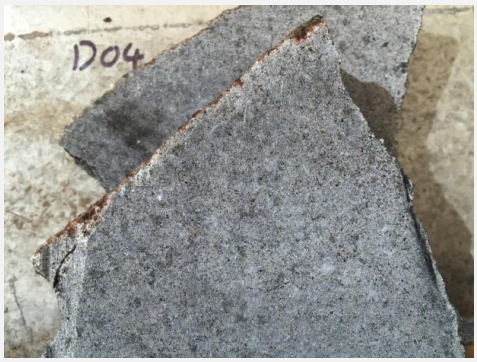


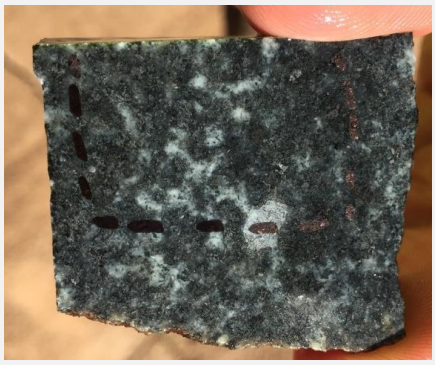

| LOCATION | D-Ring |
|---|---|
| EASTINGS | 466804 |
| NORTHINGS | 7720682 |
| LITHOLOGY | Dolerite |
| FIELD COMMENTS | Hosted in calc-silicates |

## Petrography Report

| Sample ID | DO4 D-Ring | Doleritic Non-altered |
|---|---|---|

| Mineral | Primary/ Second | Size (mm) | Abundance % | Characteristics |
|---|---|---|---|---|
| Plag | P | 0.5-3 | 45 | Very unaltered with perfect twinning |
| OPX | P | 1-5 | 25 | 45 degree extinction |
| CPX | P | 1-4 | 15 | Paralell extinction |
| Qtz | P | 0.1-0.5 | 5 | Small clasts surrounded by plagioclase |
| Mag | P | 0.1-1 | 5 | Only forms around and within cpx fractures |
| Albite | S | 0.2-0.5 | 2 | Very zoned in small areas |
| HB | S | 0.2-0.5 | 1 | Similarly zoned in small areas |
| Chlorite | S | 0.1-0.5 | 1 | Similar to biotite |
| Biotite | S | 0.1-0.5 | 1 | Small amounts, associated with zoned areas |

Areas of albitisation and hornblende/chlorite alteration of OPX
CPX tends to have magnetite within fractures and therefore a higher relief

# DO5


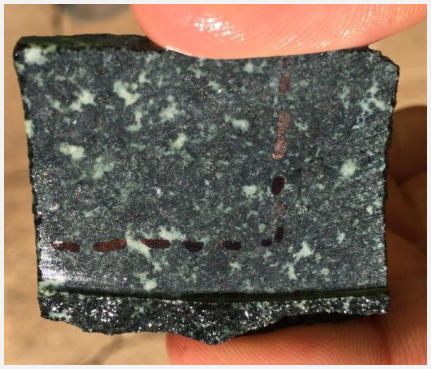

| LOCATION | Walton |
|---|---|
| EASTINGS | 460639 |
| NORTHINGS | 7709911 |
| LITHOLOGY | Dolerite |
| FIELD COMMENTS | Associated with calc-silicate, granite and ironstone. |

## Petrography Report

| Sample ID | DO5 Walton | Dolerite No Green Tinge |
|---|---|---|

| Mineral | Primary/ Second | Size (mm) | Abundance % | Characteristics |
|---|---|---|---|---|
| Sericitc Albite | S | 1-3 | 40 | Very sericitc no plagioclase |
| HB | P | 1-5 | 30 | High relief could be chlorite |
| Quartz | P | 0.5-2 | 10 | Surrounded by albite |
| CPX | P | 1-5 | 6 | Parallel extinction with high birefringence, heavily fractured |
| Mag | S | 0.1-5 | 5 | Very focused in HB areas |
| Epidote | S | 0.5-1 | 5 | High birefringence and relief |
| Scapolite | S | 0.5-1 | 3 | Borders albite grains |
| Titanite | S | 0.5-2 | 1 | Strong relief and association with Magnetite |
| | | | | |

Minerals are very altered and show large differences at grain boundaries, do not have sharp contacts
Epidote forms coeval with quartz

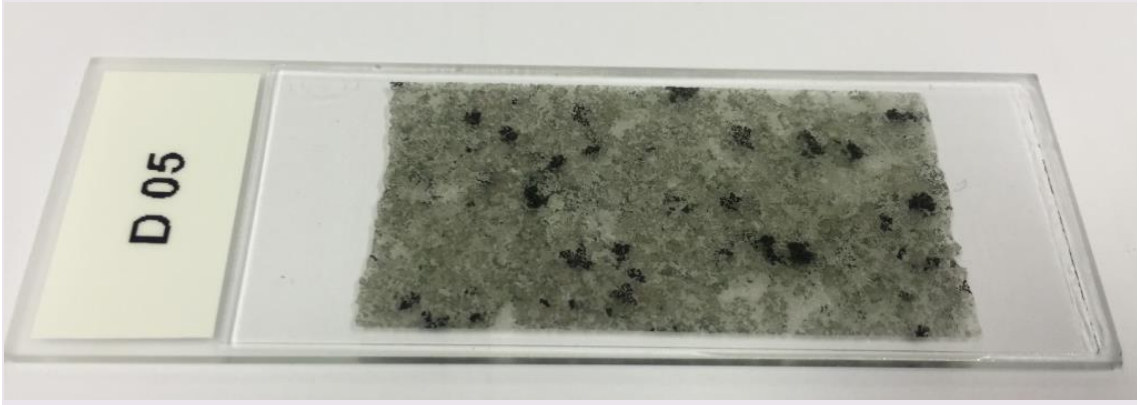

# DO6


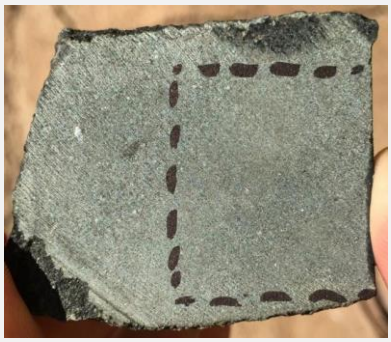

| LOCATION | Wilgar |
|---|---|
| EASTINGS | 460639 |
| NORTHINGS | 7709911 |
| LITHOLOGY | Basalt |
| FIELD COMMENTS | Truncating Mt Norna Quartzite, porphyblastic texture. |

## Petrography Report

| Sample ID | DO6 Wilgar | Basalt<br>Brown Tinge<br>Metamorphosed |
|---|---|---|

| Mineral | Primary/ Second | Size (mm) | Abundance % | Characteristics |
|---|---|---|---|---|
| Biotite | S | 0.01-0.1 | 45 | Shows orientated fabric |
| HB | P | 0.05-0.5 | 30 | Very replacive with no fabric |
| Mag | S | 0.05-0.5 | 10 | Cubic and sporadically found |
| Qtz | P | 0.05-0.1 | 10 | Smaller grains intergrown with biotite |
| Plag | P | 0.05-0.3 | 3 | Few relict plag but mainly altered to sericitic albite |
| Sericite | S | 0.05-0.3 | 2 | Replacing plag |
| | | | | |
| | | | | |
| | | | | |

**Biotite tends to show a metamorphosed fabric.**
**Sericite shows real dark brown regions.**

# DO7


| LOCATION | Walton |
|---|---|
| EASTINGS | 462196 |
| NORTHINGS | 7710534 |
| LITHOLOGY | Dolerite |
| FIELD COMMENTS | Shows small fractures, intrusion striking NW-SE 320 degrees |

## Petrography Report

| Sample ID | DO7 Walton | Dolerite Green Tinge |
|---|---|---|

| Mineral | Primary/ Second | Size (mm) | Abundance % | Characteristics |
|---|---|---|---|---|
| Sericitic Albite | P | 1-4 | 45 | Partially sericitic but shows original albite |
| HB | S | 2-6 | 30 | Replacing pyroxenes, shows twinning |
| Mag | S | 0.-6 | 10 | Commonly forming around HB very replacive textures |
| Act | S | 0.1-0.5 | 5 | Needles forming around HB |
| Scapolite | S | 0.1-2 | 5 | Forms along grain boundaries |
| K-feld | S | 1-2 | 3 | yellow-white in CPL |
| Qtz | S | 1-2 | 2 | undulose extinction |
| | | | | |
| | | | | |

**All existing pyroxenes are altered to hornblende and actinolite.**
**Higher amounts of K-feldspar and quartz in this slide compared to others**

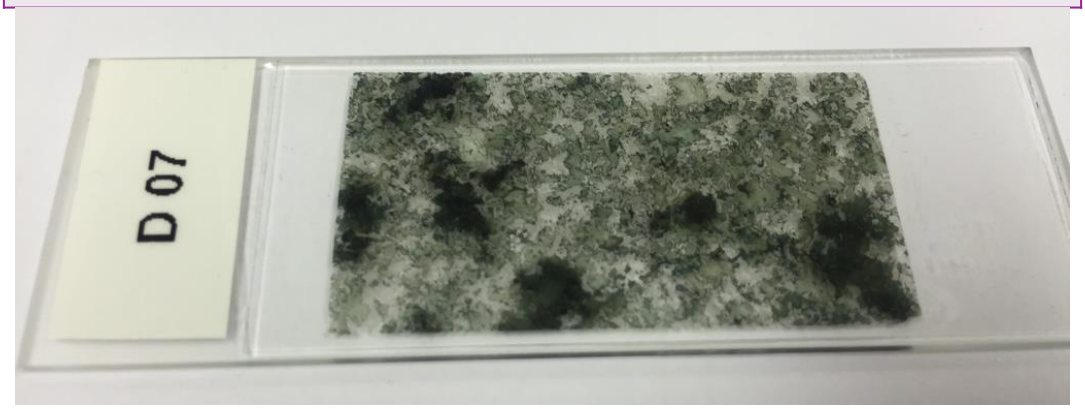

# D09

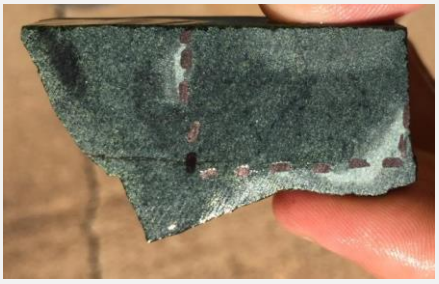

| LOCATION | Remedy |
|---|---|
| EASTINGS | 466756 |
| NORTHINGS | 7711516 |
| LITHOLOGY | Basalt |
| FIELD COMMENTS | Large dolerite-basalt region |

## Petrography Report

| Sample ID | DO9 Remedy | Basalt<br>Fractured<br>Green Tinge<br>Metamorphosed |
|---|---|---|

| Mineral | Primary/ Second | Size (mm) | Abundance % | Characteristics |
|---|---|---|---|---|
| Epidote | S | 0.01-0.08 | 40 | Strong relief and appears post metamorphism |
| HB | P | 0.01-0.1 | 30 | Dark blue-green surrounds rounded epidote grains |
| Actin | S | 0.01-0.05 | 15 | Or chlorite- creates the fabric and is a dominant mineral |
| Qtz | S | 0.01-0.05 | 10 | Within groundmass, coeval with epidote |
| Mag | S | 0.01-0.05 | 3 | Randomly spread |
| Albite | S | 0.01-0.08 | 2 | |
| | | | | |
| | | | | |
| | | | | |

**Shows a metamorphic fabric.**
**Vein is lined with chlorite and quartz**

# D10


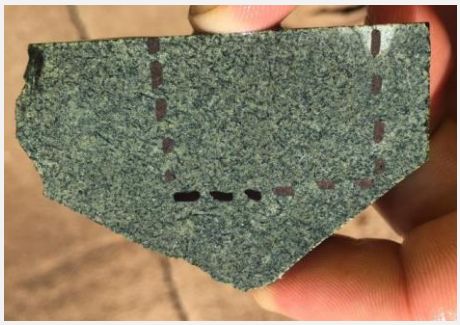

| LOCATION | Remedy |
|---|---|
| EASTINGS | 467310 |
| NORTHINGS | 7718052 |
| LITHOLOGY | Dolerite |
| FIELD COMMENTS | Appears metamorphosed |

## Petrography Report

| Sample ID | D10 Remedy | Dolerite Green Needley |
|---|---|---|

| Mineral | Primary/ Second | Size (mm) | Abundance % | Characteristics |
|---|---|---|---|---|
| Epidote | S | 0.01-0.2 | 40 | Varying in colour but has high relief |
| Actin | S | 0.1-0.2 | 20 | Dominant amphibole with no fabric |
| HB | S | 0.1-0.5 | 15 | Not as commin compared to other samples |
| Qtz | P | 0.1-0.5 | 15 | Lots of clusters, main groundmass mineral |
| Calcite | S | 0.1-0.5 | 5 | Strong distinct twinning |
| Albite | S | 0.01-0.1 | 5 | Small zones of albitised material |
| Mag | S | 0.1-0.5 | 1 | Not abundant |
| | | | | |
| | | | | |

**Calcite intergrown with quartz.**
**Slight orientation of HB and actinolite.**
**Calcite has high relief and birefringence lines.**

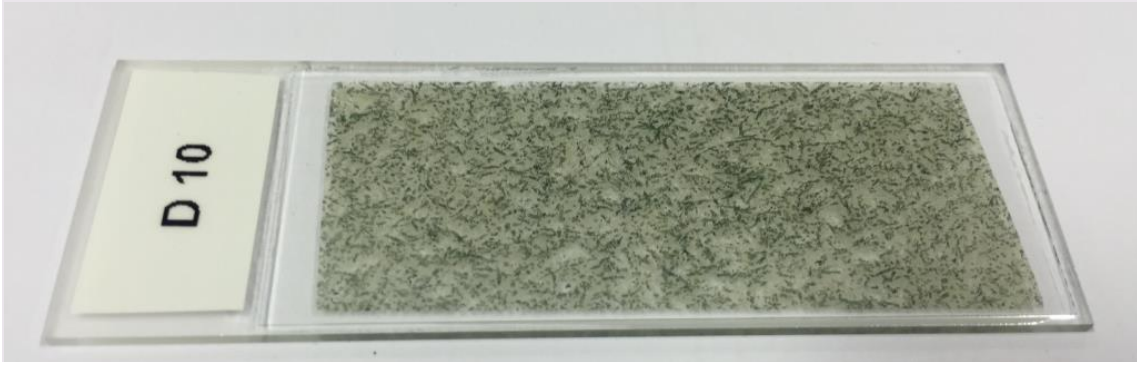

# D11

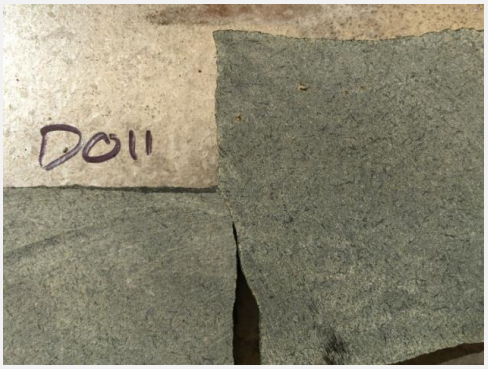


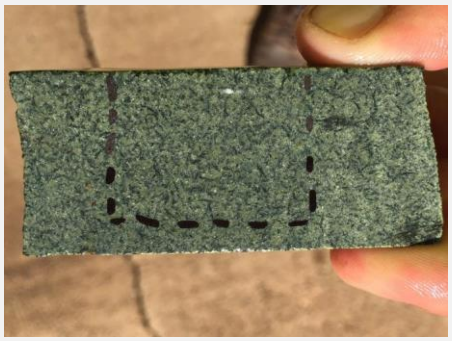

| LOCATION | Monakoff |
|---|---|
| EASTINGS | 468156 |
| NORTHINGS | 7718588 |
| LITHOLOGY | Basalt |
| FIELD COMMENTS | 4m wide intrusion, appears to be metamorphosed |

## Petrography Report

| Sample ID | D11 Monakoff | Basalt<br>Green<br>Needley<br>Fractured |
|---|---|---|

| Mineral | Primary/ Second | Size (mm) | Abundance % | Characteristics |
|---|---|---|---|---|
| Epidote | S | 0.05-0.5 | 30 | Clustered with high relief |
| Qtz | P | 0.05-0.1 | 25 | Small grains but also found within vein |
| HB | P | 0.1-0.5 | 20 | Replacing pyroxenes |
| Actin | S | 0.01-0.1 | 10 | Most abundant amphiboles |
| Calcite | S | 0.05-0.1 | 10 | In vein with sheen in CPL |
| Albite | S | 0.05-0.1 | 4 | Small clusters of sericite |
| Biotite | S | 0.05-0.1 | 1 | Altering around HB |
| | | | | |
| | | | | |

**Large abundance of epidote.**
**Veins are filled with calcite and quartz**

# D13


| LOCATION | Battleaxe |
|---|---|
| EASTINGS | 424187 |
| NORTHINGS | 7720297 |
| LITHOLOGY | Dolerite |
| FIELD COMMENTS | Intruding Mt Norna Quartzite, very small intrusion |

## Petrography Report

| Sample ID | D13 Battleaxe | Doleritic<br>Green<br>Shows a fabric |
|---|---|---|

| Mineral | Primary/ Second | Size (mm) | Abundance % | Characteristics |
|---|---|---|---|---|
| HB | P | 1-2 | 30 | Large grains altering to biotite |
| Sericite | S | 0.5-2 | 20 | Overprinting most albite grains |
| Qtz | P | 0.1-1 | 15 | Small grains throughout sample |
| Mag | S | 0.5-2 | 10 | Inside of HB |
| Biotite | S | 01.-0.8 | 10 | Forms along amphiboles but also on its own |
| Actin | S | 0.1-0.5 | 7 | Forming around sericite and magnetite |
| CPX | P | 0.5-2 | 5 | Getting replaced by HB and sericite |
| Albite | S | 0.5-1 | 2 | Replacing plagioclase in dark zones |
| Plag | S | 0.2-0.8 | 1 | Relict plagioclase grains exist |

**Orientated fabric is noticeable.**
**Minimal plag and metamorphosed.**

# D14


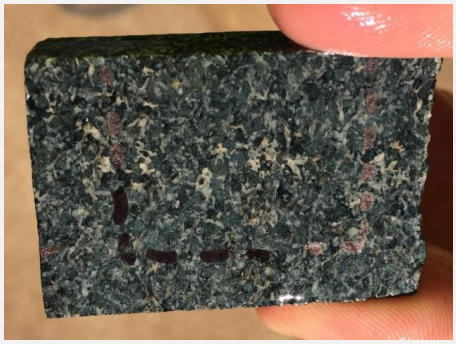

| LOCATION | Battleaxe |
|---|---|
| EASTINGS | 428698 |
| NORTHINGS | 7718658 |
| LITHOLOGY | Gabbro |
| FIELD COMMENTS | Hosted in Mt Norna Quartzite |

## Petrography Report

| Sample ID | D14 Battleaxe | Gabbroic<br>Albitised and Chlorite Altered |
|---|---|---|

| Mineral | Primary/ Second | Size (mm) | Abundance % | Characteristics |
|---|---|---|---|---|
| Sericitic Albite | S | 1-3 | 45 | Replacing plag, many grains are fractured |
| HB | P | 1-4 | 20 | Dark to light green in PPL with high birefringence in CPL |
| CPX | P | 1-3 | 10 | High relief and angular extinction being replaced by chlorite |
| Qtz | P | 0.1-0.5 | 5 | Trace amounts |
| Chlorite | S | 1-3 | 5 | Replacing pyroxene and amphiboles |
| Mag | S | 0.1-1 | 5 | Filling in free space, associated with albite granis |
| Actin | S | 0.1-1 | 3 | Small amounts of needles, late stage |
| Epidote | S | 0.1-0.5 | 2 | Small amounts and very replacive |
| | | | | |

**Accessory inerals include biotite, pyrite and various other unidentifiable minerals**

# D15


| LOCATION | Taipan |
|---|---|
| EASTINGS | 447936 |
| NORTHINGS | 7708120 |
| LITHOLOGY | Porphyritic Basalt |
| FIELD COMMENTS | Outside Taipan open pit |

## Petrography Report

| Sample ID | D15 Taipan | Basalt Mineralised |
|---|---|---|

| Mineral | Primary/ Second | Size (mm) | Abundance % | Characteristics |
|---|---|---|---|---|
| Sericite | S | 0.5-1 | 25 | Makes up groundmass |
| Biotite | S | 0.05-0.2 | 20 | Makes up groundmass |
| Mag | S | 0.01-0.8 | 20 | Strongly concentrated around bitiote grains |
| Plag | P | 0.1-2 | 20 | Edges altered by sericite, forming needles |
| Qtz | P | 0.01-0.1 | 7 | Large late stage grains |
| HB | S | 0.1-1 | 2 | Small amounts in the ground mass |
| Epidote | S | 0.01-0.1 | 2 | Late stage, makes up porphyroblasts |
| CPX | P | 0.1-0.5 | 2 | May not be clino |
| K-Feld | P | 0.1-0.5 | 2 | Associated with expected clino |

**Epidote porphyroblast surrounded by sericite.**
**2 generations of veins present, one qtz and the other amphibole and chlorite.**

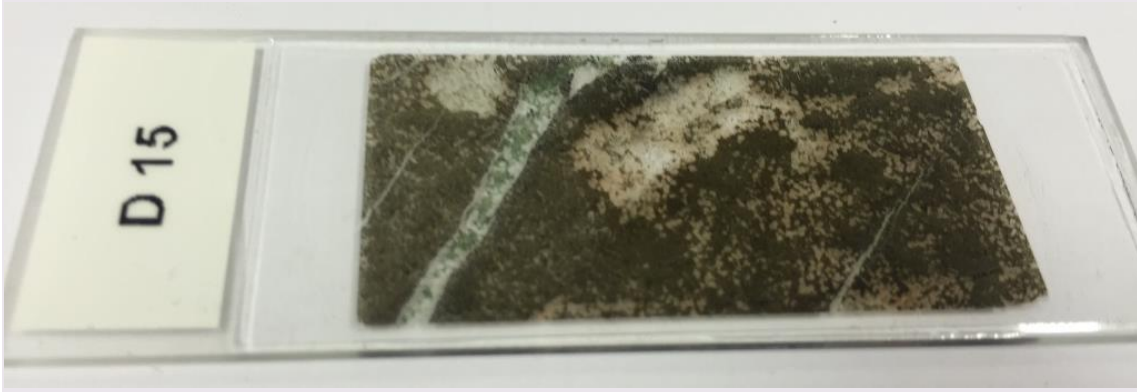

# D16


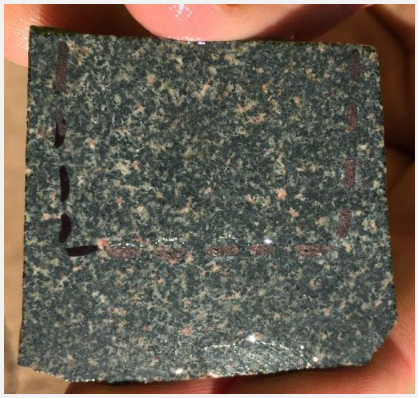

| LOCATION | Mongoose |
|---|---|
| EASTINGS | 447848 |
| NORTHINGS | 7707951 |
| LITHOLOGY | Dolerite |
| FIELD COMMENTS | Hosted in dolerite mass, possibly more than one intrusion. |

## Petrography Report

| Sample ID | D16 Mongoose | Dolerite |
|---|---|---|

| Mineral | Primary/ Second | Size (mm) | Abundance % | Characteristics |
|---|---|---|---|---|
| Albite | S | 1-2 | 40 | Sericitic and pink in some areas |
| HB | P | 1-2 | 35 | Large and mainly yellow in CPL |
| Mag | S | 0.1-2 | 15 | Always associated with HB |
| Actin | S | 01.-0.5 | 2.5 | Fine needles |
| Augite | S | 0.01-0.1 | 2.5 | Forms within quartz ?? |
| Qtz | P | 0.05-0.1 | 2 | Andulose extinction, fine grained |
| CPX | P | 1-2 | 1.5 | Colourful birefringence with sheen |
| Epidote | S | 0.01-0.1 | 0.5 | Very high relief and sheen, patchy appearance |
| | | | | |

**Epidote could likely be titanite also.**

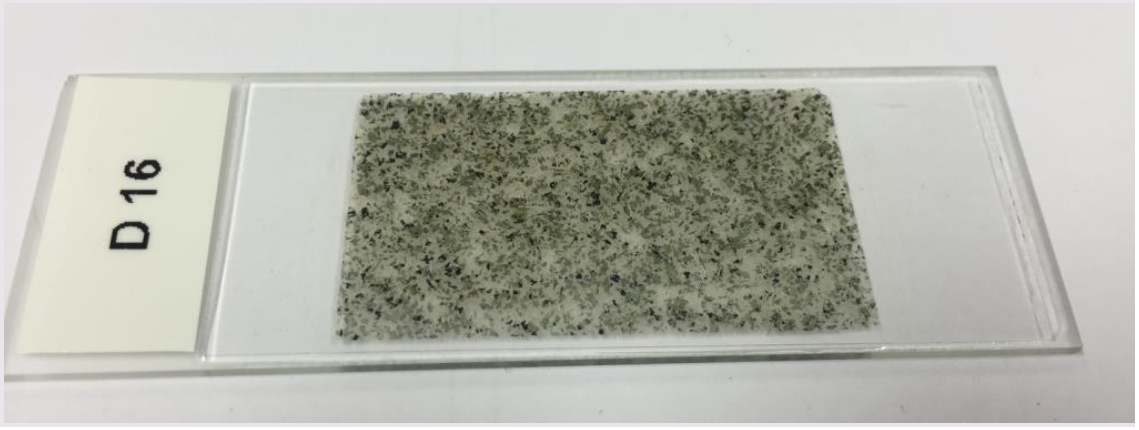

# D17


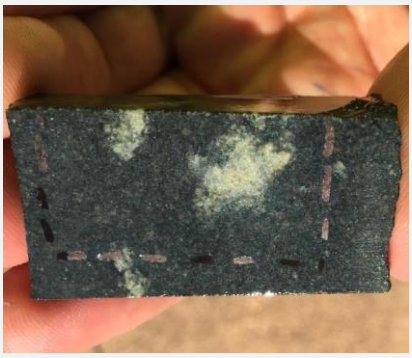

| LOCATION | Mongoose |
|---|---|
| EASTINGS | 447823 |
| NORTHINGS | 7707966 |
| LITHOLOGY | Porphyritic Dolerite |
| FIELD COMMENTS | Hosted in dolerite mass, possibly more than one intrusion. |

## Petrography Report

| Sample ID | D17 Mongoose | Dolerite Mineralised |
|---|---|---|

| Mineral | Primary/ Second | Size (mm) | Abundance % | Characteristics |
|---|---|---|---|---|
| Albite | S | 1-2 | 45 | Sericitic and pink |
| HB | P | 1-2 | 15 | High birefringence and green pleochroism |
| Actin | S | 0.1-0.5 | 15 | More abundant in this mineralized sample |
| Mag | S | 0.1-0.4 | 10 | Mainly disseminated throughout |
| Epidote | S | 0.1-0.5 | 10 | Dark green but sheen in PPL |
| Titanite | S | 0.1-0.5 | 5 | Possibly present in the mineralized area |
| | | | | |
| | | | | |
| | | | | |

**2 unidentifiable minerals within the mineralized zones**

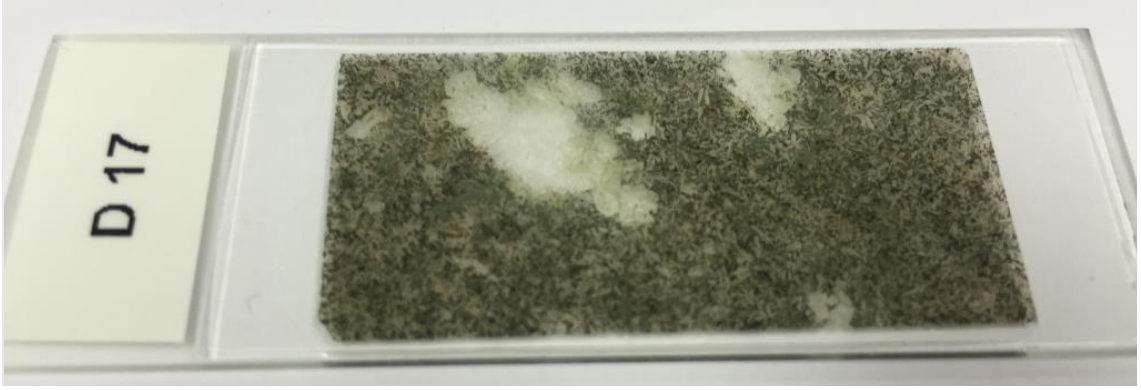

# D18


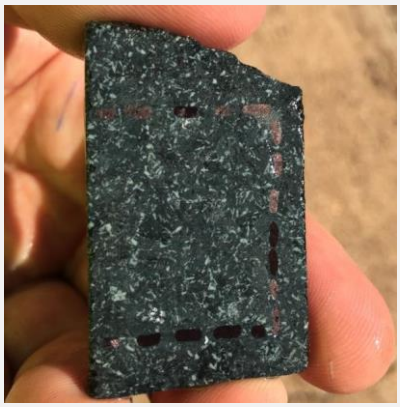

| LOCATION | Mongoose |
|---|---|
| EASTINGS | 447697 |
| NORTHINGS | 7707890 |
| LITHOLOGY | Dolerite |
| FIELD COMMENTS | Hosted in dolerite mass, possibly more than one intrusion, has lass porphyroblasts. |

## Petrography Report

| Sample ID | D18 Mongoose | Dolerite Green |
|---|---|---|

| Mineral | Primary/ Second | Size (mm) | Abundance % | Characteristics |
|---|---|---|---|---|
| HB | P | 1-5 | 50 | Large grains |
| Albite | S | 1-4 | 40 | Some grains show plag twinning |
| Mag | S | 0.5-1 | 6 | Replaces HB or chlorite |
| Actin | S | 0.1-0.3 | 4 | Strongly distinct needles |
| | | | | |
| | | | | |
| | | | | |
| | | | | |
| | | | | |

**HB/Chlorite.**
**Parallel extinction and very birefringent.**

## APPENDIX 3: GEOCHEMISTRY

### QAQC REPORT

**Sample and Assay Information**

85 dolerite pulp samples were analysed by ASL (Townsville) using the ME-MS61 multi acid digest. The process uses a crushed and ground 0.25g portion of the sample, which is pre-digested in a mixture of perchloric acid, nitric acid, hydrofluoric acid and hydrochloric acid. The remaining residue is topped up with dilute hydrochloric acid, before being analysed by inductively coupled plasma – atomic emission spectrometry (ICP-AES). Samples with high concentrations of bismuth, mercury, molybdenum, silver and tungsten are analysed by inductively coupled plasma – mass spectrometry (ICP-MS) with results then corrected for inter-element interference. Elements analysed for consist of Ag, Al, As, Ba, Be, Bi, Ca, Cd, Ce, Co, Cr, Cs, Cu, Fe, Ga, Ge, Hf, In, K, La, Li, Mg, Mn, Mo, Na, Nb, Ni, P, Pb, Rb, Re, S, Sb, Sc, Se, Sn, Sr, Ta, Te, Th, Ti, Tl, U, V, W, Y, Zn, Zr.

Amongst the 85 dolerite samples, a standard was inserted into the sample sequence at every 1:15 ratio. A duplicate sample was also inserted at this same ratio.

**Sample Preparation**

In 2014 Reverse circulation (RC) drill chips were collected from the drill rig cyclone in pre-written 1 meter RC bags. Samples were collected at 2m intervals using the spear-sample technique. Two spears were collected from each 1m interval and were sampled ('corner-to-corner') to obtain a representative sample from throughout the bag for each interval. Speared samples were tipped into calico bags, tied and then placed into poly-weave bags in groups of 5 to 8 samples. These samples were collected from drill rig locations at Battleaxe, Double Oxide, CHUM, Magpie and Turf Club.

In 2016, selected pulp remains from these rock chips were sent to ALS Townsville for re-assay. Pulp with doleritic lithology were selected from above locations.

**Standards**

A single standard material was used during the geochemical assay of dolerite pulp samples. The standard OREAS45d was obtained from Ore Research and Exploration Ltd. This standard was included into the *Compilation of analytical standards*: 2002 report, which establishes upper and lower confidence limits relating to certified values of each element within the standard. Table 1 displays the certified values of selected reference elements within the OREAS45d standard.

| **Standard Name** | Al (%) | Ca (%) | Ce ppm | Co ppm | Cu ppm | La ppm | Mn ppm | V ppm | Zn ppm |
|---|---|---|---|---|---|---|---|---|---|
| **OREAS45d** | 8.15 | 0.185 | 37.2 | 29.5 | 371 | 16.9 | 0.049 | 235 | 45.7 |

*Table 1. Shows the certified values of OREAS45d for standard reference elements.*

Table 2 displays the relative standard deviation (RSD) which reflects the average difference between standard values as a percentage of the mean value. Elements Al, Ca, Ce, Co, Cu, La, Mn, V and Zn were selected to cover concentration ranges and also on the basis of usefulness within the project. The results show the data is very good, as all elements contain RSD values under 5.5%.

| **Standard** | Al | Ca | Ce | Co | Cu | La | Mn | V | Zn |
|---|---|---|---|---|---|---|---|---|---|
| **OREAS45d** | 2.68 | 3.51 | 3.69 | 5.39 | 3.25 | 4.09 | 2.66 | 2.24 | 3.15 |

*Table 2 Relative Standard Deviation (% RSD) for selected elements for the standards used during the dolerite pulp analysis. RSD reflects the average difference between samples as a percentage of the mean value. Values under 5% are preferred.*

Standards have been plotted by sequence to determine if any pulp samples contained errors. Figures 1 to 9 display Al, Ca, Ce, Co, Cu, La, Mn, V and Zn abundances for the standard OREAS45d in sequence with sample ID.). The red dotted line represents the 95% tolerance limits of the OREAS45d standard for each element, with the tolerance limit values provided. Each figure presents the same general curve, with the two centre standard samples having larger assay values than the rest. This curve likely represents a slight drift in instrumentation, but concentration values do not vary between single elements. In total all data show a good correlation with their certified values and the majority of samples remained within their 95% confidence range. No sequential analytical differences or notable variation between samples have been noted for any element within the analytical suite.

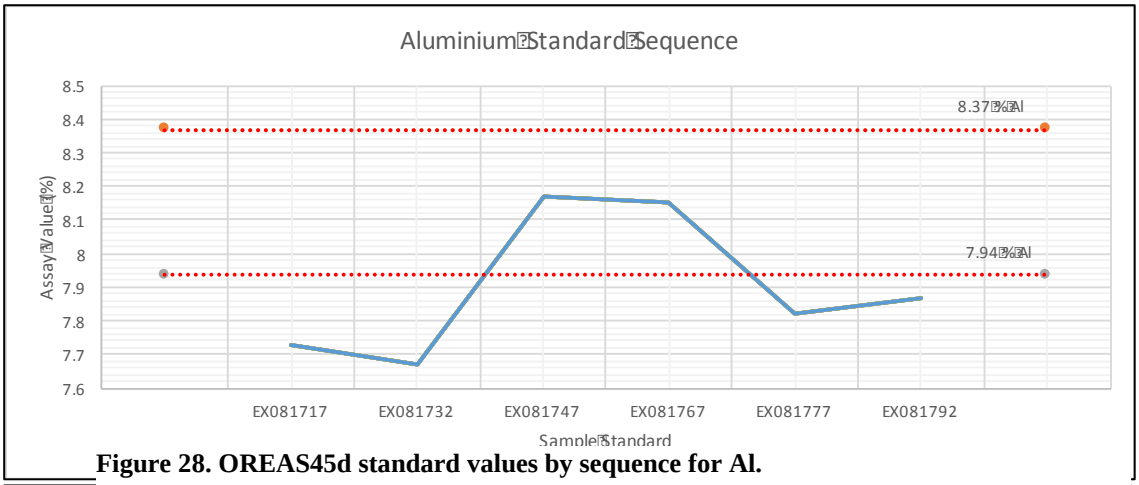


**Figure 28. OREAS45d standard values by sequence for Al.**

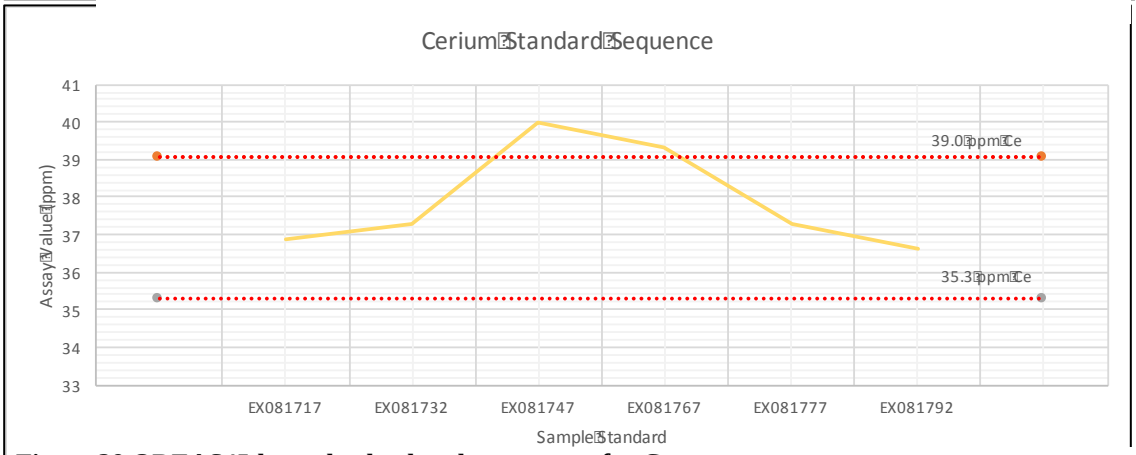


**Figure 29 OREAS45d standard values by sequence for Ca.**

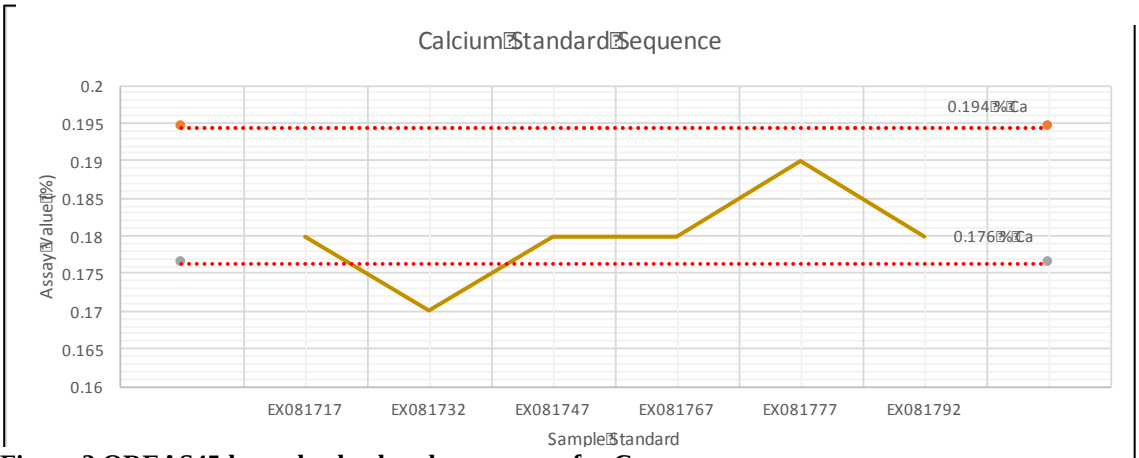


**Figure 3 OREAS45d standard values by sequence for Ce.**

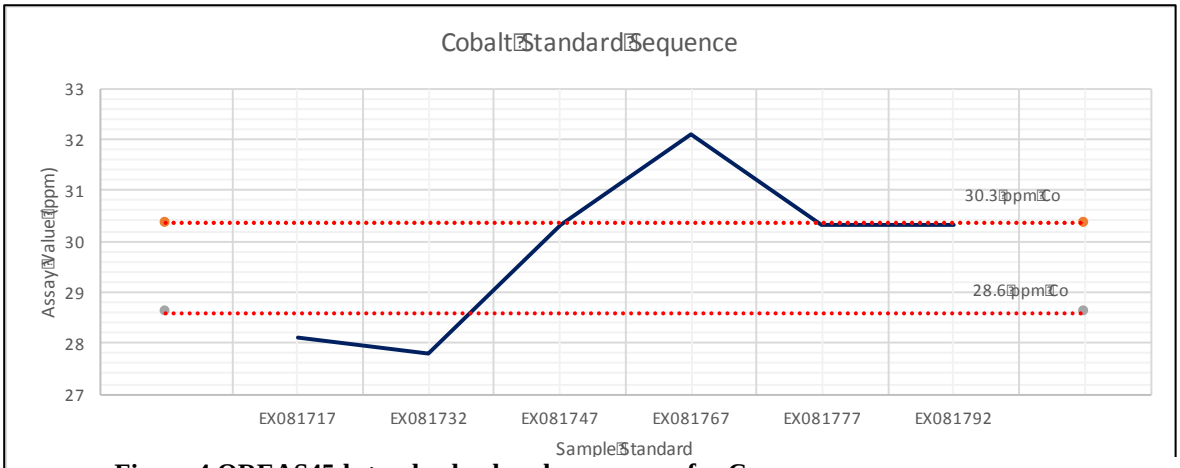


**Figure 4 OREAS45d standard values by sequence for Co.**

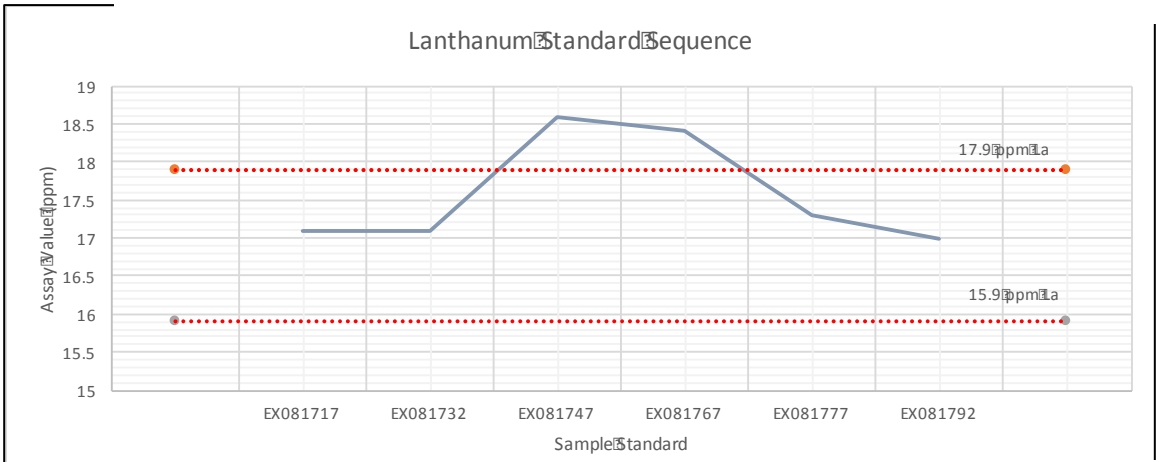


**Figure 5 OREAS45d standard values by sequence for Cu.**

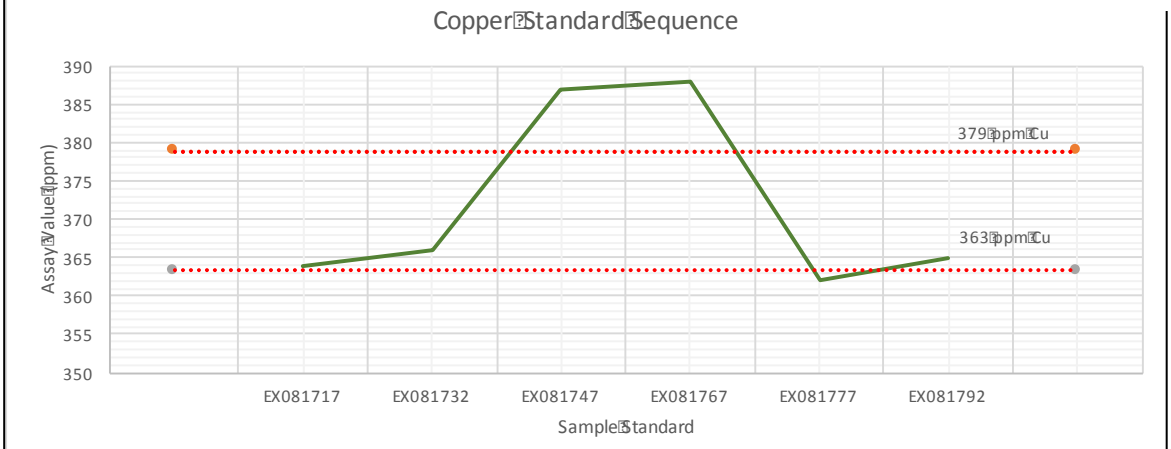


**Figure 6 OREAS45d standard values by sequence for La.**

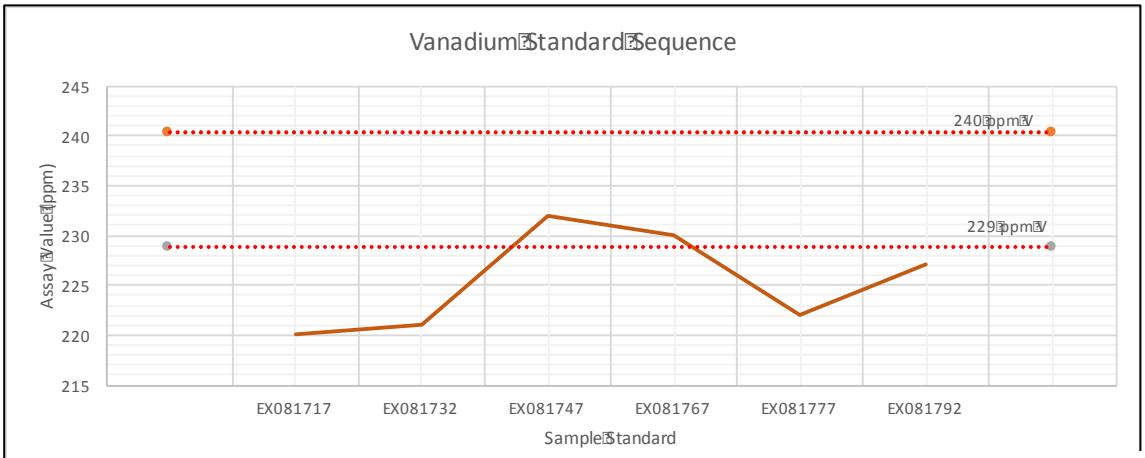


**Figure 8 OREAS45d standard values by sequence for V.**

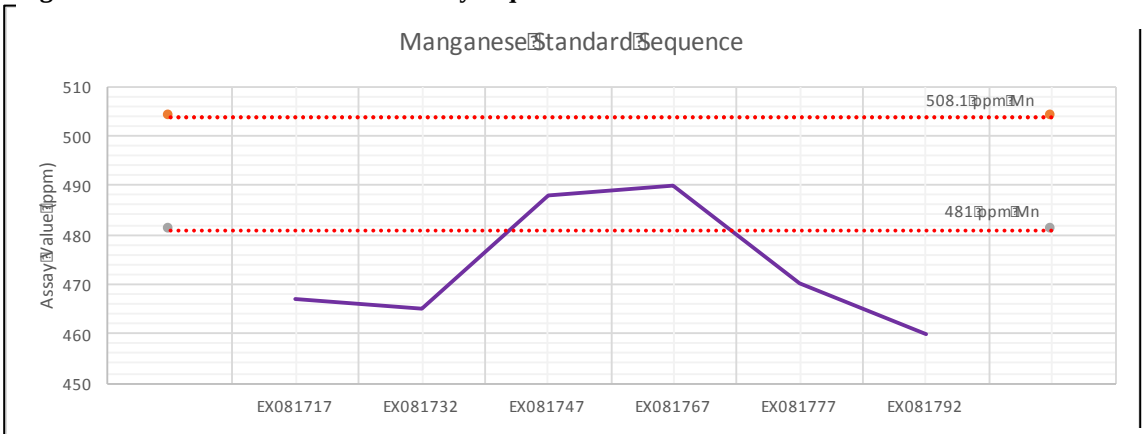


**Figure 7 OREAS45d standard values by sequence for Mn.**

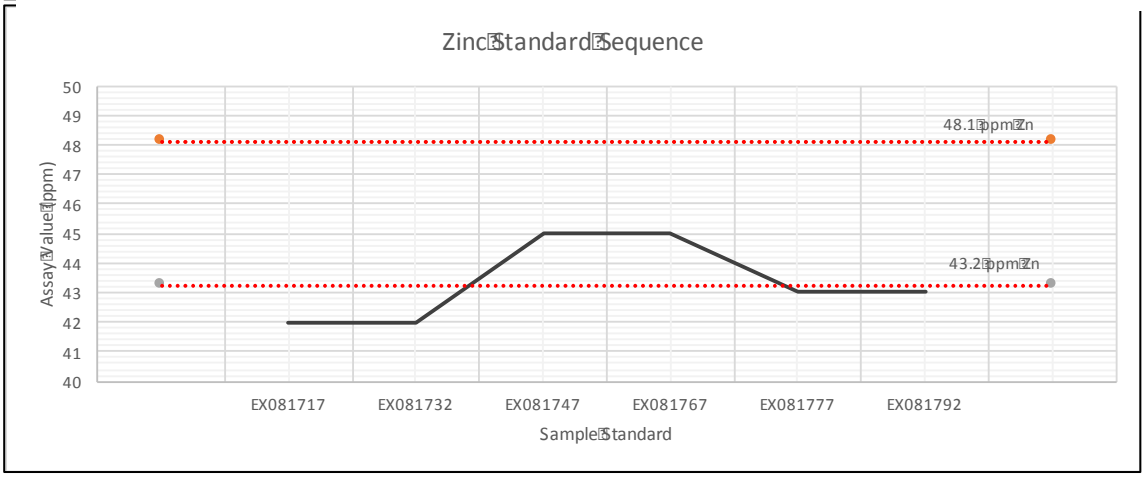


## Duplicates

Duplicate samples were included at a ratio of approximately 1:15. The original sample and its duplicate were plotted against each other to see how well the sample results correlate. Elements Al, Ca, Ce, Co, Cu, La, Mn, V and Zn were selected to cover concentration ranges and also on the basis of usefulness within the project. The results presented good correlation and are shown in Figures 10

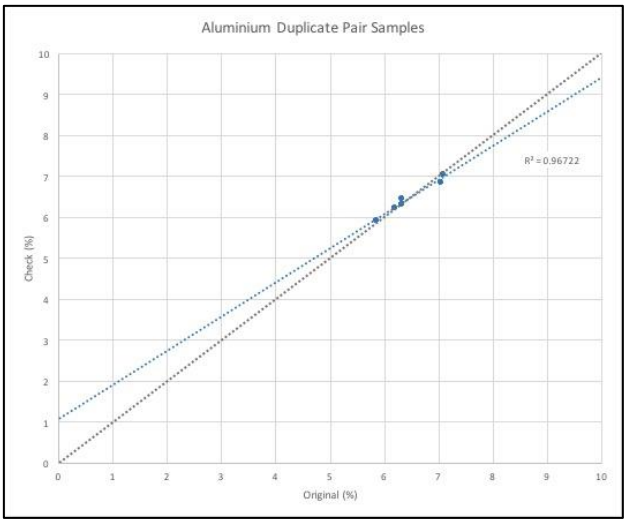


**Figure 10 Duplicate pair sample for Al, with R^2 value representing the correlation between samples.**

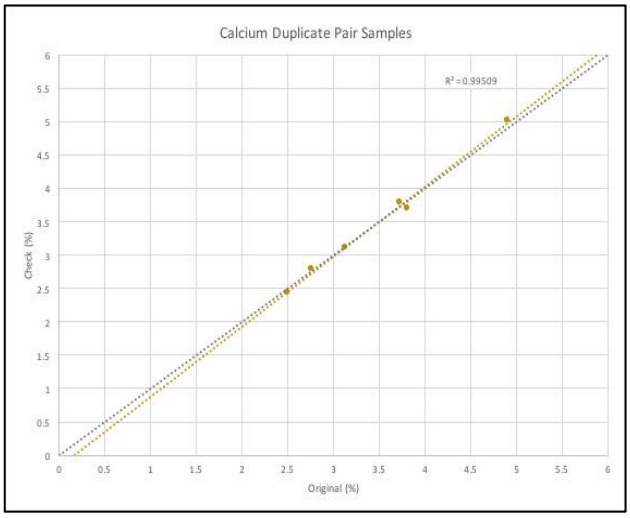


**Figure 11 Duplicate pair sample for Ca, with R^2 value representing the correlation between samples.**

to 18.

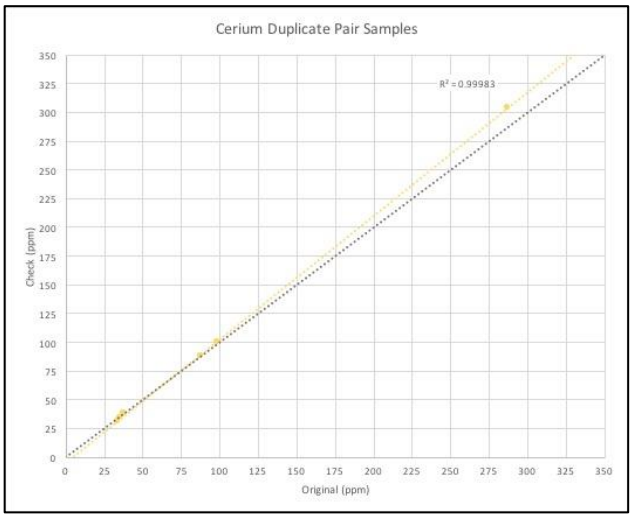


**Figure 12 Duplicate pair sample for Ce, with R^2 value representing the correlation between samples.**

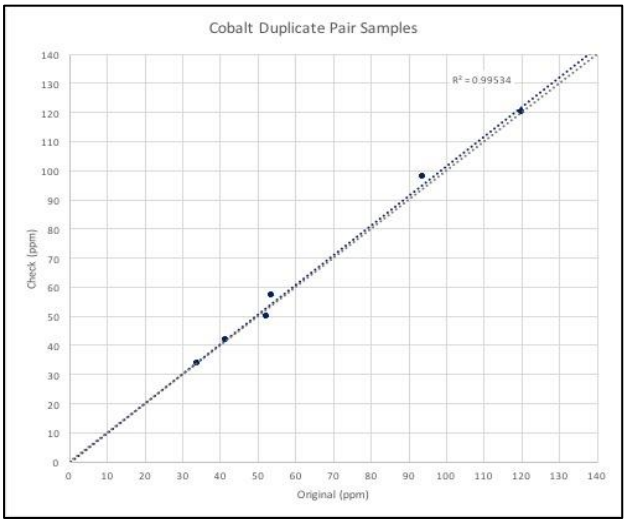


**Figure 130 Duplicate pair sample for Co, with R^2 value representing the correlation between samples.**

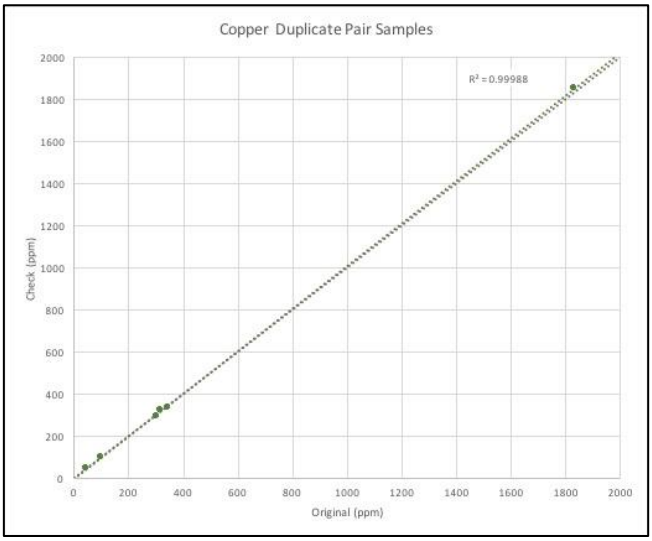


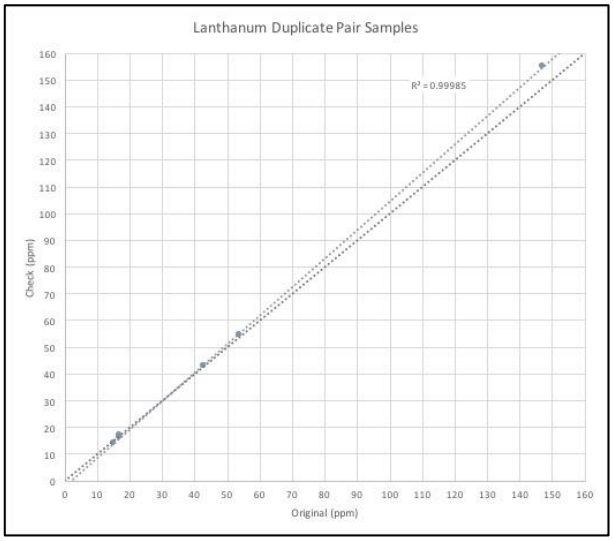


**Figure 18 Duplicate pair sample for Zn, with R^2 value representing the correlation between samples.**

**Figure 132 Duplicate pair sample for Cu, with R^2 value**

**Figure131 Duplicate pair sample for La, with R^2**

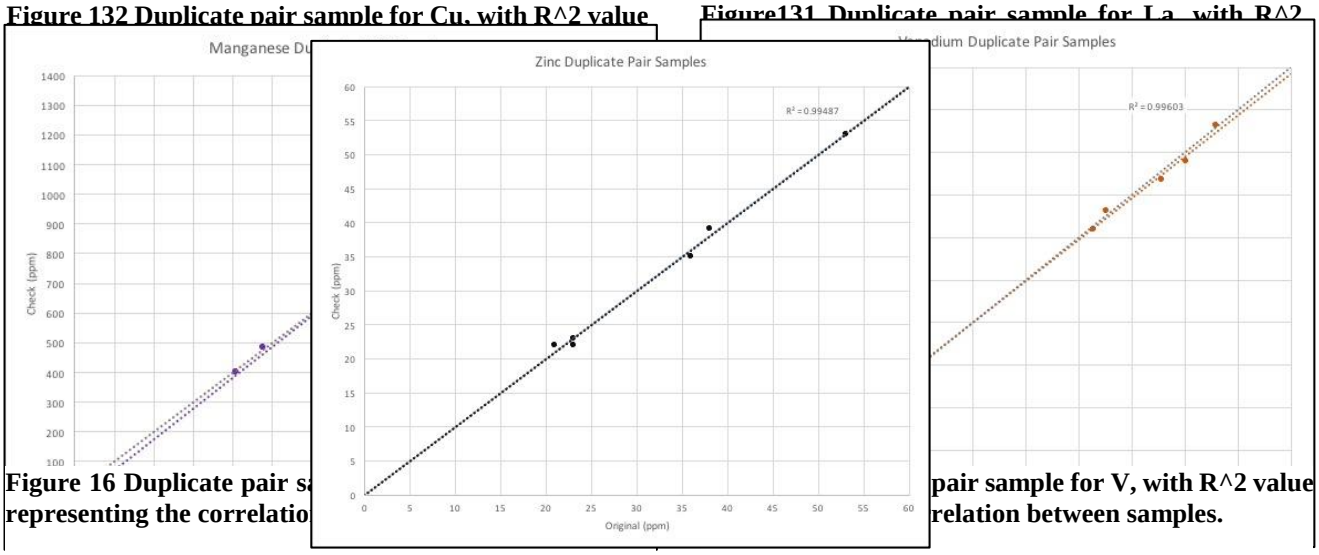


**Figure 16 Duplicate pair s pair sample for V, with R^2 value representing the correlatio relation between samples.**

Sample bias is expressed as Mean Absolute Mean Paired Relative Difference (AMPRD, also referred to as Med-APD) and represents the average difference between results for duplicate pairs for a given element. AMPRD bias profiles generally decrease with increased abundance.

| | Al | Ca | Ce | Co | Cu | La | Mn | V | Zn |
|---|---|---|---|---|---|---|---|---|---|
| **Mean AMPRD** | 1.232 | 1.768 | 3.005 | 2.611 | 2.268 | 3.210 | 2.924 | 1.797 | 2.418 |

*Table 3 Mean Absolute Mean Paired Relative Difference (AMPRD) for selected elements. This figure represents the average difference between results for duplicate pairs for a given element and is an indication of analytical bias. Values under 10 are preferred.*

Figures 19 to 28 displays duplicate pair sample Mean Paired Relative Difference (MPRD) by sequence. Variation in MPRD can be calculated to observe variations in analytical bias through time and across different batches. The red dotted line represents error and the yellow dotted line represents the maximum of preferred values. All data show no bias and plot between the preferred values.

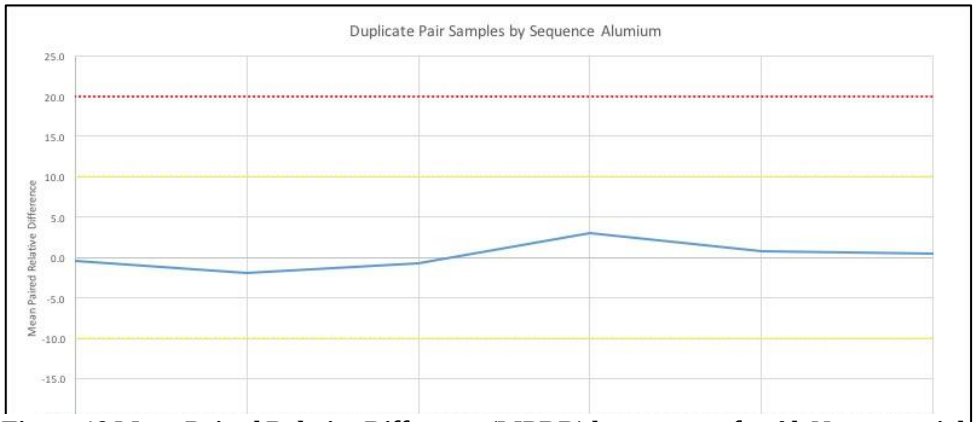


**Figure 19 Mean Paired Relative Difference (MPRD) by sequence for Al. No sequential analytical differences have been noted.**

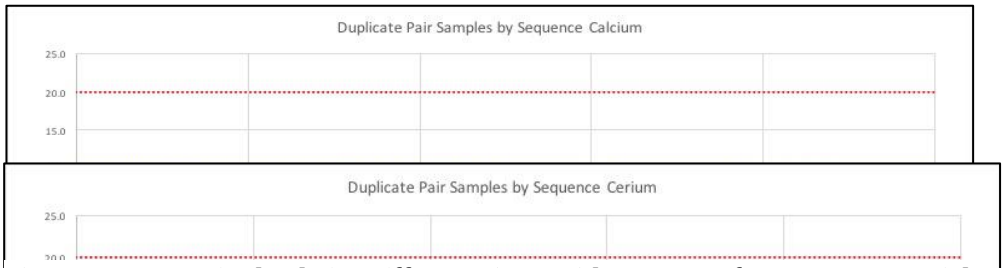


**Figure 20 Mean Paired Relative Difference (MPRD) by sequence for Ca. No sequential analytical differences have been noted.**

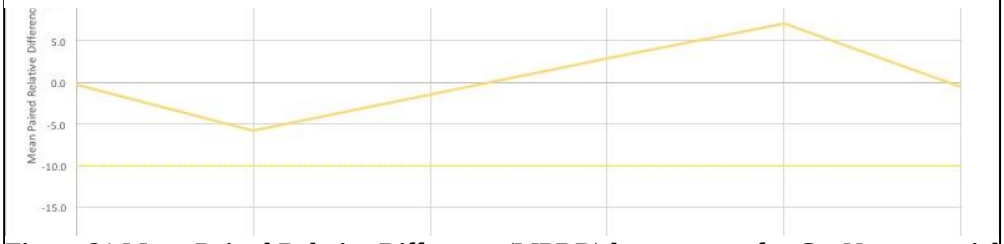


**Figure 21 Mean Paired Relative Difference (MPRD) by sequence for Ce. No sequential analytical differences have been noted.**

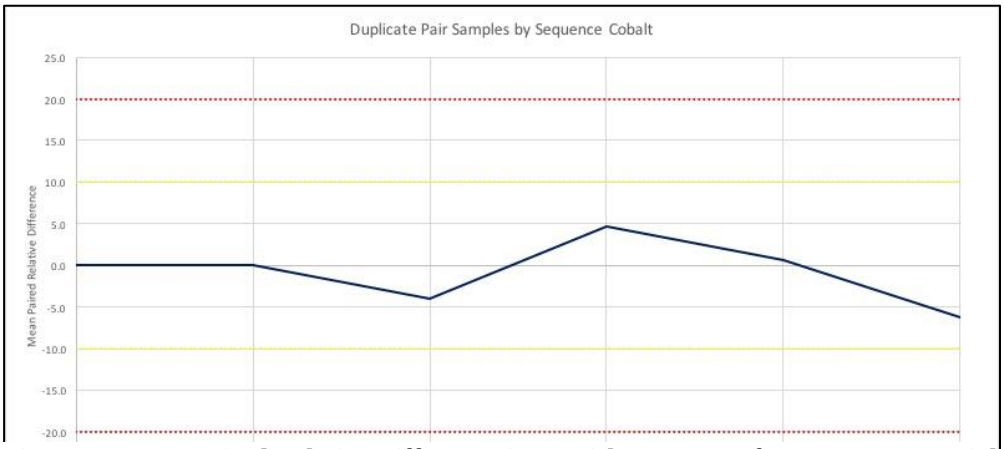


**Figure 22 Mean Paired Relative Difference (MPRD) by sequence for Co. No sequential analytical differences have been noted.**

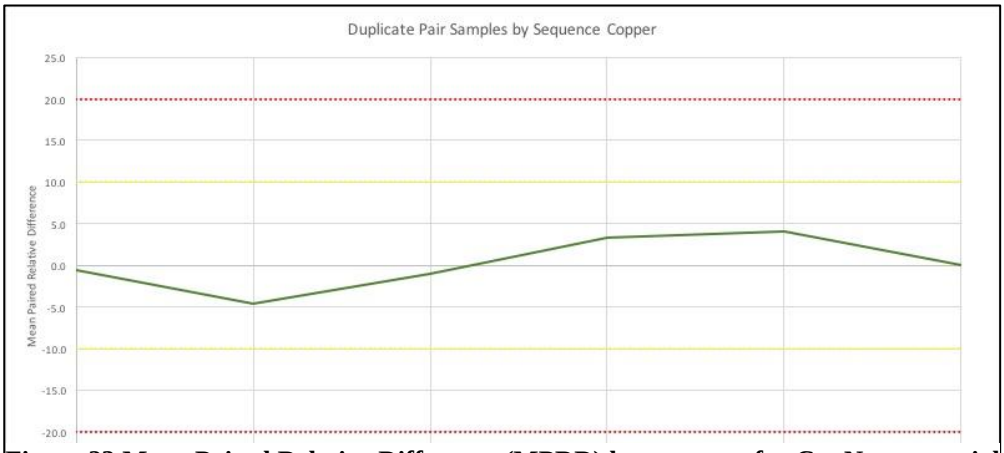


**Figure 23 Mean Paired Relative Difference (MPRD) by sequence for Cu. No sequential analytical differences have been noted.**

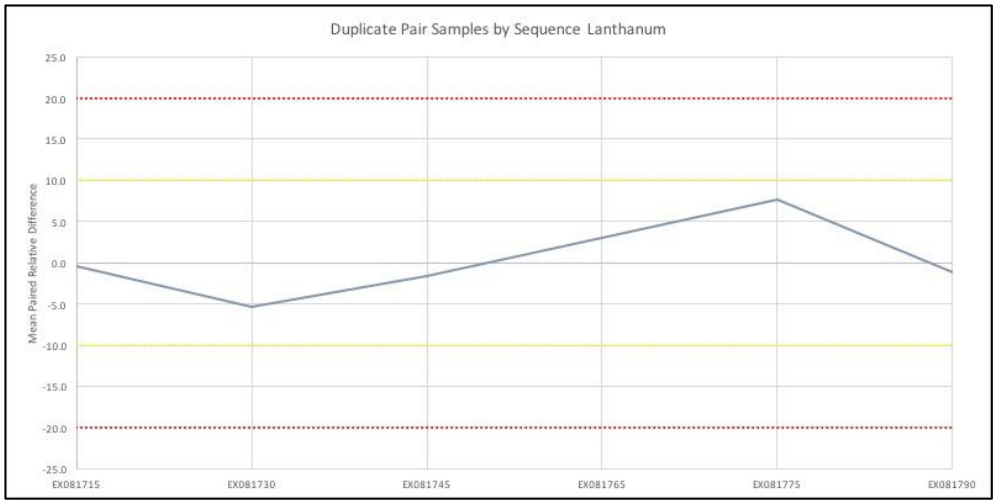


**Figure 24 Mean Paired Relative Difference (MPRD) by sequence for La. No sequential analytical differences have been noted.**

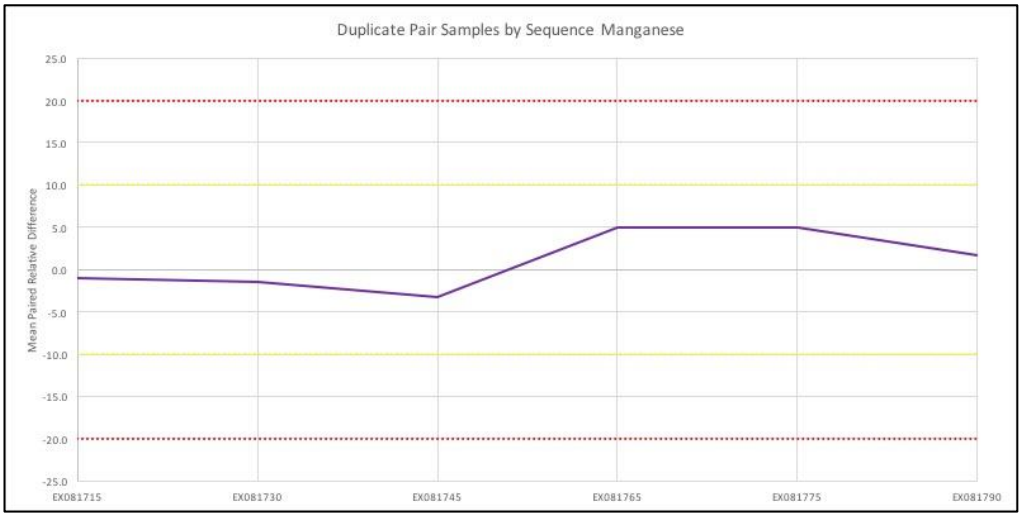


**Figure 25 Mean Paired Relative Difference (MPRD) by sequence for Mn. No sequential analytical differences have been noted.**

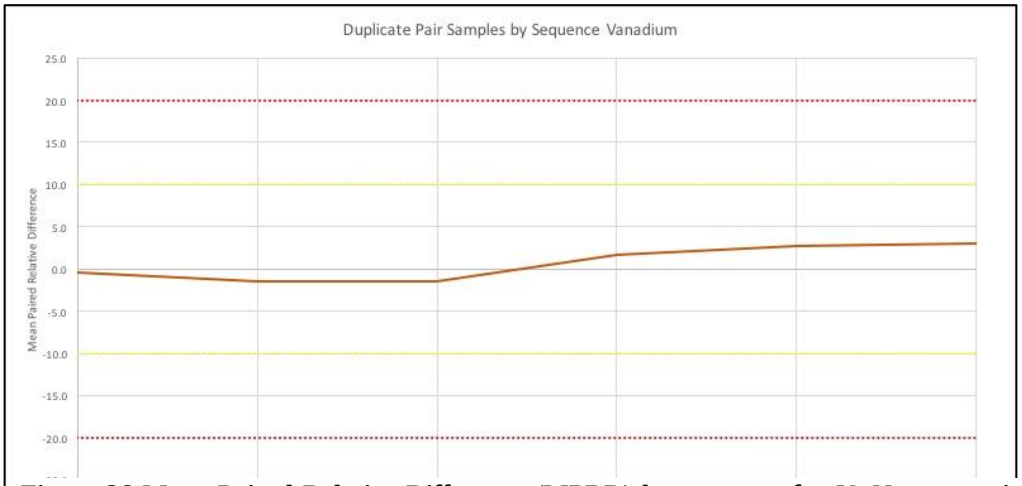


**Figure 26 Mean Paired Relative Difference (MPRD) by sequence for V. No sequential analytical differences have been noted.**

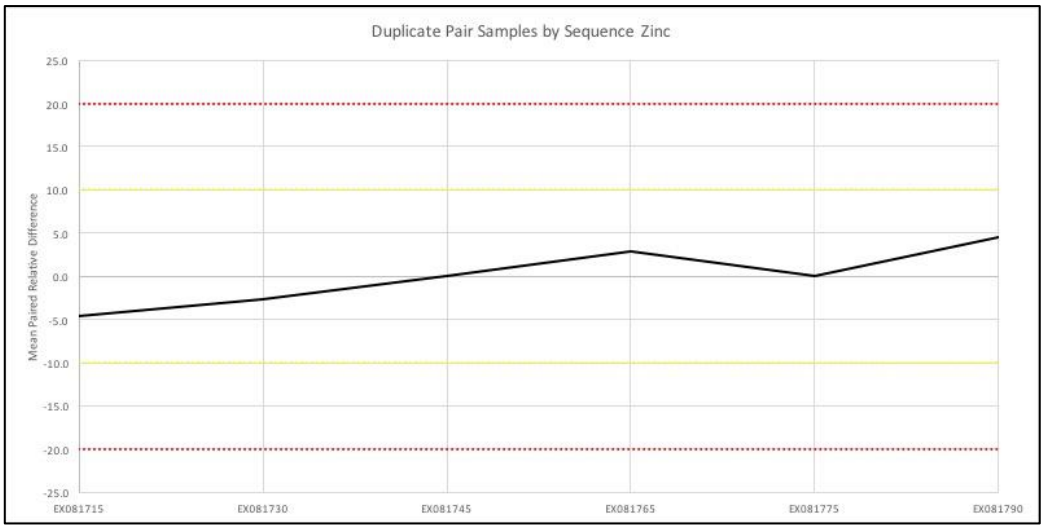

**Figure 27 Mean Paired Relative Difference (MPRD) by sequence for Zn. No sequential analytical differences have been noted.**

To establish precision (also referred to as 2APD) the AMPRD is doubled to provide a direct record of sampling precision between duplicate pairs. The precision due to concentration for each of the selected elements tends to decrease with lower concentrations. This is due to more significant statistical leverage of lower concentration values. The results are represented in Figures 27 to 30.

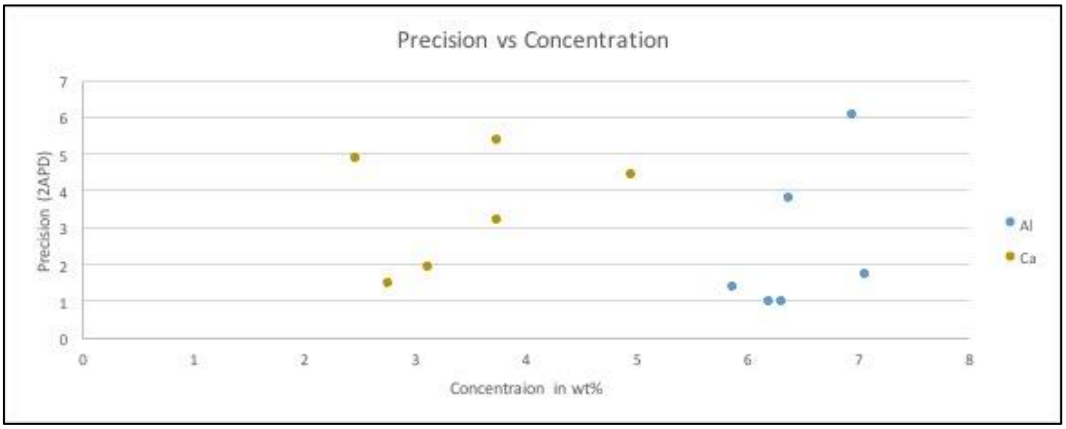


**Figure 27 Precision vs Concentrations for elements Al & Ca.**

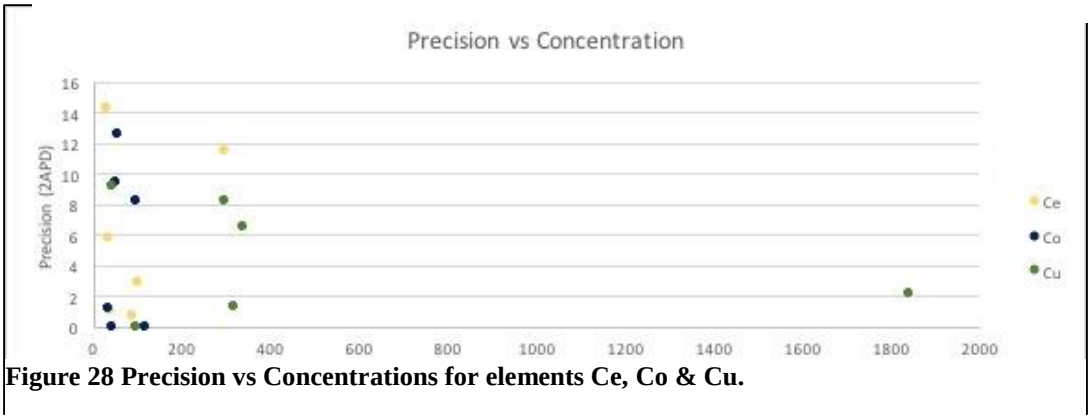


**Figure 28 Precision vs Concentrations for elements Ce, Co & Cu.**

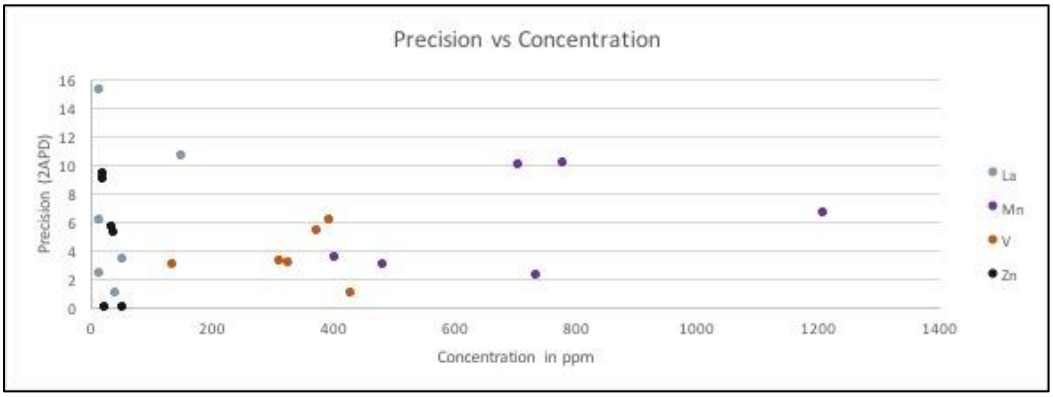


**Figure 29 Precision vs Concentrations for elements La, Mn, V & Zn.**

To establish average precision (mean 2APD) the precisions for elements Al, Ca, Ce, Co, Cu, La, Mn, V and Zn within each sample are averaged out. The average 2APRD is displayed in Figure 30.

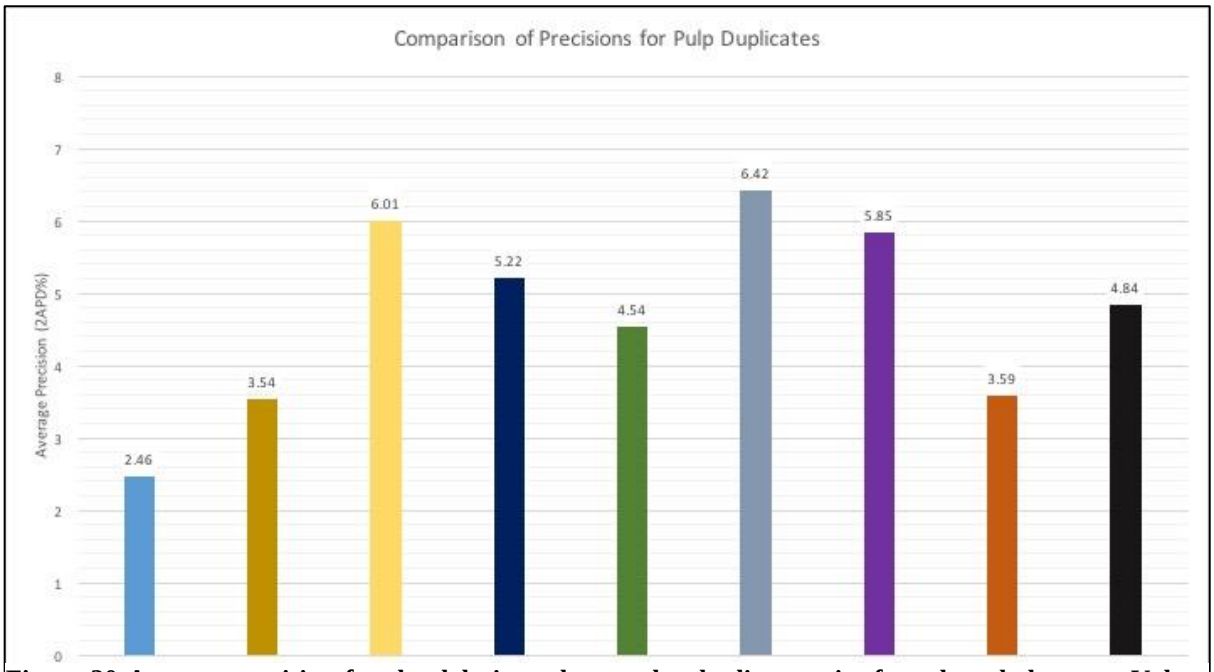


**Figure 30 Average precision for the dolerite pulp samples duplicate pairs for selected elements. Values under 20% are preferred.**

Average sample precision (2APD) generally increases for elements higher abundance such as Al and Ca, with precision decreasing with lower abundance (Ce and La) as seen in Figure 30. Overall the precision for duplicate pairs is well within the range expected for heterogeneous rock types with uneven distribution of mineral species and are interpreted to represent good quality data.

**References:**

Rough, M., Brown, A & Lilly, R. (2014). Exploration Permit for Minerals No 14303 'Big Bend' Battle Axe Prospect Drill Completion Report December 2014.

Minerals, A. (2006). Geochemical Procedure ME - MS61. In A. Minerals (Ed.): ALS Global.

# FIELD AND CUDECO SAMPLES

| NWQ16MSI | 150416 | Recvd Wt. | Al2O3 | BaO | CaO | Cr2O3 | Fe2O3 | K2O | MgO | MnO | Na2O | P2O5 | SO3 | SiO2 | SrO | TiO2 | Total | LOI |
|---|---|---|---|---|---|---|---|---|---|---|---|---|---|---|---|---|---|---|
| UNITS | | kg | % | % | % | % | % | % | % | % | % | % | % | % | % | % | % | % |
| DETECTION | | 0.02 | 0.01 | 0.01 | 0.01 | 0.01 | 0.01 | 0.01 | 0.01 | 0.01 | 0.01 | 0.01 | 0.01 | 0.01 | 0.01 | 0.01 | 0.01 | 0.01 |
| METHOD | | WEI-21 | ME-XRF26 | ME-XRF26 | ME-XRF26 | ME-XRF26 | ME-XRF26 | ME-XRF26 | ME-XRF26 | ME-XRF26 | ME-XRF26 | ME-XRF26 | ME-XRF26 | ME-XRF26 | ME-XRF26 | ME-XRF26 | ME-XRF26 | ME-GRA05 |
| CO | ME-MS61:REE's may not be totally soluble in this method. | | | | | | | | | | | | | | | | | |
| CO | | | | | | | | | | | | | | | | | | |
| RA87176 | D01 | 2 | 12.83 | 0.01 | 4.45 | -0.01 | 16.28 | 1.45 | 4.68 | 0.06 | 5.27 | 0.22 | 0.01 | 50.63 | -0.01 | 2.14 | 99.33 | 0.96 |
| RA87177 | D02 | 2.79 | 13.25 | 0.03 | 10.65 | -0.01 | 12.44 | 0.97 | 6.91 | 0.11 | 2.61 | 0.08 | 0.11 | 49.66 | 0.01 | 1.09 | 99.29 | 1.22 |
| RA87178 | D03 | 2.61 | 14.39 | 0.01 | 10.95 | 0.02 | 12 | 0.52 | 6.96 | 0.18 | 2.98 | 0.08 | 0.21 | 49.44 | 0.01 | 1.02 | 99.76 | 0.84 |
| RA87179 | D04 | 2.84 | 16.89 | -0.01 | 14.1 | 0.04 | 8.62 | 0.18 | 8.66 | 0.14 | 1.54 | 0.03 | 0.1 | 48.65 | 0.01 | 0.47 | 99.96 | 0.41 |
| RA87180 | D05 | 2.63 | 14.2 | 0.02 | 11.15 | 0.01 | 12.72 | 0.8 | 6.95 | 0.23 | 2.38 | 0.07 | 0.4 | 48.59 | 0.01 | 1 | 100.35 | 1.66 |
| RA87181 | D06 | 3.55 | 14.32 | 0.03 | 4.26 | 0.03 | 15.2 | 4.3 | 9.28 | 0.1 | 2.9 | 0.15 | 0.05 | 46.69 | 0.01 | 1.62 | 100.35 | 1.21 |
| RA87182 | D07 | 2.23 | 14.44 | 0.02 | 10.45 | 0.01 | 14.38 | 0.76 | 5.9 | 0.26 | 2.46 | 0.09 | 0.29 | 48.91 | 0.01 | 1.21 | 100.5 | 1.12 |
| RA87183 | D08 | 4.69 | 13.48 | 0.04 | 7.48 | -0.01 | 22.71 | 1.34 | 4.24 | 0.21 | 2.89 | 0.13 | 0.27 | 41.83 | 0.01 | 3.48 | 99.85 | 1.39 |
| RA87184 | D09 | 1.79 | 15.4 | -0.01 | 13.1 | 0.01 | 18.26 | 0.46 | 5.5 | 0.17 | 0.67 | 0.14 | 0.03 | 41.33 | 0.01 | 1.62 | 99.44 | 2.55 |
| RA87185 | D10 | 2.64 | 11.9 | 0.03 | 15.55 | -0.01 | 11.91 | 0.12 | 1.64 | 0.18 | 0.25 | 0.13 | 0.13 | 52.85 | 0.02 | 1.52 | 99.55 | 3.16 |
| RA87186 | D11 | 3.29 | 13.12 | -0.01 | 17.85 | -0.01 | 11.74 | 0.07 | 2.02 | 0.16 | 0.14 | 0.1 | 0.06 | 48.58 | 0.04 | 1.26 | 99.09 | 3.82 |
| RA87188 | D13 | 2.61 | 14.22 | 0.03 | 4.66 | 0.02 | 13.94 | 3.43 | 6.67 | 0.06 | 3.68 | 0.08 | 0.04 | 49.93 | 0.01 | 1.02 | 99.65 | 1.72 |
| RA87189 | D14 | 2.25 | 15.7 | 0.02 | 8.98 | -0.01 | 14.85 | 1.28 | 4.2 | 0.15 | 3.61 | 0.11 | 0.13 | 46.78 | 0.02 | 1.74 | 99.17 | 1.39 |
| RA87190 | D15 | 3.15 | 14.98 | 0.01 | 2.8 | 0.02 | 18.08 | 5.08 | 6.07 | 0.01 | 3.44 | 0.07 | 0.82 | 45.87 | 0.02 | 0.96 | 99.76 | 1.41 |
| RA87191 | D16 | 0.67 | 13.46 | 0.01 | 6.67 | 0.01 | 14.6 | 1.4 | 5.53 | 0.04 | 3.95 | 0.19 | 0.05 | 49.74 | 0.01 | 2.06 | 99.8 | 1.91 |
| RA87192 | D17 | 0.63 | 14.96 | 0.01 | 6.1 | 0.02 | 13.08 | 3.59 | 6.8 | 0.04 | 2.82 | 0.08 | 0.08 | 49.18 | 0.02 | 0.97 | 99.75 | 1.86 |
| RA87193 | D18 | 1.02 | 14.64 | -0.01 | 10.15 | 0.03 | 12.84 | 0.95 | 6.68 | 0.18 | 2.74 | 0.09 | 0.19 | 49.24 | 0.01 | 1.15 | 100.65 | 1.63 |
| RA87194 | D19 | 0.75 | 13.06 | 0.02 | 6.54 | 0.01 | 17.3 | 1.72 | 5.61 | 0.12 | 3.62 | 0.24 | 1.04 | 47.55 | 0.01 | 2.37 | 101.15 | 1.5 |
| RA87195 | D20 | 0.57 | 11.62 | -0.01 | 7.6 | 0.01 | 17.42 | 0.8 | 5.89 | 0.14 | 3.87 | 0.23 | 1.16 | 47.96 | -0.01 | 2.14 | 100.5 | 1.29 |
| RA87196 | D21 | 0.93 | 12.14 | 0.02 | 4.01 | 0.01 | 17.4 | 2.6 | 5.74 | 0.03 | 4.21 | 0.25 | 0.4 | 47.91 | -0.01 | 2.29 | 99.33 | 2.06 |
| RA87197 | D22 | 0.43 | 12.37 | -0.01 | 7.46 | -0.01 | 9.12 | 0.85 | 5.12 | 0.05 | 5.87 | 0.24 | 3.13 | 51.02 | -0.01 | 2.34 | 102 | 3.94 |
| RA87198 | D23 | 0.68 | 12.96 | 0.01 | 4.53 | -0.01 | 19.06 | 1.42 | 2.5 | 0.03 | 5.91 | 0.28 | 1.48 | 47.4 | -0.01 | 2.45 | 100.5 | 2.28 |
| RA87199 | D24 | 0.86 | 12.26 | 0.02 | 4.69 | -0.01 | 16.89 | 1.78 | 6.2 | 0.07 | 4.8 | 0.12 | 0.43 | 49.55 | -0.01 | 1.74 | 99.64 | 0.93 |

| | | | | | | | | | | | | | | | | | | | | |
|---|---|---|---|---|---|---|---|---|---|---|---|---|---|---|---|---|---|---|---|---|
| TV1604736( | | 24 | 310316 | | 546 | | | | | | | | | | | | | | | |
| NWQ16MSI | | 150416 | Recvd Wt. | Ag | | Al | | As | | Ba | | Be | | Bi | | Ca | | Cd | | Ce |
| UNITS | | | kg | ppm | | % | | ppm | | ppm | | ppm | | ppm | | % | | ppm | | ppm |
| DETECTION | | | 0.02 | 0.01 | | 0.01 | | 0.2 | | 10 | | 0.05 | | 0.01 | | 0.01 | | 0.02 | | 0.01 |
| METHOD | | | WEI-21 | ME-MS61 | | ME-MS61 | | ME-MS61 | | ME-MS61 | | ME-MS61 | | ME-MS61 | | ME-MS61 | | ME-MS61 | | ME-MS61 |
| CO | ME-MS61:REE's may not be totally soluble in this method. | | | | | | | | | | | | | | | | | | | |
| CO | | | | | | | | | | | | | | | | | | | | |
| RA87176 | D01 | | 2 | 0.05 | | 6.47 | | 8.7 | | 110 | | 0.98 | | 0.12 | | 3.1 | | 0.05 | | 47.1 |
| RA87177 | D02 | | 2.79 | 0.05 | | 6.69 | | 6.1 | | 300 | | 0.5 | | 0.1 | | 7.22 | | 0.03 | | 16.3 |
| RA87178 | D03 | | 2.61 | 0.06 | | 7.31 | | 3.5 | | 150 | | 0.58 | | 0.11 | | 7.24 | | 0.07 | | 20.3 |
| RA87179 | D04 | | 2.84 | 0.05 | | 8.57 | | 1.5 | | 60 | | 0.17 | | 0.04 | | 9.01 | | 0.09 | | 5.05 |
| RA87180 | D05 | | 2.63 | 0.31 | | 7.06 | | 7.7 | | 240 | | 0.3 | | 0.55 | | 7.4 | | 0.12 | | 12.1 |
| RA87181 | D06 | | 3.55 | 0.03 | | 7.24 | | 1.4 | | 250 | | 1.14 | | 0.04 | | 2.95 | | -0.02 | | 28.3 |
| RA87182 | D07 | | 2.23 | 0.09 | | 7.14 | | 4.8 | | 210 | | 0.4 | | 0.14 | | 6.98 | | 0.12 | | 12.95 |
| RA87183 | D08 | | 4.69 | 0.17 | | 6.6 | | 1.6 | | 420 | | 0.54 | | 0.04 | | 4.93 | | 0.05 | | 19.6 |
| RA87184 | D09 | | 1.79 | 0.05 | | 7.4 | | 3.5 | | 70 | | 0.36 | | 0.1 | | 8.01 | | 0.03 | | 23.3 |
| RA87185 | D10 | | 2.64 | 0.07 | | 6.04 | | 1.5 | | 270 | | 0.5 | | 0.24 | | 9.77 | | 0.09 | | 20.4 |
| RA87186 | D11 | | 3.29 | 0.03 | | 6.59 | | 0.7 | | 30 | | 0.4 | | 0.13 | | 11.15 | | 0.08 | | 15.65 |
| RA87188 | D13 | | 2.61 | 0.02 | | 6.76 | | 1.1 | | 290 | | 1.04 | | 0.02 | | 3.17 | | -0.02 | | 30 |
| RA87189 | D14 | | 2.25 | 0.16 | | 7.75 | | 2.7 | | 210 | | 1.01 | | 0.07 | | 6.17 | | 0.03 | | 32.1 |
| RA87190 | D15 | | 3.15 | 0.04 | | 7.33 | | 3.5 | | 150 | | 0.83 | | 0.02 | | 1.95 | | -0.02 | | 20 |
| RA87191 | D16 | | 0.67 | 0.04 | | 6.66 | | 2.4 | | 140 | | 1.09 | | 0.04 | | 4.51 | | -0.02 | | 28.9 |
| RA87192 | D17 | | 0.63 | 0.02 | | 6.99 | | 3.4 | | 150 | | 0.45 | | 0.03 | | 4.12 | | -0.02 | | 12.5 |
| RA87193 | D18 | | 1.02 | 0.04 | | 6.81 | | 1.9 | | 60 | | 0.56 | | 0.06 | | 6.68 | | 0.08 | | 17.4 |
| RA87194 | D19 | | 0.75 | 0.22 | | 6.62 | | 2.6 | | 200 | | 1.51 | | 0.2 | | 4.51 | | 0.05 | | 47.7 |
| RA87195 | D20 | | 0.57 | 0.21 | | 5.74 | | 3 | | 90 | | 1.64 | | 0.24 | | 5.13 | | 0.05 | | 49.4 |
| RA87196 | D21 | | 0.93 | 0.07 | | 6.17 | | 19.4 | | 190 | | 1.72 | | 0.15 | | 2.77 | | -0.02 | | 73.3 |
| RA87197 | D22 | | 0.43 | 0.11 | | 6.1 | | 31.2 | | 40 | | 1.83 | | 0.36 | | 4.99 | | -0.02 | | 55.9 |
| RA87198 | D23 | | 0.68 | 0.07 | | 6.56 | | 11.2 | | 140 | | 1.11 | | 0.14 | | 3.14 | | -0.02 | | 48.1 |
| RA87199 | D24 | | 0.86 | 0.03 | | 6.28 | | 3 | | 210 | | 1.2 | | 0.08 | | 3.26 | | -0.02 | | 27.3 |

| | | | | | | | | | | | | | | | | | | | | |
|---|---|---|---|---|---|---|---|---|---|---|---|---|---|---|---|---|---|---|---|---|
| TV1604736( | | | | | | | | | | | | | | | | | | | | |
| NWQ16MSI | | | | | | | | | | | | | | | | | | | | |
| UNITS | | | | | | | | | | | | | | | | | | | | |
| DETECTION | | | | | | | | | | | | | | | | | | | | |
| METHOD | | | | | | | | | | | | | | | | | | | | |
| CO | ME-MS61:REE's may not be totally soluble in this method. | | | | | | | | | | | | | | | | | | | |
| CO | | | | | | | | | | | | | | | | | | | | |
| RA87176 | D01 | | | | | | | | | | | | | | | | | | | |
| RA87177 | D02 | | | | | | | | | | | | | | | | | | | |
| RA87178 | D03 | | | | | | | | | | | | | | | | | | | |
| RA87179 | D04 | | | | | | | | | | | | | | | | | | | |
| RA87180 | D05 | | | | | | | | | | | | | | | | | | | |
| RA87181 | D06 | | | | | | | | | | | | | | | | | | | |
| RA87182 | D07 | | | | | | | | | | | | | | | | | | | |
| RA87183 | D08 | | | | | | | | | | | | | | | | | | | |
| RA87184 | D09 | | | | | | | | | | | | | | | | | | | |
| RA87185 | D10 | | | | | | | | | | | | | | | | | | | |
| RA87186 | D11 | | | | | | | | | | | | | | | | | | | |
| RA87188 | D13 | | | | | | | | | | | | | | | | | | | |
| RA87189 | D14 | | | | | | | | | | | | | | | | | | | |
| RA87190 | D15 | | | | | | | | | | | | | | | | | | | |
| RA87191 | D16 | | | | | | | | | | | | | | | | | | | |
| RA87192 | D17 | | | | | | | | | | | | | | | | | | | |
| RA87193 | D18 | | | | | | | | | | | | | | | | | | | |
| RA87194 | D19 | | | | | | | | | | | | | | | | | | | |
| RA87195 | D20 | | | | | | | | | | | | | | | | | | | |
| RA87196 | D21 | | | | | | | | | | | | | | | | | | | |
| RA87197 | D22 | | | | | | | | | | | | | | | | | | | |
| RA87198 | D23 | | | | | | | | | | | | | | | | | | | |
| RA87199 | D24 | | | | | | | | | | | | | | | | | | | |

| | | | | | | | | | | | | | | | | | | | | |
|---|---|---|---|---|---|---|---|---|---|---|---|---|---|---|---|---|---|---|---|---|
| TV1604736( | | | | | | | | | | | | | | | | | | | | |
| NWQ16MSI | | | | | | | | | | | | | | | | | | | | |
| UNITS | | | | | | | | | | | | | | | | | | | | |
| DETECTION | | | | | | | | | | | | | | | | | | | | |
| METHOD | | | | | | | | | | | | | | | | | | | | |
| CO | ME-MS61:REE's may not be totally soluble in this method. | | | | | | | | | | | | | | | | | | | |
| CO | | | | | | | | | | | | | | | | | | | | |
| RA87176 | D01 | | | | | | | | | | | | | | | | | | | |
| RA87177 | D02 | | | | | | | | | | | | | | | | | | | |
| RA87178 | D03 | | | | | | | | | | | | | | | | | | | |
| RA87179 | D04 | | | | | | | | | | | | | | | | | | | |
| RA87180 | D05 | | | | | | | | | | | | | | | | | | | |
| RA87181 | D06 | | | | | | | | | | | | | | | | | | | |
| RA87182 | D07 | | | | | | | | | | | | | | | | | | | |
| RA87183 | D08 | | | | | | | | | | | | | | | | | | | |
| RA87184 | D09 | | | | | | | | | | | | | | | | | | | |
| RA87185 | D10 | | | | | | | | | | | | | | | | | | | |
| RA87186 | D11 | | | | | | | | | | | | | | | | | | | |
| RA87188 | D13 | | | | | | | | | | | | | | | | | | | |
| RA87189 | D14 | | | | | | | | | | | | | | | | | | | |
| RA87190 | D15 | | | | | | | | | | | | | | | | | | | |
| RA87191 | D16 | | | | | | | | | | | | | | | | | | | |
| RA87192 | D17 | | | | | | | | | | | | | | | | | | | |
| RA87193 | D18 | | | | | | | | | | | | | | | | | | | |
| RA87194 | D19 | | | | | | | | | | | | | | | | | | | |
| RA87195 | D20 | | | | | | | | | | | | | | | | | | | |
| RA87196 | D21 | | | | | | | | | | | | | | | | | | | |
| RA87197 | D22 | | | | | | | | | | | | | | | | | | | |
| RA87198 | D23 | | | | | | | | | | | | | | | | | | | |
| RA87199 | D24 | | | | | | | | | | | | | | | | | | | |

| NWQ16MSI | 150416 | Recvd Wt. | Hf | In | K | La | Li | Mg | Mn | Mo | Na | Nb | Ni | P | Pb | Rb | Re | S | Sb |
|---|---|---|---|---|---|---|---|---|---|---|---|---|---|---|---|---|---|---|---|
| UNITS | | kg | ppm | ppm | % | ppm | ppm | % | ppm | ppm | % | ppm | ppm | ppm | ppm | ppm | ppm | % | ppm |
| DETECTION | | 0.02 | 0.1 | 0.005 | 0.01 | 0.5 | 0.2 | 0.01 | 5 | 0.05 | 0.01 | 0.1 | 0.2 | 10 | 0.5 | 0.1 | 0.002 | 0.01 | 0.05 |
| METHOD | | WEI-21 | ME-MS61 | ME-MS61 | ME-MS61 | ME-MS61 | ME-MS61 | ME-MS61 | ME-MS61 | ME-MS61 | ME-MS61 | ME-MS61 | ME-MS61 | ME-MS61 | ME-MS61 | ME-MS61 | ME-MS61 | ME-MS61 | ME-MS61 |
| CO | ME-MS61:REE's may not be totally soluble in this method. | | | | | | | | | | | | | | | | | | |
| CO | | | | | | | | | | | | | | | | | | | |
| RA87176 | D01 | 2 | 3.7 | 0.07 | 1.18 | 20.5 | 5 | 2.63 | 513 | 0.38 | 3.78 | 10.1 | 48.5 | 950 | 1.6 | 91.3 | -0.002 | -0.01 | 0.39 |
| RA87177 | D02 | 2.79 | 1.7 | 0.107 | 0.78 | 6.7 | 16 | 3.97 | 819 | 0.58 | 1.89 | 4.2 | 63.1 | 310 | 1.7 | 26 | -0.002 | 0.04 | 0.8 |
| RA87178 | D03 | 2.61 | 1.8 | 0.066 | 0.42 | 8.6 | 14.6 | 3.95 | 1420 | 1.07 | 2.2 | 4.7 | 79.4 | 350 | 2.4 | 15.7 | -0.002 | 0.08 | 0.28 |
| RA87179 | D04 | 2.84 | 0.7 | 0.038 | 0.15 | 2 | 4.9 | 5.01 | 1380 | 0.72 | 1.13 | 1.4 | 145.5 | 140 | 1.6 | 5.8 | -0.002 | 0.03 | 0.14 |
| RA87180 | D05 | 2.63 | 1.3 | 0.074 | 0.64 | 5.4 | 14.9 | 3.88 | 1550 | 1.95 | 1.7 | 3.1 | 98.5 | 310 | 4.9 | 43 | 0.002 | 0.15 | 0.64 |
| RA87181 | D06 | 3.55 | 2.8 | 0.069 | 3.54 | 11.9 | 26.1 | 5.45 | 730 | 0.43 | 2.1 | 7.4 | 158 | 640 | 1.2 | 179.5 | -0.002 | 0.02 | 0.23 |
| RA87182 | D07 | 2.23 | 1.4 | 0.079 | 0.62 | 5.1 | 17.6 | 3.29 | 1870 | 0.87 | 1.76 | 3.7 | 58.4 | 380 | 2.5 | 23.2 | -0.002 | 0.11 | 0.41 |
| RA87183 | D08 | 4.69 | 2 | 0.112 | 1.03 | 7.3 | 13.2 | 2.26 | 1520 | 0.58 | 2.03 | 6.1 | 79.1 | 550 | 2.3 | 52.1 | 0.004 | 0.1 | 0.43 |
| RA87184 | D09 | 1.79 | 1.3 | 0.178 | 0.36 | 8.9 | 15.2 | 2.97 | 1260 | 0.29 | 0.49 | 5.6 | 84.3 | 570 | 2.9 | 5.8 | -0.002 | -0.01 | 0.81 |
| RA87185 | D10 | 2.64 | 1.4 | 0.11 | 0.1 | 7.5 | 3 | 0.87 | 1300 | 0.31 | 0.19 | 5.9 | 19.2 | 560 | 4.8 | 1.8 | -0.002 | 0.04 | 0.62 |
| RA87186 | D11 | 3.29 | 1.5 | 0.102 | 0.06 | 5.9 | 1.9 | 1.05 | 1140 | 0.5 | 0.12 | 4.5 | 17 | 440 | 7.6 | 1.9 | 0.002 | 0.02 | 0.3 |
| RA87188 | D13 | 2.61 | 2.1 | 0.067 | 2.73 | 16.1 | 12.2 | 3.73 | 498 | 0.12 | 2.62 | 3.1 | 63.8 | 340 | 1 | 168.5 | -0.002 | 0.02 | 0.22 |
| RA87189 | D14 | 2.25 | 2.2 | 0.092 | 1.05 | 13.1 | 16.5 | 2.29 | 1150 | 0.49 | 2.63 | 10.8 | 56.5 | 490 | 2.4 | 38.4 | -0.002 | 0.05 | 0.39 |
| RA87190 | D15 | 3.15 | 1.8 | 0.043 | 4.09 | 9.7 | 12.6 | 3.41 | 157 | 0.36 | 2.46 | 3.3 | 86.6 | 310 | 1.5 | 273 | 0.003 | 0.33 | 0.39 |
| RA87191 | D16 | 0.67 | 3.8 | 0.083 | 1.12 | 11.8 | 8.3 | 3.06 | 360 | 0.6 | 2.82 | 8.5 | 54.3 | 800 | 2.1 | 77.6 | -0.002 | 0.02 | 0.59 |
| RA87192 | D17 | 0.63 | 1.8 | 0.086 | 2.83 | 5 | 15.4 | 3.73 | 311 | 0.66 | 2.01 | 3.6 | 98.9 | 330 | 1.4 | 130 | 0.002 | 0.03 | 1.07 |
| RA87193 | D18 | 1.02 | 2 | 0.058 | 0.73 | 7.2 | 5.6 | 3.54 | 1240 | 0.43 | 1.91 | 4.3 | 87.6 | 390 | 1.4 | 35.8 | -0.002 | 0.07 | 0.53 |
| RA87194 | D19 | 0.75 | 3.9 | 0.116 | 1.37 | 20 | 12.2 | 3.17 | 864 | 1.24 | 2.62 | 13 | 55.5 | 1060 | 2.7 | 149.5 | 0.002 | 0.41 | 0.62 |
| RA87195 | D20 | 0.57 | 4 | 0.191 | 0.64 | 20.5 | 7.2 | 3.29 | 1060 | 0.86 | 2.75 | 17.1 | 58.8 | 970 | 6.3 | 38.1 | 0.002 | 0.45 | 0.51 |
| RA87196 | D21 | 0.93 | 4.6 | 0.064 | 2.12 | 33.1 | 14.1 | 3.26 | 286 | 0.68 | 3.05 | 13.6 | 39.7 | 1110 | 1.3 | 133.5 | -0.002 | 0.16 | 0.43 |
| RA87197 | D22 | 0.43 | 4.3 | 0.122 | 0.65 | 18.2 | 8.6 | 2.78 | 366 | 0.58 | 4.1 | 13.5 | 72.6 | 960 | 1.5 | 41 | -0.002 | 1.19 | 0.54 |
| RA87198 | D23 | 0.68 | 5.1 | 0.016 | 1.15 | 20.1 | 6.7 | 1.34 | 282 | 3.44 | 4.28 | 18.2 | 41.3 | 1200 | 1.7 | 48.6 | 0.003 | 0.59 | 0.29 |
| RA87199 | D24 | 0.86 | 3.1 | 0.061 | 1.45 | 11.8 | 10.3 | 3.55 | 573 | 1.77 | 3.48 | 6.8 | 51.5 | 540 | 2.7 | 86.9 | 0.004 | 0.17 | 0.36 |

| NWQ16MSI | 150416 | Recvd Wt. | Sc | Se | Sn | Sr | Ta | Te | Th | Ti | Tl | U | V | W | Y | Zn | Zr |
|---|---|---|---|---|---|---|---|---|---|---|---|---|---|---|---|---|---|
| UNITS | | kg | ppm | ppm | ppm | ppm | ppm | ppm | ppm | % | ppm | ppm | ppm | ppm | ppm | ppm | ppm |
| DETECTION | | 0.02 | 0.1 | 1 | 0.2 | 0.2 | 0.05 | 0.05 | 0.01 | 0.005 | 0.02 | 0.1 | 1 | 0.1 | 0.1 | 2 | 0.5 |
| METHOD | | WEI-21 | ME-MS61 | ME-MS61 | ME-MS61 | ME-MS61 | ME-MS61 | ME-MS61 | ME-MS61 | ME-MS61 | ME-MS61 | ME-MS61 | ME-MS61 | ME-MS61 | ME-MS61 | ME-MS61 | ME-MS61 |
| CO | ME-MS61:REE's may not be totally soluble in this method. | | | | | | | | | | | | | | | | |
| CO | | | | | | | | | | | | | | | | | |
| RA87176 | D01 | 2 | 52.3 | 2 | 1.7 | 82.8 | 0.65 | 0.06 | 3.55 | 1.23 | 0.28 | 1.2 | 464 | 1.2 | 48.9 | 28 | 145.5 |
| RA87177 | D02 | 2.79 | 56.6 | 1 | 0.7 | 165.5 | 0.28 | 0.05 | 1.69 | 0.609 | 0.07 | 0.5 | 311 | 0.5 | 21.1 | 20 | 61.7 |
| RA87178 | D03 | 2.61 | 45.3 | 1 | 0.8 | 198 | 0.32 | -0.05 | 2.48 | 0.569 | 0.09 | 0.6 | 257 | 0.3 | 20.6 | 73 | 68 |
| RA87179 | D04 | 2.84 | 38.7 | 1 | 0.3 | 138.5 | 0.09 | -0.05 | 0.29 | 0.27 | 0.04 | 0.1 | 175 | 0.2 | 9.7 | 53 | 22.1 |
| RA87180 | D05 | 2.63 | 42.5 | 1 | 0.8 | 144 | 0.2 | 0.06 | 0.73 | 0.556 | 0.17 | 1 | 291 | 0.8 | 21.2 | 87 | 46.8 |
| RA87181 | D06 | 3.55 | 36.3 | 1 | 1.4 | 113.5 | 0.45 | -0.05 | 1.3 | 0.924 | 0.79 | 0.6 | 339 | 0.4 | 25.4 | 31 | 108 |
| RA87182 | D07 | 2.23 | 43.9 | 1 | 0.6 | 149 | 0.24 | 0.07 | 0.77 | 0.673 | 0.13 | 0.3 | 332 | 0.4 | 23.4 | 106 | 49.2 |
| RA87183 | D08 | 4.69 | 36.1 | 2 | 1.1 | 163.5 | 0.38 | 0.05 | 0.81 | 1.82 | 0.12 | 0.3 | 1080 | 0.3 | 34.7 | 69 | 66 |
| RA87184 | D09 | 1.79 | 50.4 | 1 | 1.2 | 117.5 | 0.35 | 0.05 | 0.64 | 0.891 | 0.03 | 0.4 | 452 | 0.7 | 40 | 27 | 38.7 |
| RA87185 | D10 | 2.64 | 36 | 1 | 1.1 | 251 | 0.38 | -0.05 | 0.88 | 0.855 | 0.03 | 0.4 | 346 | 0.5 | 32.2 | 59 | 42 |
| RA87186 | D11 | 3.29 | 37.4 | 1 | 1 | 400 | 0.29 | -0.05 | 0.92 | 0.716 | 0.04 | 0.3 | 339 | 0.2 | 25.7 | 31 | 48 |
| RA87188 | D13 | 2.61 | 39.3 | 1 | 1.2 | 164 | 0.19 | -0.05 | 1.44 | 0.446 | 0.55 | 0.7 | 301 | 0.2 | 22.5 | 11 | 76.6 |
| RA87189 | D14 | 2.25 | 34.9 | 1 | 1.3 | 251 | 0.67 | -0.05 | 3.18 | 0.976 | 0.16 | 0.5 | 490 | 0.4 | 26.1 | 38 | 80.9 |
| RA87190 | D15 | 3.15 | 38 | 1 | 0.7 | 226 | 0.22 | -0.05 | 1.15 | 0.544 | 0.69 | 0.6 | 269 | 0.2 | 13.8 | 4 | 65.7 |
| RA87191 | D16 | 0.67 | 41 | 1 | 2 | 136 | 0.56 | -0.05 | 3.31 | 1.075 | 0.15 | 2 | 384 | 0.9 | 37.2 | 10 | 144.5 |
| RA87192 | D17 | 0.63 | 33.7 | 1 | 1 | 241 | 0.24 | -0.05 | 1.28 | 0.539 | 0.5 | 0.5 | 264 | 0.6 | 18.7 | 9 | 67.2 |
| RA87193 | D18 | 1.02 | 39.2 | 1 | 0.8 | 140 | 0.28 | -0.05 | 1.64 | 0.621 | 0.15 | 0.4 | 283 | 0.2 | 23.1 | 46 | 72.4 |
| RA87194 | D19 | 0.75 | 37.7 | 2 | 3 | 108.5 | 0.84 | 0.09 | 4.76 | 1.345 | 0.52 | 2 | 422 | 2.2 | 40.4 | 36 | 148 |
| RA87195 | D20 | 0.57 | 40.5 | 2 | 5.6 | 82.4 | 0.94 | 0.1 | 5.26 | 1.205 | 0.11 | 2.6 | 354 | 4.1 | 55.9 | 36 | 155 |
| RA87196 | D21 | 0.93 | 38 | 2 | 2.6 | 38.7 | 0.88 | -0.05 | 5.1 | 1.32 | 0.29 | 2.5 | 376 | 0.8 | 45 | 20 | 176.5 |
| RA87197 | D22 | 0.43 | 31.5 | 4 | 5.2 | 38.3 | 0.85 | 0.06 | 5.33 | 1.25 | 0.08 | 3.2 | 315 | 1.1 | 62.5 | 11 | 161 |
| RA87198 | D23 | 0.68 | 25.1 | 2 | 5.8 | 28.3 | 1.19 | -0.05 | 6.42 | 1.425 | 0.12 | 3.6 | 398 | 1.4 | 66.3 | 10 | 191.5 |
| RA87199 | D24 | 0.86 | 49.4 | 1 | 1.7 | 48.9 | 0.43 | 0.06 | 2.76 | 1.01 | 0.33 | 1.3 | 390 | 0.9 | 29.6 | 24 | 112 |

FIELD REE

| | | | | | | | | | | | | | | |
|---|---|---|---|---|---|---|---|---|---|---|---|---|---|---|
| NWQ16MSM0 | | 150416 | Recvd Wt. | | | | | | | | | | | |
| UNITS | | | kg | | | | | | | | | | | |
| DETECTION | | | 0.02 | | | | | | | | | | | |
| METHOD | | | WEI-21 | | | | | | | | | | | |
| CO | ME-MS61:REE's may not be totally Soluble in this method. | | | | | | | | | | | | | |
| CO | | | | Dy | Er | Eu | Tb. | Te | Gd | Ho | Lu | Nd | Pr | Sm | Yb |
| | | | | ppm | ppm | ppm | ppm | ppm | ppm | ppm | ppm | ppm | ppm | ppm | ppm |
| RA87176 | D01 | | 2 | 7.33 | 4.9 | 2.11 | 1.21 | 0.06 | 6.85 | 1.64 | 0.59 | 23.9 | 5.85 | 5.81 | 4.28 |
| RA87177 | D02 | | 2.79 | 3.37 | 2.18 | 0.95 | 0.58 | 0.05 | 3.14 | 0.76 | 0.28 | 9.5 | 2.11 | 2.62 | 1.89 |
| RA87178 | D03 | | 2.61 | 3.46 | 2.23 | 0.99 | 0.62 | -0.05 | 3.24 | 0.74 | 0.28 | 11.5 | 2.65 | 3.02 | 2.09 |
| RA87179 | D04 | | 2.84 | 1.58 | 1.12 | 0.51 | 0.27 | -0.05 | 1.46 | 0.35 | 0.12 | 3.7 | 0.71 | 1.07 | 0.84 |
| RA87180 | D05 | | 2.63 | 3.36 | 2.27 | 0.95 | 0.54 | 0.06 | 2.93 | 0.74 | 0.29 | 7.4 | 1.57 | 2.35 | 1.89 |
| RA87181 | D06 | | 3.55 | 4.45 | 2.7 | 1.64 | 0.8 | -0.05 | 4.78 | 0.97 | 0.32 | 17.2 | 4.13 | 4.59 | 2.28 |
| RA87182 | D07 | | 2.23 | 3.81 | 2.59 | 1.05 | 0.63 | 0.07 | 3.41 | 0.86 | 0.33 | 8.4 | 1.81 | 2.54 | 2.3 |
| RA87183 | D08 | | 4.69 | 5.81 | 3.82 | 1.69 | 1.04 | 0.05 | 5.3 | 1.24 | 0.48 | 13.9 | 2.94 | 4.02 | 3.35 |
| RA87184 | D09 | | 1.79 | 7.13 | 4.48 | 3.21 | 1.25 | 0.05 | 6.78 | 1.54 | 0.54 | 18.5 | 3.76 | 5.26 | 3.81 |
| RA87185 | D10 | | 2.64 | | | | | -0.05 | | | | | | | |
| RA87186 | D11 | | 3.29 | 4.42 | 3.03 | 1.12 | 0.72 | -0.05 | 4.08 | 1.01 | 0.43 | 10.2 | 2.12 | 3.03 | 2.75 |
| RA87188 | D13 | | 2.25 | 4.29 | 2.88 | 1.38 | 0.7 | -0.05 | 3.98 | 0.94 | 0.37 | 17.2 | 4.6 | 3.63 | 2.63 |
| RA87189 | D14 | | 3.15 | | | | | -0.05 | | | | | | | |
| RA87190 | D15 | | 0.67 | 2.34 | 1.6 | 0.51 | 0.38 | -0.05 | 2.11 | 0.52 | 0.25 | 9.5 | 2.5 | 1.94 | 1.68 |
| RA87191 | D16 | | 0.63 | 6.61 | 4.16 | 2.01 | 1.12 | -0.05 | 6.22 | 1.44 | 0.51 | 18.6 | 4.06 | 5.32 | 3.61 |
| RA87192 | D17 | | 1.02 | 3.44 | 2.3 | 0.88 | 0.58 | -0.05 | 3.08 | 0.76 | 0.32 | 8.7 | 1.97 | 2.48 | 2.14 |
| RA87193 | D18 | | 0.75 | 4.1 | 2.88 | 1 | 0.7 | -0.05 | 3.79 | 0.94 | 0.38 | 10.7 | 2.36 | 2.99 | 2.64 |
| RA87194 | D19 | | 0.57 | 6.85 | 4.31 | 1.95 | 1.17 | 0.09 | 6.66 | 1.52 | 0.52 | 24.4 | 5.99 | 6.06 | 3.68 |
| RA87195 | D20 | | 0.93 | 8.76 | 5.98 | 2.15 | 1.44 | 0.1 | 7.8 | 1.98 | 0.79 | 25.8 | 6.14 | 6.88 | 5.44 |
| RA87196 | D21 | | 0.43 | 7.38 | 4.85 | 2.18 | 1.26 | -0.05 | 7.24 | 1.58 | 0.6 | 31.1 | 8.01 | 6.72 | 4.08 |
| RA87197 | D22 | | 0.68 | 9.56 | 6.93 | 3.17 | 1.61 | 0.06 | 9.48 | 2.23 | 0.85 | 32.9 | 7.79 | 8.51 | 5.81 |
| RA87198 | D23 | | 0.86 | 11.8 | 6.91 | 3.47 | 2.04 | -0.05 | 11.45 | 2.43 | 0.68 | 29.5 | 6.07 | 9.79 | 5.2 |
| RA87199 | D24 | | | | | | | 0.06 | | | | | | | |

# PULP SAMPLES

| TV16047358 | 97 | 310316 | 418 | | | | | | | | | | | | | | | | |
|---|---|---|---|---|---|---|---|---|---|---|---|---|---|---|---|---|---|---|---|
| NWQ16MSM | 120416 | Ag | Al | As | Ba | Be | Bi | Ca | Cd | Ce | Co | Cr | Cs | Cu | Fe | Ga | Ge | Hf | In |
| UNITS | | ppm | % | ppm | ppm | ppm | ppm | % | ppm | ppm | ppm | ppm | ppm | ppm | % | ppm | ppm | ppm | ppm |
| DETECTION | | 0.01 | 0.01 | 0.2 | 10 | 0.05 | 0.01 | 0.01 | 0.02 | 0.01 | 0.1 | 1 | 0.05 | 0.2 | 0.01 | 0.05 | 0.05 | 0.1 | 0.005 |
| METHOD | | ME-MS61 | ME-MS61 | ME-MS61 | ME-MS61 | ME-MS61 | ME-MS61 | ME-MS61 | ME-MS61 | ME-MS61 | ME-MS61 | ME-MS61 | ME-MS61 | ME-MS61 | ME-MS61 | ME-MS61 | ME-MS61 | ME-MS61 | ME-MS61 |
| CO | ME-MS61:REE's may not be totally soluble in this method. | | | | | | | | | | | | | | | | | | |
| CO | | | | | | | | | | | | | | | | | | | |
| EX081701 | BA | 0.1 | 5.95 | 2.7 | 140 | 1.46 | 0.13 | 3.59 | -0.02 | 102.5 | 59.8 | 52 | 6.07 | 241 | 10.7 | 21.5 | 0.37 | 3.2 | 0.06 |
| EX081702 | BA | 0.1 | 5.92 | 3.3 | 180 | 1.25 | 0.17 | 3.51 | -0.02 | 114 | 55 | 49 | 5.45 | 207 | 10.55 | 21.5 | 0.43 | 3 | 0.06 |
| EX081703 | BA | 0.06 | 5.13 | 1.2 | 980 | 1.93 | 0.07 | 4.72 | -0.02 | 254 | 54.7 | 270 | 9.92 | 156 | 7.47 | 14.75 | 0.53 | 4.5 | 0.04 |
| EX081704 | BA | 0.1 | 5.76 | 1.7 | 170 | 1.41 | 0.08 | 4.82 | 0.02 | 64.2 | 56.1 | 57 | 5.93 | 196 | 10.7 | 21.2 | 0.3 | 3.6 | 0.06 |
| EX081705 | BA | 0.07 | 6.13 | 1 | 380 | 1.2 | 0.07 | 4.22 | -0.02 | 31.8 | 40.1 | 83 | 3.77 | 258 | 10.5 | 21.2 | 0.3 | 2.9 | 0.20 |
| EX081706 | BA | 0.16 | 5.71 | 5 | 90 | 2.2 | 0.39 | 3.7 | -0.02 | 50.2 | 61.1 | 200 | 0.72 | 166 | 13.8 | 21.1 | 0.36 | 5.1 | 0.09 |
| EX081707 | BA | 0.08 | 6.02 | 1.9 | 120 | 2.07 | 0.08 | 3.61 | -0.02 | 54.7 | 39.1 | 115 | 4.01 | 71 | 10.2 | 21.7 | 0.43 | 4.3 | 0.07 |
| EX081708 | BA | 0.1 | 5.84 | 1.8 | 230 | 1.75 | 0.59 | 3.87 | -0.02 | 41.7 | 27.3 | 105 | 1.74 | 314 | 10.2 | 18.85 | 0.35 | 4 | 0.09 |
| EX081709 | BA | 0.09 | 5.77 | 2.3 | 150 | 1.93 | 0.11 | 3.86 | -0.02 | 41.4 | 44.5 | 111 | 1.88 | 171 | 10.1 | 19.7 | 0.35 | 4.2 | 0.08 |
| EX081710 | BA | 0.13 | 6.02 | 2.2 | 130 | 1.79 | 0.09 | 3.06 | -0.02 | 35.2 | 51.7 | 119 | 6.14 | 757 | 11.25 | 22.4 | 0.4 | 4.2 | 0.09 |
| EX081711 | BA | 0.14 | 5.75 | 1.5 | 170 | 1.07 | 0.11 | 4.26 | -0.02 | 93.1 | 58.8 | 55 | 8.37 | 1820 | 11.1 | 23.4 | 0.27 | 3.9 | 0.20 |
| EX081712 | BA | 0.11 | 5.8 | 2.6 | 160 | 1.16 | 0.08 | 4.21 | -0.02 | 76.6 | 38.2 | 54 | 2.94 | 479 | 11.4 | 24.8 | 0.25 | 4.4 | 0.20 |
| EX081713 | BA | 0.09 | 6 | 1.6 | 150 | 1.49 | 0.06 | 3.61 | -0.02 | 65 | 42.6 | 64 | 1.36 | 188 | 11.5 | 24.2 | 0.29 | 4.5 | 0.19 |
| EX081714 | BA | 0.1 | 6.24 | 1.2 | 190 | 1.24 | 0.06 | 3.96 | -0.02 | 55.6 | 43.5 | 62 | 1.94 | 271 | 11.9 | 24.9 | 0.44 | 4.5 | 0.23 |
| EX081715 | BA | 0.1 | 6.19 | 1.6 | 190 | 1.24 | 0.07 | 3.72 | -0.02 | 87.6 | 41.6 | 63 | 2.92 | 318 | 11.95 | 25.2 | 0.34 | 4.4 | 0.15 |
| EX081716 | | 0.1 | 6.22 | 1.5 | 190 | 1.26 | 0.07 | 3.78 | -0.02 | 87.9 | 41.6 | 64 | 2.92 | 320 | 11.95 | 25.4 | 0.3 | 4.3 | 0.16 |
| EX081717 | | 0.23 | 7.73 | 12.6 | 180 | 0.8 | 0.3 | 0.18 | 0.03 | 36.9 | 28.1 | 539 | 4.05 | 364 | 13.5 | 20.9 | 0.31 | 3.8 | 0.09 |
| EX081718 | BA | 0.15 | 5.82 | 1.4 | 210 | 1.24 | 0.09 | 4.36 | 0.02 | 48.5 | 56.2 | 62 | 8.22 | 937 | 11.65 | 21 | 0.25 | 4.1 | 0.14 |
| EX081719 | BA | 0.13 | 6.04 | 1.9 | 330 | 1.06 | 0.11 | 4.58 | -0.02 | 41.6 | 48.4 | 83 | 0.84 | 946 | 10.85 | 21.5 | 0.24 | 3.7 | 0.19 |
| EX081720 | BA | 0.11 | 6.46 | 1.7 | 200 | 1.17 | 0.09 | 4.74 | -0.02 | 41.6 | 53.4 | 89 | 0.82 | 698 | 11.3 | 21.8 | 0.35 | 4.3 | 0.19 |
| EX081721 | BA | 0.12 | 6.12 | 5.5 | 180 | 1.13 | 0.2 | 6.14 | -0.02 | 50.2 | 70.6 | 76 | 1.15 | 892 | 10.6 | 21.1 | 0.24 | 4.3 | 0.25 |
| EX081722 | BA | 0.13 | 6.35 | 3.2 | 520 | 1.29 | 0.12 | 4.26 | -0.02 | 42.1 | 45.3 | 78 | 0.88 | 867 | 11.45 | 20.2 | 0.24 | 4.2 | 0.21 |
| EX081723 | BA | 0.17 | 5.18 | 3.2 | 180 | 1.44 | 0.09 | 4.15 | 0.02 | 67.6 | 39 | 14 | 5.13 | 628 | 12 | 23.5 | 0.29 | 7.2 | 0.18 |
| EX081724 | BA | 0.18 | 5.3 | 5.9 | 200 | 1.72 | 0.09 | 4.67 | -0.02 | 67.6 | 37.7 | 14 | 1.84 | 554 | 13.15 | 24.2 | 0.3 | 6.6 | 0.26 |
| EX081725 | BA | 0.16 | 5.13 | 4.7 | 230 | 1.59 | 0.12 | 4.35 | -0.02 | 70.5 | 33.4 | 12 | 1.32 | 581 | 11.8 | 22.8 | 0.29 | 6.8 | 0.24 |
| EX081726 | BA | 0.14 | 4.26 | 5.2 | 200 | 1.13 | 0.19 | 5.8 | -0.02 | 83.4 | 41.1 | 14 | 0.82 | 596 | 8.72 | 18.75 | 0.25 | 5.4 | 0.13 |
| EX081727 | BA | 0.14 | 5.18 | 5.6 | 280 | 1.69 | 0.13 | 3.5 | 0.02 | 66.3 | 49.8 | 13 | 0.43 | 218 | 12.4 | 23.8 | 0.29 | 6.7 | 0.20 |
| EX081728 | DO | 0.1 | 5.77 | 2 | 140 | 2.36 | 0.13 | 2.8 | -0.02 | 378 | 125.5 | 93 | 8.52 | 10 | 11.55 | 25.4 | 0.66 | 3.5 | 0.05 |
| EX081729 | DO | 0.1 | 5.44 | 2 | 150 | 2.27 | 0.17 | 3.33 | -0.02 | 225 | 155 | 79 | 9.7 | 78 | 10.15 | 21.8 | 0.46 | 3.4 | 0.06 |
| EX081730 | DO | 0.09 | 6.32 | 1.2 | 210 | 3.11 | 0.12 | 2.76 | -0.02 | 287 | 120 | 81 | 15.1 | 43 | 10.95 | 26 | 0.49 | 3.5 | 0.05 |
| EX081731 | | 0.1 | 6.44 | 1.3 | 210 | 3.12 | 0.12 | 2.78 | -0.02 | 304 | 120 | 82 | 15.35 | 45 | 11.15 | 26.5 | 0.52 | 3.6 | 0.05 |
| EX081732 | | 0.22 | 7.67 | 12.5 | 180 | 0.76 | 0.29 | 0.17 | 0.03 | 37.3 | 27.8 | 544 | 4.06 | 366 | 13.25 | 20.8 | 0.29 | 3.9 | 0.09 |
| EX081733 | DO | 0.11 | 6.06 | 1.7 | 170 | 2.89 | 0.14 | 3.09 | -0.02 | 218 | 150 | 80 | 11.15 | 46 | 11.05 | 23.7 | 0.49 | 3.5 | 0.06 |
| EX081734 | DO | 0.1 | 6.26 | 1.3 | 190 | 2.66 | 0.1 | 3.05 | -0.02 | 222 | 81.6 | 82 | 10.8 | 28 | 10.7 | 23.6 | 0.41 | 3.9 | 0.06 |
| EX081735 | CHUM | 0.05 | 7.05 | 0.8 | 180 | 2.17 | 0.02 | 1.02 | -0.02 | 444 | 17.7 | 58 | 5.92 | 3 | 8.52 | 25.3 | 0.62 | 3.5 | 0.039 |
| EX081736 | CHUM | 0.09 | 6.81 | 0.6 | 160 | 1.23 | 0.02 | 1.41 | -0.02 | 97.7 | 15.3 | 48 | 5.45 | 3 | 7.59 | 20.3 | 0.3 | 3.2 | 0.03 |

| NWQ16MSN | 120416 | Ag | Al | As | Ba | Be | Bi | Ca | Cd | Ce | Co | Cr | Cs | Cu | Fe | Ga | Ge | Hf | In |
|---|---|---|---|---|---|---|---|---|---|---|---|---|---|---|---|---|---|---|---|
| UNITS | | ppm | % | ppm | ppm | ppm | ppm | % | ppm | ppm | ppm | ppm | ppm | ppm | % | ppm | ppm | ppm | ppm |
| DETECTION | | 0.01 | 0.01 | 0.2 | 10 | 0.05 | 0.01 | 0.01 | 0.02 | 0.01 | 0.1 | 1 | 0.05 | 0.2 | 0.01 | 0.05 | 0.05 | 0.1 | 0.005 |
| METHOD | | ME-MS61 | ME-MS61 | ME-MS61 | ME-MS61 | ME-MS61 | ME-MS61 | ME-MS61 | ME-MS61 | ME-MS61 | ME-MS61 | ME-MS61 | ME-MS61 | ME-MS61 | ME-MS61 | ME-MS61 | ME-MS61 | ME-MS61 | ME-MS61 |
| CO | ME-MS61:REE's may not be totally soluble in this method. | | | | | | | | | | | | | | | | | | |
| EX081737 | CHUM | 0.05 | 7.08 | 0.7 | 170 | 1.13 | 0.02 | 0.57 | -0.02 | 157.5 | 15.1 | 55 | 5.52 | 3 | 8.22 | 21.7 | 0.37 | 3.6 | 0.027 |
| EX081738 | CHUM | 0.05 | 6.92 | 0.6 | 160 | 1.48 | 0.02 | 0.8 | -0.02 | 65.7 | 15.2 | 61 | 5.3 | 3 | 8.26 | 19.65 | 0.28 | 3.5 | 0.03 |
| EX081739 | CHUM | 0.05 | 6.88 | 0.6 | 160 | 1.21 | 0.02 | 0.58 | -0.02 | 105 | 14.8 | 52 | 5.71 | 4 | 8.67 | 20.9 | 0.36 | 3.4 | 0.03 |
| EX081740 | CHUM | 0.1 | 6.43 | 2 | 90 | 1.72 | 0.19 | 3.07 | -0.02 | 186.5 | 32.5 | 12 | 7.48 | 40 | 11.8 | 23.4 | 0.49 | 7.2 | 0.044 |
| EX081741 | CHUM | 0.16 | 6.26 | 1.9 | 100 | 1.67 | 0.21 | 3.35 | -0.02 | 145 | 34.6 | 15 | 8.71 | 66 | 12.6 | 20.8 | 0.49 | 6.9 | 0.038 |
| EX081742 | CHUM | 0.13 | 6.2 | 1.9 | 90 | 1.49 | 0.14 | 2.6 | -0.02 | 142.5 | 23.1 | 15 | 8.27 | 13 | 15.15 | 21.2 | 0.65 | 6.3 | 0.027 |
| EX081743 | CHUM | 0.14 | 6.08 | 1.4 | 80 | 1.61 | 0.15 | 3.08 | 0.02 | 97.6 | 25.7 | 13 | 7.69 | 18 | 12.95 | 20.6 | 0.52 | 6.3 | 0.043 |
| EX081744 | CHUM | 0.15 | 6.49 | 1.9 | 150 | 1.5 | 0.15 | 2.69 | 0.02 | 77.7 | 38.3 | 12 | 13.5 | 51 | 11.55 | 23.3 | 0.4 | 6.8 | 0.034 |
| EX081745 | CHUM | 0.34 | 5.85 | 2.1 | 70 | 1.45 | 0.35 | 4.9 | 0.03 | 98.6 | 93.9 | 54 | 0.8 | 1830 | 11.95 | 20.9 | 0.33 | 2.8 | 0.331 |
| EX081746 | | 0.34 | 5.89 | 2.7 | 70 | 1.4 | 0.35 | 5.01 | 0.03 | 100 | 97.8 | 58 | 0.81 | 1850 | 12 | 21.3 | 0.32 | 2.9 | 0.332 |
| EX081747 | | 0.24 | 8.17 | 13.7 | 190 | 0.76 | 0.31 | 0.18 | 0.03 | 40 | 30.3 | 565 | 4.33 | 387 | 14.35 | 23 | 0.3 | 4.2 | 0.095 |
| EX081748 | CHUM | 0.09 | 7.21 | 0.5 | 150 | 1.33 | 0.09 | 3.54 | -0.02 | 49.3 | 33.8 | 85 | 7.5 | 120 | 13.4 | 22.3 | 0.34 | 2.8 | 0.097 |
| EX081749 | CHUM | 0.07 | 7.41 | 0.4 | 180 | 1.23 | 0.03 | 2.44 | -0.02 | 38.5 | 23.8 | 77 | 11.25 | 306 | 8.2 | 17.85 | 0.26 | 2.9 | 0.074 |
| EX081750 | CHUM | 0.05 | 6.99 | -0.2 | 180 | 1.08 | 0.01 | 2.41 | -0.02 | 36.6 | 19.2 | 81 | 10.85 | 97 | 8.55 | 17.95 | 0.24 | 2.8 | 0.059 |
| EX081751 | CHUM | 0.06 | 7.17 | 0.4 | 180 | 1.13 | 0.02 | 2.41 | -0.02 | 40.4 | 23.2 | 77 | 11.8 | 69 | 8.63 | 18.95 | 0.25 | 2.8 | 0.061 |
| EX081752 | CHUM | 0.11 | 6.63 | 0.9 | 200 | 1.39 | 0.07 | 5.43 | 0.02 | 50.9 | 45.3 | 64 | 1.21 | 90 | 9.52 | 20.6 | 0.27 | 3.3 | 0.09 |
| EX081753 | CHUM | 0.12 | 6.51 | 1 | 160 | 1.68 | 0.08 | 4.1 | -0.02 | 60.2 | 40.7 | 60 | 4.43 | 90 | 10 | 21.4 | 0.32 | 3.8 | 0.077 |
| EX081754 | CHUM | 0.11 | 6.7 | 0.8 | 150 | 1.76 | 0.1 | 3.89 | -0.02 | 48.8 | 45.6 | 64 | 6.31 | 71 | 9.72 | 21.8 | 0.29 | 3.9 | 0.082 |
| EX081755 | CHUM | 0.1 | 6.55 | 1.1 | 150 | 1.99 | 0.1 | 4.15 | -0.02 | 48.1 | 44.7 | 64 | 5.66 | 61 | 8.93 | 20.9 | 0.26 | 3.8 | 0.069 |
| EX081756 | CHUM | 0.1 | 6.85 | 1.1 | 120 | 2.31 | 0.07 | 3.2 | -0.02 | 56.8 | 46.8 | 62 | 9.03 | 42 | 9.1 | 22 | 0.3 | 4.3 | 0.058 |
| EX081757 | Magpie | 0.14 | 5.99 | 3.8 | 60 | 1.19 | 0.1 | 4.33 | -0.02 | 51.4 | 49.8 | 14 | 1.95 | 557 | 8.57 | 23.7 | 0.25 | 7.2 | 0.083 |
| EX081758 | Magpie | 0.11 | 5.85 | 1.8 | 40 | 1.35 | 0.06 | 3.62 | -0.02 | 75.4 | 29.5 | 16 | 0.74 | 478 | 9.36 | 24.7 | 0.3 | 7 | 0.074 |
| EX081759 | Magpie | 0.12 | 5.91 | 1.5 | 50 | 1.52 | 0.06 | 2.62 | -0.02 | 65.9 | 22.4 | 23 | 0.88 | 199 | 11.75 | 26.4 | 0.32 | 7.3 | 0.048 |
| EX081760 | Magpie | 0.12 | 5.81 | 1.4 | 50 | 1.33 | 0.04 | 2.76 | -0.02 | 48.3 | 19.6 | 14 | 0.76 | 145 | 11.35 | 24.7 | 0.31 | 7.1 | 0.04 |
| EX081761 | Magpie | 0.18 | 5.04 | 2.1 | 50 | 1.1 | 0.07 | 8.27 | -0.02 | 49.3 | 28.4 | 9 | 0.75 | 664 | 8.3 | 19.05 | 0.24 | 6.4 | 0.059 |
| EX081762 | Magpie | 0.07 | 7.08 | 2.7 | 180 | 1.11 | 0.06 | 3.43 | -0.02 | 28 | 38.7 | 77 | 1.45 | 419 | 9.79 | 21 | 0.23 | 2.8 | 0.089 |
| EX081763 | Magpie | 0.06 | 7.06 | 1.5 | 260 | 1.37 | 0.05 | 1.89 | -0.02 | 28.2 | 46.6 | 44 | 2.03 | 277 | 10.3 | 21.8 | 0.54 | 3.1 | 0.101 |
| EX081764 | Magpie | 0.08 | 6.96 | 2.4 | 190 | 1.19 | 0.06 | 3.23 | -0.02 | 30.5 | 51.8 | 47 | 2.74 | 497 | 10.55 | 21.4 | 0.29 | 2.6 | 0.096 |
| EX081765 | Magpie | 0.09 | 7.05 | 2.7 | 150 | 1.32 | 0.09 | 2.49 | -0.02 | 35.2 | 52.2 | 43 | 1.93 | 344 | 10.35 | 21.9 | 0.47 | 2.7 | 0.099 |
| EX081766 | | 0.07 | 6.84 | 2.8 | 150 | 1.36 | 0.09 | 2.43 | -0.02 | 34.2 | 49.8 | 42 | 1.82 | 333 | 9.92 | 21.8 | 0.26 | 2.9 | 0.093 |
| EX081767 | | 0.27 | 8.15 | 14.4 | 190 | 0.89 | 0.31 | 0.18 | 0.02 | 39.3 | 32.1 | 567 | 4.49 | 388 | 14.1 | 23.1 | 0.95 | 4.2 | 0.095 |
| EX081768 | Magpie | 0.07 | 6.91 | 1.7 | 200 | 1.19 | 0.05 | 4.11 | -0.02 | 35.9 | 41.6 | 42 | 1.83 | 240 | 9.38 | 22.1 | 0.28 | 2.5 | 0.086 |
| EX081769 | Magpie | 0.14 | 5.74 | 1.8 | 150 | 1.31 | 0.06 | 4.05 | -0.02 | 44.3 | 36.6 | 44 | 1.45 | 308 | 10.95 | 22.6 | 0.28 | 5.3 | 0.1 |
| EX081770 | Magpie | 0.13 | 5.94 | 2.1 | 170 | 1.28 | 0.05 | 4.47 | 0.02 | 39.8 | 35.5 | 30 | 1.63 | 292 | 10.05 | 21.5 | 0.28 | 5.2 | 0.094 |
| EX081771 | Magpie | 0.17 | 5.83 | 3 | 170 | 1.11 | 0.06 | 4.65 | -0.02 | 38.2 | 39.2 | 32 | 1.94 | 430 | 9.41 | 21 | 0.24 | 4.8 | 0.084 |
| EX081772 | Magpie | 0.16 | 6.14 | 3.3 | 180 | 1.25 | 0.06 | 4.16 | -0.02 | 35.8 | 35.3 | 20 | 2.18 | 253 | 10.25 | 22.9 | 0.26 | 4.7 | 0.077 |
| EX081773 | Magpie | 0.18 | 6.04 | 2 | 180 | 1.26 | 0.06 | 3.78 | -0.02 | 37.6 | 32.7 | 22 | 2.01 | 458 | 10.35 | 22.1 | 0.26 | 4.7 | 0.088 |
| EX081774 | Magpie | 0.1 | 6.39 | 2.4 | 320 | 1.04 | 0.06 | 4.78 | -0.02 | 30.7 | 41.9 | 63 | 2.85 | 194 | 8.66 | 20.5 | 0.24 | 3.5 | 0.088 |
| EX081775 | Magpie | 0.12 | 7.1 | 1.9 | 450 | 1.03 | 0.07 | 3.8 | -0.02 | 33.5 | 34.1 | 73 | 2.86 | 301 | 9.69 | 22.5 | 0.23 | 3.9 | 0.098 |
| EX081776 | | 0.14 | 7.04 | 2 | 440 | 1.03 | 0.07 | 3.7 | -0.02 | 31.2 | 33.9 | 73 | 2.76 | 289 | 9.33 | 22 | 0.24 | 3.7 | 0.089 |
| EX081777 | | 0.24 | 7.82 | 13.4 | 180 | 0.77 | 0.3 | 0.19 | 0.02 | 37.3 | 30.3 | 514 | 4.1 | 362 | 13.2 | 22.2 | 0.44 | 3.9 | 0.095 |

| NWQ16MSM | 120416 | Ag | Al | As | Ba | Be | Bi | Ca | Cd | Ce | Co | Cr | Cs | Cu | Fe | Ga | Ge | Hf | In |
|---|---|---|---|---|---|---|---|---|---|---|---|---|---|---|---|---|---|---|---|
| UNITS | | ppm | % | ppm | ppm | ppm | ppm | % | ppm | ppm | ppm | ppm | ppm | ppm | % | ppm | ppm | ppm | ppm |
| DETECTION | | 0.01 | 0.01 | 0.2 | 10 | 0.05 | 0.01 | 0.01 | 0.02 | 0.01 | 0.1 | 1 | 0.05 | 0.2 | 0.01 | 0.05 | 0.05 | 0.1 | 0.005 |
| METHOD | | ME-MS61 | ME-MS61 | ME-MS61 | ME-MS61 | ME-MS61 | ME-MS61 | ME-MS61 | ME-MS61 | ME-MS61 | ME-MS61 | ME-MS61 | ME-MS61 | ME-MS61 | ME-MS61 | ME-MS61 | ME-MS61 | ME-MS61 | ME-MS61 |
| CO | ME-MS61:REE's may not be totally soluble in this method. | | | | | | | | | | | | | | | | | | |
| EX081778 | Magpie | 0.11 | 6.99 | 2 | 310 | 1.15 | 0.06 | 3.58 | -0.02 | 31.2 | 28.8 | 70 | 1.85 | 188 | 9.06 | 22.5 | 0.24 | 3.7 | 0.087 |
| EX081779 | Magpie | 0.09 | 6.74 | 2.7 | 220 | 1.23 | 0.06 | 3.49 | -0.02 | 29.3 | 35 | 70 | 1.6 | 117 | 8.83 | 21.3 | 0.23 | 3.5 | 0.072 |
| EX081780 | Magpie | 0.15 | 7.1 | 4 | 260 | 1.22 | 0.07 | 4.66 | -0.02 | 32.5 | 68.4 | 73 | 2.26 | 277 | 7.67 | 23 | 0.25 | 3.5 | 0.071 |
| EX081781 | Magpie | 0.11 | 6.5 | 5.2 | 260 | 1.06 | 0.12 | 4.87 | -0.02 | 34.1 | 47 | 104 | 2.36 | 388 | 9.78 | 22.5 | 0.27 | 3.5 | 0.107 |
| EX081782 | Magpie | 0.1 | 6.69 | 6.2 | 270 | 1 | 0.12 | 4.86 | -0.02 | 36.2 | 42.6 | 96 | 1.34 | 400 | 9.86 | 22.7 | 0.34 | 3.3 | 0.112 |
| EX081783 | Magpie | 0.09 | 7.1 | 3.9 | 280 | 1.04 | 0.11 | 4.61 | -0.02 | 37.8 | 34.5 | 96 | 1.44 | 225 | 10.5 | 24 | 0.34 | 3.5 | 0.114 |
| EX081784 | Magpie | 0.09 | 7.07 | 3.6 | 280 | 0.93 | 0.09 | 4.52 | -0.02 | 34.9 | 35.6 | 99 | 1.24 | 226 | 10.75 | 23.9 | 0.27 | 3.4 | 0.101 |
| EX081785 | Magpie | 0.1 | 6.87 | 4.2 | 130 | 0.96 | 0.1 | 4.61 | -0.02 | 34.9 | 32.5 | 103 | 0.68 | 301 | 10.45 | 22.5 | 0.28 | 3.6 | 0.087 |
| EX081786 | Magpie | 0.13 | 6.54 | 7.4 | 90 | 1.65 | 0.13 | 2.59 | -0.02 | 35.1 | 105 | 81 | 1.75 | 201 | 13.1 | 21.1 | 0.28 | 4.4 | 0.065 |
| EX081787 | Magpie | 0.12 | 6.24 | 6.8 | 80 | 1.59 | 0.12 | 3.16 | -0.02 | 34.4 | 84.7 | 76 | 1.56 | 259 | 11.95 | 20.5 | 0.28 | 4 | 0.073 |
| EX081788 | Magpie | 0.15 | 6.13 | 5.8 | 80 | 1.6 | 0.11 | 3.76 | -0.02 | 36.1 | 79 | 77 | 1.49 | 923 | 11.4 | 20.4 | 0.3 | 4 | 0.089 |
| EX081789 | Magpie | 0.17 | 6.13 | 10.7 | 100 | 1.45 | 0.11 | 4.25 | -0.02 | 28.9 | 128.5 | 81 | 2.02 | 221 | 12.45 | 20.6 | 0.26 | 4 | 0.053 |
| EX081790 | Magpie | 0.07 | 6.32 | 4.5 | 140 | 1.29 | 0.09 | 3.13 | -0.02 | 37.5 | 53.8 | 87 | 2.34 | 99 | 10.75 | 21.6 | 0.25 | 3.9 | 0.077 |
| EX081791 | | 0.09 | 6.29 | 4.9 | 140 | 1.26 | 0.09 | 3.1 | -0.02 | 37.7 | 57.3 | 88 | 2.32 | 99 | 10.7 | 21.2 | 0.28 | 3.8 | 0.079 |
| EX081792 | | 0.24 | 7.87 | 13.9 | 180 | 0.83 | 0.3 | 0.18 | 0.02 | 36.6 | 30.3 | 521 | 4 | 365 | 13.55 | 22.4 | 0.29 | 3.8 | 0.091 |
| EX081793 | TCS | 0.14 | 6.47 | 1.5 | 40 | 1.12 | 0.06 | 3.86 | -0.02 | 48.5 | 41.4 | 58 | 2.12 | 854 | 12.65 | 21.4 | 0.6 | 2.3 | 0.134 |
| EX081794 | TCS | 0.11 | 6.51 | 1.4 | 50 | 2.09 | 0.06 | 3.43 | -0.02 | 35.5 | 37.6 | 50 | 4.41 | 509 | 10.95 | 22.1 | 0.34 | 2.2 | 0.1 |
| EX081795 | TCS | 0.12 | 6.53 | 1.5 | 80 | 1.28 | 0.03 | 2.85 | -0.02 | 36.9 | 47.8 | 86 | 9.92 | 279 | 11.65 | 24.2 | 0.33 | 2.4 | 0.078 |
| EX081796 | TCS | 0.08 | 6.93 | 1.1 | 80 | 1.13 | 0.03 | 3.09 | -0.02 | 46.6 | 39.1 | 62 | 9.47 | 253 | 11.85 | 25.3 | 0.37 | 2.6 | 0.073 |
| EX081797 | TCS | 0.06 | 6.59 | 1.1 | 100 | 1.24 | 0.02 | 3.57 | 0.02 | 63.8 | 40.5 | 72 | 9.81 | 161 | 10.8 | 24.6 | 0.41 | 2.3 | 0.103 |
| Ch:EX081710 | | 0.13 | 6.07 | 1.9 | 130 | 1.87 | 0.09 | 3.1 | -0.02 | 35.5 | 54 | 121 | 6.23 | 764 | 11.3 | 22.2 | 0.44 | 4.1 | 0.089 |
| Ch:EX081730 | | 0.1 | 6.23 | 1.3 | 210 | 3.18 | 0.12 | 2.71 | -0.02 | 272 | 122.5 | 80 | 14.9 | 46 | 10.7 | 25.9 | 0.52 | 3.5 | 0.049 |
| Ch:EX081745 | | 0.33 | 5.93 | 2.6 | 70 | 1.63 | 0.36 | 4.9 | 0.02 | 98.9 | 101 | 57 | 0.82 | 1840 | 12.15 | 21.3 | 0.38 | 2.8 | 0.322 |
| Ch:EX081765 | | 0.09 | 7.08 | 2.9 | 150 | 1.38 | 0.09 | 2.48 | -0.02 | 35 | 51.2 | 43 | 1.63 | 341 | 10.4 | 22 | 0.31 | 2.8 | 0.097 |
| Ch:EX081780 | | 0.14 | 7.07 | 4.2 | 260 | 1.33 | 0.07 | 4.61 | -0.02 | 31.6 | 69 | 70 | 2.23 | 273 | 7.6 | 22.7 | 0.21 | 3.6 | 0.072 |
| Blank01 | | -0.01 | -0.01 | -0.2 | -10 | -0.05 | -0.01 | -0.01 | -0.02 | -0.01 | -0.1 | -1 | -0.05 | 0 | -0.01 | -0.05 | -0.05 | -0.1 | -0.005 |
| Blank02 | | -0.01 | -0.01 | -0.2 | -10 | -0.05 | -0.01 | -0.01 | -0.02 | -0.01 | -0.1 | 1 | -0.05 | 1 | -0.01 | -0.05 | -0.05 | -0.1 | -0.005 |
| Blank03 | | -0.01 | -0.01 | -0.2 | -10 | -0.05 | -0.01 | -0.01 | -0.02 | -0.01 | -0.1 | -1 | -0.05 | 0 | -0.01 | -0.05 | -0.05 | -0.1 | -0.005 |
| St01:OREAS-45e | | 0.38 | 6.27 | 15.2 | 240 | 0.62 | 0.26 | 0.06 | 0.02 | 24.7 | 54.5 | 968 | 1.31 | 757 | 22 | 15.55 | 1.18 | 3.3 | 0.092 |
| St02:OREAS-45e | | 0.41 | 6.3 | 16.3 | 240 | 0.64 | 0.27 | 0.06 | 0.02 | 23.5 | 58.8 | 915 | 1.25 | 760 | 22 | 16.65 | 0.86 | 3.2 | 0.087 |
| St03:MRGeo08 | | 4.66 | 7.43 | 34.2 | 1070 | 3.31 | 0.62 | 2.44 | 2.32 | 81.5 | 20.4 | 91 | 13.4 | 628 | 3.78 | 20.2 | 0.29 | 3.4 | 0.177 |
| St04:GBM908-10 | | 3.06 | 6.9 | 57.2 | 1080 | 1.63 | 1.25 | 3.48 | 1.76 | 108 | 27.6 | 140 | 4.1 | 3650 | 5.34 | 21.6 | 0.36 | 3.7 | 0.073 |
| St05:OGGeo08 | | 19.75 | 6.53 | 114 | 920 | 3.1 | 9.55 | 1.99 | 18.7 | 70.2 | 93.9 | 84 | 11.1 | 8100 | 5.04 | 16.85 | 0.47 | 2.9 | 1.385 |
| St06:OGGeo08 | | 19.6 | 6.51 | 116 | 820 | 3.08 | 9.56 | 2.03 | 18.55 | 69.6 | 96.9 | 80 | 11.1 | 8060 | 5.11 | 17.6 | 0.54 | 2.9 | 1.395 |
| THEBE | | -0.5 | 5.662975 | 4.2 | 29.9 | | 0.03 | 0 | -0.5 | 79.1 | 60 | 50 | 0.15 | 1750 | 0 | 19.2 | -5 | 3.8 | 0.031 |
| THEBE | | -0.5 | 3.651825 | 0.9 | 153 | | 0.04 | 0 | -0.5 | 30 | 32 | 50 | 0.12 | 2840 | 0 | 10.6 | -5 | 2.3 | 0.061 |
| THEBE | | -0.5 | 7.6212 | 4.5 | 363 | | 0.15 | 0 | -0.5 | 24.3 | 42 | 70 | 0.41 | 62 | 0 | 19.5 | -5 | 2.2 | 0.038 |
| THEBE | | -0.5 | 6.853788 | 7 | 400 | | 0.12 | 0 | -0.5 | 17.6 | 41 | 180 | 0.22 | 1100 | 0 | 17.2 | -5 | 2 | 0.057 |
| THEBE | | -0.5 | 7.647663 | 2.9 | 178 | | 0.12 | 0 | -0.5 | 15.3 | 41 | 260 | 0.3 | 176 | 0 | 18.1 | -5 | 2 | 0.022 |

| TV16047358 | 97 | | | | | | | | | | | | | | | | | | |
|---|---|---|---|---|---|---|---|---|---|---|---|---|---|---|---|---|---|---|---|
| NWQ16MSM | 120416 | K | La | Li | Mg | Mn | Mo | Na | Nb | Ni | P | Pb | Rb | Re | S | Sb | Sc | Se | Sn |
| UNITS | | % | ppm | ppm | % | ppm | ppm | % | ppm | ppm | ppm | ppm | ppm | ppm | % | ppm | ppm | ppm | ppm |
| DETECTION | | 0.01 | 0.5 | 0.2 | 0.01 | 5 | 0.05 | 0.01 | 0.1 | 0.2 | 10 | 0.5 | 0.1 | 0.002 | 0.01 | 0.05 | 0.1 | 1 | 0.2 |
| METHOD | | ME-MS61 | ME-MS61 | ME-MS61 | ME-MS61 | ME-MS61 | ME-MS61 | ME-MS61 | ME-MS61 | ME-MS61 | ME-MS61 | ME-MS61 | ME-MS61 | ME-MS61 | ME-MS61 | ME-MS61 | ME-MS61 | ME-MS61 | ME-MS61 |
| CO | ME-MS61:REE's may not be totally soluble in this method. | | | | | | | | | | | | | | | | | | |
| CO | | | | | | | | | | | | | | | | | | | |
| EX081701 | BA | 1.84 | 50.8 | 16.6 | 2.86 | 699 | 2.38 | 2.39 | 13.8 | 47.9 | 1040 | 1.2 | 164 | 0.002 | 0.27 | 0.33 | 41.2 | 3 | 1.9 |
| EX081702 | BA | 1.79 | 57.3 | 18.3 | 2.91 | 678 | 2.41 | 2.28 | 13.4 | 49.3 | 1020 | 1 | 148.5 | 0.003 | 0.26 | 0.44 | 40.7 | 3 | 1.9 |
| EX081703 | BA | 2.72 | 122.5 | 17.4 | 3.65 | 493 | 2.24 | 1.7 | 9.2 | 85.1 | 2550 | 3.6 | 229 | -0.002 | 0.33 | 0.16 | 32.7 | 4 | 1.3 |
| EX081704 | BA | 1.59 | 30.7 | 10.5 | 2.69 | 590 | 3.39 | 2.56 | 14.1 | 50.1 | 1100 | 3.2 | 136.5 | 0.003 | 0.28 | 0.24 | 41.2 | 3 | 2 |
| EX081705 | BA | 1.65 | 14.1 | 11.6 | 2.88 | 787 | 2.7 | 2.32 | 7.5 | 57.7 | 660 | 0.9 | 120 | 0.002 | 0.1 | 0.24 | 41.3 | 2 | 1.4 |
| EX081706 | BA | 0.67 | 22.8 | 10.3 | 3.08 | 1800 | 4.42 | 3.01 | 17.1 | 73.9 | 1120 | 3.5 | 42.2 | 0.004 | 0.33 | 0.4 | 46.3 | 5 | 4.8 |
| EX081707 | BA | 1.19 | 24.9 | 14.2 | 3.49 | 1410 | 3.31 | 2.94 | 13.5 | 57.1 | 960 | 1.4 | 89.6 | 0.002 | 0.09 | 0.28 | 44.2 | 3 | 4 |
| EX081708 | BA | 1.14 | 18.5 | 16.5 | 2.91 | 1320 | 3.08 | 2.63 | 13 | 49.5 | 900 | 1.2 | 67.9 | -0.002 | 0.1 | 0.35 | 39.9 | 3 | 3.6 |
| EX081709 | BA | 0.94 | 18.5 | 11.8 | 3.11 | 1290 | 3.7 | 3.09 | 13.7 | 62.9 | 970 | 1.9 | 65.9 | 0.003 | 0.21 | 0.32 | 47.5 | 3 | 4.5 |
| EX081710 | BA | 1.59 | 16.3 | 16 | 3.43 | 1100 | 2.33 | 2.97 | 14 | 75.2 | 950 | 1.4 | 130 | 0.002 | 0.27 | 0.24 | 45.6 | 3 | 3.4 |
| EX081711 | BA | 1.68 | 45.1 | 9.7 | 2.11 | 595 | 3.2 | 2.39 | 10.7 | 50.9 | 880 | 1.1 | 160.5 | 0.002 | 0.36 | 0.22 | 38 | 4 | 2.4 |
| EX081712 | BA | 1.11 | 36.4 | 8.5 | 2.17 | 608 | 3.56 | 2.55 | 10.9 | 48.7 | 880 | 1.3 | 81.1 | 0.002 | 0.1 | 0.27 | 38.1 | 3 | 2.6 |
| EX081713 | BA | 0.94 | 31.1 | 7.4 | 2.12 | 731 | 6.39 | 2.66 | 11 | 43.6 | 950 | 1.1 | 64.7 | 0.003 | 0.05 | 0.28 | 39.8 | 3 | 2.7 |
| EX081714 | BA | 1.16 | 25.3 | 8 | 2.16 | 760 | 4.64 | 2.53 | 11.5 | 47.8 | 950 | 1.1 | 77.1 | 0.003 | 0.08 | 0.25 | 42.2 | 4 | 2.5 |
| EX081715 | BA | 1.1 | 42.8 | 8 | 2.18 | 733 | 3.89 | 2.77 | 10.9 | 44 | 1010 | 1.4 | 84 | 0.002 | 0.07 | 0.21 | 38.1 | 3 | 2.4 |
| EX081716 | | 1.09 | 43 | 8 | 2.21 | 741 | 3.75 | 2.79 | 11.1 | 43.9 | 1040 | 1.3 | 83.4 | 0.002 | 0.07 | 0.21 | 38.3 | 3 | 2.3 |
| EX081717 | | 0.38 | 17.1 | 22.3 | 0.21 | 467 | 2.36 | 0.09 | 13.9 | 229 | 400 | 19.7 | 41.4 | -0.002 | 0.05 | 0.8 | 49.7 | 4 | 2.6 |
| EX081718 | BA | 1.49 | 22.2 | 14.5 | 2.18 | 780 | 2.78 | 2.27 | 10.8 | 52.1 | 880 | 1.2 | 146.5 | 0.003 | 0.26 | 0.26 | 40.4 | 4 | 1.7 |
| EX081719 | BA | 1.62 | 18.2 | 12.5 | 2.32 | 1040 | 3.31 | 1.87 | 9.5 | 45.5 | 770 | 0.9 | 105 | 0.002 | 0.2 | 0.52 | 38.6 | 3 | 1.6 |
| EX081720 | BA | 1.1 | 19 | 8.8 | 2.23 | 1190 | 3.77 | 2.52 | 10.3 | 46.1 | 890 | 0.9 | 68 | 0.003 | 0.18 | 0.31 | 41.3 | 3 | 1.6 |
| EX081721 | BA | 1.09 | 23.1 | 10 | 2.06 | 1130 | 3.23 | 2.24 | 10 | 51.8 | 830 | 1.2 | 62.9 | 0.003 | 0.35 | 2.09 | 39.6 | 4 | 1.6 |
| EX081722 | BA | 1.86 | 18.9 | 20.1 | 2.34 | 1300 | 3.51 | 1.97 | 10.3 | 40.4 | 900 | 0.9 | 133.5 | 0.002 | 0.16 | 1.15 | 39.1 | 3 | 1.5 |
| EX081723 | BA | 1.08 | 29 | 9.4 | 1.67 | 979 | 3.53 | 2.43 | 17.8 | 20.5 | 1490 | 1.8 | 90.6 | 0.003 | 0.16 | 0.96 | 39.5 | 5 | 1.9 |
| EX081724 | BA | 0.98 | 29.1 | 9.5 | 1.66 | 1420 | 3.56 | 2.05 | 17.3 | 18.5 | 1500 | 1.4 | 52.8 | 0.003 | 0.15 | 2.11 | 41.6 | 5 | 2.2 |
| EX081725 | BA | 1.06 | 31 | 13.2 | 1.89 | 1350 | 3.17 | 1.76 | 16.6 | 20.9 | 1430 | 1.5 | 57.2 | 0.003 | 0.14 | 0.94 | 39 | 5 | 2.3 |
| EX081726 | BA | 0.74 | 39.3 | 14.1 | 1.72 | 1140 | 3.35 | 1.68 | 13.8 | 33.6 | 1220 | 1.5 | 42.5 | 0.003 | 0.23 | 0.9 | 31.7 | 4 | 2.4 |
| EX081727 | BA | 0.96 | 28 | 13.7 | 1.82 | 1220 | 3.07 | 2.33 | 17.1 | 22.8 | 1500 | 1.2 | 51.8 | 0.003 | 0.17 | 0.31 | 40.8 | 4 | 2.1 |
| EX081728 | DO | 1.5 | 190.5 | 17.5 | 3.46 | 447 | 0.78 | 2.96 | 14.2 | 60.9 | 790 | 2 | 113 | 0.002 | 0.62 | 1.17 | 45.6 | 3 | 3.1 |
| EX081729 | DO | 1.53 | 113.5 | 16.4 | 3.36 | 521 | 2.31 | 2.65 | 14 | 65 | 850 | 2 | 138.5 | 0.002 | 0.87 | 0.52 | 42.7 | 4 | 3.3 |
| EX081730 | DO | 2.2 | 147 | 23.5 | 3.83 | 478 | 1.05 | 2.82 | 14.4 | 66.5 | 940 | 1.7 | 200 | -0.002 | 0.61 | 1.2 | 42.6 | 3 | 3.1 |
| EX081731 | | 2.2 | 155 | 24.4 | 3.86 | 485 | 0.9 | 2.85 | 14.8 | 68.4 | 940 | 1.8 | 198 | 0.002 | 0.62 | 0.27 | 43.4 | 4 | 3.2 |
| EX081732 | | 0.38 | 17.1 | 22 | 0.21 | 465 | 2.37 | 0.09 | 13.9 | 226 | 400 | 19.5 | 41.4 | -0.002 | 0.05 | 1.18 | 49.7 | 4 | 2.6 |
| EX081733 | DO | 1.79 | 112.5 | 19.6 | 3.79 | 497 | 1.14 | 2.94 | 14.8 | 62.8 | 910 | 1.8 | 144 | -0.002 | 0.77 | 0.29 | 47.8 | 4 | 3.1 |
| EX081734 | DO | 1.81 | 114 | 18.6 | 3.37 | 396 | 1.08 | 3.05 | 14.9 | 53.5 | 970 | 1.6 | 141.5 | 0.002 | 0.37 | 0.52 | 42.6 | 3 | 2.7 |
| EX081735 | CHUM | 3.28 | 225 | 26.8 | 3.59 | 511 | 2.86 | 3.29 | 6.8 | 70.5 | 450 | 2 | 180 | -0.002 | 0.01 | 0.2 | 27.3 | 1 | 1.2 |
| EX081736 | CHUM | 2.97 | 49.9 | 22.9 | 3.71 | 434 | 1.89 | 3.06 | 8.3 | 58.3 | 400 | 1.7 | 195 | -0.002 | 0.01 | 0.15 | 27.7 | 1 | 1.1 |

| NWQ16MSN | 120416 | K | La | Li | Mg | Mn | Mo | Na | Nb | Ni | P | Pb | Rb | Re | S | Sb | Sc | Se | Sn |
|---|---|---|---|---|---|---|---|---|---|---|---|---|---|---|---|---|---|---|---|
| UNITS | | % | ppm | ppm | % | ppm | ppm | % | ppm | ppm | ppm | ppm | ppm | ppm | % | ppm | ppm | ppm | ppm |
| DETECTION | | 0.01 | 0.5 | 0.2 | 0.01 | 5 | 0.05 | 0.01 | 0.1 | 0.2 | 10 | 0.5 | 0.1 | 0.002 | 0.01 | 0.05 | 0.1 | 1 | 0.2 |
| METHOD | | ME-MS61 | ME-MS61 | ME-MS61 | ME-MS61 | ME-MS61 | ME-MS61 | ME-MS61 | ME-MS61 | ME-MS61 | ME-MS61 | ME-MS61 | ME-MS61 | ME-MS61 | ME-MS61 | ME-MS61 | ME-MS61 | ME-MS61 | ME-MS61 |
| CO | ME-MS61:REE's may not be totally soluble in this method. | | | | | | | | | | | | | | | | | | |
| EX081737 | CHUM | 3.18 | 80.4 | 23.3 | 3.26 | 428 | 2.56 | 3.24 | 8.9 | 62.2 | 440 | 2.1 | 188.5 | -0.002 | 0.01 | 0.14 | 27 | 1 | 1.1 |
| EX081738 | CHUM | 2.91 | 32.1 | 22.8 | 3.11 | 422 | 2.26 | 3.26 | 8.8 | 58.4 | 410 | 2.2 | 153 | -0.002 | 0.01 | 0.17 | 30.1 | 1 | 1.1 |
| EX081739 | CHUM | 2.96 | 51.7 | 22.1 | 3.09 | 398 | 2.28 | 3.26 | 8.4 | 58.3 | 410 | 1.7 | 169.5 | -0.002 | 0.01 | 0.17 | 26.5 | 1 | 1.1 |
| EX081740 | CHUM | 1.3 | 92.3 | 13.4 | 2.6 | 645 | 7.94 | 3.43 | 21.1 | 44.1 | 1670 | 3.3 | 139 | 0.005 | 0.11 | 0.43 | 50 | 4 | 5.7 |
| EX081741 | CHUM | 1.35 | 70.1 | 9.5 | 2.47 | 564 | 12.5 | 3.64 | 20.6 | 41.3 | 1620 | 2.7 | 150 | 0.006 | 0.16 | 0.47 | 70 | 5 | 6 |
| EX081742 | CHUM | 1.38 | 68.5 | 10.4 | 2.07 | 470 | 4.44 | 3.65 | 19.3 | 41 | 1500 | 2.7 | 143.5 | 0.002 | 0.03 | 0.37 | 46.9 | 5 | 7.1 |
| EX081743 | CHUM | 1.23 | 47.1 | 9.9 | 2.3 | 581 | 4.07 | 3.57 | 20.3 | 40 | 1350 | 2.6 | 132.5 | 0.003 | 0.05 | 0.39 | 52.7 | 5 | 6.9 |
| EX081744 | CHUM | 2.24 | 36.2 | 21.9 | 2.86 | 579 | 5.05 | 2.89 | 20.5 | 49.5 | 1580 | 3.1 | 238 | 0.003 | 0.15 | 0.36 | 40.2 | 6 | 6.9 |
| EX081745 | CHUM | 0.69 | 53.8 | 4.9 | 2.25 | 1190 | 7.28 | 2.58 | 11.1 | 58.7 | 590 | 11.8 | 36.2 | 0.004 | 1.29 | 0.52 | 15.6 | 4 | 9.4 |
| EX081746 | | 0.69 | 54.7 | 5 | 2.27 | 1230 | 7.36 | 2.6 | 11.1 | 61.5 | 580 | 11.9 | 36.5 | 0.004 | 1.31 | 0.51 | 16.1 | 3 | 9.6 |
| EX081747 | | 0.4 | 18.6 | 22.9 | 0.22 | 488 | 2.71 | 0.1 | 15.8 | 238 | 420 | 20.7 | 44.4 | -0.002 | 0.05 | 0.92 | 53.2 | 4 | 2.8 |
| EX081748 | CHUM | 1.91 | 24.8 | 14.5 | 3.65 | 972 | 1.68 | 3.19 | 7.4 | 57.2 | 470 | 3 | 154.5 | -0.002 | 0.1 | 0.23 | 28.4 | 2 | 2.8 |
| EX081749 | CHUM | 2.68 | 19.2 | 20.2 | 4.65 | 704 | 0.76 | 3.14 | 6.7 | 65.1 | 460 | 3.2 | 213 | -0.002 | 0.11 | 0.1 | 33.2 | 2 | 1.8 |
| EX081750 | CHUM | 2.57 | 18.1 | 19.5 | 4.38 | 641 | 0.7 | 2.9 | 6.7 | 61.8 | 480 | 2 | 208 | -0.002 | 0.02 | 0.08 | 33.3 | 1 | 1.4 |
| EX081751 | CHUM | 2.65 | 19.9 | 21.1 | 4.51 | 621 | 0.8 | 2.91 | 6.7 | 64.2 | 470 | 3.4 | 221 | -0.002 | 0.06 | 0.08 | 34.7 | 1 | 1.5 |
| EX081752 | CHUM | 1.62 | 23.5 | 11.3 | 3 | 1030 | 2.32 | 2.49 | 16.1 | 46.6 | 890 | 6 | 124.5 | 0.003 | 0.17 | 0.32 | 36.8 | 3 | 2.1 |
| EX081753 | CHUM | 1.42 | 28.3 | 13.7 | 3.39 | 730 | 2.21 | 2.96 | 16.4 | 47.2 | 860 | 6 | 121 | 0.003 | 0.15 | 0.28 | 39.8 | 3 | 3.2 |
| EX081754 | CHUM | 1.52 | 22.7 | 14.3 | 3.15 | 840 | 2.36 | 2.78 | 16.5 | 51 | 890 | 4.6 | 142.5 | 0.002 | 0.15 | 0.27 | 40.7 | 3 | 3.4 |
| EX081755 | CHUM | 1.43 | 22.3 | 14.2 | 3.16 | 779 | 2.29 | 2.96 | 16.2 | 55.4 | 920 | 4.5 | 127.5 | 0.002 | 0.12 | 0.25 | 43.4 | 3 | 3.6 |
| EX081756 | CHUM | 1.67 | 26.8 | 17 | 3.27 | 697 | 1.82 | 3.33 | 17.6 | 61.2 | 1010 | 4.8 | 154 | -0.002 | 0.07 | 0.21 | 48.6 | 3 | 5.5 |
| EX081757 | Magpie | 0.52 | 23.2 | 9.2 | 2.07 | 667 | 3.52 | 3.6 | 17.1 | 26.6 | 1320 | 1.7 | 30.9 | 0.003 | 0.23 | 0.3 | 35.8 | 4 | 1.8 |
| EX081758 | Magpie | 0.31 | 35.3 | 10.4 | 2.08 | 610 | 4.53 | 3.61 | 17.6 | 20.9 | 1420 | 1.4 | 15.3 | 0.005 | 0.09 | 0.31 | 35.3 | 4 | 2 |
| EX081759 | Magpie | 0.38 | 29.5 | 7.9 | 2 | 567 | 3.82 | 3.79 | 17.3 | 20.6 | 1370 | 1.3 | 19.2 | 0.004 | 0.03 | 0.3 | 38.5 | 4 | 2.2 |
| EX081760 | Magpie | 0.38 | 20.8 | 9.1 | 1.92 | 483 | 3.68 | 3.58 | 16.7 | 20.7 | 1260 | 1.4 | 18.6 | 0.003 | 0.02 | 0.3 | 36.9 | 4 | 2.3 |
| EX081761 | Magpie | 0.39 | 21.4 | 8.6 | 1.74 | 714 | 2.43 | 3 | 15.6 | 19.5 | 1140 | 1.6 | 19 | 0.002 | 0.1 | 0.3 | 30.8 | 4 | 2 |
| EX081762 | Magpie | 1.27 | 13 | 19.7 | 4.08 | 850 | 1.92 | 2.74 | 6.1 | 85.9 | 750 | 0.9 | 57.9 | 0.002 | 0.11 | 0.33 | 33.3 | 2 | 1 |
| EX081763 | Magpie | 1.55 | 13.1 | 35.4 | 5.25 | 723 | 1.77 | 1.85 | 6.9 | 101 | 700 | 1 | 79.4 | 0.002 | 0.09 | 0.38 | 32.3 | 2 | 1 |
| EX081764 | Magpie | 1.36 | 14.4 | 20.5 | 4.32 | 879 | 1.96 | 2.44 | 6.3 | 111 | 730 | 1.1 | 66.9 | 0.002 | 0.19 | 0.36 | 33.6 | 2 | 1.2 |
| EX081765 | Magpie | 1.05 | 16.7 | 24.2 | 4.53 | 798 | 1.54 | 2.69 | 6.7 | 118 | 710 | 1 | 54.9 | 0.002 | 0.19 | 0.35 | 33.4 | 3 | 1.2 |
| EX081766 | | 1.02 | 16.2 | 23.6 | 4.39 | 759 | 1.54 | 2.61 | 6.5 | 113.5 | 700 | 0.9 | 54.2 | 0.002 | 0.18 | 0.35 | 32.8 | 3 | 1.1 |
| EX081767 | | 0.41 | 18.4 | 25.9 | 0.22 | 490 | 2.72 | 0.1 | 15.9 | 239 | 420 | 20.8 | 44.5 | -0.002 | 0.05 | 0.89 | 57.7 | 4 | 2.7 |
| EX081768 | Magpie | 1.32 | 19 | 19 | 3.96 | 898 | 1.92 | 2.64 | 7.1 | 96.2 | 710 | 0.9 | 69.2 | 0.002 | 0.12 | 0.36 | 32.9 | 2 | 1.1 |
| EX081769 | Magpie | 0.72 | 20 | 6.5 | 2.52 | 794 | 8.34 | 3.3 | 12.8 | 63.2 | 970 | 1.3 | 37.5 | 0.004 | 0.04 | 0.36 | 46.1 | 4 | 1.9 |
| EX081770 | Magpie | 0.8 | 17.7 | 6.8 | 2.51 | 786 | 5.39 | 3.46 | 13.1 | 47.1 | 880 | 1.5 | 44.6 | 0.002 | 0.05 | 0.38 | 45.8 | 4 | 2.3 |
| EX081771 | Magpie | 0.88 | 16.8 | 5.5 | 2.3 | 778 | 7.85 | 3.29 | 12.1 | 52.8 | 900 | 1.6 | 51.2 | 0.004 | 0.12 | 0.38 | 42 | 4 | 2.7 |
| EX081772 | Magpie | 0.94 | 15.5 | 5.9 | 2.54 | 809 | 5.1 | 3.51 | 11.5 | 47.2 | 870 | 1.6 | 54.7 | 0.002 | 0.1 | 0.37 | 45.7 | 3 | 2.6 |
| EX081773 | Magpie | 0.89 | 16.9 | 5.6 | 2.64 | 720 | 4.52 | 3.49 | 11.3 | 47.1 | 830 | 1.6 | 52.1 | 0.003 | 0.07 | 0.37 | 45.6 | 3 | 2.3 |
| EX081774 | Magpie | 1.19 | 13.6 | 7.5 | 3.4 | 781 | 3.3 | 3.32 | 8.8 | 55.1 | 660 | 1.2 | 70.8 | -0.002 | 0.16 | 0.3 | 39 | 3 | 1.7 |
| EX081775 | Magpie | 1.49 | 15 | 6.3 | 3.07 | 723 | 2.83 | 3.74 | 9.2 | 56 | 710 | 1.2 | 86.4 | 0.002 | 0.1 | 0.38 | 41.9 | 3 | 1.6 |
| EX081776 | | 1.44 | 13.9 | 6.1 | 2.98 | 688 | 3.17 | 3.59 | 9.1 | 56.6 | 690 | 1.3 | 84.5 | -0.002 | 0.1 | 0.36 | 41.8 | 3 | 1.6 |
| EX081777 | | 0.4 | 17.3 | 23.2 | 0.22 | 470 | 2.52 | 0.1 | 14.7 | 227 | 400 | 20.1 | 43.3 | -0.002 | 0.05 | 0.86 | 53.5 | 4 | 2.6 |

| NWQ16MSM | 120416 | K | La | Li | Mg | Mn | Mo | Na | Nb | Ni | P | Pb | Rb | Re | S | Sb | Sc | Se | Sn |
|---|---|---|---|---|---|---|---|---|---|---|---|---|---|---|---|---|---|---|---|
| UNITS | | % | ppm | ppm | % | ppm | ppm | % | ppm | ppm | ppm | ppm | ppm | ppm | % | ppm | ppm | ppm | ppm |
| DETECTION | | 0.01 | 0.5 | 0.2 | 0.01 | 5 | 0.05 | 0.01 | 0.1 | 0.2 | 10 | 0.5 | 0.1 | 0.002 | 0.01 | 0.05 | 0.1 | 1 | 0.2 |
| METHOD | | ME-MS61 | ME-MS61 | ME-MS61 | ME-MS61 | ME-MS61 | ME-MS61 | ME-MS61 | ME-MS61 | ME-MS61 | ME-MS61 | ME-MS61 | ME-MS61 | ME-MS61 | ME-MS61 | ME-MS61 | ME-MS61 | ME-MS61 | ME-MS61 |
| CO | | ME-MS61:REE's may not be totally soluble in this method. | | | | | | | | | | | | | | | | | |
| EX081778 | Magpie | 1.09 | 13.8 | 9.5 | 3.08 | 713 | 2.69 | 3.61 | 8.8 | 54.3 | 690 | 1.1 | 61.5 | 0.002 | 0.06 | 0.35 | 40.9 | 3 | 1.4 |
| EX081779 | Magpie | 0.87 | 12.8 | 13 | 2.99 | 659 | 2.45 | 3.78 | 8.6 | 53 | 650 | 1.1 | 49 | 0.002 | 0.1 | 0.33 | 38.9 | 3 | 1.6 |
| EX081780 | Magpie | 1.13 | 14.9 | 12.5 | 3.24 | 680 | 4.98 | 3.77 | 8.6 | 62.2 | 680 | 1.2 | 63.9 | 0.002 | 0.27 | 0.34 | 38.2 | 3 | 1.8 |
| EX081781 | Magpie | 1.57 | 14.8 | 10.9 | 3.13 | 668 | 5.6 | 2.66 | 9.2 | 78.1 | 810 | 1.5 | 90.6 | 0.003 | 0.22 | 0.69 | 41.2 | 3 | 1.5 |
| EX081782 | Magpie | 1.56 | 15.9 | 10.6 | 3.14 | 665 | 4.43 | 2.7 | 9.4 | 66.3 | 820 | 1 | 82.5 | 0.002 | 0.19 | 0.62 | 42.7 | 3 | 1.6 |
| EX081783 | Magpie | 1.54 | 16.8 | 10.5 | 3.3 | 694 | 3.38 | 3.1 | 10.1 | 67.9 | 890 | 1.1 | 80.1 | 0.003 | 0.12 | 0.59 | 44.8 | 3 | 1.5 |
| EX081784 | Magpie | 1.53 | 15.2 | 9.5 | 3.31 | 715 | 3.3 | 3.11 | 9.3 | 67.2 | 870 | 1 | 73.7 | 0.003 | 0.15 | 0.47 | 43.2 | 3 | 1.4 |
| EX081785 | Magpie | 0.89 | 15.3 | 10 | 3.13 | 805 | 4.12 | 3.49 | 9.4 | 64.8 | 860 | 1.3 | 39.7 | 0.002 | 0.19 | 0.38 | 42.2 | 3 | 1.4 |
| EX081786 | Magpie | 0.85 | 15.7 | 14.2 | 3.15 | 382 | 10.1 | 3.77 | 10.3 | 57 | 940 | 1.3 | 46.8 | 0.016 | 0.55 | 0.53 | 40.7 | 3 | 1.6 |
| EX081787 | Magpie | 0.74 | 15.6 | 16 | 3.21 | 463 | 4.91 | 3.49 | 9.9 | 53.6 | 890 | 1.2 | 41.9 | 0.006 | 0.4 | 0.49 | 41.5 | 3 | 1.8 |
| EX081788 | Magpie | 0.76 | 16.4 | 12.9 | 3.09 | 497 | 4.72 | 3.53 | 10 | 56.6 | 900 | 1.6 | 43.2 | 0.004 | 0.41 | 0.54 | 40 | 4 | 1.9 |
| EX081789 | Magpie | 0.95 | 13 | 11.5 | 2.84 | 456 | 4.43 | 3.45 | 9.8 | 58.8 | 900 | 2.2 | 53.4 | 0.004 | 0.66 | 0.61 | 38.7 | 3 | 2.1 |
| EX081790 | Magpie | 1.13 | 16.8 | 11.5 | 3.11 | 408 | 4.57 | 3.32 | 9.7 | 59.1 | 860 | 1.4 | 66.8 | 0.003 | 0.2 | 0.45 | 41.4 | 3 | 1.7 |
| EX081791 | | 1.13 | 17 | 11.9 | 3.11 | 401 | 5.4 | 3.3 | 9.9 | 62.8 | 870 | 1.4 | 66.2 | 0.002 | 0.21 | 0.43 | 42.5 | 3 | 1.6 |
| EX081792 | | 0.4 | 17 | 23.2 | 0.22 | 460 | 2.51 | 0.1 | 14.9 | 228 | 410 | 19.9 | 42.5 | -0.002 | 0.05 | 0.81 | 53 | 4 | 2.5 |
| EX081793 | TCS | 0.64 | 24.8 | 10.5 | 3.21 | 270 | 3.17 | 3.81 | 7.3 | 75.4 | 610 | 7.3 | 54.7 | 0.005 | 0.66 | 0.39 | 51.4 | 4 | 2.3 |
| EX081794 | TCS | 0.88 | 17 | 7.6 | 3.14 | 305 | 1.08 | 3.91 | 10.4 | 40.3 | 550 | 4.2 | 107.5 | 0.002 | 0.22 | 0.31 | 49.9 | 3 | 2.1 |
| EX081795 | TCS | 1.82 | 17.8 | 16.5 | 3.79 | 279 | 1 | 3.36 | 6.3 | 72.8 | 520 | 4.2 | 213 | 0.004 | 0.48 | 0.18 | 50.7 | 3 | 1.8 |
| EX081796 | TCS | 1.73 | 23 | 14.8 | 3.91 | 324 | 1.86 | 3.75 | 7.1 | 54.3 | 630 | 4.2 | 217 | 0.002 | 0.21 | 0.19 | 52.8 | 3 | 2.2 |
| EX081797 | TCS | 1.87 | 35 | 17.1 | 4.12 | 341 | 3.8 | 3.11 | 6.5 | 50.3 | 560 | 3.2 | 231 | 0.004 | 0.15 | 0.19 | 52.3 | 3 | 1.6 |
| Ch:EX081710 | | 1.58 | 16.6 | 16.4 | 3.45 | 1110 | 2.69 | 2.96 | 14.3 | 78.4 | 960 | 1.5 | 128 | 0.002 | 0.27 | 0.32 | 46.3 | 4 | 3.5 |
| Ch:EX081730 | | 2.14 | 139.5 | 24.1 | 3.72 | 466 | 0.99 | 2.78 | 14.6 | 69.6 | 930 | 2.1 | 194.5 | 0.002 | 0.62 | 0.24 | 43.2 | 4 | 3.1 |
| Ch:EX081745 | | 0.69 | 54.5 | 5.4 | 2.26 | 1190 | 7.29 | 2.62 | 11.3 | 63.3 | 580 | 12.1 | 36.1 | 0.005 | 1.31 | 0.47 | 16.6 | 4 | 9.4 |
| Ch:EX081765 | | 1.04 | 16.6 | 23.9 | 4.47 | 766 | 1.57 | 2.71 | 6.4 | 117.5 | 720 | 1.1 | 54.5 | 0.002 | 0.19 | 0.35 | 33.8 | 2 | 1.2 |
| Ch:EX081780 | | 1.16 | 14.4 | 13.3 | 3.19 | 678 | 4.29 | 3.76 | 8.7 | 59.2 | 660 | 1.3 | 64.1 | 0.002 | 0.28 | 0.33 | 38.8 | 3 | 1.8 |
| Blank01 | | -0.01 | -0.5 | -0.2 | -0.01 | -5 | -0.05 | -0.01 | -0.1 | -0.2 | 10 | -0.5 | -0.1 | -0.002 | -0.01 | -0.05 | -0.1 | -1 | -0.2 |
| Blank02 | | -0.01 | -0.5 | -0.2 | -0.01 | -5 | -0.05 | -0.01 | -0.1 | -0.2 | -10 | -0.5 | -0.1 | -0.002 | -0.01 | -0.05 | -0.1 | -1 | -0.2 |
| Blank03 | | -0.01 | -0.5 | -0.2 | -0.01 | -5 | -0.05 | -0.01 | -0.1 | -0.2 | -10 | -0.5 | -0.1 | -0.002 | -0.01 | -0.05 | -0.1 | -1 | -0.2 |
| St01:OREAS-45e | | 0.3 | 11.4 | 6.7 | 0.13 | 513 | 2.29 | 0.06 | 7.1 | 441 | 320 | 17.1 | 20.5 | -0.002 | 0.04 | 0.96 | 94.9 | 4 | 1.3 |
| St02:OREAS-45e | | 0.32 | 11 | 7.1 | 0.13 | 522 | 2.46 | 0.06 | 7.6 | 445 | 330 | 17.2 | 21.5 | -0.002 | 0.05 | 1.03 | 101.5 | 4 | 1.2 |
| St03:MRGeo08 | | 2.93 | 40.7 | 33.2 | 1.26 | 549 | 15.95 | 1.93 | 22 | 699 | 1020 | 1060 | 219 | 0.009 | 0.29 | 4.76 | 12.7 | 3 | 4.2 |
| St04:GBM908-10 | | 2 | 55.9 | 11.7 | 1.69 | 802 | 67.4 | 2.1 | 11.1 | 2220 | 970 | 2010 | 173 | -0.002 | 0.36 | 1.68 | 19 | 3 | 3.3 |
| St05:OGGeo08 | | 2.68 | 35.2 | 32.4 | 1.16 | 486 | 901 | 1.73 | 16.8 | 8450 | 820 | 7020 | 190 | 1.35 | 2.64 | 25.4 | 10.1 | 11 | 13.2 |
| St06:OGGeo08 | | 2.79 | 34.5 | 34.3 | 1.15 | 483 | 865 | 1.72 | 17.5 | 8570 | 820 | 6960 | 187.5 | 1.395 | 2.72 | 25.5 | 10.3 | 12 | 13.5 |
| THEBE | | 0 | 41.1 | -10 | 0 | 0 | 3 | 0 | 14.5 | 46 | 0 | 4 | 6.2 | 0.001 | | 0.08 | 33 | 1.3 | 5 |
| THEBE | | 0 | 8.2 | 10 | 0 | 0 | 2 | 0 | 9.1 | 60 | 0 | 46 | 26.5 | 0.001 | | 0.08 | 21 | 1.4 | 3 |
| THEBE | | 0 | 11.7 | -10 | 0 | 0 | -1 | 0 | 4 | 54 | 0 | 2 | 28.2 | -0.001 | | 0.26 | 38 | 0.6 | 1 |
| THEBE | | 0 | 8.8 | -10 | 0 | 0 | 1 | 0 | 3.9 | 59 | 0 | 6 | 105 | -0.001 | | 0.39 | 34 | 1.2 | 2 |
| THEBE | | 0 | 6.4 | -10 | 0 | 0 | 1 | 0 | 3.7 | 93 | 0 | -2 | 62.5 | -0.001 | | 0.27 | 41 | 0.5 | 1 |

| TV16047358 | 97 | | | | | | | | | | | | | |
|---|---|---|---|---|---|---|---|---|---|---|---|---|---|---|
| NWQ16MSM | 120416 | Sr | Ta | Te | Th | Ti | Tl | U | V | W | Y | Zn | Zr | Pass75um |
| UNITS | | ppm | ppm | ppm | ppm | % | ppm | ppm | ppm | ppm | ppm | ppm | ppm | % |
| DETECTION | | 0.2 | 0.05 | 0.05 | 0.01 | 0.005 | 0.02 | 0.1 | 1 | 0.1 | 0.1 | 2 | 0.5 | 0.01 |
| METHOD | | ME-MS61 | ME-MS61 | ME-MS61 | ME-MS61 | ME-MS61 | ME-MS61 | ME-MS61 | ME-MS61 | ME-MS61 | ME-MS61 | ME-MS61 | ME-MS61 | LOG-QC |
| CO | ME-MS61:REE's may not be totally soluble in this method. | | | | | | | | | | | | | |
| CO | | | | | | | | | | | | | | |
| EX081701 | BA | 107.5 | 0.89 | 0.07 | 2.81 | 1.405 | 0.54 | 1.5 | 441 | 1.2 | 35.5 | 26 | 119 | |
| EX081702 | BA | 124 | 0.85 | 0.06 | 2.77 | 1.405 | 0.51 | 1.6 | 438 | 1.5 | 32.9 | 29 | 110.5 | |
| EX081703 | BA | 177.5 | 0.48 | 0.11 | 31.8 | 0.642 | 0.82 | 5.5 | 300 | 1.3 | 24.6 | 23 | 181 | |
| EX081704 | BA | 198.5 | 0.89 | 0.08 | 2.88 | 1.305 | 0.45 | 1.6 | 391 | 1.5 | 42 | 21 | 134.5 | |
| EX081705 | BA | 180.5 | 0.47 | 0.06 | 2.14 | 1.075 | 0.32 | 0.7 | 381 | 1.3 | 30.6 | 26 | 104 | |
| EX081706 | BA | 58 | 1.09 | 0.08 | 4.93 | 1.805 | 0.13 | 3.5 | 548 | 2 | 55.1 | 21 | 178 | |
| EX081707 | BA | 56.6 | 0.83 | 0.07 | 4.36 | 1.265 | 0.31 | 2.8 | 371 | 1.3 | 41 | 22 | 153 | |
| EX081708 | BA | 59.9 | 0.8 | 0.05 | 3.98 | 1.2 | 0.19 | 2.4 | 340 | 2.7 | 45.1 | 17 | 145 | |
| EX081709 | BA | 63 | 0.81 | 0.07 | 4.15 | 1.25 | 0.2 | 3.4 | 369 | 1.7 | 51.2 | 17 | 152 | |
| EX081710 | BA | 43.5 | 0.82 | 0.07 | 4.4 | 1.315 | 0.42 | 2.8 | 412 | 1.2 | 34.3 | 18 | 151 | |
| EX081711 | BA | 150.5 | 0.67 | 0.14 | 3.25 | 1.35 | 0.68 | 1.8 | 407 | 2.1 | 37.8 | 22 | 143 | |
| EX081712 | BA | 151 | 0.67 | 0.07 | 3.23 | 1.33 | 0.26 | 1.9 | 402 | 2.2 | 43.4 | 22 | 158 | |
| EX081713 | BA | 146.5 | 0.7 | 0.06 | 3.31 | 1.405 | 0.18 | 1.6 | 408 | 2.1 | 42.6 | 23 | 161 | |
| EX081714 | BA | 160.5 | 0.73 | 0.07 | 3.52 | 1.415 | 0.22 | 1.5 | 418 | 2.3 | 42.8 | 24 | 157.5 | |
| EX081715 | BA | 169 | 0.69 | 0.08 | 3.42 | 1.385 | 0.28 | 2.2 | 430 | 1.7 | 39.1 | 21 | 160 | |
| EX081716 | | 170.5 | 0.69 | 0.07 | 3.4 | 1.405 | 0.28 | 2.2 | 432 | 1.7 | 38.8 | 22 | 155 | |
| EX081717 | | 30.9 | 1.04 | 0.11 | 13.95 | 0.726 | 0.24 | 2.6 | 220 | 1.6 | 10.4 | 42 | 140 | |
| EX081718 | BA | 161 | 0.71 | 0.09 | 3.52 | 1.38 | 0.61 | 1.2 | 432 | 2.6 | 38.7 | 25 | 145 | |
| EX081719 | BA | 179.5 | 0.6 | 0.06 | 3.18 | 1.185 | 0.28 | 1.1 | 379 | 1.7 | 37.4 | 33 | 131 | |
| EX081720 | BA | 189 | 0.66 | 0.05 | 3.47 | 1.32 | 0.19 | 1.3 | 407 | 1.7 | 38.2 | 29 | 156.5 | |
| EX081721 | BA | 242 | 0.64 | 0.07 | 3.45 | 1.27 | 0.18 | 1.3 | 388 | 1.9 | 39.8 | 29 | 154.5 | |
| EX081722 | BA | 135 | 0.66 | 0.05 | 3.33 | 1.355 | 0.35 | 1.2 | 410 | 1.9 | 35.7 | 36 | 153.5 | |
| EX081723 | BA | 73.5 | 1.09 | 0.07 | 5.47 | 1.755 | 0.4 | 1.9 | 227 | 2.1 | 58.2 | 22 | 263 | |
| EX081724 | BA | 92.2 | 1.06 | 0.07 | 5.6 | 1.77 | 0.19 | 1.8 | 233 | 2.8 | 61.4 | 25 | 239 | |
| EX081725 | BA | 85.2 | 1.03 | 0.08 | 5.44 | 1.67 | 0.17 | 1.9 | 220 | 2.6 | 65.4 | 27 | 252 | |
| EX081726 | BA | 51.4 | 0.9 | 0.06 | 4.53 | 1.46 | 0.13 | 2.2 | 184 | 2.9 | 51.8 | 19 | 192 | |
| EX081727 | BA | 70 | 1.06 | 0.06 | 5.51 | 1.69 | 0.14 | 2.1 | 225 | 2.4 | 60.2 | 22 | 243 | |
| EX081728 | DO | 52.2 | 0.85 | 0.05 | 11.6 | 1.085 | 0.58 | 2 | 304 | 1.7 | 37.4 | 28 | 129 | |
| EX081729 | DO | 57.7 | 0.82 | 0.06 | 7.93 | 1.015 | 0.68 | 2.1 | 279 | 2 | 33.4 | 32 | 127.5 | |
| EX081730 | DO | 70.4 | 0.87 | 0.06 | 6.72 | 1.14 | 1.1 | 1.7 | 326 | 1.6 | 36.8 | 38 | 129 | |
| EX081731 | | 71.7 | 0.89 | 0.06 | 6.86 | 1.155 | 1.09 | 1.7 | 331 | 1.7 | 37.1 | 39 | 134 | |
| EX081732 | | 30.7 | 1.03 | 0.14 | 13.9 | 0.728 | 0.25 | 2.6 | 221 | 1.6 | 10.1 | 42 | 140 | |
| EX081733 | DO | 55.6 | 0.87 | 0.06 | 7.01 | 1.145 | 0.79 | 1.9 | 325 | 1.7 | 35.8 | 34 | 131 | |
| EX081734 | DO | 90 | 0.92 | 0.05 | 6.02 | 1.18 | 0.71 | 1.9 | 362 | 1.6 | 35.8 | 24 | 143.5 | |
| EX081735 | CHUM | 75.8 | 0.62 | -0.05 | 10.9 | 0.424 | 0.77 | 2.2 | 221 | 0.3 | 20.5 | 32 | 124.5 | |
| EX081736 | CHUM | 59.3 | 0.64 | 0.05 | 8.15 | 0.388 | 0.69 | 1.9 | 173 | 0.3 | 17 | 28 | 113.5 | |

| NWQ16MSN | 120416 | Sr | Ta | Te | Th | Ti | Tl | U | V | W | Y | Zn | Zr | Pass75um |
|---|---|---|---|---|---|---|---|---|---|---|---|---|---|---|
| UNITS | | ppm | ppm | ppm | ppm | % | ppm | ppm | ppm | ppm | ppm | ppm | ppm | % |
| DETECTION | | 0.2 | 0.05 | 0.05 | 0.01 | 0.005 | 0.02 | 0.1 | 1 | 0.1 | 0.1 | 2 | 0.5 | 0.01 |
| METHOD | | ME-MS61 | ME-MS61 | ME-MS61 | ME-MS61 | ME-MS61 | ME-MS61 | ME-MS61 | ME-MS61 | ME-MS61 | ME-MS61 | ME-MS61 | ME-MS61 | LOG-QC |
| CO | ME-MS61:REE's may not be totally soluble in this method. | | | | | | | | | | | | | |
| EX081737 | CHUM | 55.7 | 0.72 | 0.05 | 8.06 | 0.431 | 0.73 | 2.1 | 196 | 0.3 | 14.9 | 29 | 127.5 | |
| EX081738 | CHUM | 69 | 0.67 | 0.05 | 7.98 | 0.41 | 0.68 | 2.2 | 192 | 0.3 | 17.8 | 28 | 124 | |
| EX081739 | CHUM | 61 | 0.65 | 0.05 | 7.72 | 0.398 | 0.7 | 2 | 204 | 0.3 | 15.4 | 28 | 121 | |
| EX081740 | CHUM | 38 | 1.28 | 0.07 | 8.09 | 1.675 | 0.62 | 4.1 | 355 | 2.1 | 62.8 | 45 | 261 | 95.2 |
| EX081741 | CHUM | 39.4 | 1.28 | 0.08 | 8.83 | 1.905 | 0.68 | 4.7 | 377 | 2.2 | 63.6 | 39 | 255 | |
| EX081742 | CHUM | 31 | 1.16 | 0.06 | 9.03 | 1.695 | 0.67 | 4.4 | 396 | 1.8 | 63.4 | 35 | 233 | |
| EX081743 | CHUM | 34.2 | 1.16 | 0.07 | 6.87 | 1.65 | 0.62 | 4.2 | 352 | 2.1 | 68 | 39 | 232 | |
| EX081744 | CHUM | 29.9 | 1.25 | 0.08 | 6.6 | 1.88 | 1.19 | 3.9 | 341 | 2.3 | 79.1 | 44 | 249 | |
| EX081745 | CHUM | 90.9 | 0.91 | 0.2 | 12.7 | 0.301 | 0.19 | 2.7 | 135 | 580 | 23 | 53 | 99.4 | |
| EX081746 | | 91.7 | 0.9 | 0.21 | 12.6 | 0.299 | 0.2 | 2.7 | 137 | 580 | 23 | 53 | 99.8 | |
| EX081747 | | 33 | 1.15 | 0.15 | 14.9 | 0.775 | 0.26 | 2.7 | 232 | 2.1 | 10.8 | 45 | 153.5 | |
| EX081748 | CHUM | 79.6 | 0.56 | 0.05 | 7.05 | 0.411 | 0.62 | 2.1 | 244 | 41.2 | 20.6 | 50 | 99.1 | |
| EX081749 | CHUM | 66.2 | 0.5 | -0.05 | 5.73 | 0.426 | 0.91 | 1.7 | 185 | 14.9 | 23 | 44 | 99.4 | |
| EX081750 | CHUM | 71.5 | 0.5 | -0.05 | 5.74 | 0.45 | 0.81 | 1.7 | 196 | 1.4 | 23 | 37 | 98.7 | |
| EX081751 | CHUM | 79 | 0.52 | 0.05 | 6.16 | 0.422 | 0.88 | 1.6 | 183 | 1.8 | 21.7 | 40 | 97.8 | |
| EX081752 | CHUM | 173.5 | 1 | -0.05 | 4.66 | 1.095 | 0.4 | 1.5 | 362 | 1.5 | 31.3 | 46 | 119.5 | |
| EX081753 | CHUM | 123.5 | 1.01 | 0.05 | 4.8 | 1.075 | 0.48 | 2.4 | 358 | 1.5 | 37.5 | 39 | 138 | |
| EX081754 | CHUM | 139.5 | 1.03 | 0.06 | 4.66 | 1.12 | 0.59 | 2.3 | 368 | 2.4 | 32.3 | 39 | 138.5 | |
| EX081755 | CHUM | 108 | 1.02 | 0.05 | 4.77 | 1.065 | 0.55 | 2.4 | 360 | 1.9 | 34.1 | 37 | 134.5 | |
| EX081756 | CHUM | 82.3 | 1.09 | -0.05 | 5.17 | 1.135 | 0.7 | 3.1 | 386 | 2.3 | 46.5 | 40 | 154 | |
| EX081757 | Magpie | 47.1 | 1.08 | 0.12 | 6.01 | 1.635 | 0.2 | 2.3 | 336 | 1.7 | 45.2 | 23 | 257 | |
| EX081758 | Magpie | 39.6 | 1.13 | 0.07 | 6.13 | 1.615 | 0.09 | 2.1 | 305 | 1.8 | 49.1 | 22 | 248 | |
| EX081759 | Magpie | 31.6 | 1.08 | 0.08 | 6.37 | 1.495 | 0.1 | 2 | 340 | 1.4 | 50.1 | 19 | 261 | |
| EX081760 | Magpie | 30.1 | 1.07 | 0.06 | 6.17 | 1.525 | 0.09 | 2 | 328 | 1.8 | 48 | 20 | 252 | |
| EX081761 | Magpie | 51.8 | 0.99 | 0.09 | 5.2 | 1.48 | 0.1 | 2.5 | 277 | 2.3 | 50.4 | 18 | 227 | |
| EX081762 | Magpie | 55.7 | 0.41 | 0.05 | 1.99 | 0.869 | 0.19 | 0.6 | 339 | 1.4 | 23.6 | 36 | 96.3 | |
| EX081763 | Magpie | 46.1 | 0.44 | -0.05 | 2.43 | 0.819 | 0.25 | 0.8 | 304 | 2.3 | 25.1 | 39 | 114 | |
| EX081764 | Magpie | 54 | 0.38 | 0.07 | 1.9 | 0.803 | 0.25 | 0.6 | 329 | 1 | 25.6 | 36 | 93.9 | |
| EX081765 | Magpie | 61.8 | 0.43 | -0.05 | 2.02 | 0.877 | 0.19 | 0.7 | 314 | 1.6 | 25.9 | 36 | 101.5 | |
| EX081766 | | 60.8 | 0.42 | -0.05 | 2 | 0.846 | 0.18 | 0.7 | 309 | 1.6 | 25.6 | 35 | 102 | |
| EX081767 | | 32.9 | 1.13 | 0.12 | 15.25 | 0.766 | 0.26 | 2.8 | 230 | 1.6 | 10.5 | 45 | 152.5 | |
| EX081768 | Magpie | 63.9 | 0.43 | -0.05 | 1.83 | 0.904 | 0.23 | 0.6 | 311 | 1.6 | 25.9 | 36 | 90.1 | |
| EX081769 | Magpie | 63.4 | 0.8 | 0.06 | 4.55 | 1.58 | 0.18 | 1.7 | 612 | 1.6 | 38.6 | 23 | 192.5 | |
| EX081770 | Magpie | 71.2 | 0.81 | 0.07 | 4.35 | 1.59 | 0.18 | 1.8 | 570 | 1.7 | 40.2 | 25 | 190 | |
| EX081771 | Magpie | 83.3 | 0.75 | 0.07 | 3.98 | 1.575 | 0.22 | 1.9 | 618 | 1.8 | 40.8 | 22 | 174 | |
| EX081772 | Magpie | 86.1 | 0.74 | 0.07 | 3.98 | 1.655 | 0.25 | 1.8 | 701 | 1.7 | 36.9 | 23 | 168.5 | |
| EX081773 | Magpie | 78.7 | 0.72 | 0.06 | 3.84 | 1.625 | 0.24 | 1.5 | 716 | 1.8 | 36.1 | 22 | 168.5 | |
| EX081774 | Magpie | 113 | 0.55 | -0.05 | 2.96 | 1.025 | 0.32 | 1.2 | 338 | 1.2 | 30.3 | 23 | 128.5 | |
| EX081775 | Magpie | 153 | 0.6 | -0.05 | 3.23 | 1.095 | 0.36 | 1.1 | 378 | 1.1 | 31.1 | 23 | 136.5 | |
| EX081776 | | 150 | 0.57 | 0.05 | 3.15 | 1.065 | 0.36 | 1.1 | 368 | 1.1 | 30.4 | 23 | 133.5 | |
| EX081777 | | 32.3 | 1.05 | 0.11 | 14.45 | 0.737 | 0.25 | 2.7 | 222 | 1.6 | 10.3 | 43 | 143.5 | |

| NWQ16MSM | 120416 | Sr | Ta | Te | Th | Ti | Tl | U | V | W | Y | Zn | Zr | Pass75um |
|---|---|---|---|---|---|---|---|---|---|---|---|---|---|---|
| UNITS | | ppm | ppm | ppm | ppm | % | ppm | ppm | ppm | ppm | ppm | ppm | ppm | % |
| DETECTION | | 0.2 | 0.05 | 0.05 | 0.01 | 0.005 | 0.02 | 0.1 | 1 | 0.1 | 0.1 | 2 | 0.5 | 0.01 |
| METHOD | | ME-MS61 | ME-MS61 | ME-MS61 | ME-MS61 | ME-MS61 | ME-MS61 | ME-MS61 | ME-MS61 | ME-MS61 | ME-MS61 | ME-MS61 | ME-MS61 | LOG-QC |
| CO | ME-MS61:REE's may not be totally soluble in this method. | | | | | | | | | | | | | |
| EX081778 | Magpie | 138 | 0.55 | 0.05 | 3.08 | 1.025 | 0.25 | 1 | 355 | 1.3 | 29.8 | 22 | 132.5 | |
| EX081779 | Magpie | 125 | 0.53 | -0.05 | 2.99 | 0.992 | 0.18 | 1.1 | 347 | 1.2 | 29 | 20 | 127.5 | |
| EX081780 | Magpie | 99.3 | 0.54 | -0.05 | 2.96 | 1.015 | 0.25 | 1.7 | 327 | 1.1 | 28.1 | 25 | 129.5 | 97.1 |
| EX081781 | Magpie | 193.5 | 0.57 | 0.06 | 2.56 | 1.16 | 0.41 | 0.9 | 399 | 1.6 | 34.4 | 27 | 131 | |
| EX081782 | Magpie | 196 | 0.56 | -0.05 | 2.65 | 1.18 | 0.31 | 0.9 | 397 | 1.9 | 34.5 | 28 | 127.5 | |
| EX081783 | Magpie | 172 | 0.62 | 0.05 | 2.77 | 1.285 | 0.31 | 0.8 | 429 | 1.6 | 36.5 | 27 | 132 | |
| EX081784 | Magpie | 147 | 0.59 | -0.05 | 2.63 | 1.265 | 0.25 | 0.8 | 433 | 1.5 | 33.7 | 28 | 128 | |
| EX081785 | Magpie | 101 | 0.57 | -0.05 | 2.63 | 1.25 | 0.14 | 0.8 | 420 | 1.7 | 34.7 | 30 | 135 | |
| EX081786 | Magpie | 43.1 | 0.63 | 0.07 | 2.99 | 1.27 | 0.23 | 1.5 | 402 | 0.9 | 36 | 21 | 157 | |
| EX081787 | Magpie | 49.3 | 0.61 | 0.07 | 2.8 | 1.205 | 0.19 | 1.4 | 378 | 1 | 36 | 20 | 147.5 | |
| EX081788 | Magpie | 50.1 | 0.61 | 0.08 | 2.84 | 1.185 | 0.2 | 1.4 | 368 | 0.9 | 36 | 21 | 148 | |
| EX081789 | Magpie | 55.2 | 0.59 | 0.07 | 2.61 | 1.24 | 0.22 | 1.8 | 390 | 1.2 | 35.1 | 21 | 147 | |
| EX081790 | Magpie | 64.2 | 0.61 | 0.05 | 2.88 | 1.23 | 0.28 | 1.1 | 401 | 1 | 34.5 | 23 | 141.5 | |
| EX081791 | | 63.6 | 0.59 | 0.06 | 2.96 | 1.215 | 0.28 | 1.2 | 389 | 1 | 34.3 | 22 | 141 | |
| EX081792 | | 31.9 | 1.07 | 0.11 | 14.4 | 0.762 | 0.25 | 2.6 | 227 | 1.6 | 10.2 | 43 | 141.5 | |
| EX081793 | TCS | 77.7 | 0.43 | 0.12 | 2.41 | 0.97 | 0.15 | 2.6 | 384 | 0.4 | 39.4 | 18 | 74.6 | |
| EX081794 | TCS | 67.5 | 0.88 | 0.06 | 3.61 | 0.926 | 0.34 | 3.8 | 386 | 0.3 | 38.1 | 19 | 70.4 | |
| EX081795 | TCS | 57.2 | 0.39 | 0.06 | 2.23 | 0.872 | 0.93 | 1.8 | 378 | 0.2 | 30.1 | 29 | 80.1 | |
| EX081796 | TCS | 50.8 | 0.45 | 0.06 | 2.41 | 1.015 | 0.81 | 1.9 | 413 | 0.2 | 36.4 | 32 | 88.7 | |
| EX081797 | TCS | 68.3 | 0.42 | 0.06 | 2.54 | 0.922 | 0.84 | 1.7 | 391 | 0.2 | 29.7 | 26 | 78.8 | |
| Ch:EX081710 | | 43.1 | 0.81 | 0.08 | 4.32 | 1.35 | 0.42 | 2.9 | 417 | 1.1 | 33.9 | 18 | 152 | |
| Ch:EX081730 | | 69.5 | 0.84 | 0.05 | 6.31 | 1.12 | 1.06 | 1.7 | 320 | 1.6 | 35.8 | 38 | 130 | |
| Ch:EX081745 | | 90.5 | 0.92 | 0.19 | 13.1 | 0.303 | 0.2 | 2.8 | 134 | 580 | 23.1 | 52 | 98.6 | |
| Ch:EX081765 | | 61.8 | 0.41 | 0.05 | 2.04 | 0.839 | 0.18 | 0.7 | 315 | 2 | 25.8 | 36 | 101.5 | |
| Ch:EX081780 | | 97.7 | 0.54 | -0.05 | 2.98 | 1.015 | 0.25 | 1.7 | 330 | 1.2 | 28.3 | 25 | 129.5 | |
| Blank01 | | -0.2 | -0.05 | -0.05 | -0.01 | -0.005 | -0.02 | -0.1 | -1 | -0.1 | -0.1 | -2 | -0.5 | |
| Blank02 | | -0.2 | -0.05 | -0.05 | -0.01 | -0.005 | -0.02 | -0.1 | -1 | -0.1 | -0.1 | -2 | -0.5 | |
| Blank03 | | -0.2 | -0.05 | -0.05 | -0.01 | -0.005 | -0.02 | -0.1 | -1 | -0.1 | -0.1 | -2 | -0.5 | |
| St01:OREAS-45e | | 15.2 | 0.56 | 0.21 | 12.85 | 0.513 | 0.15 | 2.4 | 299 | 1.1 | 8.1 | 43 | 109 | |
| St02:OREAS-45e | | 15.9 | 0.57 | 0.19 | 12.75 | 0.525 | 0.15 | 2.5 | 304 | 1.1 | 8.2 | 43 | 112.5 | |
| St03:MRGeo08 | | 304 | 1.55 | -0.05 | 20.7 | 0.474 | 1.07 | 5.9 | 108 | 4.9 | 28.4 | 798 | 112 | |
| St04:GBM908-10 | | 292 | 0.81 | 0.08 | 17.05 | 0.635 | 1.25 | 2.2 | 138 | 3.4 | 37.6 | 1080 | 136 | |
| St05:OGGeo08 | | 242 | 1.27 | 0.2 | 17.7 | 0.37 | 1.68 | 5.1 | 84 | 4.5 | 23.4 | 6930 | 96.4 | |
| St06:OGGeo08 | | 245 | 1.28 | 0.25 | 17.85 | 0.38 | 1.7 | 5.2 | 85 | 4.4 | 23.6 | 7050 | 93.8 | |
| THEBE | | 27.9 | 1 | 0.1 | 4.21 | 6.414757 | -0.5 | 3.37 | 466 | 2 | 50.5 | 3 | 148 | 10.7 |
| THEBE | | 163 | 0.4 | 0.12 | 2.14 | 4.136619 | -0.5 | 1.39 | 301 | 1 | 54.5 | 47 | 86 | 6.9 |
| THEBE | | 176.5 | 0.1 | 0.02 | 1.74 | 8.632944 | -0.5 | 0.56 | 351 | 1 | 26.6 | 86 | 82 | 14.4 |
| THEBE | | 144 | 0.1 | 0.12 | 1.47 | 7.763655 | -0.5 | 0.67 | 334 | 1 | 24.9 | 28 | 73 | 12.95 |
| THEBE | | 122 | 0.1 | 0.02 | 1.57 | 8.66292 | -0.5 | 0.42 | 350 | 1 | 22.7 | 54 | 75 | 14.45 |

# APPENDIX 4: GEOCHRONOLOGY

D163APATITE

| Final207_235 | Final207_235_ | Final206_238 | Final206_238_Error | Correlati | Final238_206 | Final238_206_ | Final207_206 | Final207Age | Final207Age_Int2SE |
|---|---|---|---|---|---|---|---|---|---|
| ~~28~~ | ~~6.2~~ | ~~0.394~~ | ~~0.072~~ | ~~0.65875~~ | ~~0.444~~ | ~~0.077~~ | ~~-0.19951~~ | ~~-1.80E+03~~ | ~~2.10E+03~~ |
| ~~44~~ | ~~11~~ | ~~0.55~~ | ~~0.1~~ | ~~0.56974~~ | ~~0.471~~ | ~~0.067~~ | ~~0.072192~~ | ~~320~~ | ~~410~~ |
| 6.12 | 0.63 | 0.254 | 0.016 | 0.34043 | 0.148 | 0.018 | -0.19823 | ~~590~~ | ~~310~~ |
| ~~49~~ | ~~15~~ | ~~0.67~~ | ~~0.18~~ | ~~0.93208~~ | ~~0.49~~ | ~~0.17~~ | ~~0.74723~~ | ~~610~~ | ~~340~~ |
| 7.5 | 1.1 | 0.262 | 0.023 | 0.076404 | 0.18 | 0.035 | 0.34484 | ~~640~~ | ~~370~~ |
| 10.6 | 4.2 | 0.262 | 0.027 | 0.45852 | 0.255 | 0.08 | -0.32462 | ~~680~~ | ~~350~~ |
| 4.1 | 1.1 | 0.252 | 0.032 | 0.64652 | 0.098 | 0.023 | -0.36462 | ~~790~~ | ~~330~~ |
| 4.06 | 0.43 | 0.216 | 0.012 | 0.69588 | 0.127 | 0.023 | -0.21316 | ~~800~~ | ~~210~~ |
| 4.3 | 1.5 | 0.215 | 0.034 | 0.86511 | 0.187 | 0.073 | 0.067253 | ~~830~~ | ~~420~~ |
| 5.6 | 1.3 | 0.217 | 0.017 | 0.70409 | 0.158 | 0.037 | -0.23108 | ~~830~~ | ~~780~~ |
| ~~8.3~~ | ~~3.4~~ | ~~0.251~~ | ~~0.06~~ | ~~0.88912~~ | ~~0.25~~ | ~~0.11~~ | ~~0.49832~~ | ~~880~~ | ~~220~~ |
| ~~6.3~~ | ~~1.7~~ | ~~0.2~~ | ~~0.033~~ | ~~0.81162~~ | ~~0.222~~ | ~~0.068~~ | ~~-0.083949~~ | 940 | 390 |
| ~~8.7~~ | ~~1.8~~ | ~~0.323~~ | ~~0.035~~ | ~~0.86212~~ | ~~0.181~~ | ~~0.036~~ | ~~-0.45547~~ | 950 | 290 |
| ~~17.3~~ | ~~4.4~~ | ~~0.376~~ | ~~0.06~~ | ~~0.71618~~ | ~~0.325~~ | ~~0.086~~ | ~~-0.40455~~ | 950 | 190 |
| 6.7 | 1.3 | 0.238 | 0.016 | 0.89345 | 0.18 | 0.038 | -0.50549 | 960 | 460 |
| 4.11 | 0.82 | 0.241 | 0.021 | 0.2949 | 0.119 | 0.023 | -0.20247 | 1020 | 360 |
| 3.16 | 0.62 | 0.218 | 0.02 | 0.78151 | 0.101 | 0.024 | -0.4746 | 1020 | 390 |
| 6.21 | 0.78 | 0.255 | 0.03 | 0.41562 | 0.176 | 0.03 | 0.035221 | 1060 | 290 |
| 5.31 | 0.59 | 0.23 | 0.013 | 0.44932 | 0.16 | 0.022 | -0.042883 | 1060 | 160 |
| 5.2 | 1.8 | 0.27 | 0.031 | 0.4595 | 0.148 | 0.056 | -0.065434 | 1100 | 120 |
| 4.5 | 1.7 | 0.257 | 0.046 | 0.91389 | 0.143 | 0.056 | -0.023282 | 1130 | 120 |
| 8.5 | 1.3 | 0.274 | 0.017 | 0.65309 | 0.214 | 0.04 | -0.4063 | 1140 | 110 |
| ~~6.68~~ | ~~0.89~~ | ~~0.293~~ | ~~0.018~~ | ~~0.94658~~ | ~~0.155~~ | ~~0.022~~ | ~~-0.59117~~ | 1150 | 230 |
| 8.2 | 1.5 | 0.252 | 0.023 | 0.50448 | 0.256 | 0.056 | -0.11366 | 1150 | 270 |
| 16 | 7.6 | 0.39 | 0.12 | 0.99035 | 0.3 | 0.1 | -0.37667 | 1151 | 93 |
| ~~23.1~~ | ~~8.8~~ | ~~0.38~~ | ~~0.11~~ | ~~0.93591~~ | ~~0.396~~ | ~~0.09~~ | ~~0.089266~~ | 1180 | 160 |
| ~~22.9~~ | ~~7.9~~ | ~~0.43~~ | ~~0.11~~ | ~~0.92453~~ | ~~0.408~~ | ~~0.086~~ | ~~-0.1249~~ | 1180 | 150 |
| ~~11~~ | ~~1.6~~ | ~~0.281~~ | ~~0.024~~ | ~~0.95636~~ | ~~0.312~~ | ~~0.065~~ | ~~-0.70363~~ | 1190 | 180 |
| ~~26.1~~ | ~~7.9~~ | ~~0.69~~ | ~~0.18~~ | ~~0.97488~~ | ~~0.3~~ | ~~0.073~~ | ~~-0.2985~~ | 1200 | 140 |
| 7 | 3 | 0.264 | 0.067 | 0.9446 | 0.209 | 0.087 | 0.12054 | 1220 | 190 |
| 7.6 | 1.1 | 0.27 | 0.015 | 0.90264 | 0.204 | 0.042 | -0.66235 | 1230 | 200 |
| ~~7.7~~ | ~~2.7~~ | ~~0.229~~ | ~~0.047~~ | ~~0.86693~~ | ~~0.29~~ | ~~0.1~~ | ~~-0.25356~~ | 1260 | 120 |
| 3.6 | 1.2 | 0.201 | 0.024 | 0.45225 | 0.115 | 0.033 | -0.093769 | 1260 | 120 |
| 6.4 | 1 | 0.259 | 0.015 | 0.91708 | 0.192 | 0.044 | -0.5915 | 1270 | 260 |
| 5.4 | 1 | 0.252 | 0.03 | 0.8357 | 0.189 | 0.053 | -0.29448 | 1280 | 190 |
| 5.12 | 0.59 | 0.253 | 0.018 | 0.067167 | 0.158 | 0.023 | -0.087271 | 1320 | 230 |
| 7.4 | 1.1 | 0.286 | 0.019 | 0.68635 | 0.203 | 0.046 | -0.18568 | 1340 | 140 |
| 9.4 | 1.5 | 0.302 | 0.03 | 0.88327 | 0.233 | 0.041 | -0.44535 | 1340 | 190 |
| 7.4 | 2.5 | 0.235 | 0.044 | 0.85134 | 0.24 | 0.13 | 0.46473 | ~~1410~~ | ~~130~~ |
| 8.6 | 3.9 | 0.279 | 0.04 | 0.67862 | 0.28 | 0.13 | -0.31767 | ~~1510~~ | ~~200~~ |

D183APATITE

| Final207 | Final207 | Final206 | Final206 | ErrorCor | Final238 | Final238 | Final207 | Final207Age | Final207Age_Int2SE |
|---|---|---|---|---|---|---|---|---|---|
| ~~126~~ | ~~32~~ | ~~1.08~~ | ~~0.37~~ | ~~0.5961~~ | ~~0.67~~ | ~~0.12~~ | ~~0.8737~~ | ~~-1.00E+03~~ | ~~2.00E+03~~ |
| ~~11.3~~ | ~~2.3~~ | ~~0.281~~ | ~~0.034~~ | ~~0.5275~~ | ~~0.209~~ | ~~0.036~~ | ~~0.72~~ | ~~100~~ | ~~660~~ |
| 10.2 | 2.4 | 0.232 | 0.02 | 0.2912 | 0.219 | 0.04 | 0.4478 | ~~280~~ | ~~950~~ |
| ~~40~~ | ~~12~~ | ~~0.42~~ | ~~0.14~~ | ~~0.3385~~ | ~~0.74~~ | ~~0.33~~ | ~~0.6984~~ | ~~400~~ | ~~1000~~ |
| 9.4 | 2.5 | 0.227 | 0.023 | 0.4289 | 0.216 | 0.04 | 0.3723 | ~~730~~ | ~~420~~ |
| ~~41~~ | ~~20~~ | ~~0.59~~ | ~~0.29~~ | ~~0.8738~~ | ~~0.44~~ | ~~0.13~~ | ~~-0.698~~ | ~~850~~ | ~~390~~ |
| ~~107~~ | ~~37~~ | ~~1.23~~ | ~~0.47~~ | ~~0.2515~~ | ~~0.66~~ | ~~0.28~~ | ~~0.8895~~ | ~~940~~ | ~~160~~ |
| 10.6 | 3.3 | 0.272 | 0.045 | 0.4507 | 0.215 | 0.051 | 0.49 | ~~970~~ | ~~390~~ |
| ~~4.6~~ | ~~0.28~~ | ~~0.18~~ | ~~0.13~~ | ~~0.4372~~ | ~~0.71~~ | ~~0.66~~ | ~~0.954~~ | 1050 | 250 |
| 9.9 | 2.3 | 0.246 | 0.027 | 0.1533 | 0.231 | 0.047 | 0.5469 | 1080 | 170 |
| 5.5 | 1.1 | 0.219 | 0.021 | 0.4542 | 0.122 | 0.014 | 0.254 | 1110 | 170 |
| 9.2 | 3 | 0.231 | 0.043 | 0.266 | 0.249 | 0.032 | 0.733 | 1120 | 140 |
| 14.4 | 3.2 | 0.282 | 0.023 | 0.0639 | 0.295 | 0.054 | -0.061 | 1140 | 130 |
| 14.3 | 2.8 | 0.271 | 0.023 | 0.2078 | 0.288 | 0.038 | 0.4918 | 1170 | 140 |
| 13.6 | 3.3 | 0.247 | 0.028 | 0.3836 | 0.299 | 0.057 | 0.3872 | 1190 | 140 |
| 13.2 | 3.1 | 0.269 | 0.027 | 0.2211 | 0.258 | 0.048 | 0.4045 | 1200 | 180 |
| 8.8 | 2.2 | 0.247 | 0.021 | 0.2761 | 0.216 | 0.055 | -0.234 | 1200 | 150 |
| 13.4 | 2.3 | 0.28 | 0.022 | 0.0114 | 0.27 | 0.045 | 0.1019 | 1210 | 130 |
| ~~19.7~~ | ~~6.7~~ | ~~0.364~~ | ~~0.047~~ | ~~0.3037~~ | ~~0.24~~ | ~~0.056~~ | ~~-0.139~~ | 1220 | 150 |
| 9.2 | 2.7 | 0.226 | 0.024 | 0.2486 | 0.227 | 0.052 | 0.533 | 1240 | 130 |
| ~~45~~ | ~~20~~ | ~~0.328~~ | ~~0.08~~ | ~~0.574~~ | ~~0.54~~ | ~~0.28~~ | ~~0.7619~~ | 1250 | 190 |
| ~~43~~ | ~~18~~ | ~~0.37~~ | ~~0.11~~ | ~~0.109~~ | ~~0.44~~ | ~~0.22~~ | ~~0.3806~~ | 1280 | 220 |
| 10.5 | 2.9 | 0.245 | 0.026 | 0.5174 | 0.204 | 0.031 | 0.2519 | ~~1410~~ | ~~220~~ |
| ~~11.6~~ | ~~2.1~~ | ~~0.223~~ | ~~0.025~~ | ~~0.1974~~ | ~~0.321~~ | ~~0.064~~ | ~~0.2417~~ | ~~1630~~ | ~~240~~ |

D16T

| Final207_235 | Final207_235_Int2 | Final206_238 | Final206_238_Int2SE | ErrorCorrelation_6_38vs7 | Final207_206 | Final207_206_Prop2 | ErrorCorrelation_38_6vs7_i | Final207Age | Final207Age_Prop2SE |
|---|---|---|---|---|---|---|---|---|---|
| 4.33 | 0.51 | 0.304 | 0.018 | 0.502708978 | 0.097 | 0.011 | 0.113402062 | 1630 | 160 |
| 3.44 | 0.38 | 0.26 | 0.015 | 0.522267206 | 0.093 | 0.011 | 0.11827957 | 1470 | 140 |
| 4.9 | 0.28 | 0.294 | 0.013 | 0.773809524 | 0.115 | 0.0069 | 0.06 | 1570 | 150 |
| 4.25 | 0.27 | 0.2752 | 0.013 | 0.743566968 | 0.1064 | 0.0077 | 0.072368421 | 1520 | 140 |
| 4.59 | 0.31 | 0.2838 | 0.011 | 0.573893473 | 0.1109 | 0.0069 | 0.062218215 | 1507 | 100 |
| 4.64 | 0.82 | 0.31 | 0.019 | 0.346813533 | 0.104 | 0.02 | 0.192307692 | 1460 | 230 |
| 8.6 | 1.1 | 0.328 | 0.023 | 0.548226164 | 0.182 | 0.027 | 0.148351648 | 1150 | 270 |
| 5.04 | 0.33 | 0.302 | 0.015 | 0.758579169 | 0.114 | 0.0074 | 0.064912281 | 1590 | 130 |
| 4.64 | 0.19 | 0.2884 | 0.011 | 0.931454851 | 0.1102 | 0.0045 | 0.040834846 | 1563 | 110 |
| 5.54 | 0.41 | 0.299 | 0.015 | 0.67786932 | 0.128 | 0.011 | 0.0859375 | 1470 | 150 |
| 4.71 | 0.4 | 0.284 | 0.016 | 0.663380282 | 0.114 | 0.01 | 0.087719298 | 1500 | 160 |
| 4.21 | 0.42 | 0.265 | 0.014 | 0.529559748 | 0.11 | 0.012 | 0.109090909 | 1400 | 150 |
| ~~7.7~~ | ~~1.6~~ | ~~0.334~~ | ~~0.029~~ | 0.417851796 | ~~0.167~~ | ~~0.033~~ | 0.19760479 | ~~1120~~ | ~~260~~ |
| ~~5.27~~ | ~~0.8~~ | ~~0.331~~ | ~~0.022~~ | 0.437839879 | ~~0.112~~ | ~~0.017~~ | 0.151785714 | ~~1350~~ | ~~350~~ |
| 5.72 | 0.39 | 0.315 | 0.016 | 0.744973545 | 0.1251 | 0.0083 | 0.066346922 | 1544 | 120 |
| ~~7.1~~ | ~~1.2~~ | ~~0.323~~ | ~~0.034~~ | 0.622807018 | ~~0.166~~ | ~~0.035~~ | 0.210843373 | ~~1160~~ | ~~320~~ |
| 5.33 | 0.53 | 0.293 | 0.016 | 0.549166076 | 0.125 | 0.013 | 0.104 | 1440 | 160 |
| 5.8 | 0.67 | 0.296 | 0.021 | 0.614158935 | 0.134 | 0.016 | 0.119402985 | 1340 | 160 |
| 5.12 | 0.47 | 0.306 | 0.018 | 0.640801001 | 0.119 | 0.013 | 0.109243697 | 1580 | 180 |
| 6.18 | 0.67 | 0.333 | 0.023 | 0.637084846 | 0.13 | 0.016 | 0.123076923 | 1400 | 190 |
| 5.87 | 0.59 | 0.329 | 0.016 | 0.483849364 | 0.122 | 0.011 | 0.090163934 | 1630 | 160 |
| 5.27 | 0.28 | 0.319 | 0.013 | 0.767017465 | 0.114 | 0.0073 | 0.064035088 | 1680 | 150 |
| 7.16 | 0.56 | 0.317 | 0.023 | 0.927670122 | 0.158 | 0.016 | 0.101265823 | 1290 | 200 |
| ~~11.9~~ | ~~2.1~~ | ~~0.335~~ | ~~0.031~~ | 0.524378109 | ~~0.26~~ | ~~0.051~~ | 0.196153846 | ~~640~~ | ~~420~~ |
| ~~6.8~~ | ~~1.9~~ | ~~0.339~~ | ~~0.04~~ | 0.422294675 | ~~0.148~~ | ~~0.045~~ | 0.304054054 | ~~990~~ | ~~380~~ |
| ~~9.8~~ | ~~2.9~~ | ~~0.359~~ | ~~0.047~~ | 0.442416675 | ~~0.187~~ | ~~0.036~~ | 0.192513369 | ~~950~~ | ~~320~~ |
| 3.62 | 0.19 | 0.2723 | 0.012 | 0.839631212 | 0.0912 | 0.005 | 0.054824561 | 1611 | 120 |